68-17,597

SHENG, Henry Pa-Houng, 1931-
HYDRODYNAMIC STUDY OF LIQUID-LIQUID SEPARATION IN A CONVENTIONAL CYCLONE.

The University of Oklahoma, Ph.D., 1968
Engineering, chemical

University Microfilms, Inc., Ann Arbor, Michigan

THE UNIVERSITY OF OKLAHOMA

GRADUATE COLLEGE

HYDRODYNAMIC STUDY OF LIQUID-LIQUID SEPARATION IN A CONVENTIONAL CYCLONE

A DISSERTATION

SUBMITTED TO THE GRADUATE FACULTY

in partial fulfillment of the requirements for the

degree of

DOCTOR OF PHILOSOPHY

BY

Henry Pa-Houng Sheng

Norman, Oklahoma

1968

HYDRODYNAMIC STUDY OF LIQUID-LIQUID SEPARATION

IN A CONVENTIONAL CYCLONE

APPROVED BY

C.M. Sliepcevich

J.M. Campbell

S.D. Christian

F.B. Campbell

Fred Weller

DISSERTATION COMMITTEE

ACKNOWLEDGMENT

As I am reaching the terminal of my academic journey after an unexpectedly long and tortuous path, I feel compelled to take this opportunity to say a few words to those whom I shall cherish in my memory.

First, I wish to express my deep appreciation and profound admiration to Professor C. M. Sliepcevich for his guidance and encouragement in directing this study. Both his classroom pedagogy and tutorial sessions, in which he elucidated a multitude of interdisciplinary subjects, were part of my rewarding experiences at the University of Oklahoma.

Gratitude is also due to members of my dissertation committee: Prof. Sherril Christian, Prof. John Campbell, Prof. Frank Canfield for their generous effort in contributing many hours of discussion as well as advice; and particularly to Dr. J. Reed Welker for his meticulous examination of this manuscript. Personal communication with Prof. K. Rietema of Technological University of Eindhoven, Holland is also thankfully acknowledged.

Special mention must be given to Dwight Pfenning, my colleague, for his competent assistance in computer programming which made the processing of massive raw data possible. Indebtedness must also extend to Dr. Hadi Hashemi and Jerry Havens for their analytical interpretations on several problems. Credits should be given to Mrs. Ruth Hogan, Mrs. Joyce Meyer and Miss Connie Ellender for the preparation of the manuscript and to Mrs. Billy Ann Brown for general administrative guidance on this project.

Both Continental Oil Company of Ponca City, Oklahoma and U.S. Industries of Kansas City, Mo. are responsible for the donation of hydrocarbon and polyethylene particles, respectively, for the laboratory experiment.

Finally, the financial support of the E-C Corporation of Chicago, Illinois made this investigation possible.

ABSTRACT

In a conventional hydrocyclone, two vortices take place when a sufficient amount of two or more liquid phases is charged tangentially to the upper base. The primary vortex is responsible for discharging the heavier phase in a rotating spray at the apex of the underflow. Simultaneously, at this apex a column of air, usually known as the air core, is drawn spirally upward to carry the lighter phase through the vortex finder tube and to exit as the overflow.

A mathematical model postulating a combined streamline flow and centrifugal action is proposed. However, by testing against the processed experimental data, it is discovered that only at phase ratio (oil/water) of 1/2, the streamline flow governs the mechanics of phase separation. In this respect, the fate of a solid or liquid to exit in the overflow is ultimately determined by its path and the momentum of the air core relative to the terminal velocity of the particle in question. The prevalent assumption, which attributes the centrifugal action to be the sole controlling factor in a cyclone, is therefore not adequate for a liquid-liquid system.

Unlike the common centrifuge which draws on external power for the separation on phases, the source of power in a hydrocyclone is inherent within the system. Consequently, any separation in a hydrocyclone is inevitably complemented by a certain degree of turbulence. Through the theoretical formulation outlined in this thesis, it is possible to express the macroscopic turbulent length in a dimensional form.

A total of 240 runs was conducted by incorporating three levels of flow rates and feed compositions and two levels of solid (polyethylene sp. gr. = 0.92) sizes and solid contents as parameters. The system is consisted of water and hydrocarbon (sp. gr. = 0.76). The relative efficiency value and effective volume fraction for each run are tabulated.

A method for estimating the relative efficiency values for an undetermined system is presented. In addition the practical application of relative efficiencies for comparing the performance of two cyclone systems is illustrated.

TABLE OF CONTENTS

TABLE OF CONTENTS (continued)

TABLE OF CONTENTS (continued)

TABLE OF CONTENTS (continued)

LIST OF TABLES

LIST OF ILLUSTRATIONS

LIST OF ILLUSTRATIONS (continued)

HYDRODYNAMIC STUDY OF LIQUID-LIQUID SEPARATION IN A CONVENTIONAL CYCLONE

CHAPTER I

INTRODUCTION

Generally a cyclone can be either a cylindrical tube, a hollow truncated cone, or a combination of both. The latter is the most common design today. The feed entrance tube is always installed tangentially but usually in the upper portion of the cylindrical section. Two concentric outlets are provided at opposite ends. The upper outlet is commonly known as the vortex finder tube or overflow discharge and the lower outlet the discharge nozzle or underflow apex.

The most attractive feature of the cyclone is its simplicity in both construction and operation (e.g., no moving parts) and low capital investment (as compared with a centrifuge, for example). However, the practical advantage of a cyclone is that almost any mixture of immiscible fluids or solid-containing suspension with a density gradient can be separated into two enriched portions, provided the flow throughput is substantial enough to generate adequate vortex action within the cyclone. When a clear liquid is present in the feed, two vortex phenomena can be observed. The outer vortex represents the bulk flow swirling downward in a rotating spray at the apex where the inner vortex, essentially a column of air usually known as the air core, is drawn spirally and co-directionally upward to carry the lighter phase through the vortex finder tube and to exit as the overflow (Figure 1). Since most liquid fluids are several hundred times denser than air and owing to the conservation of momentum at the apex, the tangential velocity of the air-column can be expected to be several hundred times* greater than that of the bulk flow at the discharge nozzle. It is mainly due to this air core that the lighter phase of the feed mixture is separated through the vortex finder tube. One may also note that the dual-vortex mechanism experienced in a hydrocyclone is different from the single-vortex flow which has been extensively investigated by hydrodynamicists.

The flow pattern of a single fluid in a hydrocyclone has been determined by several investigators with findings in good agreement. Both Crainer (5) and Kelsall (11) maintained that the product of tangential velocity and radius to the nth power is constant.

$$V_\theta \, r^n = \text{constant} \qquad (1)$$

*Estimated from high-speed motion pictures.

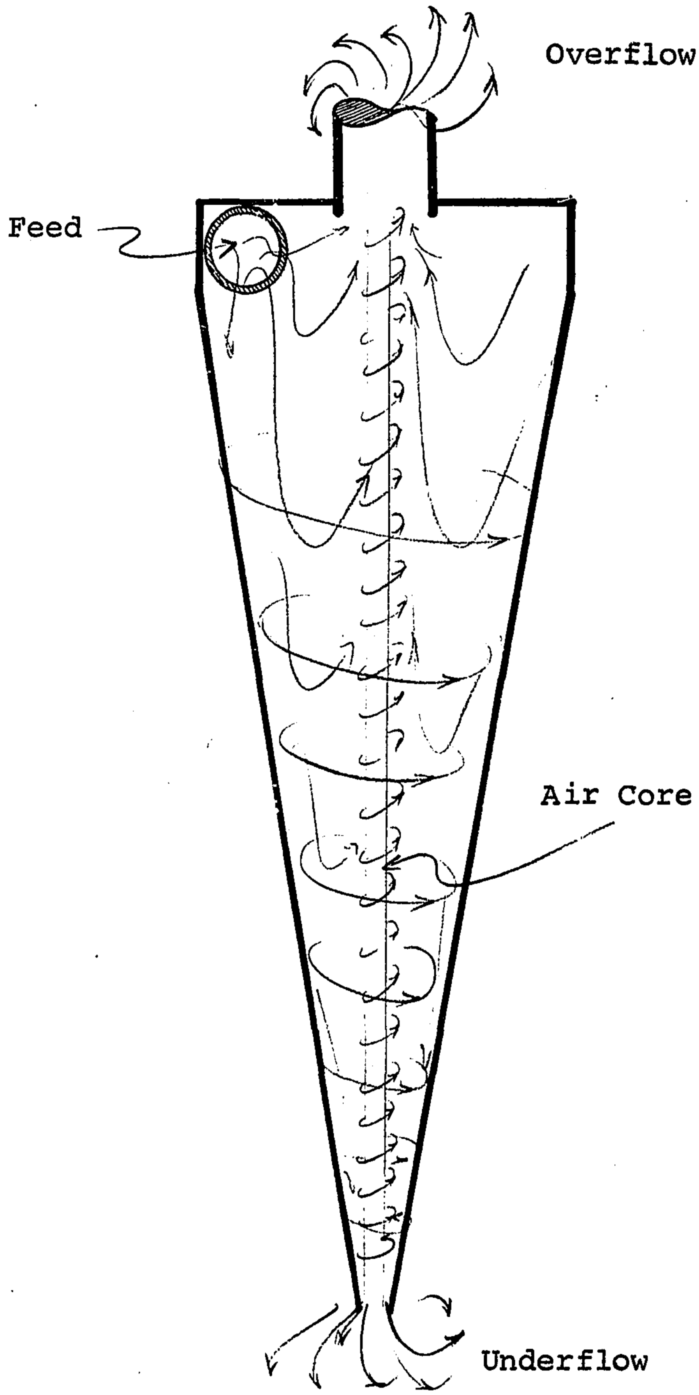

Figure 1. Vertical, Radial, and Tangential
Flow Pattern

as long as the total input energy to the systems remains unchanged; i.e., the law of conservation of angular momentum is applicable. However, as shown in Figure 2, n can vary from -1 to +1 depending on the internal friction loss. For a fluid of infinite viscosity n is -1. Driessen (6) derived the basic mathematical relationship between tangential velocity and radius for a vortex flow involving a single fluid, which compared favorably with the measured values. Rietema (16) has plotted the reduced tangential velocity as a function of the reduced radius using the sum of kinematic viscosity and turbulent viscosity as a parameter, and it provided correlations for the optimum design of solid-liquid separation, which has since been a standard reference in this technology. Mixon (14) further substantiated the correlation by reinterpretations which are expected to pave the way for the future study of three-phase separations.

In contrast to numerous publications on solid-liquid separation by the technology of hydrocyclone, the study on liquid-liquid separation has been meager. The major differences between these two mechanisms are: 1) solid particles remain intact while liquid particles tend to split into finer sizes due to high shear streeses near the air core and 2) solid particles to be separated from the liquid nearly always have a density much greater than that of the liquid, whereas the dispersed liquid particles may have a density either slightly greater or less than that of the continuous phase.

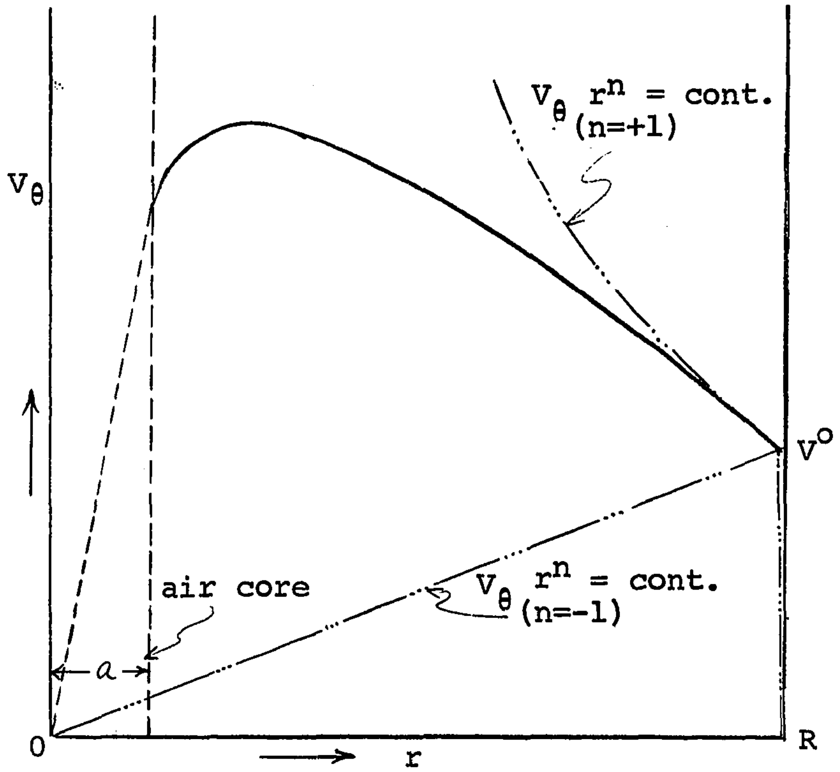

Figure 2(a). Typical Tangential Velocity Profile Near The Entrance Tube (17)

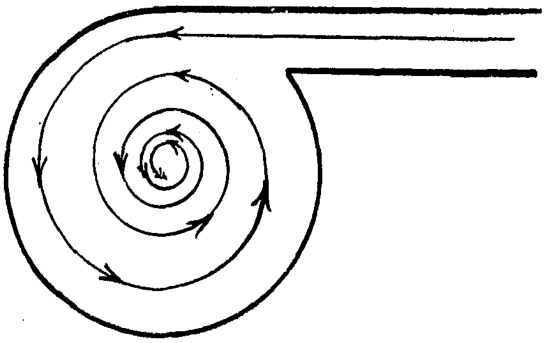

Figure 2(b). Streamline Flow Pattern

Unlike the centrifuge in which a particle, either of liquid or solid, experiences a unique force, the particle moving through a fluid medium in a hydrocyclone experiences unbalanced pressures on opposite sides of the particle normal to the direction of flow. In addition, the source of power for the separation of phases in a hydrocyclone is inherent in the stream; hence, any separation in a hydrocyclone is always complemented by a certain degree of turbulent mixing of the phases, notably in the upper conic section near the feed entrance tube. This inevitable turbulence causes a damaging effect in a solid-liquid case where solids could be dynamically "retained" near the air core and then mechanically carried off to the overflow. In the case of a liquid-liquid system, the effect is even more detrimental if the liquid particles tend to emulsify with the continuous medium. When an emulsion is formed, the function of a hydrocyclone is merely reduced to the separation of the denser emulsion from the lighter emulsion of an essentially homogeneous mixture. However, the presence of a solid phase in a liquid-liquid system tends to discourage the emulsion forming presumably due to the reduction of surface contact area--especially when the solid is preferentially wetted by one of the liquids. It is mainly from the standpoint of academic interest that this investigation is devoted mostly to the study of turbulent mixing in a hydrocyclone by a proposed mathematical model. The purpose of this model is to express the turbulence in terms of dimensional "length" when the required experimental variables become available.

One of the major factors in the commercial acceptance of a unit of equipment is its economic feasibility. The main reason that the hydrocyclone has not yet been generally adopted for liquid-liquid separation by commercial operations is its low efficiency at the present state-of-art. Therefore, one of the objectives of this investigation is to measure the separation efficiency of a two-phase, liquid system in the presence of a solid. It is hoped that this study will eventually yield some perspective knowledge leading to the amelioration of economic feasibility of liquid separation by the technology of hydrocyclone.

CHAPTER II

HISTORICAL BACKGROUND AND PRIOR WORK

Of all the cyclones in existence today, the gas-solid cyclone, commonly known as the cyclone separator, probably has the longest history of usage.

Although the first hydrocyclone patent was granted in the U.S. in 1891 to Bretney and a five-foot diameter hydrocyclone was employed by the phosphate industry as early as 1914, commercial installations were not too prevalent until the late 1930's--mostly confined to the pulp and paper industry for cleaning dilute pulp stock.

It was not until the early 1940's when the Dutch State Mines inaugurated coal-washing and ore-processing in large tonnage that the acceptance of hydrocyclone generated any appreciable momentum. From then on, numerous papers appeared in the literature and many ingenious designs and modifications for a broad spectrum of applications became available on the market. The art of hydrocyclone technology then began to flourish.

With the exception of independent theoretical studies on vortex hydrodynamics, engineering research on the hydrocyclone, particularly in correlation of performance and applicability to various processes, was meager until it received concerted support from both the U.S. Atomic Energy Commission and U.K. Atomic Energy Authority during World War II. In the ensuing years, more sophisticated efforts, incorporating hydrocynamic principles and analyses, appeared in published papers. It is due to the limited scope of this investigation that readers are referred to the book <u>The Hydrocyclone</u> (3) which contains the most complete bibliography available. Over 600 papers on hydrocyclone and related subjects and 55 patent reviews are presented.

While the hydrocyclone has been standard equipment in various fields of technology for solid-liquid separation, the 1960's saw a revived interest in special laboratory uses and diversified applications—notably in the chemical industry for liquid-liquid extraction, solid-liquid leaching, crystallization, and in space technology where separation in a zero-gravitational field is required. Recently, in the petrochemical industry, considerable effort has been expended to increase the operating efficiency of the cyclone separator in order to permit its use in general liquid-liquid separation on a commercial scale. A cursory review of current information seems to indicate that the general trend is toward adopting a system consisting of multiple, small- or even miniature-cyclones with common feed entrance and discharge exits. It is generally regarded that a small cyclone yields a higher efficiency. Hence, for handling large capacities, multiple, small units can be used to circumvent the problems of scale-up. In addition, the effect of various dimensions and apex angles on separation efficiency can be minimized in a smaller cyclone.

Since the scope of this investigation is primarily in the realm of liquid-liquid separations, a brief review of the previous work in this aspect is pertinent.

While the literature is abundant in solid-liquid separation work, little is available on liquid-liquid separations. The earliest recorded investigation was conducted by Tepe and Woods (21) of the U.S. Atomic Energy Commission in 1943 in which the separation efficiency was derived. Van Rossum (23) in 1953 conducted investigations on the separation of water-in-oil emulsions in a 3-inch cyclone using oils of different viscosities and densities as the continuous phase. Effects of viscosity on separation efficiency were also determined. Simkin and Olney (18) in 1956 determined by a series of experiments the most favorable conditions for separating liquids in a 4-inch cyclone. Values of separation efficiencies as a function of effluent split at various feed compositions, feed rates, and geometric factors of the cyclone were obtained. The relationship between the mass transfer efficiency and the degree of phase seaparation was also discussed. In the same year, Bradley (2) proposed a scheme to use the cyclone as an extractor-separator which was followed by Hitchon's (10) experiment to measure both the separation efficiencies and mass transfer efficiencies in a 10 mm. cyclone as an extracting-separating device for a tri-component system. In similar manner, Molyneaux (15) investigated the possibility of liquid-liquid extraction and solid-liquid leaching in a dual-cyclone for other tri-component systems and reported the findings in the form of mass-transfer coefficients. In addition, Breeze (4) reported some separation results and qualitative conclusions from a high-speed "dual jet-clone" as a substitute for a mixer-settler unit.

Academically, Klein (12) in 1950 investigated the applicability of a cyclone to the separation of a liquid mixture in a 3-inch cyclone. Although optimum effluent splits were obtained for various feed compositions and pressure drops across the cyclone, emulsification remained serious. Ellefson (7) continued the work by employing an 8-inch cyclone in order to simulate the commercial-scale operation. He reported the range of optimum volume at various parameters as well as the correlation of energy requirement to the inlet and overflow diameters. Recently, Sweet Water Development (19) has conducted massive experimental runs using various designs and modifications of cyclone for a liquid-solid-liquid system in which the solid, a propane hydrate, has an intermediate density between brine and propane. However, no tabulation of separation efficiency and correlation of data are presented.

CHAPTER III

THEORETICAL ANALYSIS

This theoretical study is presented in two parts. In the first part the separation mechanics, in which the motion of a particle, whether it be a solid or liquid, is thoroughly investigated with due consideration for influential factors, and a mathematical model is proposed in order to determine the ineffective separation region. In the second part the definitions of multicomponent separation efficiency and ideal efficiency are presented.

Separation Mechanics

The flow mechanism in the separation of immiscible liquids in a hydrocyclone involves two vortices — the inner vortex primarily responsible for carrying the lighter phase to the overflow and the outer vortex for discharging the heavier phase to the apex. In the absence of any well-established theory for a dual-vortex flow involving two immiscible liquids, it seems appropriate to derive the desired equation of state from the Navier-Stokes Equation (1). Since steady-state is expected for a cyclone in operations and the fluid under consideration is assumed to be incompressible,

$$\nabla \cdot \vec{V} = 0 \qquad (2)$$

where $\vec{V}$ is the fluid velocity. In cylindrical coordinates for a Newtonian fluid with constant density, ρ, and viscosity, μ, the following equations of motion are pertinent:

r-component

$$V_r \frac{\partial V_r}{\partial r} + V_z \frac{\partial V_z}{\partial Z} - \frac{V_\theta^2}{r} = - \frac{1}{\rho} \frac{\partial P}{\partial r} = \nu \left[\frac{1}{r} \frac{\partial}{\partial r} \left(r \frac{\partial V_r}{\partial r}\right) + \frac{\partial^2 V_r}{\partial Z^2} - \frac{V_r}{r^2}\right] \qquad (3)$$

θ-component

$$V_r \frac{\partial V_\theta}{\partial r} + V_z \frac{\partial V_\theta}{\partial Z} + \frac{V_r V_\theta}{r} = \nu \left[\frac{1}{r} \frac{\partial}{\partial r} \left(r \frac{\partial V_\theta}{\partial r}\right) + \frac{\partial^2 V_\theta}{\partial Z^2} - \frac{V_\theta}{r^2}\right] \qquad (4)$$

Z-component

$$V_r \frac{\partial V_z}{\partial r} + \frac{V_\theta}{r} \frac{\partial V_z}{\partial \theta} + V_z \frac{\partial V_z}{\partial Z} = - \frac{1}{\rho} \frac{\partial P}{\partial Z} + \nu \left[\frac{1}{r} \frac{\partial}{\partial r} \left(r \frac{\partial V_z}{\partial r}\right) + \frac{\partial^2 V_z}{\partial Z^2}\right] + g \qquad (5)$$

The vertical velocity component as measured by Kelsall (10) indicates that a null region generally prevails within the cyclone in operation except in the neighborhood of the air core or the inner vortex where the liquid is carried to the overflow by a spiral action of the inner vortex, i.e., the tangential velocity predominates over the others. Therefore it appears reasonable that the vertical velocity component is negligible. (Note: For a short laboratory size cyclone, the hydrostatic pressure attributed by the gravitational force is also negligible in comparison with the centrifugal force generated within the cyclone. Reported values indicate sometimes a magnitude of 15,000 g is possible).

Tangential Velocity at the Air Core: The tangential velocity profile of a single fluid in a hydrocyclone has been well investigated (5), (6), (10). However, the analytical expression of the velocity at the air core is extremely complex. As an academic exercise, this author presents two additional methods for determining the velocity at the air core which have not been reported in the literature. The analytical method is shown in Appendix A and the experimental method which requires several measured variables and a set of trial and error procedures is under the last section "Method of Determining the Macroscopic Turbulent Length" of this chapter.

Of all the equations presented in the derivation of air core velocity (shown in Appendix A), the two most important ones are:

$$V_\theta = \frac{aV_o}{a^{\xi+2} - b^{\xi+2}}\left(r^{\xi+1} - \frac{b^{\xi+2}}{r}\right) \qquad (6)*$$

*Identical with Eq. A-41.

where a = air core radius

V_o = tangential velocity at the periphery of the air core

r = radius of the cyclone

b = radius of the upper base of the cyclone

$\xi = \frac{(Q/L)}{\nu}$, a dimensionless quantity

and
$$V_o \simeq \frac{a^{\xi+2} - b^{\xi+2}}{a}\sqrt{\frac{P_{in}(h_2{}^2 \tan^2\alpha)}{\rho\,[K \cdot E \cdot (2)]}} \qquad (7)^*$$

where P_{in} = inlet pressure to the cyclone

h_2 = height of conic section of the cyclone

α = apex angle of the cyclone

ρ = density of the fluid

$[K \cdot E \cdot (2)]$ = kinetic energy of the fluid in the conic section of the cyclone (See Eq. A-48)

Definition of the "Apparent Mass": Neumark (15) has proved analytically that the so-called "apparent mass"—the mass of a particle moving through a non-viscous and incompressible fluid—is dependent on the density and volume of the fluid being displaced as well as the geometric shape of the particle in question. A table of the shape factor is also provided by Neumark ranging from zero to infinity. For a spherical particle, the shape factor is 0.50. Thus, for example, the apparent mass of a spheroid moving in water would be

---

* Identical with Eq. A-52.

$$m_o = m + 0.5\ M \tag{8}$$

where m is the static mass of the spheroid and M is the mass of water being displaced by the spheroid. It is evident that the apparent mass will only be identical to the static mass when the particle is traveling in an absolute vacuum. In applying this principle to particles flowing in a hydrocyclone, the apparent mass of the particle will be used as the correct term in place of the static mass for the derivation of equation of motion shown in the following section.

Mechanism of Solid-Liquid Separation: In dealing with the problems encountered in hydrodynamics, it is sometimes necessary to designate particle velocities relative to the fluid with overbars; hence $\bar{v}_x$, $\bar{v}_y$, $\bar{v}_z$, $\bar{v}_\theta$, $\bar{v}_r$ must be distinguished from the fluid velocities, v_x, v_y, . . . respectively. Thus if W is an arbitrary function of the X, Y, Z components, we have

$$dW = \frac{\partial W}{\partial X}\,dX + \frac{\partial W}{\partial Y}\,dY + \frac{\partial W}{\partial Z}\,dZ + \frac{\partial W}{\partial t}\,dt \tag{9}$$

$$\frac{dW}{dt} = \frac{\partial W}{\partial X}\frac{dX}{dt} + \frac{\partial W}{\partial Y}\frac{dy}{dt} + \frac{\partial W}{\partial Z}\frac{\partial Z}{\partial t} + \frac{\partial W}{\partial t}$$

$$= \frac{\partial W}{\partial X}\,\bar{\bar{v}}_x + \frac{\partial W}{\partial Y}\,\bar{\bar{v}}_y + \frac{\partial W}{\partial Z}\,\bar{\bar{v}}_z + \frac{\partial W}{\partial t} \tag{10}$$

where $\frac{dW}{dt}$ is the rate of change of W as seen by a co-moving observer with the same velocity as the streamline and $\bar{\bar{v}}_x$, $\bar{\bar{v}}_y$, $\bar{\bar{v}}_z$ are absolute reference frames. For cylindrical coordinates

$$\frac{D}{Dt} = \frac{\partial}{\partial t} + V_r \frac{\partial}{\partial r} + \frac{V_\theta}{r}\frac{\partial}{\partial \theta} + V_z \frac{\partial}{\partial Z}$$

$$\begin{aligned}\frac{D\vec{v}}{Dt} = \frac{\partial \vec{v}}{\partial t} &= \bar{v}_r \frac{\partial \vec{v}}{\partial r} + \frac{\bar{v}_\theta}{r}\frac{\partial \vec{v}}{\partial \theta} + \bar{v}_z \frac{\partial \vec{v}}{\partial Z} \\ &= \left(\frac{\partial \bar{v}_x}{\partial t} + \bar{v}_r \frac{\partial \bar{v}_x}{\partial r} + \frac{\bar{v}_\theta}{r}\frac{\partial \bar{v}_x}{\partial \theta} + \bar{v}_z \frac{\partial \bar{v}_x}{\partial Z}\right)\hat{i} \\ &+ \left(\frac{\partial \bar{v}_y}{\partial t} + \bar{v}_r \frac{\partial \bar{v}_y}{\partial r} + \frac{\bar{v}_\theta}{r}\frac{\partial \bar{v}_y}{\partial \theta} + \bar{v}_z \frac{\partial \bar{v}_y}{\partial Z}\right)\hat{j} \\ &+ \left(\frac{\partial \bar{v}_z}{\partial t} + \bar{v}_r \frac{\partial \bar{v}_z}{\partial r} + \frac{\bar{v}_\theta}{r}\frac{\partial \bar{v}_z}{\partial \theta} + \bar{v}_z \frac{\partial \bar{v}_z}{\partial Z}\right)\hat{k}\end{aligned} \tag{11}$$

$$\hat{i} = \cos\theta\ \hat{e}_r - \sin\theta\ \hat{e}_\theta \tag{12}$$

$$\hat{j} = \sin\theta\ \hat{e}_r + \cos\theta\ \hat{e}_\theta \tag{13}$$

$$\hat{k} = \hat{e}_z \tag{14}$$

and

$$\bar{v}_x = \cos\theta\ \bar{v}_r - \sin\theta\ \bar{v}_\theta \tag{15}$$

$$\bar{v}_y = \sin\theta\ \bar{v}_r + \cos\theta\ \bar{v}_\theta \tag{16}$$

$$\bar{v}_z = \bar{v}_z \tag{17}$$

By using Eqs. 12 through 17 for transformation, we have

$$\frac{Dv}{Dt} = \left(\frac{\partial \vec{v}_r}{\partial t} + \bar{v}_r \frac{\partial \bar{v}_r}{\partial r} + \frac{\bar{v}_\theta}{r}\frac{\partial \bar{v}_r}{\partial \theta} - \frac{\bar{v}_\theta^2}{r} + \bar{v}_z \frac{\partial \bar{v}_r}{\partial Z}\right) \quad \ldots$$

. . . . . r-component

$$+\left(\frac{\partial\bar{v}_\theta}{\partial t} + \bar{v}_r\frac{\partial\bar{v}_\theta}{\partial r} + \frac{\bar{v}_\theta}{r}\frac{\partial\bar{v}_\theta}{\partial\theta} + \frac{\bar{v}_r\bar{v}_\theta}{r} + \bar{v}_z\frac{\partial\bar{v}_\theta}{\partial Z}\right) \ldots$$

. . . . . θ-component

$$+\left(\frac{\partial\bar{v}_z}{\partial t} + \bar{v}_r\frac{\partial\bar{v}_z}{\partial r} + \frac{\bar{v}_\theta}{r}\frac{\partial\bar{v}_z}{\partial\theta} + \bar{v}_z\frac{\partial\bar{v}_z}{\partial Z}\right) \ldots$$

. . . . . Z-component

From Newtonian mechanics the basic equation for a particle moving in a fluid with a velocity $\bar{v}$ is (9)

$$m_o\frac{D\vec{v}}{Dt} = -\ k\ \vec{v} + m^\circ\vec{Z} - 2m^\circ\vec{\omega}\times\vec{v}_\theta - m^\circ\vec{\omega}\times(\vec{\omega}\times r) + \int Pd\vec{A} \tag{19}$$

where $\frac{D\vec{v}}{Dt}$ denotes the righthand side of Eq. 18.

$-k\ \vec{v}$ is the viscous force

$m^\circ\vec{Z}$ is the body force equal to $m^\circ g\ \hat{e}_z$ in this case

$-2\ m^\circ\vec{\omega}\times\vec{v}_\theta$ is the Coriolis force caused by the rotating force

$m^\circ\vec{\omega}\times(\vec{\omega}\times\vec{r})$ is the centrifugal force caused by the rotating force

$\int Pd\vec{A}$ is the net pressure force acting on the particle and $dA = ds\cdot\vec{n}$ where $\vec{n}$ is the normal unit vector with respect to the surface element of the particle.

For the r-component:

$$m_o\left(\frac{\partial\bar{v}_r}{\partial t} + \bar{v}_r\frac{\partial\bar{v}_r}{\partial r} + \frac{\bar{v}_\theta}{r}\frac{\partial\bar{v}_r}{\partial\theta} - \frac{\bar{v}_\theta^{\ 2}}{r} + \bar{v}_z\frac{\partial\bar{v}_r}{\partial Z}\right) = -\ k\ \bar{v}_r + m^\circ\vec{Z}$$

$$- 2\ m^\circ \vec{\omega} \times \vec{v}_r - m^\circ \vec{\omega} \times (\vec{\omega} \times \vec{r}) + \int P ds \cdot \vec{n}_{\theta z} = - k\ \bar{v}_r$$

$$- 2\ m^\circ \omega\ \bar{v}_r \sin \varphi_{v_z v_r} - m^\circ [\vec{\omega} (\vec{\omega} \cdot \vec{r}) - \vec{r} (\vec{\omega} \cdot \vec{\omega})] + \int P ds \cdot \vec{n}_{\theta z}$$

$$= - k\ \bar{v}_r + 2\ m^\circ \omega\ \bar{v}_r - m^\circ [\vec{\omega} (\omega r \cos \varphi_{v_z r}) - r(\omega^2)] + \int P ds \cdot \vec{n}_{\theta z}$$

$$= - k\ \bar{v}_r + 2\ m^\circ \omega\ \bar{v}_r + m^\circ r\ \omega^2 + \int P ds \cdot \vec{n}_{\theta z} \tag{20}$$

For the θ-component:

$$m_o \left(\frac{\partial \bar{v}_\theta}{\partial t} + \bar{v}_r \frac{\partial \bar{v}_\theta}{\partial r} + \frac{\bar{v}_\theta}{r} \frac{\partial \bar{v}_\theta}{\partial \theta} + \frac{\bar{v}_r \bar{v}_\theta}{r} + \bar{v}_z \frac{\partial \bar{v}_\theta}{\partial Z} \right) = - k\ \bar{v}_\theta + m^\circ \vec{Z}$$

$$- 2\ m^\circ \omega \times \vec{v}_\theta - m^\circ \vec{\omega} \times (\vec{\omega} \times \vec{r}) + \int P ds \cdot \vec{n}_{rz} = - k\ \bar{v}_\theta - 2\ m^\circ \omega \times \bar{v}_\theta$$

$$\sin \Phi_{v_z v_\theta} - m^\circ (0 - 0) + \int P ds \cdot \vec{n}_{rz} = - k\ \bar{v}_\theta - 2\ m^\circ \omega\ \bar{v}_\theta$$

$$+ \int P ds \cdot \vec{n}_{rz} \tag{21}$$

For the Z-component:

$$m_o \left(\frac{\partial \bar{v}_z}{\partial t} + \bar{v}_r \frac{\partial \bar{v}_z}{\partial r} + \frac{\bar{v}_\theta}{r} \frac{\partial v_z}{\partial \theta} + \bar{v}_z \frac{\partial \bar{v}_z}{\partial \theta} \right) = - k\ \bar{v}_z + m^\circ g - 2\ m^\circ \vec{\omega} \times \vec{\omega}$$

$$- m^\circ \vec{\omega} \times (\vec{\omega} \times \vec{r}) + \int P ds \cdot \vec{n}_{\theta r} = - k\ \bar{v}_z + m^\circ g - 0 - 0 + \int P ds \cdot \vec{n}_{\theta r}$$

$$= - k\ \bar{v}_z + m^\circ g + \int P ds \cdot \vec{n}_{\theta r} \tag{22}$$

Here, the approximations for $\frac{\partial \bar{v}_r}{\partial Z}$, $\frac{\partial \bar{v}_\theta}{\partial Z}$, $\frac{\partial \bar{v}_z}{\partial Z}$, $\frac{\partial \bar{v}_z}{\partial Z}$, $\frac{\partial \bar{v}_z}{\partial r}$, $\frac{\partial \bar{v}_z}{\partial \theta}$, can all be neglected. Further we are only concerned over the separation of solid or liquid particles from a liquid by means of the vertical component. Therefore, only Eq. 22 is useful. Unfortunately, Eq. 22 cannot be solved analytically because of the presence of the pressure force term. However, for an approximate solution, it is proposed to exclude this term temporarily and to reinstate it later in an empirical fashion as shown in Eq. 43.

$$m_o \left(\frac{\partial \bar{v}_z}{\partial t}\right) = - k \ \bar{v}_z + m^\circ g \tag{23}$$

$$\frac{d\bar{v}_z}{dt} = - \frac{k' \bar{v}_z}{m_o} + \frac{m^\circ}{m_o} g \tag{24}$$

Eq. 24 is essentially a first order linear equation and the solution is

$$e^{\int \frac{k}{m_o} dt} \frac{d\bar{v}_z}{dt} + e^{\int \frac{k}{m_o} dt} \frac{k}{m_o} \bar{v}_z = e^{\int \frac{k}{m_o} dt} \frac{m^\circ g}{m_o}$$

$$\bar{v}_z \, e^{\int \frac{k}{m_o} dt} = e^{\int \frac{k}{m_o} dt} \frac{m^\circ g}{m_o} \left(\frac{m_o}{k}\right) + K'$$

$$\bar{v}_z \, e^{\frac{k}{m_o} t} = e^{\frac{k}{m_o} t} \frac{m^\circ g}{k} + K' \tag{25}$$

when $\qquad t = 0, \ \bar{v}_z = 0$

$$K' = - \frac{m^\circ g}{k}$$

$$\bar{v}_z \, e^{\frac{k}{m_o} t} = e^{\frac{k}{m_o} t} \frac{m^\circ g}{k} - \frac{m^\circ g}{k} = \frac{m^\circ g}{k} \left(e^{\frac{k}{m_o} t} - 1\right)$$

$$v_z = \frac{m^{\circ}g}{k}\left(1 - e^{-\frac{k}{m_o}t}\right) \tag{26}$$

By considering the force of buoyancy which is equal to

$$F = - Mg$$

we have

$$m_o\left(\frac{dv_z}{dt}\right) = (m - M)g - k\ \bar{v}_z$$

and consequently (neglecting the pressure force term)

$$\bar{v}_z = \frac{(m - M)g}{k}\left(1 - e^{-\frac{k}{m_o}t}\right) \tag{27}$$

Now, we can determine the constant term k by comparing Eq. 27 with Stoke's Law which describes the terminal velocity of a free-falling body in a viscous, hydrostatic fluid. Thus, we have

$$m = \frac{4}{3}\pi\sigma^3\rho' \text{ and } M = \frac{4}{3}\pi\sigma^3\rho$$

$$\bar{v}_z = \frac{4}{3}\pi\sigma^3\frac{(\rho'-\rho)g}{k}\left(1 - e^{-\frac{k}{m_o}t}\right)$$

$$= \frac{2}{9}\frac{(\rho'-\rho')\sigma^2}{\mu}g$$

$$k = 6\pi\sigma\mu\left(1 - e^{-\frac{k}{m_o}t}\right)$$

when $t \to \infty$

$$k = 6\pi\sigma\mu \tag{28}$$

Flow Path of Particles Traveling in a Cyclone: In the case of oil-water separation, with water being the continuous phase, the oil is mostly divided into fine particles which will most probably follow the streamline of the water. Thus, to predict the streamline path traveled by a particle of negligible weight and dimension, let us assume the streamline function in cylindrical coordinates

$$\psi = f(r,\theta), \text{ so } d\psi = \frac{\partial\psi}{\partial r} dr + \frac{\partial\psi}{\partial\theta} d\theta$$

$$= \frac{\partial\psi}{\partial r} dr + \frac{1\partial\psi}{r\partial\theta} r\, d\theta \qquad (29)$$

If the stream function has a value ψ_A at A and ψ_B at B, the difference in the ψ-values, $d\psi = \psi_B - \psi_A$, equals the rate of flow across the line AB, as a consequence of the definition of ψ. This flow rate can be considered as the total of two flow rates; namely, in cylindrical coordinates, the radial velocity V_r in the outward radial direction, and $-V_\theta$ in the tangential direction. Since the radial flow rate is $rV_r d\theta$, and the tangential flow rate is $-V_\theta dr$, we have

$$d\psi = rV_r d\theta - V_\theta dr \qquad (30)$$

Previously, we know from the derivation of air core velocity, (Eq. A-12)

$$rV_r \cong (Q/L) \qquad (31)$$

However, rV_r, which is mainly responsible for the spiral downward flow, is not strictly a constant throughout the entire cyclone because of the overflow Q_o. Therefore, an approximate method must be devised. Recognizing the material balance equation for steady state

$$Q_f = Q_o + Q_u \tag{32}$$

we can consider the terminal conditions where measured variables can be obtained. For the limiting case,

$$Q_o = 0, \text{ then } Q_f = Q_u$$

we have
$$(Q/L) \cong rV_r \cong Q_f/2\pi H \tag{33}$$

on the other hand, if

$$Q_u = 0, \text{ then } Q_f = Q_o$$

the distance for Q to travel downward before it reaches the air core to reverse its direction and exit in the overflow will be doubled. Hence

$$(Q/L) \cong rV_r \cong \tfrac{1}{2}(Q_f/2\pi H) \tag{34}$$

and an approximate equation based on terminal conditions can be

$$(Q/L) = \frac{(Q_f + Q_u)}{2} \frac{1}{2\pi H} \cong rV_r \tag{35}$$

Recalling Eq. 6, we have

$$V_\theta = \frac{aV_o}{a^{\xi+2} - b^{\xi+2}} \left(r^{\xi+1} - \frac{b^{\xi+2}}{r} \right) \tag{6}$$

By the relationship of

$$V_\theta = \frac{r \cdot d\theta}{dt} \tag{36}$$

and

$$V_r \; dt = dr \tag{37}$$

Eq. 36 can be written as

$$d\theta = V_\theta \frac{dr}{r \; V_r} \tag{38}$$

Substituting Eq. 38 into Eq. 30 yields

$$\int d\psi = \int rV_r d\theta - \int V_\theta dr$$

$$\psi = -(rV_r) \frac{V_\theta dr}{(r \; V_r)} - (- V_\theta dr) + K' = \text{constant}$$

which signifies that the flow pattern of the stream function is specified.

In case the downward flow pattern is desired, Eq. 38 can be integrated to yield

$$d\theta = \int \frac{V_\theta dr}{(Q/2\pi H)} = \int \frac{aV_o}{(Q/2\pi H)\,(a^{\xi+2} - b^{\xi+2})} \left(r^{\xi+1} - \frac{b^{\xi+2}}{r} \right) dr$$

$$\theta = \frac{aV_o}{(Q/2\pi H)\,(a^{\xi+2} - b^{\xi+2})} \left(\frac{r^{\xi+2}}{\xi+2} - b^{\xi+2} \ln r \right) + k' \tag{39}$$

If we assign C_o as the initial radial distance of the particle from the center of the hydrocyclone when $\theta = 0$, then we have the initial condition

$$\theta = 0, \; r = C_o$$

and
$$\theta = \frac{aV_o}{(Q/2\pi H)\,(a^{\xi+2}-b^{\xi+2})}\left(\frac{r^{\xi+2}-C_o{}^{\xi+2}}{\xi+2} - b^{\xi+2}\,\ln\frac{r}{C_o}\right) \tag{40}$$

which should adequately describe the path of the particle traveling in a hydrocyclone provided both the tangential velocity of the fluid at the air core and the initial radial distance of the particle are known.

In order to determine the time required for a liquid particle of the dispersed phase to fall freely in a viscous medium over a distance Z_m, Eq. 27 can be rewritten as

$$\frac{dZ_m}{dt} = \frac{(m-M)g}{k}\left(1 - e^{-\frac{k}{m_o}t}\right) \tag{41}$$

Integrating Eq. 41 yields

$$\int dZ_m = \frac{(m-M)}{k}g\left[t + \frac{m_o}{k}\,e^{-\frac{k}{m_o}t}\right] + K'$$

when
$$t = 0, \; Z = 0$$

$$K' = \frac{(m-M)}{k}g\;\frac{m_o}{k}$$

$$Z_m = \frac{(m-M)}{k}g\left[t - \frac{m_o}{k}\,e^{-\frac{k}{m_o}t}\right] - \frac{(m-M)}{k^2}g\;m_o$$

$$= \frac{m_o(m-M)g}{k^2}\left[\frac{k}{m_o}t - 1 + e^{-\frac{k}{m_o}t}\right] \tag{42}$$

As mentioned earlier, in order to solve Eq. 22 with the inclusion of the pressure term, it is necessary to resort to an empirical procedure. Fortunately, Fontein's (8) citing of dye injection experiments provided a physical model which indicated that the overflow fluid mostly initiates from the area near the cyclone wall after traveling downward in a certain distance Z_o in order to exit reversely through vortex finder tube. Thus, we have

$$2\,Z_o = \frac{Q_o t}{\frac{\pi(b^2-a^2)}{2}} \tag{43}$$

and

$$Z = Z_m + Z_o = \frac{(m-M)\,m_o g}{k^2}\left[\frac{k}{m_o}t - 1 + e^{-\frac{k}{m_o}t}\right] + \frac{Q_o t}{\pi(b^2-a^2)} \tag{44}$$

<u>Effective Separation Region in a Cyclone</u>: In reality, when a mixture of immiscible liquids is charged into a hydrocyclone at a given rate, Q_f, substantial enough to generate some centrifugal action, there will be a certain turbulent mixing region extending a length "d" from the upper base (Figure 3). Therefore, at least this much of the hydrocyclone

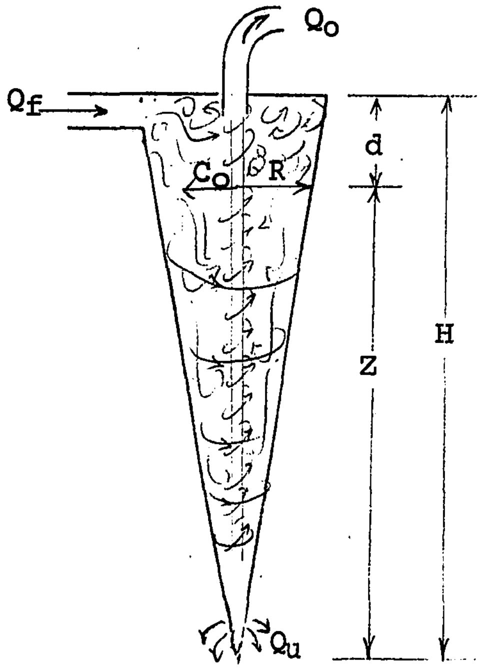

Figure 3. Cyclone Hypothetically Partitioned into a Turbulent and An Effective Separation Region.

is extremely ineffective for separation. However, as the liquid mixture moves from the turbulent region into the separation region, a particle of the dispersed (discontinuous) phase at a radial distance, say C_o, will take a certain time to reach the air core of radius "a". By combining Eq. 37 and Eq. 31

$$V_r \, dt = dr \qquad (37)$$

$$(Q/L) = r \, V_r \qquad (31)$$

$$dt = \frac{rdr}{(Q/L)} \tag{45}$$

$$\int_o^t dt = \int_a^{C_o} \frac{rdr}{(Q/L)}$$

$$t = \frac{C_o^2 - a^2}{2(Q/L)} \tag{46}$$

the time requirement can be determined. Since the particle travels downward until it reaches the air core to be carried off in the overflow, the downward distance covered by this particle is also equal to "Z" as represented by Eq. 44. With the presence of the turbulent region, the maximum distance of "Z" is therefore

$$Z = H - d \tag{47}$$

where H is the height of the cyclone.

In case the centrifugal force becomes the dominating factor, it is necessary to incorporate it into Eq. 45.

As we know the centrifugal acceleration = $\omega^2 r$ where ω is the angular velocity at the radius r (Note: In contrast to solid-body rotation, ω is not a constant but is a function of r). Hence, the force experienced by an oil particle = $(M-m)\,\omega^2 r$, assuming that locally the flow is slow so that the hydrostatic pressure law holds. Referring to Eq. 27 the terminal velocity of the particle will be equal to $\frac{(M-m)\omega^2}{k} r$. Since $\omega = \frac{V_\theta}{r}$

$$(\bar{v}_r)_t = \frac{(M-m)}{k}\frac{V_\theta^{\,2}}{r^2}(r) = \frac{(M-m)}{k}\frac{V_\theta^{\,2}}{r}$$

and Eq. 6 states that the tangential velocity

$$V_\theta = \frac{aV_o}{a^{\xi+2}-b^{\xi+2}}\left(\frac{r^{\xi+2}-b^{\xi+2}}{r}\right)$$

$$(\bar{v}_r)_t = \frac{(M-m)}{k\ r^3}\frac{a^2V_o^{\,2}}{(a^{\xi+2}-b^{\xi+2})^2}(r^{\xi+2}-b^{\xi+2})^2 \qquad (48)$$

Since $\xi = \frac{(Q/L)}{\nu}$ and $\nu = \frac{\mu}{\rho}$

ξ is a fairly large number*, and

$$\left(\frac{r^{\xi+2}-b^{\xi+2}}{a^{\xi+2}-b^{\xi+2}}\right)^2 \approx 1$$

$$\therefore\ (\bar{v}_r)_t = \frac{(M-m)}{k\ r^3}a^2V_o^{\,2} = \left(\frac{dr}{dt}\right)_t$$

$$dt = \frac{dr}{\dfrac{(M-m)\,a^2V_o^{\,2}}{k\ r^3}} \qquad (49)\ \#$$

Combining Eq. 45 with Eq. 49 yields

---

*The magnitude can be estimated by assuming $Q=Q_f$ = 60 cc/sec. for an actual run, so L = 2πx 16 cm. and ν = 0.01 cm^2/sec. $\xi \cong 60$.

#Integrating Eq. 49 will yield

$$t = \frac{9\ \mu(C_o^4 - a^4)}{8(\rho - \rho')(\sigma_\ell^3)a^2V_o^2} \qquad (49\ a)$$

$$dr = \frac{(Q/L)}{r}dt + \frac{(M-m)\,a^2 V_o^{\,2}}{k\,r^3}dt = \frac{[r^2\,k\,(Q/L) + (M-m)\,a^2 V_o^{\,2}]dt}{k\,r^3}$$

$$dt = \frac{r^3 dr}{r^2 (Q/L) + \dfrac{(M-m)\,a^2 V_o^{\,2}}{k}} \qquad (50)$$

$$t = \frac{1}{(Q/L)} \int_a^{C_o} \frac{r^3 dr}{r^2 + \dfrac{(M-m)}{k\,(Q/L)} a^2 V_o^{\,2}}$$

$$M = \frac{4}{3}\pi\rho\sigma^3, \quad m = \frac{4}{3}\pi\rho'\sigma^3, \quad k = 6\pi\sigma\mu$$

Equation 50 can be integrated by consulting an integral table where

$$\int \frac{X^3 dX}{(K^2 + X^2)} = \frac{X^2}{2} - \frac{K^2}{2} \ln (K^2 + X^2)$$

$$t = \frac{C_o^{\,2} - a^2}{2\,(Q/L)} - \frac{(\rho-\rho')\sigma^2 a^2 V_o^{\,2}}{9\,\mu (Q/L)^2} \ln\left(\frac{C_o^{\,2} + \dfrac{2\,(\rho-\rho')\sigma^2 a^2 V_o^{\,2}}{9\mu\,(Q/L)}}{a^2 + \dfrac{2(\rho-\rho')\sigma^2 a^2 V_o^{\,2}}{9\mu\,(Q/L)}}\right) \qquad (51)$$

Now, from Eq. 35 and Eq. 47 we have the relationship between (Q/L) and Z if experimentally measured flow rates are available. We also have the relationship between Z and t from Eq. 44 provided the mass of the dispersed liquid particle and the overflow rate are known. However, it appears Eq. 51 is handicapped by the fact that C_o, the radial distance from the center which determines whether the dispersed liquid particle will exit in the overflow or the underflow, cannot be measured directly by any simple experimental scheme. Therefore, in order to remedy this situation, it is necessary to establish another relationship between C_o and some experimentally measurable variables so we can bridge the proposed theoretical model described in the foregoing sections and the experimental results--yet to be obtained--to test the validity of the model.

Assuming the oil-water mixture in the hydrocyclone is consistently well-proportioned as in the feed, we can propose that the ratio of a hypothetical conic volume of radius C_o (Figure 4) to that of a radius R is proportional to the ratio

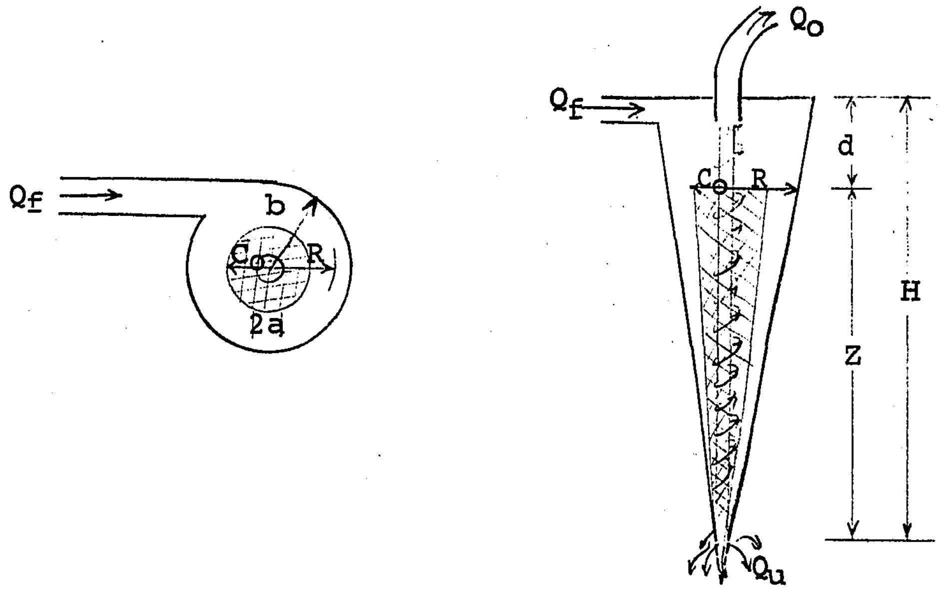

Fig. 4. Vertical and Cross-Sectional View of a Hypothetical Model Within a Cyclone.

of the actual fraction of the volumetric rate of oil exiting in the overflow to that of its ideal fraction, thus

$$\frac{\frac{1}{3}\, Z\pi (C_o{}^2 - a^2)}{\frac{1}{3}\, Z\pi (R^2 - a^2)} = \frac{(Q_o x_o / Q_f x_f)_{exp.}}{(Q_o x_o / Q_f x_f)_{ideal}}$$

or

$$\frac{(C_o{}^2 - a^2)}{(R^2 - a^2)} = \frac{(Q_o x_o / Q_f x_f)_{exp.}}{(Q_o x_o / Q_f x_f)_{ideal}} \tag{52}$$

$$R = \frac{b\,Z}{H} \tag{53}$$

Both b and H are physical dimensions of the cyclone, and $(x_o,\ x_f)_{exp.}$ are measured volumetric fractions of the oil in the overflow and in the feed, respectively. The $(x_o,\ x_f)_{ideal}$ are defined in the second part of this chapter (p.41). One must bear in mind that this hypothetical model has no physical meaning.

<u>Method of Determining the Macroscopic Turbulent Length</u>: In the previous section we have obtained the means for calculating C_o from a proposed model requiring measured experimental variables. However, Eq. 51 is of no use unless V_o, the tangential velocity at the air core, is known. Although an analytical method is available (Eq. 7) for computing V_o at two parameters, P_{in} and (Q/L), it is not only very tedious but also, in applying it to Eq. 51, the correct

pair of P_{in} and (Q/L) values corresponding to each run must be known. This requirement demands an additional measurement, P_{in}, which cannot be obtained accurately due to pressure fluctuations within the cyclone during operation. Fortunately, the tangential velocity at the air core varies largely with the feed rate but less with the underflow (Eq. 35); i.e., both P_{in} and (Q/L) are affected by the feed, whereas (Q/L) is only slightly affected by the underflow. In view of Eq. 51 which still contains two unknowns, t and V_o, we can employ a pair of simultaneous equations representing two adjacent runs and a trial and error scheme to obtain t and an average value of V_o between any two adjacent runs of the same feed rate. The procedure is shown in the following steps:

A) Let

$$t_1 = \frac{C_{o1}^{\;2}-a^2}{2(Q/L)_1} - \frac{(\rho-\rho')\sigma^2 a^2 V_o^{\;2}}{9\mu (Q/L)_1^2} \ln\left(\frac{C_{o1}^{\;2}+\dfrac{2(\rho-\rho')\sigma^2 a^2 V_o^{\;2}}{9\mu (Q/L)_1}}{a^2+\dfrac{2(\rho-\rho')\sigma^2 a^2 V_o^{\;2}}{9\mu (Q/L)_1}}\right) \quad (51a)$$

$$t_2 = \frac{C_{o2}^{\;2}-a^2}{2(Q/L)_2} - \frac{(\rho-\rho')\sigma^2 a^2 V_o^{\;2}}{9\mu (Q/L)_2^2} \ln\left(\frac{C_{o2}^{\;2}+\dfrac{2(\rho-\rho')\sigma^2 a^2 V_o^{\;2}}{9\mu (Q/L)_2}}{a^2+\dfrac{2(\rho-\rho')\sigma^2 a^2 V_o^{\;2}}{9\mu (Q/L)_2}}\right) \quad (51b)$$

where $(C_o)_1$ and $(C_o)_2$ can be obtained by using Eq. 52 with experimental information and an assumed "d" from which

$$Z = [H-d] \qquad (47)$$

$$R = \frac{bZ}{H} \qquad (53)$$

and

$$\frac{C_o^{\,2}-a^2}{R^2-a^2} = \frac{\left(\frac{Q_o x_o}{Q_f x_f}\right)_{exp.}}{\left(\frac{Q_o x_o}{Q_f x_f}\right)_{ideal}} \qquad (52)$$

B) Likewise, let

$$Z_1 = \frac{(m-M)m_o g}{k^2}\left[\frac{k}{m}t_1 - 1 + e^{-\frac{k}{m_o}t_1}\right] + \frac{(Q_o)_1 t_1}{\pi(b^2-a^2)} \qquad (44a)$$

$$Z_2 = \frac{(m-M)m_o g}{k^2}\left[\frac{k}{m}t_2 - 1 + e^{-\frac{k}{m_o}t_1}\right] + \frac{(Q_o)_2 t_2}{\pi(b^2-a^2)} \qquad (44b)$$

represent the same two adjacent runs where

$$Z_1 \cong Z_2$$

for a unique "d". If the m and m_o values were negligibly small, Eq. 44a and Eq. 44b can be approximated to

$$\frac{(Q_o)_1 t_1}{\pi(b^2-a^2)} = \frac{(Q_o)_2 t_2}{\pi(b^2-a^2)}$$

or

$$\frac{t_1}{t_2} = \frac{(Q_o)_2}{(Q_o)_1} \qquad (54)$$

C) Now Eq. 51a and Eq. 51b can be fully utilized by substituting $(Q/L)_1$ and $(Q/L)_2$ (from Eq. 35) and an assumed value of V_o in order to obtain t_1 and t_2 values. The value of t_1/t_2 must satisfy Eq. 54 before proceeding to the next step. If not, a new value for V_o is assumed and Step (A) to (C) are repeated until the calculated t_1/t_o matches the t_1/t_2 value from Eq. 54.

D) Finally, after the calculated t_1/t_2 satisfies Eq. 54, Z_1 or Z_2 can be calculated (Eq. 44). A calculated value of d is then found from Eq. 47. If the calculated value of d does not equal the assumed value of d, the procedure is repeated from Step (B) downward until the assumed and calculated values of d are equal.

Separation Efficiency

Before the overall separation efficiency for a three-phase system is defined, it is worthy to note some nomenclature and material balance equations for a two-phase system.

$$Q_f = Q_o + Q_u \tag{32}$$

where Q_f, Q_o, Q_u = volumetric flow rate of the feed, overflow and underflow, respectively.

$$x_o + y_o = 1.0 \tag{55}$$

where x_o, y_o = volumetric fraction of the lighter phase and the denser phase in the overflow, respectively.

The following material balance equations are also useful:

$$x_u + y_u = 1.0 \tag{56}$$

$$Q_o x_o + Q_u x_u = Q_f x_f \tag{57}$$

$$Q_o y_o + Q_u y_u = Q_f y_f \tag{58}$$

Tepe and Woods' (21) definition of overall separation efficiency for a liquid-liquid system is not only confined to the hydrocyclone but is also applicable to other separating devices as well. Briefly, the overall efficiency is the sum of each liquid phase (immiscible) efficiency. Thus

$$E = E_1 + E_2 \tag{59}$$

where E_1 is the phase efficiency of the lighter liquid phase and E_2 that of the denser phase. Since the lighter phase is expected to exit in the overflow and the denser in the underflow, by definition

$$E_1 = \frac{1}{Q_f}\left[Q_o x_o - Q_o \ (1-x_o) \ \frac{\cancel{Q_f} x_f}{\cancel{Q_f}(1-x_f)}\right] \tag{60}$$

$Q_o x_o$ is the measured volumetric flow rate of the lighter phase in the overflow, and $Q_o(1-x_o) \ (\frac{x_f}{1-x_f})$ is the proportional amount of the lighter phase in the overflow had there been no enrichment of the lighter phase based on the presence of the heavier phase.

$$E_2 = \frac{1}{Q_f}\left[Q_u y_u - Q_u \ (1-y_u) \ \frac{\cancel{Q_f} y_f}{\cancel{Q_f}(1-y_f)}\right] \tag{61}$$

Combining Eq. 60 with Eq. 61 yields

$$E = E_1 + E_2 = \frac{Q_o \ (x_o - x_f)}{Q_f \ (1 - x_f)} + \frac{Q_u \ (y_u - y_f)}{Q_f \ (1 - y_f)} \tag{62}$$

With the aid of material balance equations, Eq. 62 could be reduced further to

$$E = \frac{Q_o \; (x_o - x_f)}{Q_f \; x_f \; (1-x_f)} \tag{63}$$

<u>Overall Separation Efficiency for a Three-Phase System</u>: In the case of a three-phase separation in a conventional hydrocyclone where only two outlets are accessible, the third phase will have to exit either through the vortex finder tube or the discharge apex, or both simultaneously. Hence, in defining the overall separation efficiency, the desirability of the third phase to exit in either outlet dictates the format of the equation. If it is desired that the third phase exit in the overflow, the phase efficiency for the lighter phase would be

$$E_1 = \frac{1}{Q_f}\left[Q_o x_o - Q_o \; (1-x_o-Z_o) \; \frac{\cancel{Q_f} x_f}{\cancel{Q_f}(1-x_f-Z_f)}\right] = \frac{Q_o}{Q_f}$$

$$\left[\frac{(x_f Z_o - x_o Z_f) \; + \; (x_o - x_f)}{(1-x_f-Z_f)}\right] \tag{64}$$

where z_o = fraction of third component in the overflow.

z_f = fraction of third component in the feed.

The phase efficiency for the denser phase is identical to Eq. 61. Likewise, the phase efficiency for the third phase would be

$$E_3 = \frac{1}{Q_f}\left[Q_oZ_o - Q_o(1-x_o-z_o)\,\frac{Q_fZ_f}{Q_f(1-x_f-Z_f)}\right]$$

$$= \frac{Q_o}{Q_f}\left[\frac{(x_oZ_f - x_fZ_o) + (Z_o - Z_f)}{(1-x_f-Z_f)}\right] \tag{65}$$

The overall separation efficiency for a three-phase system is therefore

$$E = E_1 + E_2 + E_3 = \frac{Q_o[(x_o-x_f) + (Z_o-Z_f)]}{Q_f\ (1-x_f-Z_f)} + \frac{Q_u\ (y_u-y_f)}{Q_f\ (1-y_f)} \tag{66}$$

In case it is desired that the third phase exit in the underflow,

$$E = \frac{Q_o\ (x_o-x_f)}{Q_f\ (1-x_f)} + \frac{Q_u[(y_u-y_f) + (Z_u-Z_f)]}{Q_f\ (1-y_f-Z_f)} \tag{67}$$

Tengbergen and Rietema (20) listed eleven basic requirements for an acceptable overall separation efficiency value. The major points were

1. The highest value should be reached only when both phases are obtained completely pure after separation.
2. If one effluent stream contains a pure phase, the efficiency should be equal to the ratio of the quantity of this pure stream over the quantity of this phase in the feed.
3. If the feed is split up into 2 streams having the same composition as the feed, the efficiency number should be zero.

4. The efficiency should remain the same if the 2 phases or the 2 effluent streams are interchanged.

For a two-phase system, they defined the efficiency to be

$$E = \left| \frac{Q_o x_o}{Q_f x_f} - \frac{Q_o y_o}{Q_f y_f} \right| = \left| \frac{Q_o x_u}{Q_f x_f} - \frac{Q_u y_u}{Q_f y_f} \right| \tag{68}$$

which is identical to Eq. B-2 (Appendix B)

Extending this definition to a multiphase system yields

$$E = \left| \frac{\sum_{1}^{A_n}(A)_o}{\sum_{1}^{A_n}(A)_f} - \frac{\sum_{1}^{B_n}(B)_o}{\sum_{1}^{B_n}(B)_f} \right| = \left| \frac{\sum_{1}^{A_n}(A)_u}{\sum_{1}^{A_n}(A)_f} - \frac{\sum_{1}^{B_n}(B)_u}{\sum_{1}^{B_n}(B)_f} \right| \tag{69}$$

where A_1, A_2, A_3, . . . A_n are lighter phases desired to leave the overflow.

B_1, B_2, B_3, . . . B_n are denser phases desired to leave in the underflow, and

$$(A_1 + A_2 + A_3 + \ldots + A_n)_o + (B_1 + B_2 + B_3 + \ldots + B_n)_o = Q_o \tag{70}$$

$$(A_1 + A_2 + A_3 + \ldots + A_n)_u + (B_1 + B_2 + B_3 + \ldots + B_n)_u = Q_u \tag{71}$$

$$(A_1 + A_2 + A_3 + \ldots + A_n)_f + (B_1 + B_2 + B_3 + \ldots + B_n)_f = Q_f \tag{72}$$

Examples illustrating the identity of Eq. 63 with Eq. 68 and Eq. 66 with Eq. 69 are shown in Appendix B. It has been demonstrated in the literature (20) that numerous different algebraic manipulations are available to compute the identical overall efficiency value.

Definition of Ideal Separation Efficiency: When a feed stream containing two immiscible fluid phases of a given proportion is charged to a hydrocyclone, the most ideal separation would be for the overflow to contain only the pure lighter phase and the underflow the pure denser phase. Consequently, the ratio of the overflow to underflow (effluent split) will be identical to the ratio of the lighter phase to denser phase (x_f/y_f) in the feed. With reference to Eq. 62 both

$$(x_o)_s = 1.0, \quad (y_u)_s = 1.0$$

and the ideal efficiency, E_s, is unity.

$$E_s = \frac{Q_o + Q_u}{Q_f} = 1.0 \tag{73}$$

In case the desired effluent split is not identical to x_f/y_f, the best separation would be for one exit flow to contain a pure phase; i.e., either x_o, or y_u, equals 1.0. In such a case the shape of the curve of the ideal efficiency, E_s, versus effluent split will be of a "roof-type" with the highest E_s value (1.0) at $Q_o/Q_u = x_f/y_f$. Since the ideal efficiency values can be obtained independent of experimental data, a

FORTRAN computer program has been developed to generate these values which are shown in Table C-1 for subsequent reference. For a three-phase system, the determination of E_s values follows the same logic as discussed in this section. If it is desired to have the third phase exit with the lighter phase, then

$$(x_o + z_o)_s = 1.0, \quad (y_u)_s = 1.0 \tag{74}$$

otherwise

$$(x_o)_s = 1.0, \quad (y_u + Z_u)_s = 1.0 \tag{75}$$

and both Eq. 66 and Eq. 67 can be reduced to unity respectively at $Q_o/Q_u = x_f/y_f$.

The utilization of the ideal efficiency curve is not only limited to hydrocyclones in general but to any phase separation device as well. In employing the ideal curve as a guide (in a somewhat similar manner as the equilibrium curve in the extraction operation), it enables the designer to select the most optimum range of effluent split when the actual efficiency values are available for comparison.

CHAPTER IV

EXPERIMENTAL APPARATUS AND PROCEDURES

A conventional hydrocyclone normally consists of three stationary parts: 1) Vortex finder tube (VFT), 2) Main body with tangential feed entrance tube, and 3) Discharge apex nozzle. For a certain size of a main body, which is essentially a short cylindrical section in conjunction with a truncated cone, a given interchangeable vortex finder tube and certain discharge apex nozzles are combined to satisfy a specific requirement for separation. In the case of solid-liquid separation, for instance, the larger the diameter of the vortex finder tube, the coarser the separation; i.e., more solid particles exit with the liquid in the overflow. On the other hand, a large discharge apex orifice yields greater underflow. Thus the primary function of the apex nozzle is to control the effluent split (Q_o/Q_u). In certain industrial applications, apex nozzles with variable diameters are often employed in order to suit a range of specific needs.

Laboratory Equipment

For the convenience of visual observations in the present study, a glass, laboratory hydrocyclone test set was purchased from Liquid-Solid Separation, Ltd. of London (Fig. 5). It contains two hydrocyclones, 30 mm and 15 mm ID measured at the cylindrical section. Each cyclone is equipped with three vortex finder tubes and five discharge apex nozzles. Because the maximum solid size used in the experiments reported herein was 0.832 mm, it was not possible to use the 15 mm cyclone since the largest discharge apex nozzle, being 1.5 mm, could not accommodate a free slurry flow. In the case of the 30 mm cyclone, this restriction also permitted the use of only the largest discharge nozzle (3.0 mm, designated as No. 1) and occasionally the second largest nozzle (2.6 mm, designated as No. 2).

One of the primary objectives of this study was to determine the separation efficiency as a function of effluent split (Q_o/Q_u). However, the restrictions imposed on the range of volume splits by the limited combinations of vortex finder tube and discharge apex nozzle precluded obtaining the desired range of values from 0.2 to 8.0. In order to obtain the desired range of values, a screwclamp and copper wires were used to restrict the overflow through a chlorinated Tygon tubing attached to the vortex finder tube. All of the three vortex finder tubes (ID 8.5 mm, 6.0 mm, 4.2 mm, designated as large, medium, and small respectively) were used. The dimensions of the cyclone in detail are shown in Figure 6.

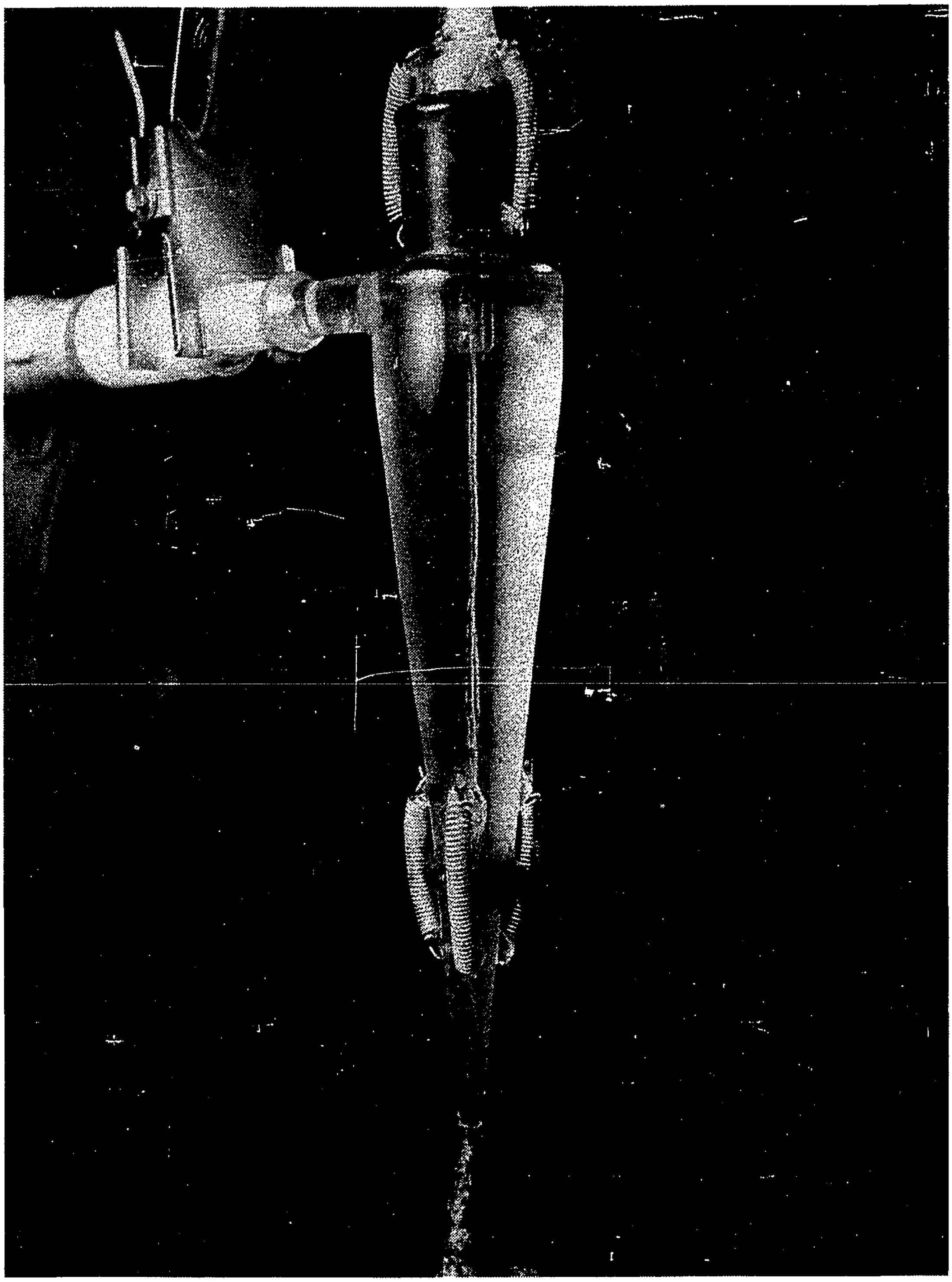

Figure 5. Views of the Air Core and Rotating Spray at the Apex

Physical Dimensions of the Laboratory Hydrocyclone

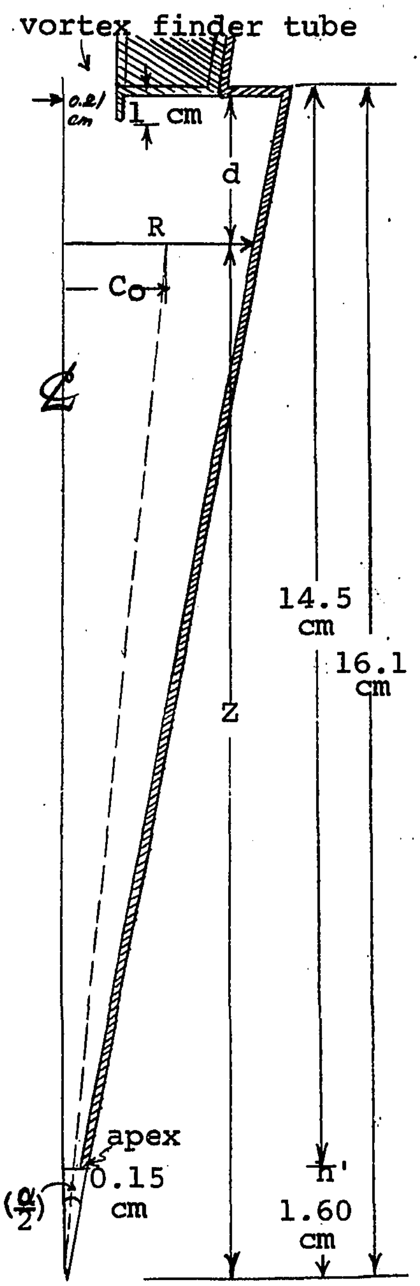

Figure 6. Dimensions of The Laboratory Hydrocyclone

The laboratory hydrocyclone has the shape of a truncated cone. In order to simplify the mathematics involved in describing the geometry of a truncated cone, extrapolation was made from the apex so the cyclone can be considered as a cone. Since it is the ratio of the cone volumes (hypothetical cone volume over the effective cone volume as defined by Eq. 52) which is applicable to calculations, any error incurred by considering a full cone instead of a truncated cone will be relatively insignificant.

By use of the physical dimensions of the laboratory hydrocyclone, the apex angle, α, the extrapolated height, H, can be calculated as follows (See Figure 6 for dimensions of the cyclone).

$$\tan(\alpha/2) = \frac{1.50 - 0.15}{14.5}$$

$$= 0.0931$$

$$\alpha = 10° \; 40'$$

$$\frac{0.15}{h'} = \tan(\alpha/2) = 0.0931$$

$$h' = 1.60 \text{ cm}$$

Hence,

$$H = h + h'$$

$$= 14.5 + 1.6 = 16.1 \text{ cm}$$

The volume of the cone at a distance Z from the apex is $\frac{\pi R^2 Z}{3}$ whereas $R/b = Z/16.1$

$$R^2 = b^2 \left(\frac{16.1 - d}{16.1}\right)^2$$

$$= (1.5)^2 \left(\frac{16.1 - d}{16.1}\right)^2$$

The air core radius is estimated to be about 0.1 cm. The conic volume of a height Z is

$$\frac{\pi}{3} R^2 Z - \pi(a)^2 Z = \frac{\pi Z}{3}(R^2 - 3a^2)$$

The hypothetical conic volume of a height Z with a radius C_o is

$$\frac{\pi}{3} C_o^2 Z - \pi(a)^2 Z = \frac{\pi Z}{3}(C_o^2 - 3a^2)$$

As stated in Chapter III (p. 33) the relationship between the measured variables and the assumed hypothetical model is represented by

$$\left(\frac{Q_o x_o}{Q_f x_f}\right) \Bigg/ \left(\frac{Q_o x_o}{Q_f x_f}\right)_{\text{ideal}} = \frac{\pi (C_o^2 - 3a^2)\frac{Z}{3}}{\pi (R^2 - 3a^2)\frac{Z}{3}} \qquad (52)$$

Experimental Installation

It is generally due to the simplicity of the hydrocyclone operation that the entire experimental configuration is quite minimal. A duplicate set could be assembled within a few days provided all the parts are available.

The major part of the installation was a Teel conveyor pump (Model 1P610) driven by a ½ HP motor. Since variable speeds for the pump were requred, a Variac was attached to the motor and different sizes of pulleys incorporated between the motor and pump. A 55-gal drum equipped with a low-speed mixer was also employed for mixing the premeasured solid particles with the hydrocarbon. The details of the experimental setup are shown in Figure 7.

Materials Used

The hydrocarbon used throughout this project was a mixture of C_{12}, C_{13}, and C_{14} defined as "heavy paraffin" and was donated by Continental Oil Co. of Ponca City. The specific gravity was determined by a Westphal balance to be 0.756.

The solid particles, trade-named Microthene, were donated by U.S. Industrial Chemical Co. Two sizes, 0.832 mm and 0.294 mm, both having the same specific gravity of 0.923, were tested. Since the particles are only preferentially wetted by the hydrocarbon, they were mixed with the hydrocarbon prior to merging with the water stream.

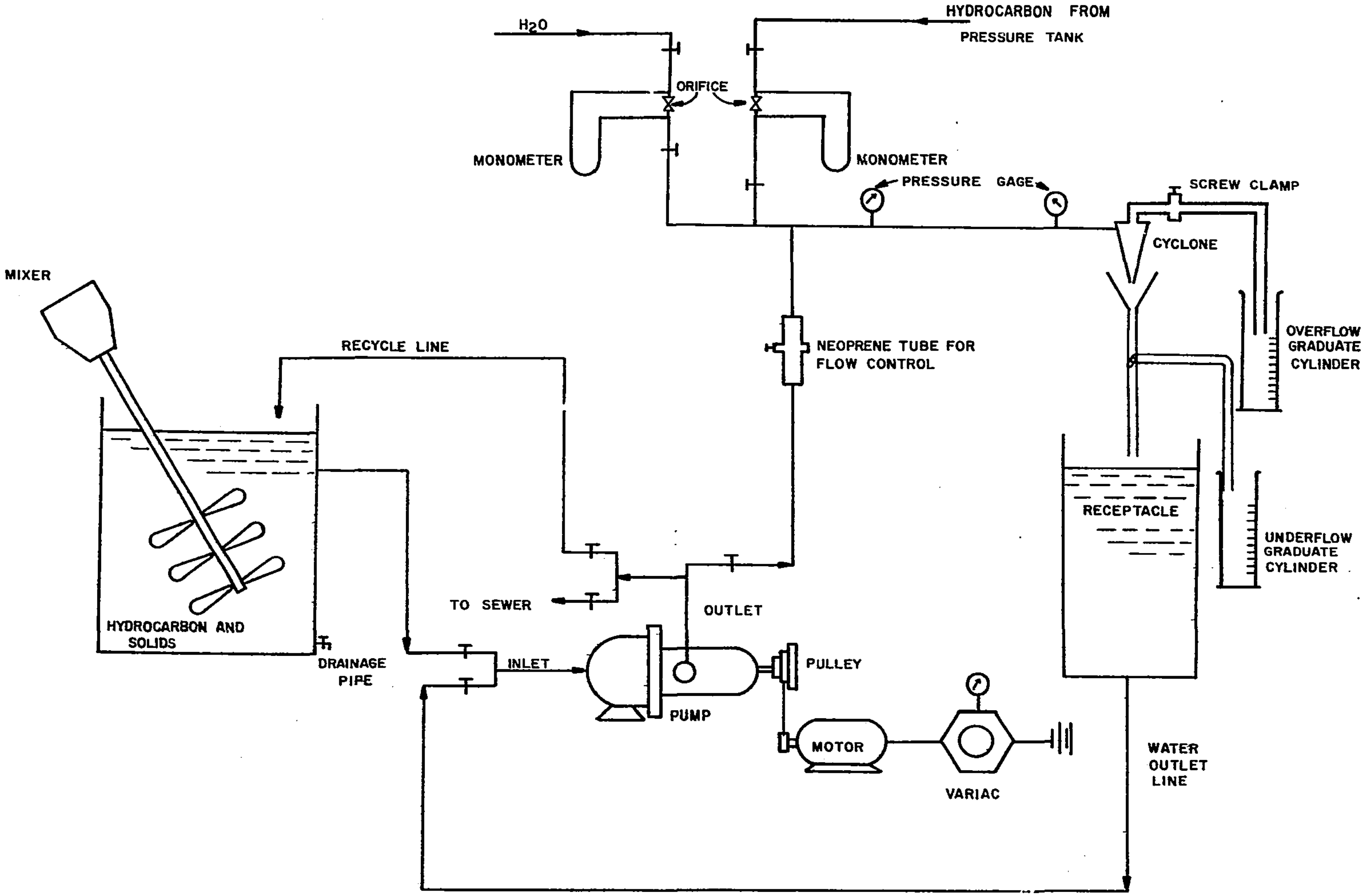

Figure 7. Schematic Diagram of Experimental Installation.

Whenever emulsion occurred as a result of the intense turbulence in the cyclone created during high flow rates, a few drops of water-soluble "emulsion breaker" (trade-named Tretolite) was added to disperse the emulsion layer.

Experimental Procedure

Because a density change of any material is not expected in this experiment, all the percentages are conveniently expressed on a volume basis. The experimental procedures are:

1) Once all the requirements for a particular run were assigned, the mixer in the solid-hydrocarbon tank and the conveyor pump were turned on to allow mixing and recycling of solid and hydrocarbon between the pump and the tank for five minutes before merging with the water to enter into the hydrocyclone. The water flow rate was determined by using a calibrated monometer.

2) With the aid of a stop-clock, a run began with the simultaneous placing of overflow and underflow tubes each in separate cylinders. For a feed rate of 50 cc/sec., a 60 seconds duration was assigned; for 50 cc/sec., 60 seconds; and for 40 cc/sec., 75 seconds, respectively.

3) At the end of each run, both the volume of aqueous and of hydrocarbon-solid phases in overflow and underflow were measured and recorded.

4) The solids were then vacuum-filtered through a Buchner funnel and collected in a pre-weighed paper

basket prior to drying. Each sample was oven dried for about 3 hours at 100°C prior to weight determination in an analytical balance.

A data sheet including sample calculations is given in Appendix D.

Operating Parameters

As evident in the foregoing chapters, the determination of separation efficiency (E) as a function of effluent split (Q_o/Q_u) demands the measurement of x_o, y_u, and z_o as dependent variables. In order to observe any significant effect on these variables, the following parameters and levels were chosen:

A) Feed rate (Q_f): 50, 60, and 75 cc/sec.

B) Feed phase ratio ($(x_f+z_f)/y_f$): 0.5,1.0, and 2.0.

C) Solid concentration in oil: 2% and 4%.

D) Solid Diameter: 0.832 and 0.294 mm.

Thus, the minimum number of sets required would be identical to the maximum number of combinations of parameter levels, so

$$\text{No. of Sets} = 3 \times 3 \times 2 \times 2 = 36$$

In view of the possibility that the dimensions of both the vortex finder tube and the discharge nozzle might exert strong influence on the measured variables, three additional sets of runs using different combinations of vortex tube and discharge nozzles were conducted (Figures E-5, 6, and 14) for comparision. All the 39 sets of efficiency curves are presented in Appendix E.

CHAPTER V

MEASUREMENT ERRORS

Although efforts have been made to minimize all the possible measurement errors in the system, an estimate of the errors is still appropriate.

Before estimating the relative errors inherent in the overall efficiency value and various volume splits, it will be recalled that the resultant relative errors of the four arithmetic operations are (13)

Addition:
$$\frac{e_{x+y}}{\bar{x}+\bar{y}} = \frac{\bar{x}}{\bar{x}+\bar{y}}\left(\frac{e_x}{\bar{x}}\right) + \frac{\bar{y}}{\bar{x}+\bar{y}}\left(\frac{e_y}{\bar{y}}\right) \tag{76}$$

Subtraction:
$$\frac{e_{x-y}}{\bar{x}-\bar{y}} = \frac{\bar{x}}{\bar{x}-\bar{y}}\left(\frac{e_x}{\bar{x}}\right) - \frac{\bar{y}}{\bar{x}-\bar{y}}\left(\frac{e_y}{\bar{y}}\right) \tag{77}$$

Multiplication:
$$\frac{e_{x\cdot y}}{\bar{x}\cdot\bar{y}} \simeq \frac{e_x}{\bar{x}} + \frac{e_y}{\bar{y}} \tag{78}$$

Division:
$$\frac{e_{x/y}}{\bar{x}/\bar{y}} \simeq \frac{e_x}{\bar{x}} - \frac{e_y}{\bar{y}} \tag{79}$$

where $\bar{x}$, $\bar{y}$ = measured quantity of variables x, y, respectively.

e_x, e_y = known error in the measured quantity x, y, respectively.

In this experiment, the errors in the measurement arise from the volumetric measurement of the effluents and the gravimetric measurement of the solids. The relative error in measuring the oil (and also water) volume in the overflow as well as in the underflow is estimated to be approximately ± 0.5%. By applying Eq. 76 the resultant maximum relative error in either overflow (or underflow) volumetric measurement should be

$$\frac{e_{Q_o t}}{Q_o t} \leq 1.0\%$$

Since x_o is the volume fraction of oil (with solids) in the overflow, the resultant relative error by applying Eq. 79 is

$$\frac{e_{x_o}}{\bar{x}_o} \leq 2.0\%$$

The maximum relative error for the feed volume is the combined relative error of both the overflow and underflow because the feed volume was determined by adding the overflow and underflow volumes. Hence, by Eq. 76

$$\frac{e_{Q_f t}}{\overline{Q_f t}} \leq 2.0\%$$

Likewise, by Eq. 79, the relative error in computing x_f should be

$$\frac{e_{xf}}{\bar{x}_f} \le 3.0\%$$

With reference to Eq. 63 the overall efficiency can be expressed in terms of

$$E = \frac{(Q_o t)(x_o - x_f)}{(Q_f t)(x_f)(1-x_f)} \tag{80}$$

The resultant relative error of Q_o/Q_f can be estimated as ≤ 3.0% and for $(x_o - x_f)$, the relative error is ≤ 4.5%. Similarly, for the term $x_f(1-x_f)$, the relative error is ≤ 6.0%. By combining the relative errors of all measurements pertaining to the efficiency, the error analysis shows that the maximum relative error in calculating the efficiency is

$$\frac{e_E}{\bar{E}} \le 13.5\%$$

The maximum relative errors for each of the volume splits were also estimated. In summary:

Volume Split	Relative Error
effluent $(\frac{Q_o}{Q_u})$	≤ 2.0%
water $(\frac{Q_u y_o}{Q_u y_u})$	≤ 1.0%
oil + solids $(\frac{Q_o(x_o+Z_o)}{Q_u(x_u+Z_u)})$	≤ 1.0%

oil $\left(\frac{Q_o x_o}{Q_u x_u}\right)$	$\leq 1.0\%$
solids $\left(\frac{Q_o Z_o}{Q_u Z_u}\right)$	$\leq 0.08\%$

CHAPTER VI

DISCUSSION OF RESULTS

Efficiency Curves

A total of 240 runs grouped in 39 sets of various parameter combinations was conducted for this experiment. An index table and description for the preliminary treatment of raw data are included in Appendix E with two summaries of data and 39 sets of efficiency curves. Each set comprises both an actual and an ideal efficiency curve plotted as functions of effluent split (Q_o/Q_u). Since there are only three phase ratios (oil/water = 1/2, 1/1, 2/1) included in this experiment and each phase ratio dictates the shape of an ideal efficiency curve, the actual efficiency curve is compared with its own ideal efficiency curve at the same phase ratio. Figures 8, 9, and 10 (identical to Figures E-1, 2, and 3) are representative samples at Q_f = 60 cc/sec.

Among the 39 sets of efficiency curves presented here, three sets are duplicates of identical parameter combinations. The purpose was to investigate the possible influence of both vortex finder and discharge nozzle sizes

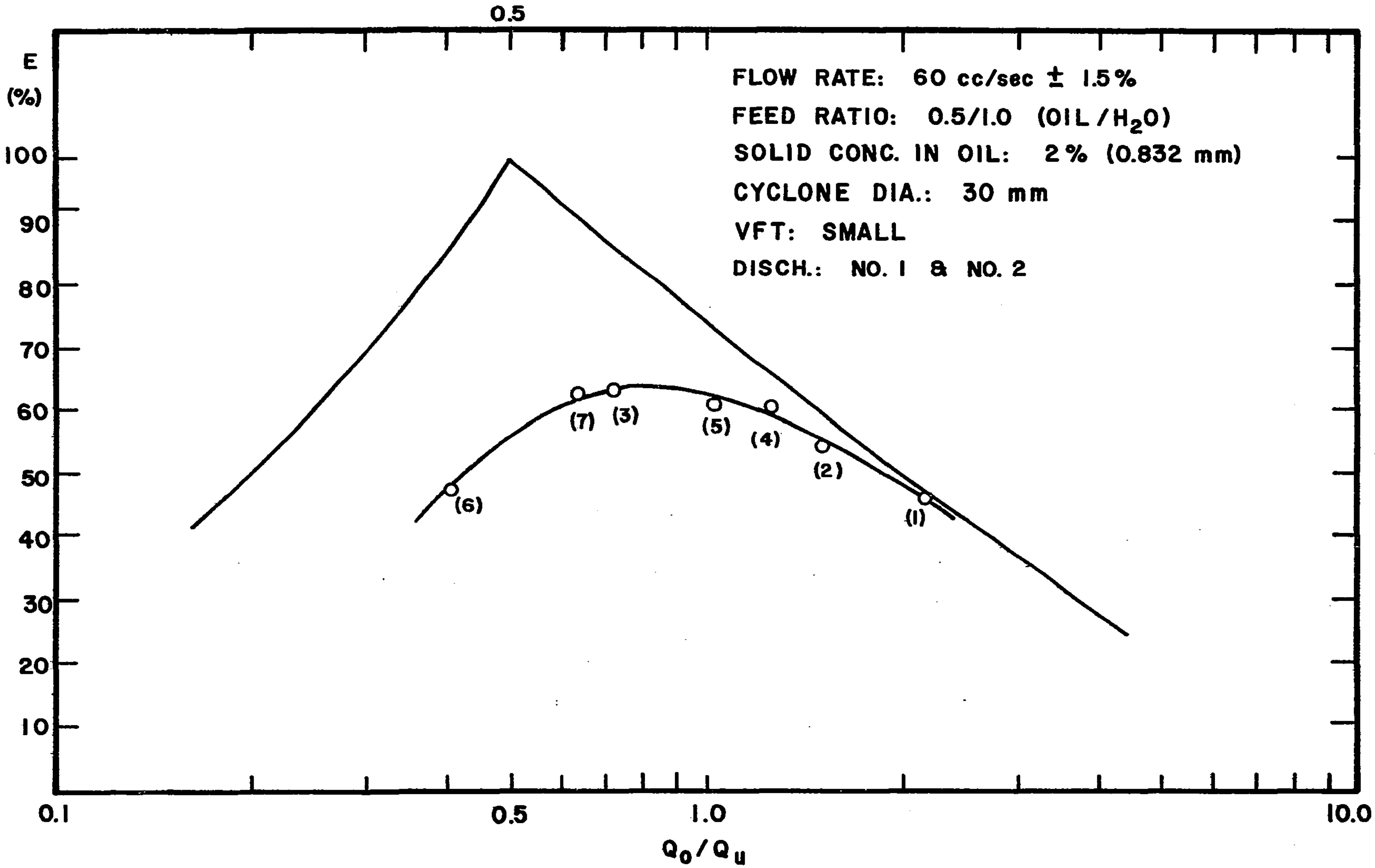

Figure 8. Overall Efficiency vs. Effluent Split (oil/water = 1/2, Q_f = 60.0 cc/sec).

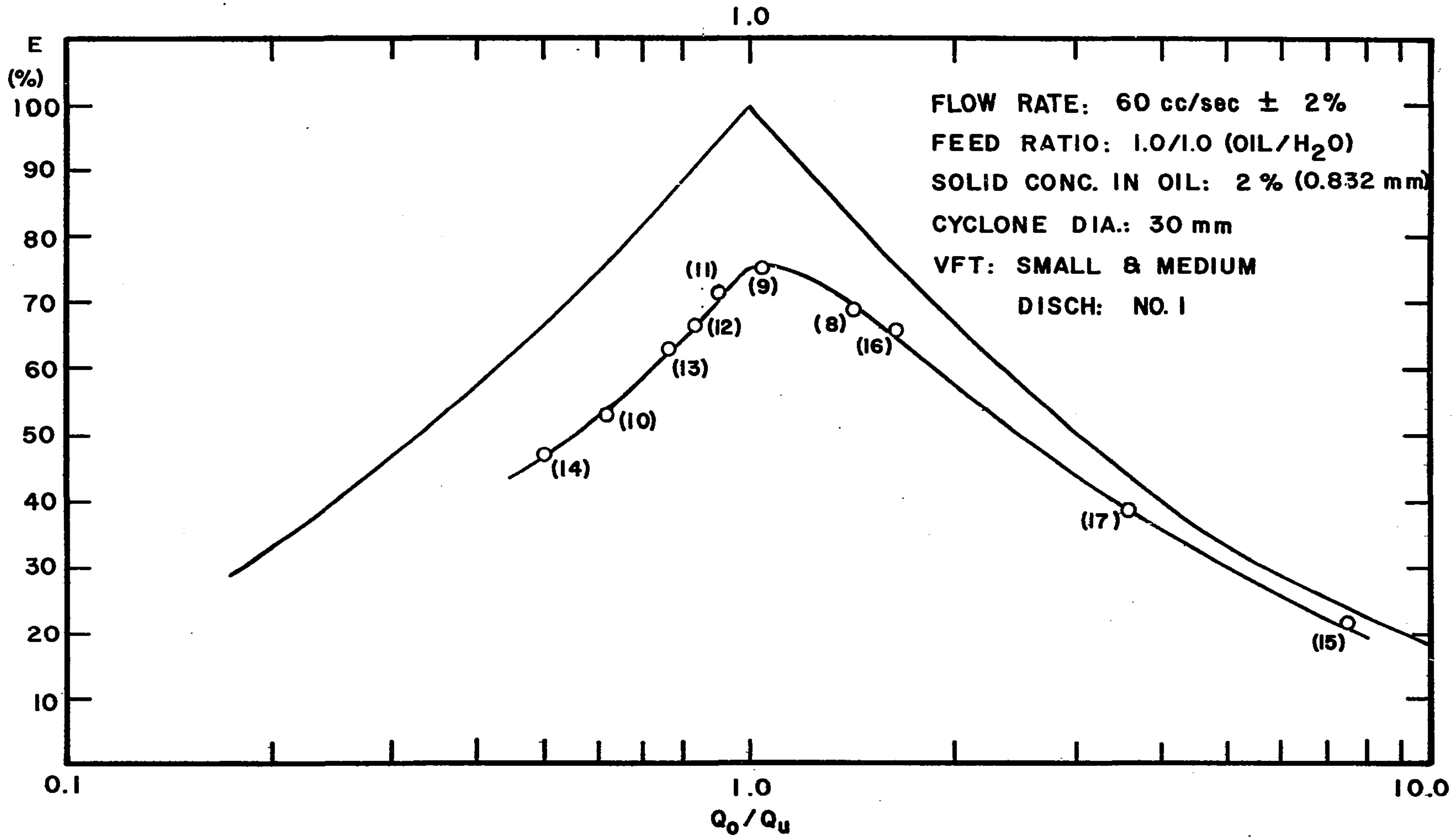

Figure 9. Overall Efficiency vs. Effluent Split (oil/water = 1/1, Q_f = 60.0 cc/sec).

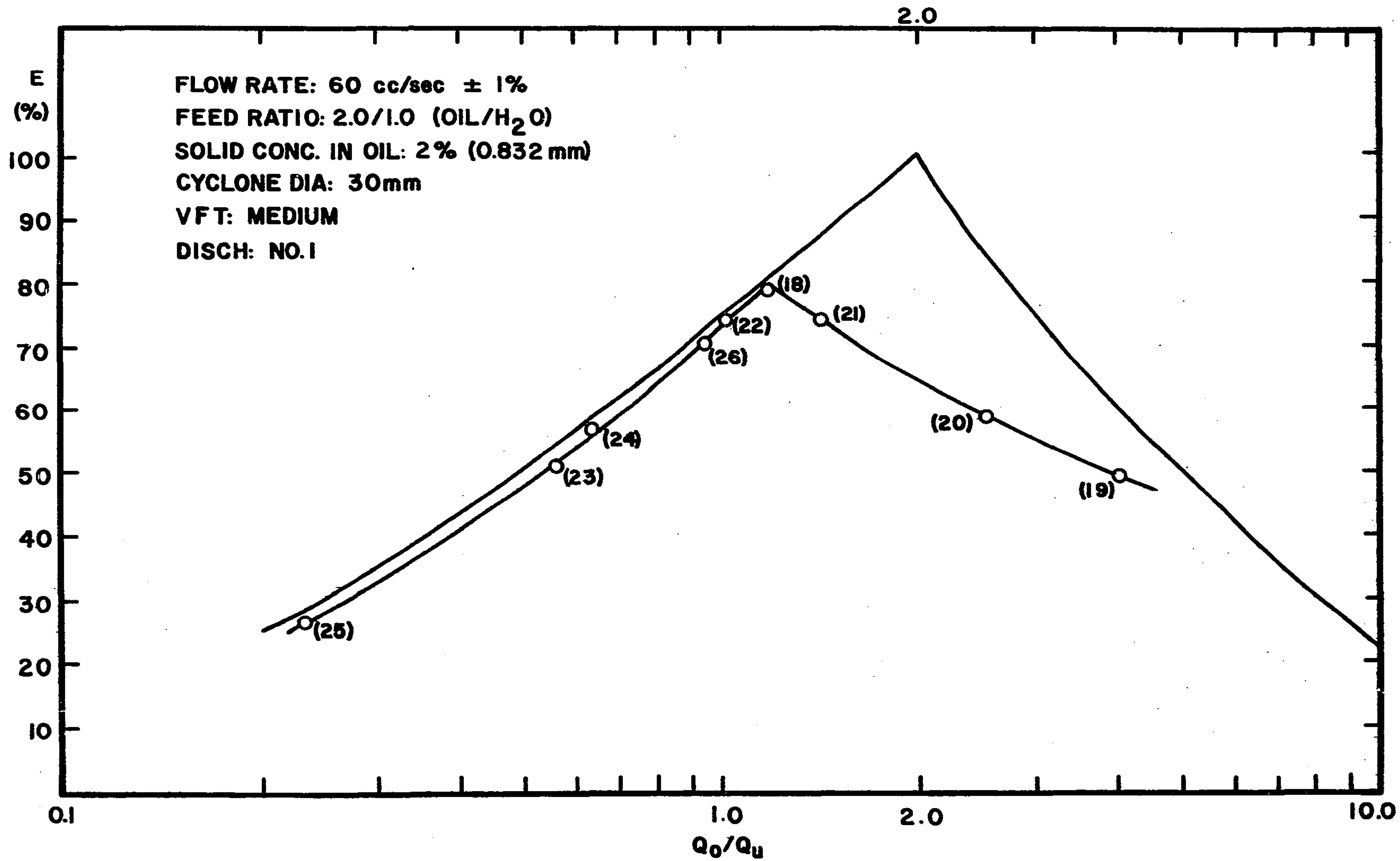

Figure 10. Overall Efficiency vs. Effluent Split (oil/water = 2/1, Q_f = 60.0 cc/sec).

on the actual efficiency. Runs in Figures 11, 12, and 13 (identical to Figures E-4, 5, and 6) were conducted under identical operating conditions with different tube and nozzle combinations. As evident from the shape of the curves, no appreciable effect on actual efficiency could be detected. However, in contrast to Figure 14 (Figure E-13), Figure 15 (Figure E-14) displays a sharp decline in actual efficiency under a large vortex finder tube. The logical explanation is that at phase ratio (oil/water) of 1/2, the vortex tube's cross-sectional area not only covers most of the oil particles congregating around the air core but also the water phase as well. Hence, the size of the tube is of importance. In the previous case where the phase ratio (oil/water) is 2/1, both the overflow and the underflow contain large portions of oil, particularly in the overflow. Therefore, it could be reasoned that the vortex finder tube, from the smallest to the largest used in this experiment, is likely to be occupied by oil flowing through. From the exhibits of all the three duplicate runs, it may be concluded that both vortex tube and discharge nozzle size would have no effect on the actual efficiency for runs of phase ratio (oil/water) 2/1.

It can also be noted from all the actual efficiency curves that nearly all the maximum values are located in the vicinity where $Q_o/Q_u = 1.0$, irrespective of any phase ratio. This consistency may be attributed to the fact that the

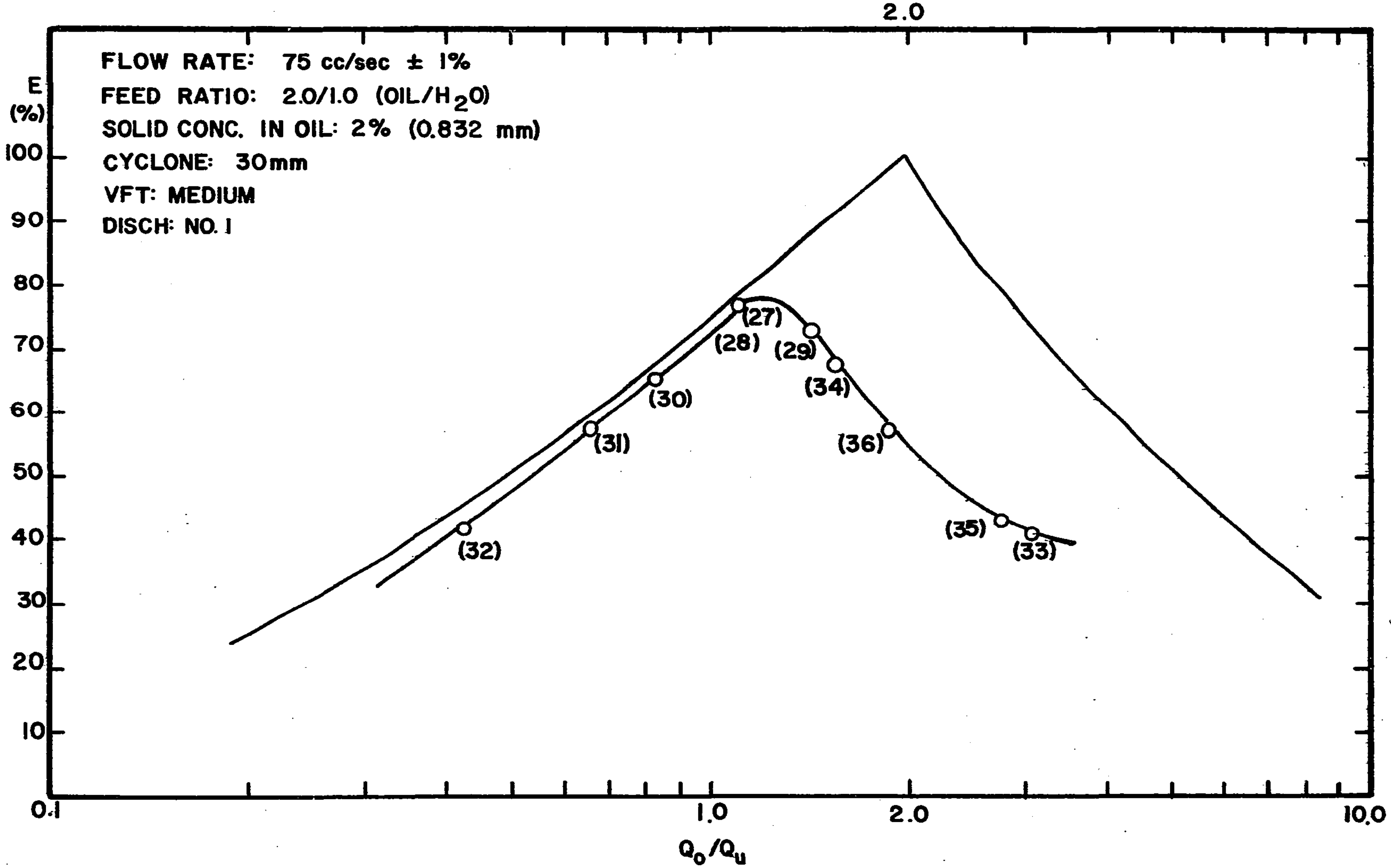

Figure 11. Overall Efficiency vs. Effluent Split (oil/water = 2/1, Q_f = 75.0 cc/sec, VFT = medium, Apex = No. 1.

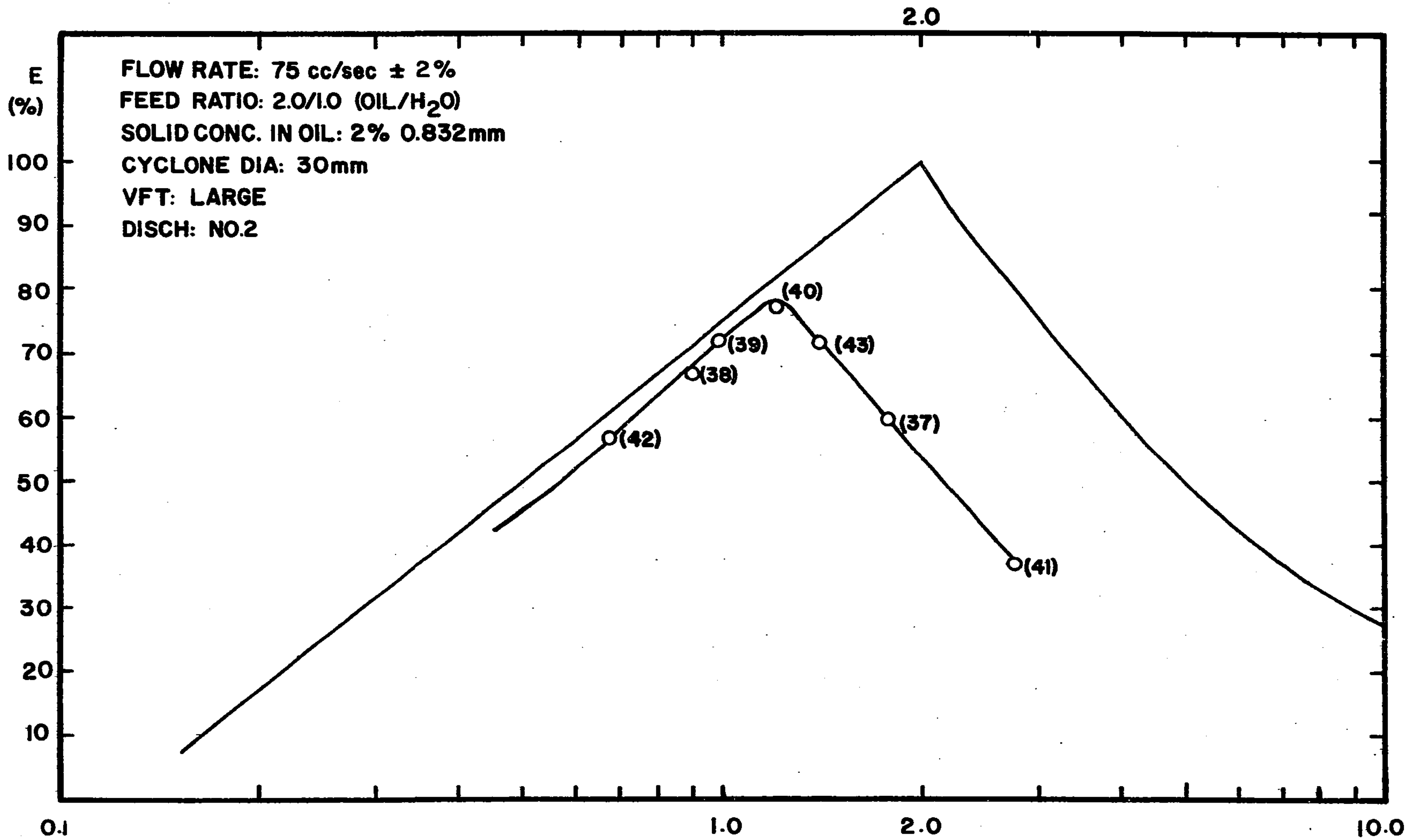

Figure 12. Overall Efficiency vs. Effluent Split (oil/water = 2/1, Q_f = 75.0 cc/sec, VFT = large, Apex = No. 2).

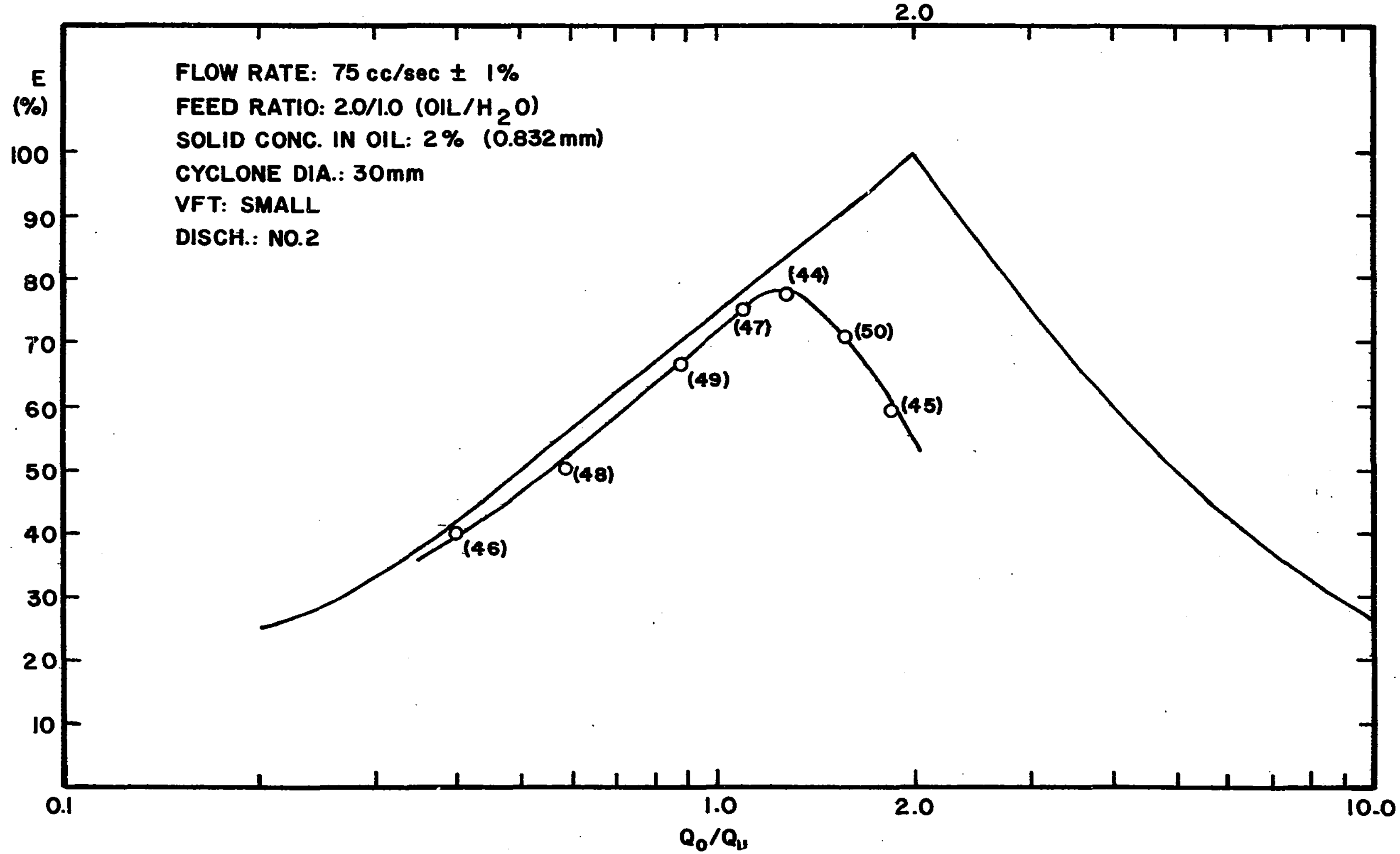

Figure 13. Overall Efficiency vs. Effluent Split (oil/water = 2/1, Q_f = 75.0 cc/sec, VFT = small, Apex = No. 2).

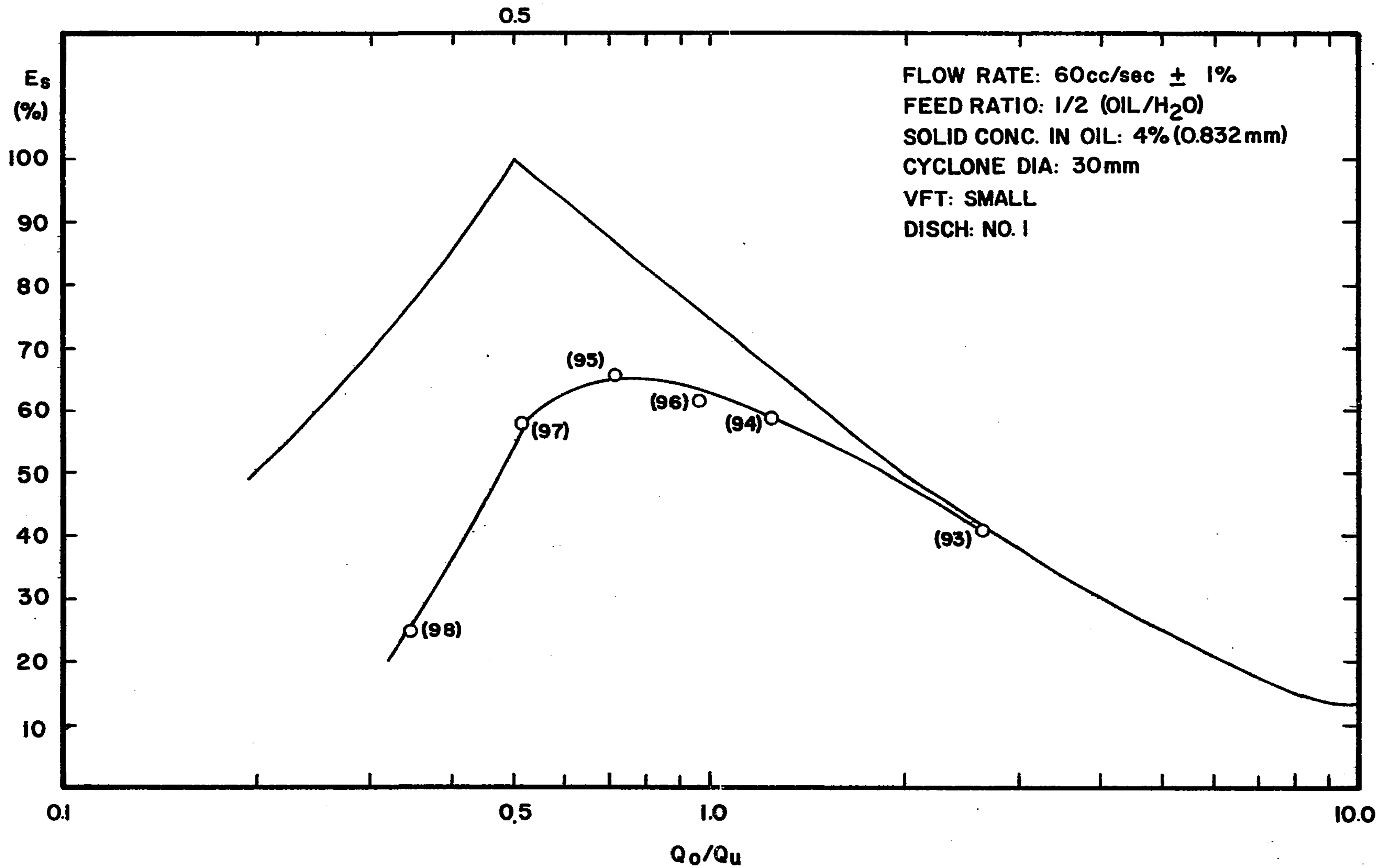

Figure 14. Overall Efficiency vs. Effluent Split (oil/water = 1/2, Q_f = 60.0 cc/sec, VFT = small, Apex = No. 1).

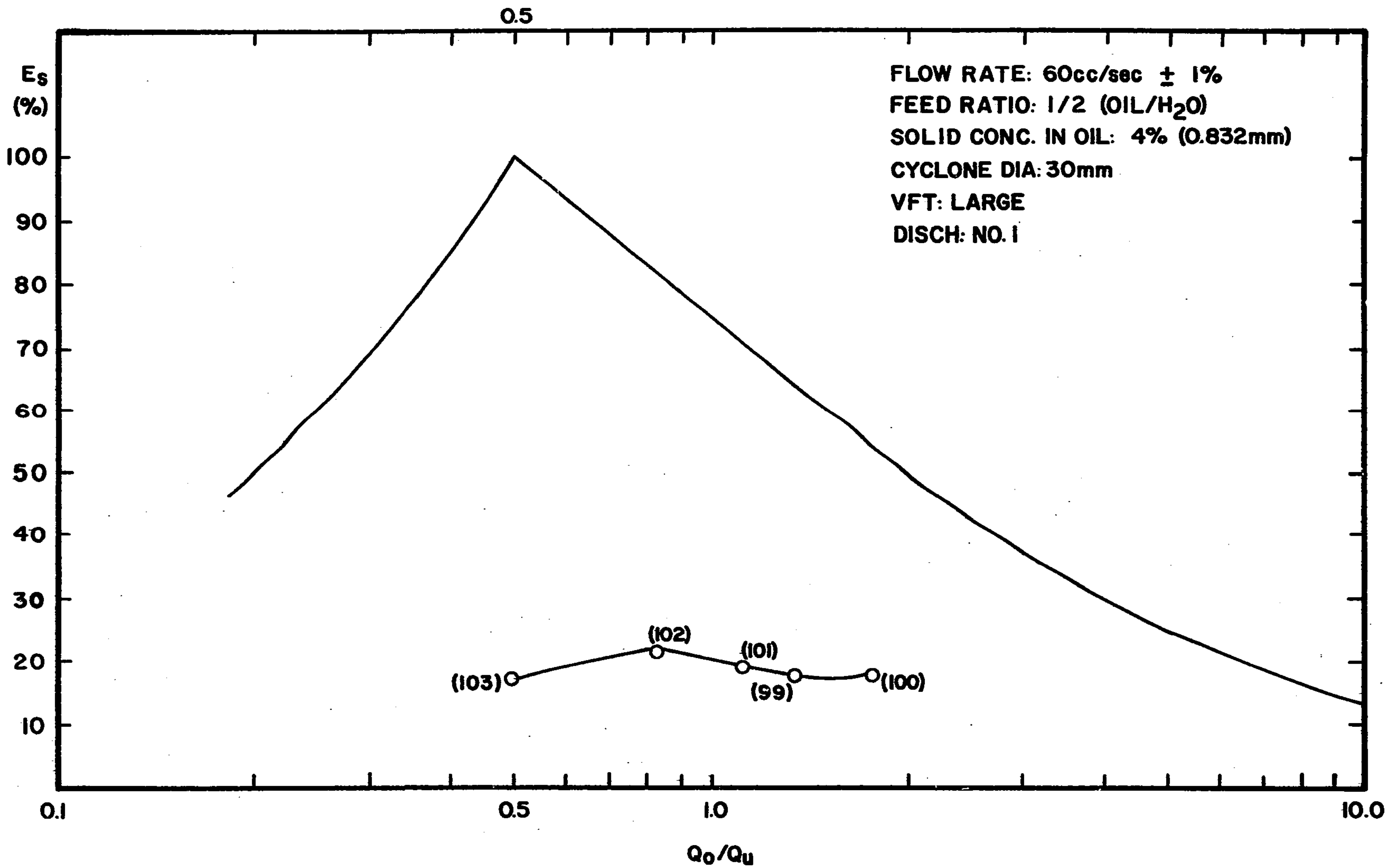

Figure 15. Overall Efficiency vs. Effluent Split (oil/water = 1/2, Q_f = 60.0 cc/sec, VFT = large, Apex No. 2.)

geometrical shape of the cyclone exerts a unique influence on the actual separation efficiency since all the runs were conducted in the 30 mm cyclone.

As a result of this investigation, a novel term—relative efficiency (E/E_s)--is introduced. It is defined as the ratio of the actual efficiency to its corresponding ideal efficiency at the same effluent split (Q_o/Q_u) and phase ratio (x_f/y_f). While the utility value of this term is exemplified in the following chapter, the values of relative efficiency are plotted against effluent split (Q_o/Q_u) in Figure 16 for the runs shown in Figures 8, 9, and 10. It may be of some interest to note that practically all of the lowest values of the relative efficiency occur in the neighborhood where the effluent split (Q_o/Q_u) approximates the phase ratio (x_f/y_f).

With reference to the section on "Separation Efficiency" in Chapter III, it has been mentioned that the peak of the ideal efficiency (100%) can only occur where effluent split (Q_o/Q_u) coincides with phase ratio (x_f/y_f). Therefore, the low value of relative efficiency where Q_o/Q_u equals to x_f/y_f only substantiates the belief that this particular cyclone is not well designed for the liquid-liquid separation and process designers must select a cyclone most suitable for a known phase ratio (x_f/y_f) in order to obtain a maximum investment return.

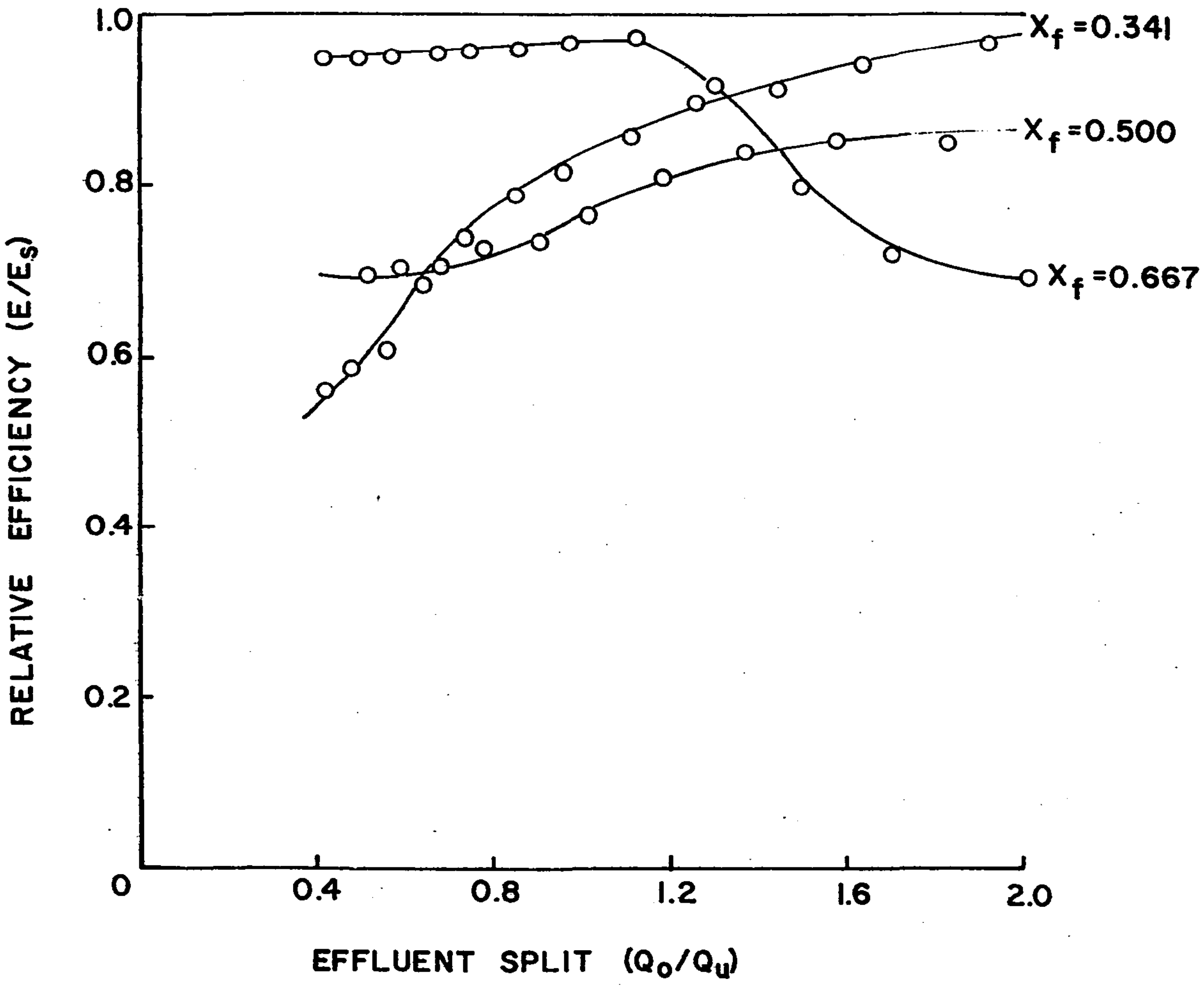

Figure 16. Relative Efficiency vs. Effluent Split at Three Phase Ratios (Q_f = 60.0 cc/sec).

<u>Emulsification</u>

According to the established theory, an emulsion consists of two liquid phases of which the dispersed phase is distributed in the continuous phase in the form of micro-droplets (0.2 to 5 microns). When the volume concentration of these droplets exceeds 74%, they must cease to be spherical and the structure resembles that of foams. It is also known that an emulsion is formed when the dispersed liquid particle in a mixture traveling in a continuous medium experiences intense shear force as a result of momentum transfer. In the case of a hydrocyclone, the phenomenon occurs only at higher feed rates as observed in this experiment. Under these circumstances, the dispersed particles congregating in the vicinity of the air core apparently are not able to transfer all of the momentum from the air core to the next adjacent layer and consequently are broken into micro-droplets. This phenomenon is more pronounced for a mixture having a phase ratio (oil/water) of 1.0, probably due to the maximum interfacial contact surface area separating these two phases. The momentum transfer across an interface is always hindered to some extent presumably due to the interfacial tension. It is natural that the momentum flux generated from the air core can cause a larger particle to break up into smaller ones. The "breaking-up" process will continue until the interfacial forces of the particle are large enough to withhold further reduction in size due to shearing forces.

During the experimental runs one could also observe the intense emulsification taking place at the region immediately below the upper base where turbulence is more prominent. When emulsions are formed within a hydrocyclone, separation becomes minimal because the particles of smaller size are less mobile, particularly in a very crowded space. Hence, no meaningful comparison can be made between an emulsified run and its emulsion-free counterpart under otherwise identical operating conditions.

Effective Volume Fraction and Cyclone Performance

The so-called "effective volume fraction" (EVF) is defined as the complementary fraction of the ineffective volume representing turbulence, emulsification, mixing, entrainment and any unknown hydrodynamic cause detrimental to the separation of phases in a cyclone. Although the ineffective volume fraction can be obtained by direct conversion from the macroscopic turbulent length defined in Chapter III (Note: both values are tabulated in Table E-3), the term "volume fraction" is preferred over "length" which might suggest that ineffectiveness is present only in a particular locality. Nevertheless, before arriving at the value of a volume fraction, it is necessary to determine the turbulent length by the scheme outlined in the final section of Chapter III; the selection of the appropriate model by fitting it with experimental data is fully explained in Appendix F. However, one must bear in mind that the derivation of relative velocity, and hence the vertical distance (Eq. 27 and Eq. 40) traveled by a dispersed particle, was performed for the case where the density of the continuous phase is greater than that of the dispersed phase. Hence both $\overline{v}_\theta$ and $\overline{v}_r$ are negligible. If, on the converse, these two quantities are not negligible, the turbulent length, d, obtained without the inclusion of them cannot be too realistic. Unfortunately, the mathematics would be insurmountable if both $\overline{v}_\theta$ or $\overline{v}_r$ were included in the derivation for an analytical solution.

From a series of solid-liquid separation experiments Rietema (17) has reported, in terms of minimum turbulence, various optimum ratios of cyclone component parts to the cyclone's upper base diameter, e.g.,

$$L/D = 5.0 \text{ and } b/D = 0.28$$

where L is the cyclone height and b the internal feed tube diameter. By comparing with the present cyclone in question where

$$L/D = 14.5/30.0 \cong 5.0$$

$$\text{and} \quad b/D = 6.0/30.0 = 0.20$$

It is conceivable that some turbulence may be attributed to the small feed entrance tube.

One may also note from the tabulation of effective volume fraction that the value is in increasing order with effluent split (Q_o/Q_u). This phenomenon could very well mean the moderation of turbulence as more fluid (in both phases) exits in the vortex finder tube as the overflow. Since the vortex tube is located very near the feed entrance tube, a high overflow rate also suggests that a short and direct route could exist between these two tubes.

Superficially, the relative efficiency value and the effective volume fraction may seem to be identical. A close examination of the equations and derivations indicates that the former is a measure of enrichment of both liquid phases by means of effluent compositions, while the latter reveals the hydrodynamic aspect of a cyclone in operation. A comparison of these two terms is meaningful only for identical cyclones under identical operating conditions. For example, a replacement of the small vortex finder by a medium size for higher overflow rate would lower the value of relative efficiency because a more dense liquid phase would exit in the overflow. Yet in the meantime, the effective volume fraction increases due to less turbulence.

In order to measure the performance of a cyclone, a new term, Φ, designated as the product of relative efficiency and effective volume fraction is introduced. It is interesting to note from Figures 17, 18, and 19 that for

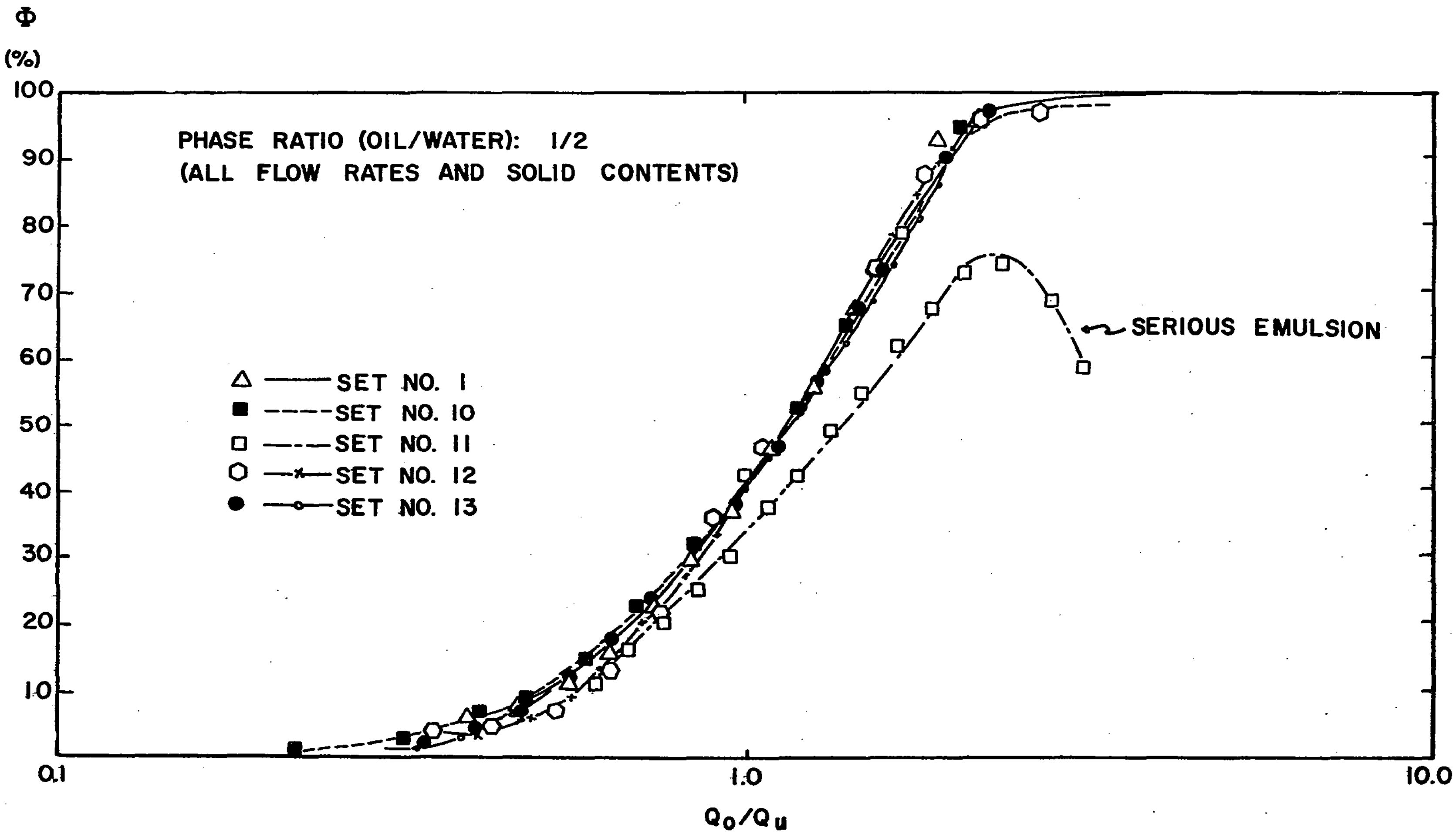

Figure 17. Cyclone Performance vs. Effluent Splits (Run Set No's. 1, 10, 11, and 13).

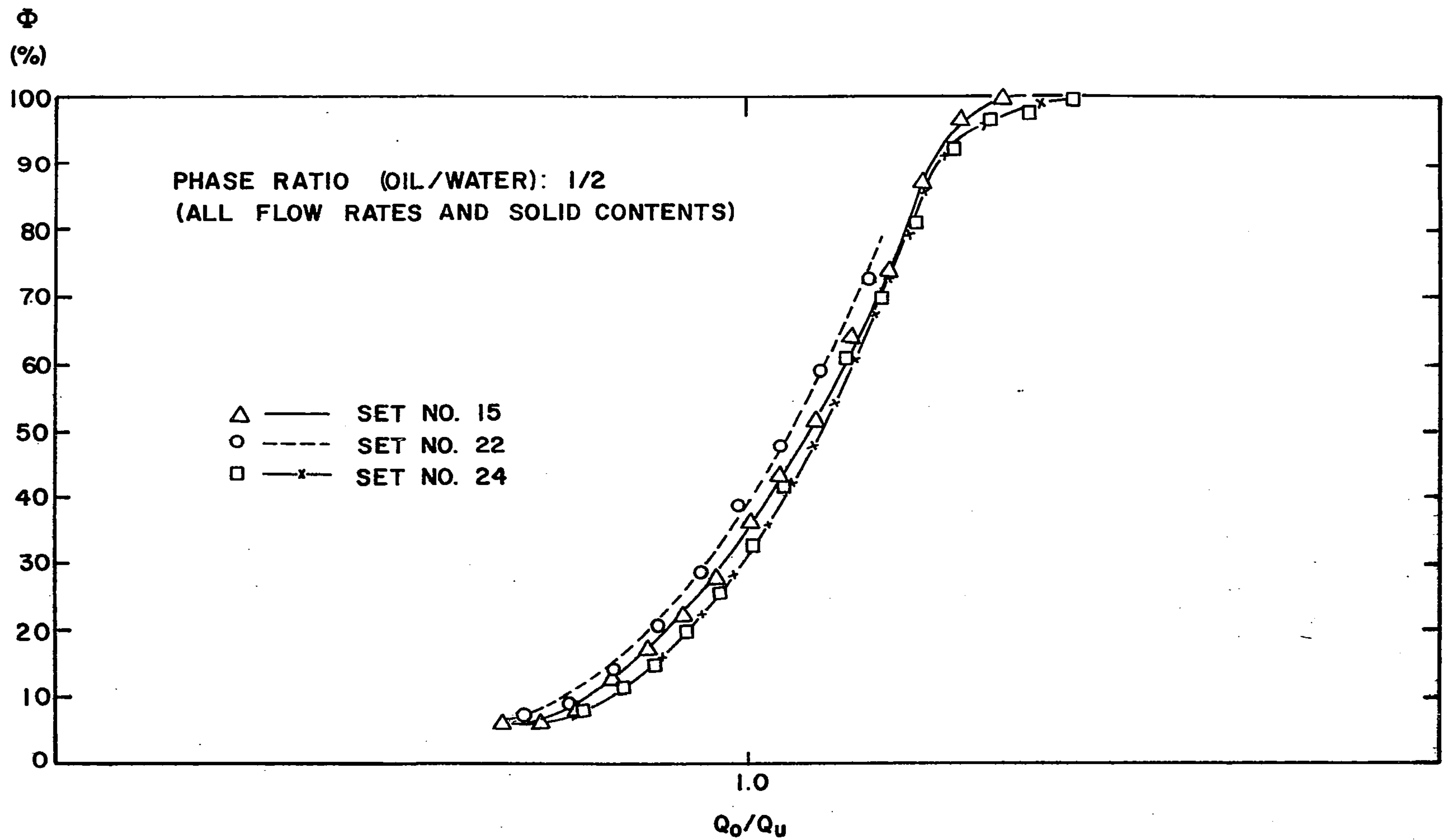

Figure 18. Cyclone Performance vs. Effluent Splits
(Run Set No's. 15, 22, and 24).

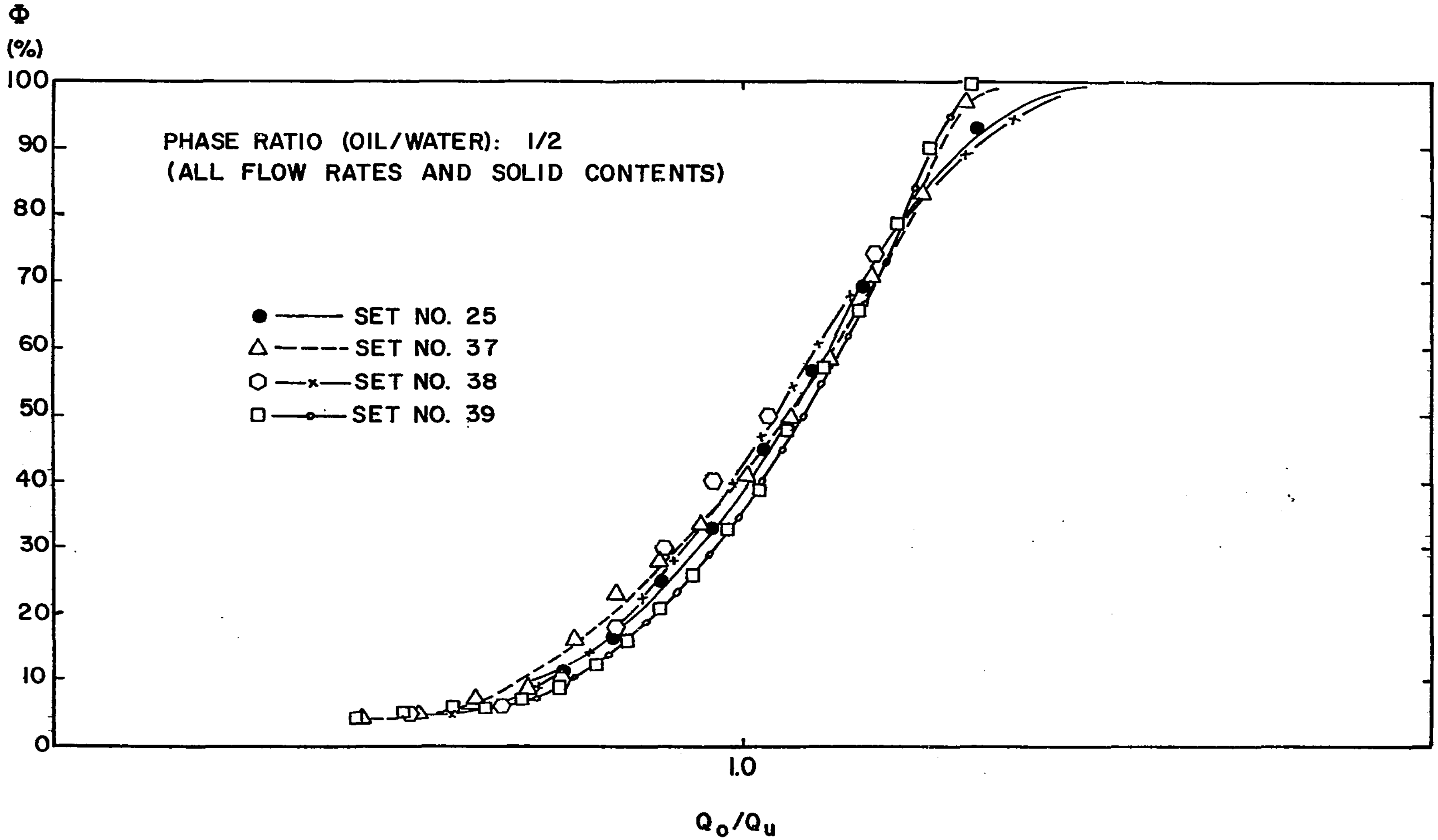

Figure 19. Cyclone Performance vs. Effluent Splits (Run Set No's. 25, 37, 38, and 39).

all the runs with x_f = 0.33 (phase ratio - oil/water = 0.5), an "S" shape curve results when the performance is plotted against effluent splits, except when intense emulsification is encountered. However, no fixed shape curve could be identified for runs with x_f = 0.50 and x_f = 0.67. This phenomenon further substantiates the fact that the mathematical model postulating a streamline flow is more suitable for a system in which the dispersed phase is of a density less than that of the continuous phase (for more details see Appendix F).

CHAPTER VII

APPLICATION OF RELATIVE EFFICIENCY VALUES TO CYCLONE PROCESS DESIGN

Method of Estimating Relative Efficiency Values

The relative efficiency has been defined to be the actual separation efficiency divided by the ideal efficiency at the same effluent split (Q_o/Q_u) and feed composition (x_f) (Appendix C). Briefly, it is a measure of the proximity to an ideal state and its maximum value is unity. Since relative efficiency values (E/E_s) as a function of effluent split (Q_o/Q_u) for three x_f values (0.33, 0.50, and 0.67) at a particular feed rate have been determined experimentally, the E/E_s value at, say, $x_f = 0.8$ can be readily obtained by cross-plotting the known relative efficiency value versus x_f at various effluent splits and extrapolating to $x_f = 0.8$. The results of a set of such extrapolations is given in Table 1. The overall efficiency curve of this new estimated system is simply the extrapolated relative efficiency values multiplied by the corresponding ideal efficiency (E_s) values at the same effluent split (Q_o/Q_u). In Figure 20 the estimated overall efficiency curve at 60 cc/sec and $x_f = 0.8$ (or $x_f/y_f = 4.0$) in a 30 mm cyclone is shown as an illustration of the usefulness of the relative efficiency values.

TABLE 1

ESTIMATING THE OVERALL EFFICIENCY VALUES BY EXTRAPOLATION

Q_o/Q_u	E/E_s (Q_f = 60 cc/sec) x_f=0.34	x_f=0.50	x_f=0.67	x_f=0.80 (extrapolated)	E_s^* x_f=0.80	$E^{\#}$ x_f=0.80
0.5	0.55	0.70	0.96	0.99	0.42	0.42
0.7	0.70	0.73	0.96	0.99	0.51	0.51
0.9	0.80	0.75	0.97	0.99	0.59	0.59
1.1	0.86	0.79	0.97	0.99	0.66	0.65
1.3	0.91	0.82	0.94	0.99	0.71	0.70
1.5	0.94	0.84	0.80	0.78	0.75	0.59
1.7	0.96	0.85	0.74	0.68	0.79	0.54
2.0	0.97	0.86	0.69	0.56	0.83	0.47

*See Table C-1

#See Figure 20 next page

Comparison of Two Cyclone Systems

A practical example of the application of relative efficiency to cyclone process design utilizing the aforementioned efficiency curve is of interest.

In making a comparison, two cyclone systems are considered. System 1 operates at a flow rate of 60 cc/sec and contains 50% oil in the feed. It is now desired to separate the feed stream into two effluents with the overflow containing

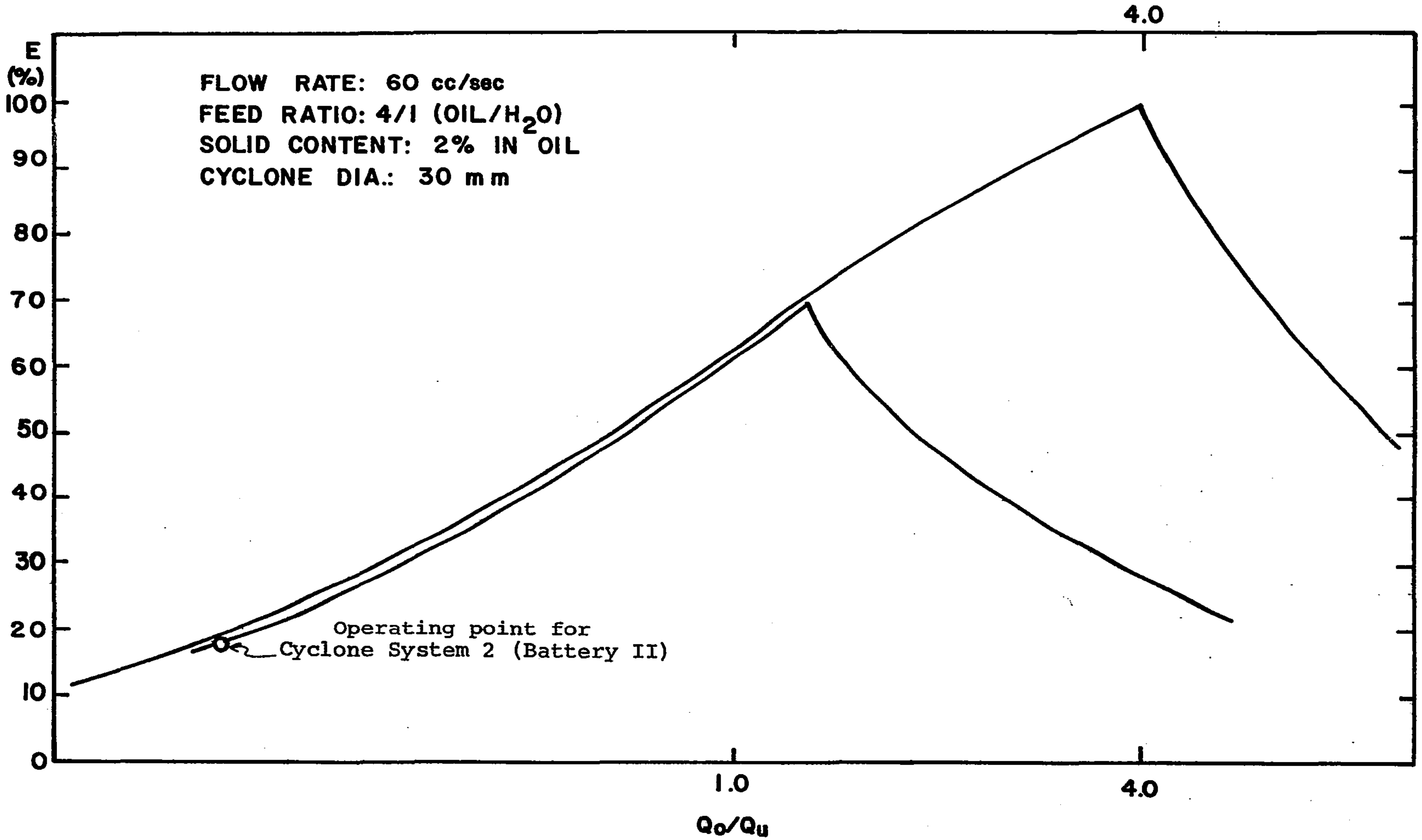

Figure 20. Estimated Overall Efficiency vs. Effluent Splits (oil/water = 4/1, Q_f = 60.0 cc/sec).

about 86% oil. Separation is to be accomplished by using a 30-mm cyclone, and the operating effluent splits (Q_o/Q_u) are chosen from the actual efficiency curve given in Figure 9 (or Figure E-2) because the information on the feed conditions and the overflow composition are available. The data also show that

$$Q_o = 27 \text{ cc/sec}, \; Q_u = 33 \text{ cc/sec}$$
$$x_u = 0.20, \; E/E_s = 71\%$$

The flow sheet for System 1 is shown as follows:

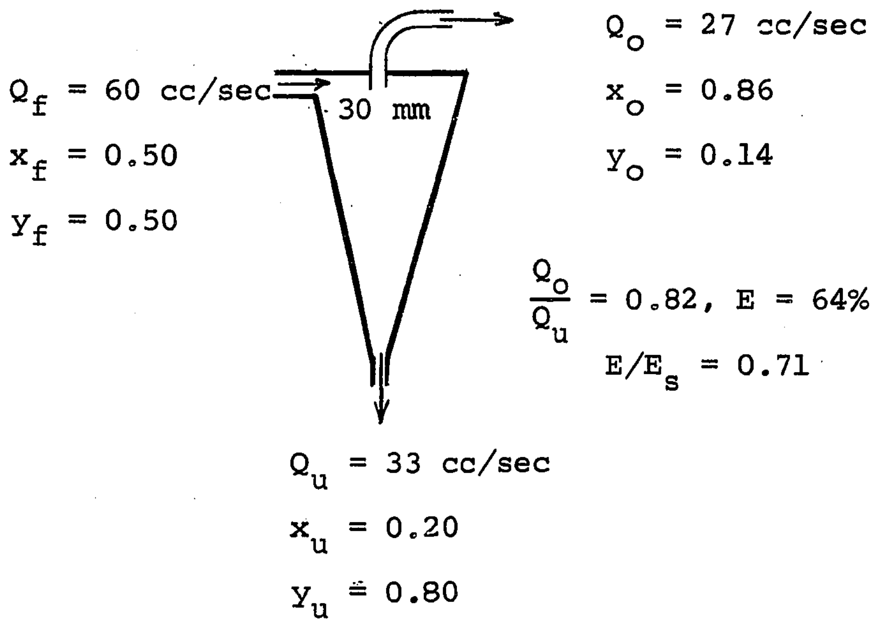

Figure 21. Cyclone System 1.

Here, the total flow requires pumping is 60 cc/sec and only one cyclone unit is needed.

Suppose it is now desired to upgrade the oil content in the overflow to $x_o = 0.98$ while maintaining the same feed rate, feed composition, and overall effluent splits as in System 1. Two cyclone batteries in series, designated as System 2, are devised for comparative study. By assuming an effluent ratio for each battery and by using efficiency curves (Figures 10 and 20), one can determine the interstream flow rate and flow composition with the aid of simple material balance equations (Equations 55-58). Thus

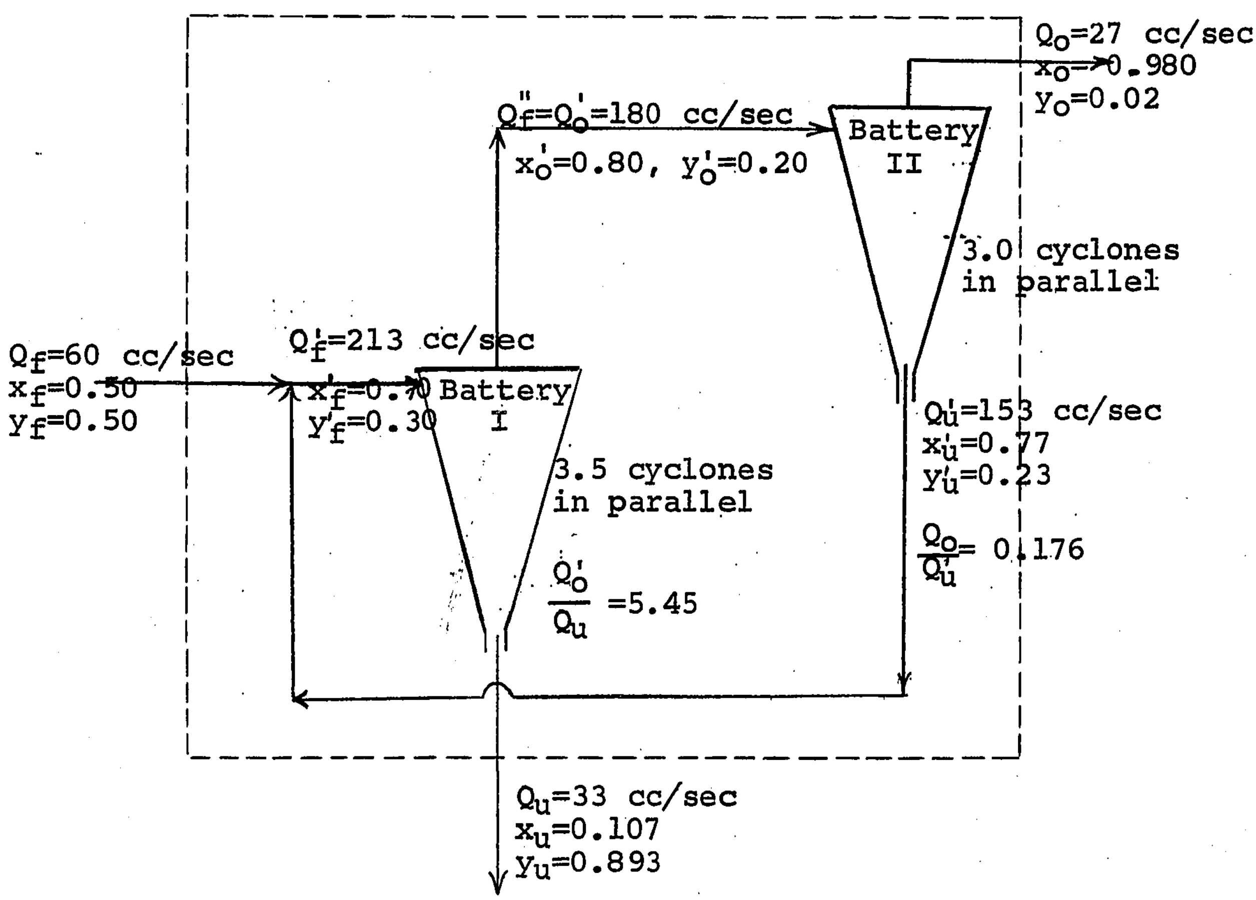

Figure 22. Cyclone System 2.
(Dual-battery in Series)

it is discovered that for

Battery I: $Q_f' = 213$ cc/sec

Battery II: $Q_f'' = Q_o' = \underline{180 \text{ cc/sec}}$

Total flow requires pumping $= 393$ cc/sec

If each unit cyclone is to process the same feed rate (60 cc/sec) as in System 1

$$\frac{393 \text{ cc/sec}}{60 \text{ cc/sec-unit}} = 6.5 \text{ units}$$

will be required. A summary of pertinent information for these two systems is shown in Table 2.

TABLE 2

SUMMARY OF CYCLONE DESIGN INFORMATION

System 1

1) $Q_f = 60$ cc/sec = 1370 gal/day
2) $x_f = 0.5$, $y_f = 0.5$
3) $Q_o = 27$ cc/sec = 615 gal/day
4) $x_o = 0.86$, $y_f = 0.14$
5) $Q_u = 33$ cc/sec = 755 gal/day
6) $x_u = 0.20$, $y_u = 0.80$
7) Overall effluent split $(Q_o/Q_u) = 0.82$
8) Overall efficiency E = 0.655
9) Relative efficiency $(E/E_s) = (0.66/0.90) = 0.710$
10) Total flow requires pumping = 60 cc/sec
11) Total No. of cyclone in operation = 1.0

TABLE 2 (continued)

System 2

1) Q_f = 60 cc/sec = 1370 gal/day

2) x_f = 0.5, y_f = 0.5

3) Q_o = 27 cc/sec = 615 gal/day

4) x_o = 0.98, y_o = 0.02

5) Q_u = 33 cc/sec = 755 gal/day

6) x_u = 0.107, y_u = 0.893

7) Overall effluent split (Q_o/Q_u) = 0.82

8) Overall efficiency E = 0.867

9) Relative Efficiency (E/E_s) = 0.867/0.900
= 0.964

Battery I

No. of Cyclone = 3.5 in parallel

Q_f' = 213 cc/sec (x_f' = 0.70, y_f' = 0.30)

Q_o' = 180 cc/sec (x_o' = 0.80, y_o' = 0.20

Q_u = 33 cc/sec (x_u = 0.11, y_u = 0.89)

Effluent split (Q_o/Q_u) = 5.45

Efficiency E_I = 0.410

E_I/E_s = 0.410/0.47 = 0.875

Battery II

No. of cyclone = 3.0 in parallel

$Q_f' = Q_o'$ = 180 cc/sec (x_f' = 0.80, y_f' = 0.20)

Q_o = 27 cc/sec (x_o = 0.98, y_o = 0.02)

Q_u' = 153 cc/sec (x_u' = 0.77, y_u' = 0.23)

TABLE 2 (continued)

Effluent split $(Q_o/Q_u) = 0.176$

Efficiency $E_{II} = 0.170$

$E_{II}/E_s = 0.167/0.19 = 0.880$

10) Total flow requires pumping = 393 cc/sec

11) Total No. of cyclone in operation = 6.5

Additional power for inter-cyclone pumping (393 cc/sec - 60 cc/sec = 333 cc/sec) will also be required as a result of further enrichment of both the overflow and underflow streams. In essence, the upgrading process is accomplished by taking advantage of extreme effluent splits ($Q_o'/Q_u = 5.45$ in Battery I and $Q_o/Q_u' = 0.176$ in Battery II) where relative efficiency values are close to unity. One may also note that the overall relative efficiency value for System II is 0.964 in comparison with 0.710 for System I.

CHAPTER VIII

CONCLUSIONS

As a summary of experience accumulated during the laboratory investigation, the following conclusions are apropos:

1. In a laboratory hydrocyclone, the mechanics of liquid-liquid separation is governed by the postulated streamline flow when an air core is present. In brief, the fate of a solid or liquid dispersed particle to exit either in the overflow or underflow is determined by a host of interrelated factors; such as the air core momentum, size, shape, density of the particle, the viscosity of the surrounding fluid, the net pressure force on the particle as well as the local acceleration.

2. The most intensely turbulent region was observed to be near the entrance tube immediately below the upper base. It is believed that the turbulence was caused by the geometric incongruity of the cyclone design with respect to the flow pattern. Hence, turbulence mitigation could be effected by the modification of the geometric configuration of the cyclone.

3. The utility of an ideal efficiency curve designated for each feed composition can be realized in the form of relative efficiency values for the estimation of the overall efficiency value of a heretofore undetermined system.

4. As expected, the dispersed liquid particles decrease in size with increasing flow rate. Emulsions became detrimental to the separation in most cases at 75 cc/sec --notably at phase ratio (oil/water) = 1.0) However, emulsification can be inhibited by the presence of solid which is preferentially wetted by the dispersed phase but not by the continuous liquid phases.

5. Both vortex tube and discharge apex dimensions showed negligible effect in the determination of overall separation efficiency except in the case where the feed contains one-third oil or any lighter phase. In such a case, a large vortex tube covers not only the cross-sectional area of the air associated with oil particles but also the continuous phase surrounding the air core as well.

6. The effective volume fraction (converted from macroscopic turbulent length) is in increasing order with the effluent splits. This fact probably indicated that as more fluid is leaving in the overflow, less turbulence is taking place within the cyclone.

7. The cyclone performance as defined shows a consistent pattern as a function of effluent split only for systems of $x_f = 0.33$. Since the performance is the product

of effective volume fraction (EVF) and relative efficiency, it could also imply that the mathematical model derived for determining the EVF is more suitable for systems having a density of the dispersed phase less than that of the continuous phase.

APPENDIX A

MATHEMATICAL DERIVATION OF AIR CORE VELOCITY

As stated in the beginning of Separation Mechanics Part, the vertical velocity component of a fluid in a hydrocyclone is negligible in comparison with the radial and tangential components. Hence, for a two-dimensional model, Eq. 3 and Eq. 4 can be simplified

$$V_r \frac{\partial V_r}{\partial r} - \frac{{V_\theta}^2}{r} = -\frac{1}{\rho}\frac{\partial P}{\partial r} + \nu \left[\frac{1}{r}\frac{\partial}{\partial r}\left(r\frac{\partial V_r}{\partial r}\right) - \frac{V_r}{r^2}\right] \tag{A-1}$$

$$V_r \frac{\partial V_\theta}{\partial r} + \frac{V_r V_\theta}{r} = \nu \left[\frac{1}{r}\frac{\partial}{\partial r}\left(r\frac{\partial V_\theta}{\partial r}\right) - \frac{V_\theta}{r^2}\right] \tag{A-2}$$

Rearranging Eq. A-1 yields

$$V_r \frac{\partial V_r}{\partial r} - \frac{{V_\theta}^2}{r} = -\frac{1}{\rho}\frac{\partial P}{\partial r} + \nu \left[\frac{1}{r}\left(\frac{\partial V_r}{\partial r} + r\frac{\partial^2 V_r}{\partial r^2}\right) - \frac{V_r}{r^2}\right]$$

$$= -\frac{1}{\rho}\frac{\partial P}{\partial r} + \nu \left[\frac{1}{r}\frac{\partial V_r}{\partial r} + \frac{\partial^2 V_r}{\partial r^2} - \frac{V_r}{r^2}\right] \tag{A-3}$$

Noting

$$\frac{1}{r}\frac{\partial (r\ V_r)}{\partial r} = \frac{V_r}{r} + \frac{\partial V_r}{\partial r} \tag{A-4}$$

and differentiating Eq. A-4 yields

$$\frac{\partial}{\partial r}\ \frac{1}{r}\ \frac{\partial (r\ V_r)}{\partial r} = \frac{1}{r}\ \frac{\partial V_r}{\partial r} - \frac{V_r}{r^2} + \frac{\partial^2 V_r}{\partial r^2} \qquad \text{(A-5)}$$

We can rewrite Eq. A-3 as

$$V_r \frac{\partial V_r}{\partial r} - \frac{V_\theta{}^2}{r} = -\frac{1}{\rho}\frac{\partial P}{\partial r} + \nu\left[\frac{\partial}{\partial r}\ \frac{1}{r}\ \frac{\partial (r\ V_r)}{\partial r}\right] \qquad \text{(A-6)}$$

Likewise, Eq. A-2 can be written as

$$V_r \frac{\partial V_\theta}{\partial r} + \frac{V_r V_\theta}{r} = \nu\ \frac{\partial}{\partial r}\left[\frac{1}{r}\ \frac{\partial (r\ V_\theta)}{\partial r}\right] \qquad \text{(A-7)}$$

In the case of steady state, the product of r and V_r can be approximated to a constant. Thus

$$\frac{\partial (rV_r)}{\partial r} \cong 0 \qquad \text{(A-8)}$$

which further reduces Eq. A-6 to

$$V_r \frac{\partial V_r}{\partial r} - \frac{V_\theta{}^2}{r} = -\frac{1}{\rho}\ \frac{\partial P}{\partial r} \qquad \text{(A-9)}$$

Rearranging Eq. A-7

$$V_r\left[\frac{\partial V_\theta}{\partial r} + \frac{V_\theta}{r}\right] = \nu\ \frac{\partial}{\partial r}\left[\frac{1}{r}\ \frac{\partial (rV_\theta)}{\partial r}\right] \qquad \text{(A-10)}$$

$$\left(\frac{V_r}{r}\right)\ \frac{\partial (rV_\theta)}{\partial r} = \nu\ \frac{\partial}{\partial r}\left[\frac{1}{r}\ \frac{\partial (rV_\theta)}{\partial r}\right] \qquad \text{(A-11)}$$

By taking advantage of

$$r\,V_r \cong \text{constant} = (Q/L) \qquad \text{(A-12)}$$

where Q is volumetric rate, Eq. A-11 can be expressed as

$$\frac{(Q/L)}{r^2}\left[\frac{\partial(rV_\theta)}{\partial r}\right] = \nu\,\frac{\partial}{\partial r}\left[\frac{1}{r}\,\frac{\partial(rV_\theta)}{\partial r}\right] \qquad \text{(A-13)}$$

of

$$\frac{(Q/L)}{\nu}\,\frac{1}{r^2}\,\frac{d(rV_\theta)}{dr} = \frac{d}{dr}\left[\frac{1}{r}\,\frac{d(rV_\theta)}{dr}\right] \qquad \text{(A-14)}$$

Let

$$\frac{1}{r}\,\frac{d(rV_\theta)}{dr} = g(r) \qquad \text{(A-15)}$$

Eq. A-14 is therefore

$$\frac{(Q/L)}{\nu}\,\frac{g(r)}{r} = \frac{d[g(r)]}{dr} \qquad \text{(A-16)}$$

or

$$\frac{(Q/L)}{\nu}\,\frac{dr}{r} = \frac{d[g(r)]}{g(r)}$$

$$\frac{(Q/L)}{\nu}\,\ln r = \ln\,[g(r)] + C$$

or

$$g(r) = K\,r^{\frac{(Q/L)}{\nu}} \qquad \text{(A-17)}$$

Equating Eq. A-17 and Eq. A-15

$$K\,r^{\frac{(Q/L)}{\nu}} = \frac{1}{r}\,\frac{d(rV_\theta)}{dr}$$

$$\frac{d(rV_\theta)}{dr} = K\,r^{\frac{(Q/L)}{\nu} + 1}$$

$$r\,V_\theta = \frac{K_1}{\frac{(Q/L)}{\nu} + 2}\,r^{\frac{(Q/L)}{\nu} + 2} + K_2$$

$$V_\theta = \frac{K_1}{\frac{(Q/L)}{\nu} + 2} r^{\frac{(Q/L)}{\nu} + 1} + \frac{K_2}{r} \tag{A-18}$$

If $\frac{(Q/L)}{\nu} = -2$, the solution approaches ∞. However, by substituting the value of -2 for $\frac{(Q/L)}{\nu}$ in Eq. A-16 we have

$$-2\frac{g(r)}{r} = \frac{d[g(r)]}{dr}$$

$$-2 \ln r = \ln g(r) + K$$

with Eq. A-15
$$g(r) = K_1 r^{-2} = \frac{1}{r}\frac{d(rV_\theta)}{dr} \tag{A-19}$$

$$K_1 r^{-1} = \frac{d(rV_\theta)}{dr}$$

$$K_2 + K_1 \ln r = rV_\theta$$

$$V_\theta = \frac{K_1 \ln r}{r} + \frac{K_2}{r} \tag{A-20}$$

Equation A-12 states that

$$V_r r = (Q/L), \text{ or } V_r = \frac{(Q/L)}{r}$$

$$\frac{\partial V_r}{\partial r} = -\frac{(Q/L)}{r^2} \text{ or } \frac{(Q/L)}{r}\frac{\partial V_r}{\partial r} = \frac{-(Q/L)^2}{r^3}$$

or
$$V_r \frac{\partial V_r}{\partial r} = \frac{-(Q/L)^2}{r^3} \tag{A-21}$$

Combining with Eq. A-9

$$V_r \frac{\partial V_r}{\partial r} - \frac{V_\theta^{\,2}}{r} = -\frac{1}{\rho}\frac{\partial P}{\partial r}$$

$$\frac{(Q/L)^2}{r^3} + \frac{V_\theta^2}{r} = \frac{1}{\rho}\frac{\partial P}{\partial r} \qquad \text{(A-22)}$$

Eq. A-18 can be squared to

$$V_\theta^2 = \frac{K_1^2}{\left[2 + \frac{Q/L}{\nu}\right]^2} r^{2\left[\frac{Q/L}{\nu}+1\right]} + \frac{K_2^2}{r^2} + \frac{2\,K_1K_2}{\left(2 + \frac{Q/L}{\nu}\right)} r^{\frac{(Q/L)}{\nu}}$$

(A-23)

Substituting Eq. A-23 into Eq. A-22 we have

$$\frac{dP}{dr} = \frac{\rho(Q/L)^2}{r^3} + \frac{\rho\,K_1^2}{\left(2 + \frac{(Q/L)}{\nu}\right)^2} r^{\left[2\frac{(Q/L)}{\nu}+1\right]} + \frac{\rho K_2^2}{r^3}$$

$$+ \frac{2\,\rho\,K_1K_2}{2 + \frac{(Q/L)}{\nu}} r^{\left[\frac{Q/L}{\nu}-1\right]} \qquad \text{(A-24)}$$

$$P(r) = -\frac{\rho\,[(Q/L)^2 + K_2^2]}{2r^2} + \frac{\rho\,K_1^2}{\left[2 + \frac{(Q/L)}{\nu}\right]^2\left(2+\frac{2(Q/L)}{\nu}\right)} r^{2\left[\frac{(Q/L)}{\nu}+1\right]}$$

(A-25)

$$+ \frac{2\,\rho\,K_1\,K_2}{\left[2 + \frac{(Q/L)}{\nu}\right]\left(\frac{(Q/L)}{\nu}\right)} r^{\frac{(Q/L)}{\nu}}$$

For Eq. A-24, when $\frac{(Q/L)}{\nu} = -1$.

$$\frac{dP}{dr} = \frac{[\rho(Q/L)^2 + \rho K^2{}_2]}{r^3} + \frac{\rho K_1{}^2}{r} + \frac{2\rho\ K_1K_2}{r^2} \qquad \text{(A-26)}$$

$$\therefore\ P(r) = \frac{-\rho[(Q/L)^2 + K_2{}^2]}{2r^2} + \rho K_1{}^2\ \ln r - \frac{2\rho\ K_1K_2}{r} \qquad \text{(A-27)}$$

By squaring Eq. A-20

$$V_\theta{}^2 = \frac{K_1{}^2\ (\ln r)^2}{r^2} + \frac{2\ K_1K_2\ \ln r}{r^2} + \frac{K_2{}^2}{r^2}$$

$$= \frac{1}{r^2}\ [K_1{}^2\ (\ln r)^2 + 2\ K_1K_2\ \ln r + K_2{}^2] \qquad \text{(A-28)}$$

Substituting Eq. A-28 into Eq. A-22

$$\frac{dP}{dr} = \frac{\rho(Q/L)^2}{r^3} + \frac{\rho}{r^3}\ [K_1{}^2\ (\ln r)^2 + 2\ K_1K_2\ \ln r + K_2{}^2]$$

$$= \frac{\rho}{r^3}\ [K_1{}^2\ (\ln r)^2 + 2\ K_1K_2\ \ln r + K_2{}^2 + (Q/L)^2] \qquad \text{(A-29)}$$

$$P(r) = \rho\ K_1{}^2 \int \frac{(\ln r)^2}{r^3} dr + 2\ K_1K_2\ \rho \int \frac{\ln r}{r^3}\ dr - \frac{\rho[K_2{}^2 + (Q/L)^2]}{2r^2} \qquad \text{(A-30)}$$

$$\int \frac{(\ln r)^2}{r^3}\ dr = \frac{r^{-2}\ (\ln r)^2}{-2} - \frac{2}{2}\int r^{-3}\ (\ln r)\, dr$$

$$= -\frac{(\ln r)^2}{2r^2} + \int \frac{(\ln r)}{r^3} dr \qquad \text{(A-31)}$$

Substituting Eq. A-31 into Eq. A-30

$$P(r) = -\rho\, K_1^{\,2}\, \frac{(\ln r)^2}{2r^2} + (2\, K_1 K_2\, \rho + K_1^{\,2}\rho) \int \frac{(\ln r)\, dr}{r^3}$$

$$- \frac{\rho\, [K_2^{\,2} + (Q/L)^2]}{2r^2} \qquad \text{(A-32)}$$

$$\int \frac{\ln r}{r^3}\, dr = \frac{r^{-2}}{-2} \ln r - \frac{r^{-2}}{4} = \frac{-\ln r}{2r^2} - \frac{1}{4r^2} = (\ln r + \tfrac{1}{2})(\frac{-1}{2r^2}) \qquad \text{(A-33)}$$

$$P(r) = -\rho\, K_1^{\,2}\, \frac{(\ln r)^2}{2r^2} - (2\, K_1 K_2\, \rho + K_1^{\,2}\rho) \frac{(\ln r + \frac{1}{2})}{2r^2}$$

$$- \frac{\rho [K_2^{\,2} + (Q/L)^2]}{2r^2}$$

$$= - \frac{\rho}{2r^2} [K_1^{\,2} (\ln r)^2 + K_2^{\,2} + (Q/L)^2$$

$$+ (\ln r + \tfrac{1}{2}) + K_2^{\,2} + (Q/L)^2] \; (2\, K_1 K_2 + K_1^{\,2}) \qquad \text{(A-34)}$$

To calculate the air core rotating velocity, we know from Eq. A-18

$$V_\theta = \frac{K_1}{2 + \frac{(Q/L)}{\nu}}\, r^{(\frac{Q/L}{\nu} + 1)} + \frac{K_2}{r}$$

$$(\frac{Q/L}{\nu} \neq -2) \qquad \text{(A-18)}$$

where $(Q/L) = V_r r$, and K_1 and K_2 are determined by the boundary conditions at r = a, and r = b (Figure A-1)

where $V_\theta = V_o$ at $r = a$

$V_\theta = 0$ at $r = b$

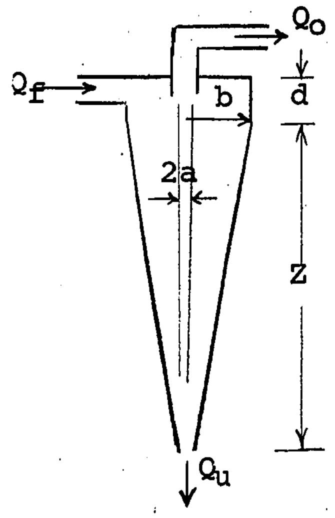

Figure A-1. Conventional Cyclone With Both Cylindrical and Conic Sections

$$V_o = \frac{K_1}{2 + \frac{(Q/L)}{\nu}} a^{(\frac{Q/L}{\nu} + 1)} + \frac{K_2}{a} \tag{A-35}$$

$$0 = \frac{K_1}{2 + \frac{(Q/L)}{\nu}} b^{(\frac{Q/L}{\nu} + 1)} + \frac{K_2}{b} \tag{A-36}$$

Multiplying Eq. A-35 by 1/b and Eq. A-36 by 1/a

$$\frac{V_o}{b} = \frac{K_1 \, a^{(\frac{Q/L}{\nu} + 1)}}{2 + \frac{(Q/L)}{\nu} b} + \frac{K_2}{ab} \tag{A-35a}$$

$$0 = \frac{K_1 \; b^{(\frac{Q/L}{\nu} + 1)}}{2 + (\frac{Q/L}{\nu})a} + \frac{K_2}{ab} \tag{A-36a}$$

$$\frac{V_o}{b} = \frac{K_1}{2 + (\frac{Q/L}{\nu})} \left[\frac{a^{(\frac{Q/L}{\nu} + 1)}}{b} - \frac{b^{(\frac{Q/L}{\nu} + 1)}}{a}\right], \text{ let } (\frac{Q/L}{\nu}) = \xi$$

$$K_1 = \frac{(\frac{V_o}{b})\;(2 + \xi)}{\frac{a^{\xi+1}}{b} - \frac{b^{\xi+1}}{a}} = \frac{2 + \xi}{a^{\xi+1} - \frac{b^{\xi+2}}{a}} \;(V_o)$$

$$= \frac{2 + \xi}{a^{\xi+2} - b^{\xi+2}} \;(a\;V_o) \tag{A-37}$$

Multiplying Eq. A-35 by $b^{(\xi+1)}$ and Eq. A-36 by $a^{(\xi+1)}$

$$V_o \; b^{\xi+1} = \frac{K_1}{2+\xi} \;(ab)^{\xi+1} + \frac{K_2 \; b^{\xi+1}}{a} \tag{A-38}$$

$$0 = \frac{K_1}{2+\xi} \;(ab)^{\xi+1} + \frac{K_2 \; a^{\xi+1}}{b} \tag{A-39}$$

Subtracting Eq. A-37 from Eq. A-38 we have

$$V_o \; b^{\xi+1} = K_2 \;(\frac{b^{\xi+1}}{a} - \frac{a^{\xi+1}}{b}) = K_2 \;(\frac{b^{\xi+2} - a^{\xi+2}}{ab})$$

$$K_2 = \frac{b^{\xi+2}}{b^{\xi+2} - a^{\xi+2}}(a\;V_o) \tag{A-40}$$

Substituting Eq. A-37 and Eq. A-40 into Eq. A-18 we have

$$V_\theta = \frac{a\ V_o}{a^{\xi+1}-b^{\xi+2}}\ r^{\xi+1} + \frac{b^{\xi+2}\ a\ V_o}{b^{\xi+2}-a^{\xi+2}}\ \frac{1}{r}$$

$$= \frac{a\ V_o}{a^{\xi+2}-b^{\xi+2}}\ (r^{\xi+1} - \frac{b^{\xi+2}}{r}) \qquad \text{(A-41)}$$

Now we can find the approximate value of V_o by energy conservation. The kinetic energy of the liquid in the hydrocyclone with the parameters as shown in Fig. A-1 is

$$\text{K.E.} = \frac{1}{2}\rho\ h_1 \int_a^b V_\theta^2\ 2\pi r dr + \frac{1}{2}\rho \int_o^{h_2}\int_a^{R=h_2\tan\alpha} (2\pi) V_\theta^2 r dr dh/3$$

$$= [\pi\rho h_1 \int_a^b V_\theta^2 r dr] + [\frac{\pi\rho}{3} \int_o^{h_2}\int_a^{h_2\tan\alpha} V_\theta^2 r dr dh] \qquad \text{(A-42)}$$

Squaring Eq. A-41 yields

$$V_\theta^2 = \frac{a^2\ V_o^2}{(a^{\xi+2}-b^{\xi+2})^2}\ [r^{2(\xi+1)} - 2b^{\xi+2} r^{\xi} + \frac{b^{2(\xi+2)}}{r^2}] \qquad \text{(A-43)}$$

$$\int V_\theta^2 r dr = \frac{a^2 V_o^2}{(a^{\xi+2} - b^{\xi+2})^2} \int (r^{2\xi+3} - 2b^{\xi+2}\ r^{\xi+1} + \frac{b^{2(\xi+2)}}{r})\, dr$$

$$= \frac{a^2\ V_o^2}{(a^{\xi+2}-b^{\xi+2})^2} \left[\frac{r^{2\xi+4}}{2\xi+4} - 2b^{\xi+2}\ \frac{r^{\xi+2}}{\xi+2} + b^{2(\xi+2)} \ln r\right]$$

$$\text{(A-44)}$$

For the first term of Eq.A-42

$$\int_a^b V_\theta^{\,2}\, rdr = \frac{a^2\, V_o^{\,2}}{(a^{\xi+2}-b^{\xi+2})^2}\left\{\left[\frac{b^{2\xi+4}}{2\ (\xi+2)} - \frac{2b^{2\xi+4}}{\xi+2} + b^{2(\xi+2)}\ell n\ b\right]\right.$$

$$\left.-\left[\frac{a^{2\xi+4}}{2\xi+4} - \frac{2b^{\xi+2}\ a^{\xi+2}}{\xi+2} + b^{2\ (\xi+2)}\ell n\ a\right]\right\} \qquad \text{(A-45)}$$

$$= \frac{a^2\ V_o^{\,2}}{(a^{\xi+2}-b^{\xi+2})^2}\left[b^{2\,(\xi+2)}\ell n\ b - (\tfrac{3}{2})\,\frac{b^{2\xi+4}}{\xi+2} - b^{2\,(\xi+2)}\ell n\ a\right.$$

$$\left.+ \frac{2(ab)^{\xi+2}}{\xi+2} - \frac{1}{2}\,\frac{a^{2\xi+4}}{(\xi+2)}\right]$$

$$= \frac{a^2 V_o^{\,2}}{a^{\xi+2}-b^{\xi+2})^2}\left[b^{2\,(\xi+2)}\ell n\,\frac{b}{a} - \frac{1}{2}\,\frac{3b^{2\xi+4}-a^{2\xi+4}}{\xi+2}\right.$$

$$\left.+ \frac{2\,(ab)^{\xi+2}}{\xi+2}\right] \qquad \text{(A-46)}$$

Substituting h_2 tan α for r in Eq. A-44

$$\int_o^{h_2}\int_a^{h_2\ \tan\ \alpha} V_\theta^{\,2} rdrdh = \frac{a^2 V_o^{\,2}}{(a^{\xi+2}+b^{\xi+2})^2}\int_o^{h_2}\left[\frac{(h_2\ \tan\ \alpha)^{2\xi+4}}{2\,(\xi+2)}\right.$$

$$- \frac{2b^{\xi+2}(h_2\ \tan\ \alpha)^{\xi+2}}{\xi+2}$$

$$\left.+ \ell n\ (h_2\ \tan\ \alpha)\ (b^{2\,(\xi+2)})\right] dh$$

$$= \frac{a^2\ V_o^{\,2}}{(a^{\xi+2}+b^{\xi+2})^2}\left[\frac{h_2^{\,2\xi+5}(\tan\ \alpha)^{2\xi+4}}{(2\xi+4)\ (2\xi+5)}\right.$$

$$- \frac{2b^{\xi+2}h_2^{\ \xi+3}\ (\tan\ \alpha)^{\xi+2}}{(\xi+2)\ (\xi+3)} \qquad \text{(A-47)}$$

$$\left.+ b^{2\,(\xi+2)}h_2\ \ (\ell n\ h_2\ - 1 + \ell n\ \tan\ \alpha)\right]$$

$$\text{Total K. E.} = \frac{\pi\rho\, h_1\, a^2\, V_o^2}{(a^{\xi+2}-b^{\xi+2})^2}\left[b^{2(\xi+2)}\,\ell n\,\frac{b}{a} - \frac{1}{2}\,\frac{3b^{2\xi+4}-a^{2\xi+4})}{(\xi+2)}\right.$$

$$\left. + \frac{2(ab)^{\xi+2}}{\xi+2}\right] + \frac{\pi\rho\, h_2\, a^2\, V_o^2}{3(a^{\xi+2}+b^{\xi+2})^2}\left[\frac{(h_2 \tan\alpha)^{2\xi+4}}{(2\xi+4)(2\xi+5)}\right.$$

$$- \frac{2b^{\xi+2}(h_2 \tan\alpha)^{\xi+2}}{(\xi+2)(\xi+3)} + b^{2(\xi+2)}(\ell n\, h_2 - 1$$

$$\left. + \ell n \tan\alpha)\right]$$

$$= \frac{a^2\,\rho\pi\, V_o^2}{(a^{\xi+2}-b^{\xi+2})^2}\left[h_1\ \text{K. E. (1)} + \frac{h_2}{3}\ \text{K. E. (2)}\right] \qquad \text{(A-48)}$$

By neglecting the gravitational potential energy, the net potential energy is = Inlet pressure x Volume of the cyclone.

$$\text{Volume} = \pi b^2\, h_1 + \int_o^{h_2} \pi(h \tan\alpha)^2 dh = \pi b^2 h_1 + \frac{\pi h_2^{\,3}}{3}\tan^2\alpha$$

$$\text{Total P. E.} = P_{in}\left[\pi b^2 h_1 + \frac{\pi h_2^{\,3}}{3}\tan^2\alpha\right] \qquad \text{(A-49)}$$

Assuming no energy loss due to viscous shear we have

$$\text{Total P. E.} = \text{Total K. E.} \qquad \text{(A-50)}$$

$$\frac{a^2\rho\pi\, V_o^2}{(a^{\xi+2}-b^{\xi+2})^2}\left[h_1\ \text{K. E. (1)} + \frac{h_2}{3}\ \text{K. E. (2)}\right] = P_{in}\left[\pi b^2 h_1\right.$$

$$+ \frac{\pi h_2^{\,3}}{3} \tan^2 \alpha \Big]$$

$$V_o = \frac{a^{\xi+2} - b^{\xi+2}}{a} \sqrt{\frac{P_{in} \left(b^2 h_1 + \frac{h_2^{\,3}}{3} \tan^2 \alpha\right)}{\rho\left[h_1 \text{ K.E.}(1) + \frac{h_2}{3} \text{ K.E.}(2)\right]}} \qquad \text{(A-51)}$$

For a cyclone of negligible vertical section, Eq. 56 can be reduced to

$$V_o \cong \frac{a^{\xi+2} - b^{\xi+2}}{a} \sqrt{\frac{P_{in} \left(h_2^{\,2} \tan^2 \alpha\right)}{\rho[\text{K.E.}(2)]}} \qquad \text{(A-52)}$$

APPENDIX B

COMPARISON OF TWO DEFINITIONS OF SEPARATION EFFICIENCY

1) The general equation for the separation efficiency involving any number of phases is

$$E_{overall} = \left| \frac{\sum_{1}^{A_n} (A)_o}{\sum_{1}^{A_n} (A)_f} - \frac{\sum_{1}^{B_n} (B)_o}{\sum_{1}^{B_n} (B)_f} \right| = \left| \frac{\sum_{1}^{A_n} (A)_u}{\sum_{1}^{A_n} (A)_f} - \frac{\sum_{1}^{B_n} (B)_u}{\sum_{1}^{B_n} (B)_f} \right| \quad \text{(B-1)}$$

where $A_1, A_2, A_3, \ldots A_n$ are lighter phases desired to leave in the overflow

$B_1, B_2, B_3, \ldots B_n$ are heavier phase desired to leave in the underflow

Subscript o, f, u denote overflow, feed, underflow and

$$(A_1 + A_2 + A_3 + \ldots)_o + (B_1 + B_2 + B_3 + \ldots)_o = Q_o \quad (70)$$

$$(A_1 + A_2 + A_3 + \ldots)_u + (B_1 + B_2 + B_3 + \ldots)_u = Q_u \quad (71)$$

$$(A_1 + A_2 + A_3 + \ldots)_f + (B_1 + B_2 + B_3 + \ldots)_f = Q_f \quad (72)$$

For a two-phase system (A and B)

let $A_o = Q_o x_o$ $\quad B_o = Q_o y_o$

$A_u = Q_u x_u$ $\quad B_u = Q_u y_u$

$A_f = Q_f x_f$ $\quad B_f = Q_f y_f$

Eq. B-1 is reduced to Eq. 68

$$E_{overall} = \left| \frac{Q_o x_o}{Q_f x_f} - \frac{Q_o y_o}{Q_f y_f} \right| = \left| \frac{Q_u x_u}{Q_f x_f} - \frac{Q_u y_u}{Q_f y_f} \right| \qquad \text{(B-2)}$$

For a three-phase system (A_1, A_2 and B) where phase A_2 is, say, a solid preferentially wetted by the lighter phase, A_1, and is desired to exit in the overflow

$$(A_1)_o = Q_o x_o,\ (A_2)_o = Q_o z_o,\ B_o = Q_o y_o$$

$$(A_1)_u = Q_u x_u,\ (A_2)_u = Q_u z_u,\ B_u = Q_u y_u$$

$$(A_1)_f = Q_f x_f,\ (A_2)_f = Q_f z_f,\ B_f = Q_f y_f$$

$$E_{overall} = \left| \frac{Q_o(x_o+z_o)}{Q_f(x_f+z_f)} - \frac{Q_o y_o}{Q_f y_f} \right| = \left| \frac{Q_u(x_u+z_u)}{Q_f(x_f+z_f)} - \frac{Q_u y_u}{Q_f y_f} \right| \qquad \text{(B-3)}$$

2) In this investigation, the general equation for the separation efficiency involving any number of phases is

$$E_{overall} = \sum_1^n E_{A_1, A_2 \ldots, B_1, B_2 \ldots} = \sum_1^{A_n} E_A + \sum_1^{B_n} E_B$$

$$= \frac{1}{Q_f}\left[Q_o \left(\frac{\sum_1^{A_n} \frac{(A)_o}{Q_o} - \sum_1^{A_n} \frac{(A)_f}{Q_f}}{\frac{\sum_1^{B_n} (B)_f}{Q_f}} \right) + Q_u \left(\frac{\sum_1^{B_n} \frac{(B)_u}{Q_u} - \sum_1^{B_n} \frac{(B)_f}{Q_f}}{\frac{\sum_1^{A_n} (A)_f}{Q_f}} \right) \right] \qquad \text{(B-4)}$$

For a two-phase system (A-B), Eq. B-4 is reduced to Eq. 62.

$$E_{overall} = E_A + E_B = \frac{Q_o}{Q_f}\left[x_o - (1-x_o)\frac{x_f}{1-x_f} \right] + \frac{Q_u}{Q_f}\left[y_u - (1-y_u)\frac{x_f}{1-x_f} \right] \qquad (62)$$

For a three-phase system (A_1-A_2-B) Eq. B-4 is reduced to Eq. 66

$$E_{overall} = E_{A_1} + E_{A_2} + E_B$$

$$= \frac{Q_o}{Q_f}\ \frac{(x_o - x_f + x_f z_o - x_o z_f)}{(1 - x_f - Z_f)} + \frac{Q_o}{Q_f}\ \frac{(z_o - z_f + z_f x_o - x_f z_o)}{(1 - x_f - Z_f)}$$

$$+ \frac{Q_u}{Q_f}\ \frac{(y_u - y_f)}{(1 - y_f)}$$

$$= \frac{Q_o}{Q_f}\ \frac{(x_o - x_f + z_o - z_f)}{(1 - x_f - z_f)} + \frac{Q_u}{Q_f}\ \frac{(y_u - y_f)}{(1 - y_f)} \qquad (66)$$

For the purpose of illustrating the identity between Eq. 63 and Eq. 68, the following algebraic proof is provided:

a) For a two-phase system, Eq. 68 is

$$E = \frac{Q_o x_o}{Q_f x_f} - \frac{Q_o y_o}{Q_f y_f} = \frac{Q_o x_o y_f - Q_o y_o x_f}{Q_f x_f y_f}$$

$$= \frac{Q_o x_o (1 - x_f) - Q_o x_f (1 - x_o)}{Q_f x_f (1 - x_f)}$$

$$= \frac{Q_o x_o - Q_o x_o x_f - Q_o x_f + Q_o x_f x_o}{Q_f x_f (1 - x_f)}$$

$$= \frac{Q_o x_o - Q_o x_f}{Q_f x_f (1 - x_f)} = \frac{Q_o (x_o - x_f)}{Q_f x_f (1 - x_f)} \qquad (63)$$

b) For a three-phase system (Run No. 55) given

$$Q_f = 75.0 \qquad Q_o = 56.70 \qquad Q_u = 18.30$$

$$x_f = 0.654 \qquad x_o = 0.773 \qquad x_u = 0.277$$

$$y_f = 0.332 \qquad y_o = 0.211 \qquad y_u = 0.699$$

$$z_f = 0.014 \qquad z_u = 0.016 \qquad z_u = 0.024$$

$$Q_f x_f = 49.0 \qquad Q_f y_f = 24.9 \qquad Q_f z_f = 1.05$$

$$Q_o x_o = 43.9 \qquad Q_o y_o = 12.0 \qquad Q_o z_o = 0.90$$

$$Q_u x_u = 5.1 \qquad Q_u y_u = 12.9 \qquad Q_u z_u = 0.15$$

$$E = \frac{Q_o(x_o+z_o)}{Q_f(x_f+z_f)} - \frac{Q_o y_o}{Q_f y_f} = \frac{56.7(0.789)}{75.0(0.668)} - \frac{12.0}{24.9} = 0.409$$

and

$$E_{A_1} = \frac{Q_o}{Q_f}\left[\frac{x_o-x_f + x_f z_o - x_o z_f}{1-x_f-z_f}\right] = 0.756\left[\frac{0.119 + 0.0115-0.011}{0.332}\right] = 0.271$$

$$E_{A_1} = \frac{Q_o}{Q_f}\left[\frac{z_o-z_f + x_o z_f - z_o x_f}{1-x_f-z_f}\right] = 0.756\left[\frac{0.002 + 0.011-0.011}{0.332}\right] = 0.0046$$

$$E_B = \frac{Q_u}{Q_f}\left[\frac{y_u-y_f}{1-y_f}\right] = 0.244\left(\frac{0.699-0.332}{0.668}\right) = 0.244\left(\frac{0.367}{0.668}\right) = 0.134$$

$$E = E_{A_1} + E_{A_2} + E_B = 0.409$$

APPENDIX C

IDEAL EFFICIENCY VALUES VERSUS EFFLUENT SPLITS

Although ideal separation efficiencies are independent of feed rates, it is necessary to assume a number (Q_f) in order to obtain the values. By applying the prescribed conditions outlined on Page 41 to Eq. 62 and by enlisting the aid of a FORTRAN computer program shown below, a table of values is given in the following pages.

```
C       IDEAL SEPARATION EFFICIENCY CALCULATION
        QF = 60.0
        LNCT = 54
        XOY = 0.0
        DO 650 K = 1,6
        QO = 0.0
        IF (XOY-1.0) 110, 115, 115
110     XOY = XOY + 0.5
        GO TO 116
115     XOY = XOY + 1.0
116     XF = XOY/(1.0 + XOY)
        DO 600 J = 1,7
        QO = QO + 10.0
        QU = QF - QO
        IF (QU) 650, 650, 100
100     IF ((QO/QU)-XOY) 200, 300, 400
200     XO = 1.0
        YU = 1.0 - ((QF*XF-QO)/QU)
        GO TO 500
300     XO = 1.0
        YU = 1.0
        GO TO 500
400     YU = 1.0
        XO = 1.0 - (QF*(1.0-XF)-QU)/QO
```

```
500     YF = 1.0 - XF
        A1 = ((XO-XF) / (1.0-XF))*QU/QF
        A2 = ((YU-YF) / (XF))*QU/QF
        A3 = QO/QU
        ES = A1 +A2
        A4 = XF/YF
        IF(LNCT-54) 550, 510, 510
510     WRITE (3,5000)
        LNCT = 0
550     LNCT = LNCT + 1
        WRITE (3,5100) QF, XO, YU, XF, YF, A4, A1,
          A2, ES, A3
5100    FORMAT (' '10F7.3)
5000    FORMAT ('0'/'0')
600     CONTINUE
650     CONTINUE
        END
```

TABLE C-1

IDEAL SEPARATION EFFICIENCY (E_s) VS. EFFLUENT SPLIT (Q_o/Q_u) FOR VARIOUS FEED PHASE RATIOS (x_f/y_f)

Q_f*	x_o	y_u	x_f	y_f	x_f/y_f	E_x	E_y	E_s	Q_o/Q_u
60.000	1.000	0.800	0.333	0.667	0.500	0.167	0.333	0.500	0.200
60.000	1.000	1.000	0.333	0.667	0.500	0.333	0.667	1.000	0.500
60.000	0.667	1.000	0.333	0.667	0.500	0.250	0.500	0.750	1.000
60.000	0.500	1.000	0.333	0.667	0.500	0.167	0.333	0.500	2.000
60.000	0.400	1.000	0.333	0.667	0.500	0.083	0.167	0.250	5.000
60.000	1.000	0.600	0.500	0.500	1.000	0.167	0.167	0.333	0.200
60.000	1.000	0.750	0.500	0.500	1.000	0.333	0.333	0.667	0.500
60.000	1.000	1.000	0.500	0.500	1.000	0.500	0.500	1.000	1.000
60.000	0.750	1.000	0.500	0.500	1.000	0.333	0.333	0.667	2.000
60.000	0.600	1.000	0.500	0.500	1.000	0.167	0.167	0.333	5.000
60.000	1.000	0.400	0.667	0.333	2.000	0.167	0.083	0.250	0.200
60.000	1.000	0.500	0.667	0.333	2.000	0.333	0.167	0.500	0.500
60.000	1.000	0.667	0.667	0.333	2.000	0.500	0.250	0.750	1.000
60.000	1.000	1.000	0.667	0.333	2.000	0.667	0.333	1.000	2.000
60.000	0.800	1.000	0.667	0.333	2.000	0.333	0.167	0.500	5.000
60.000	1.000	0.300	0.750	0.250	3.000	0.167	0.056	0.222	0.200
60.000	1.000	0.375	0.750	0.250	3.000	0.333	0.111	0.444	0.500
60.000	1.000	0.500	0.750	0.250	3.000	0.500	0.167	0.667	1.000
60.000	1.000	0.750	0.750	0.250	3.000	0.667	0.222	0.889	2.000
60.000	0.900	1.000	0.750	0.250	3.000	0.500	0.167	0.667	5.000
60.000	1.000	0.240	0.800	0.200	4.000	0.167	0.042	0.208	0.200
60.000	1.000	0.300	0.800	0.200	4.000	0.333	0.083	0.417	0.500
60.000	1.000	0.400	0.800	0.200	4.000	0.500	0.125	0.625	1.000
60.000	1.000	0.600	0.800	0.200	4.000	0.667	0.167	0.833	2.000
60.000	0.960	1.000	0.800	0.200	4.000	0.667	0.167	0.833	5.000
60.000	1.000	0.200	0.833	0.167	5.000	0.167	0.033	0.200	0.200
60.000	1.000	0.250	0.833	0.167	5.000	0.333	0.067	0.400	0.500
60.000	1.000	0.333	0.833	0.167	5.000	0.500	0.100	0.600	1.000

*Ideal efficiency values are independent of feed rates.

TABLE C-1 (Continued)

Q_f*	x_o	y_u	x_f	y_f	x_f/y_f	E_x	E_y	E_s	Q_o/Q_u
60.000	1.000	0.500	0.833	0.167	5.000	0.667	0.133	0.800	2.000
60.000	1.000	1.000	0.833	0.167	5.000	0.833	0.167	1.000	5.000
60.000	1.000	0.171	0.857	0.143	6.000	0.167	0.028	0.194	0.200
60.000	1.000	0.214	0.857	0.143	6.000	0.333	0.056	0.389	0.500
60.000	1.000	0.286	0.857	0.143	6.000	0.500	0.083	0.583	1.000
60.000	1.000	0.429	0.857	0.143	6.000	0.667	0.111	0.778	2.000
60.000	1.000	0.857	0.857	0.143	6.000	0.833	0.139	0.972	5.000
60.000	1.000	0.150	0.875	0.125	7.000	0.167	0.024	0.190	0.200
60.000	1.000	0.188	0.875	0.125	7.000	0.333	0.048	0.381	0.500
60.000	1.000	0.250	0.875	0.125	7.000	0.500	0.071	0.571	1.000
60.000	1.000	0.375	0.875	0.125	7.000	0.667	0.095	0.762	2.000
60.000	1.000	0.750	0.875	0.125	7.000	0.833	0.119	0.952	5.000

*Ideal efficiency values are independent of feed rates.

APPENDIX D

SAMPLE DATA SHEET AND CALCULATIONS

In the following page is a sample data sheet of a typical run (No. 198) conducted under the prescribed conditions as indicated. The calculation procedure for obtaining the overall separation efficiency is quite simple.

$$x_o + z_o = \frac{\text{oil + solid}}{\text{run volume}} = \frac{25.73}{26.06} = 0.988$$

$$y_u = \frac{\text{water volume}}{\text{run volume}} = \frac{19.74}{34.02} = 0.580$$

$$x_f + z_f = 0.666$$

$$y_f = 0.334$$

$$E = \frac{Q_o[(x_o+z_o) - (x_f+z_f)]}{Q_f[\ 1 \quad - (x_f+z_f)]} + \frac{Q_u(y_u-y_f)}{Q_f(1 - y_f)}$$

$$= \frac{26.06\ (0.988 - 0.666)}{60.08\ (\ 1 \quad - 0.666)} + \frac{34.02\ (0.580 - 0.334)}{60.08\ (\ 1 \quad - 0.334)}$$

$$= 0.627$$

$$Q_o/Q_u = 26.06/34.02 = 0.766$$

Data Sheet
(Liquid-Solid-Liquid Separation)

Date 10/10/1967 Run No. 197

(1) Diameter 30 mm. Discharge orifice 3.0 mm. VFT Small

(2) Pressure 5.0 - 5.5 lb/in^2, % solids in oil tank 4.0%, D_p 0.294 mm.

Desired Flow Rate 60 cc/sec. Oil/H_2O = 2.0

Overflow

(A)

water vol.	34	cc.
oil + solids	2585	cc.
dry sol. + tare	46.79	gm.
tare wt.	4.02	gm.
dry solid	42.77	gm.
	46.3	cc.

solid content in oil = 1.79%

(B)

run vol. = 2619 cc/100.5 sec = 26.06 cc/sec
water vol. = 34 cc/100.5 sec = 0.34 cc/sec
oil + sol. = 2585 cc/100.5 sec = 25.73 cc/sec

Underflow

(A)

water vol.	1984	cc.
oil + solids	1435	cc.
dry sol. + tare	114.69	gm.
tare wt.	5.42	gm.
dry solid	109.27	gm.
	118.4	cc.

solid content in oil = 8.27%

(B)

run vol. = 3419 cc/100.5 sec = 34.02 cc/sec
water vol. = 1984 cc/100.5 sec = 19.74 cc/sec
oil + sol. = 1435 cc/100.5 sec = 14.28 cc/sec

Total throughput = 60.08 cc/sec. = 100.00%
Total water vol. = 20.08 cc/sec. = 33.43%
Total oil + solids = 40.00 cc/sec. = 66.57%

Total solids in overflow = 0.461 cc/sec.
Total solids in underflow = 1.180 cc/sec.
Total solids entering = 1.641 cc/sec.

Solid conc. in oil = 4.07%

Solid conc. in fluid = 2.71%

Overflow/underflow (solids) = o.391
Overflow/underflow (oil + solids = 1.80
Overflow/underflow (total) = 0.766

Overflow/underflow (oil) = 1.93
Overflow/underflow (water) = 0.017

APPENDIX E

PRESENTATION OF DATA

There are three tables presented in this appendix. Table E-1 serves as an index for the reader to locate a particular run of a given set of parameters. Table E-2 contains all the unprocessed experimental data as well as calculated actual efficiencies. The measurement error inherent within each column in Table E-2 is given in Chapter V. In Table E-3 are included the treated data and the detailed calculation procedures in a FORTRAN computer program.

Preliminary Treatment of Raw Data

Since all the feed rates (Q_f) varied less than ±1.5% from the desired values, it is assumed that such a deviation will have very little effect on the measured variables. To achieve the uniqueness within each set of runs and to facilitate the processing of raw data for subsequent computations, a factor was applied to each Q_f in order to adjust it to the exact desired feed rates: 50.00, 60.00 and 75.00 cc/sec. Consequently both Q_o and Q_u were also adjusted proportionally.

The trial and error procedure outlined previously for determining the average macroscopic turbulent length between a pair of adjacent runs further requires the Q_o or Q_u interval between each pair to be consistent throughout the entire set. In order to permit the turbulent length calculations to be made, it was therefore necessary to obtain values of the efficiency at Q_o/Q_u ratios other than the measured ratios. These interpolated values for efficiency and Q_o/Q_u ratios were obtained for each difference in overflow or underflow rate of 2.0 cc/sec. Interpolation was carried out only between measured values for efficiency and Q_o/Q_u. A total of 445 interpolated data points were obtained based on the original 240 measured data points. All the interpolated points are contained in Table E-3 and are prefixed by a letter C in the discussions. While the separation efficiency value for each interpolated effluent split (Q_o/Q_u) could be located from the original efficiency curve, it was not possible to reassign a new value of an independent variable ($x_f + z_f$) from another independent variable--effluent split (Q_o/Q_u)--without further experimental work. To remedy this situation, it was again necessary to resort to the assumption applied earlier that slight variations from the desired feed phase ratio (0.5, 1.0 and 2.0) were also insignificant to the measured dependent variables x_o, y_u, etc. Hence an average value of ($x_f + z_f$)

within each set of runs was obtained by the following method.

$$(x_f + z_f)_{ave.} = \frac{\sum_1^n [Q_f(x_f + z_f)]_i}{\sum_1^n [(Q_f)]_i}$$

where n is the total number of runs in the original set, and subscript i is designated to each individual run. Once the value of $(x_f + z_f)$ was estimated, the $(x_o + z_o)$ and y_u corresponding to each interpolated effluent split was readily obtained from the efficiency,

$$E = \frac{Q_o[(x_o + z_o)-(x_f + z_f)]}{Q_f[1 - (x_f + z_f)]} + \frac{Q_u(y_u-y_f)}{Q_f(1 -y_f)} \qquad (66)$$

and the material balance,

$$[1 - (x_o + z_o)]Q_o + y_uQ_u = Q_f[1 - (x_f + z_f)] \qquad (58)$$

A computer program was written to make the desired calculations. The program is listed later in this appendix and the results of the calculations for $(x_o + z_o)$ and y_u are included in Table E-3.

Overall Separation Efficiency Curve vs. Effluent Split at Various Specified Parameters

For the convenience of locating a particular run or an efficiency curve, the following table is provided. Thus, if it is desired to locate the efficiency curve of a given set of parameters, say Q_f = 60 cc/sec, phase ratio (oil/water) = 1.0, solid content 2% and solid size 0.832 mm, the number will be Figure E-2 as indicated in this case by the superscript o in the following table

TABLE E-1

Index Table for Sets and Run Numbers

oil/water ↓	$2\sigma_s$ = 0.832 mm			$2\sigma_s$ = 0.294 mm		
	2% solids					
1/2 (run No)	10 (75-82)	1 (1-7)	$11^{\square}$ (82-85)	25 (169-72)	22 (153-57)	24 (164-68)
1/1	8 (60-68)	2^{o} (8-17)	7* (51-59)	26 (173-77)	23 (158-63)	27* (178-81)
2/1	9 (69-74)	3 (18-26)	4,5,6 (27-50)	30 (191-94)	29 (186-90)	28 (182-85)
	4% solids					
1/2	12 (86-92)	13,14 (93-103)	15 (104-9)	38 (229-33)	37 (222-28)	39 (234-39)
1/1	21 (147-52)	16 (110-15)	17* (116-26)	36 (217-21)	33 (202-7)	32* (199-01)
2/1	20 (142-46)	18 (127-34)	19 (135-41)	34 (208-12)	31 (195-8)	35 (213-16)
Q_f cc/sec	50	60	75	50	60	75

* Separation disrupted seriously by intense emulsification.

$\square$ Separation interfered by moderate emulsification.

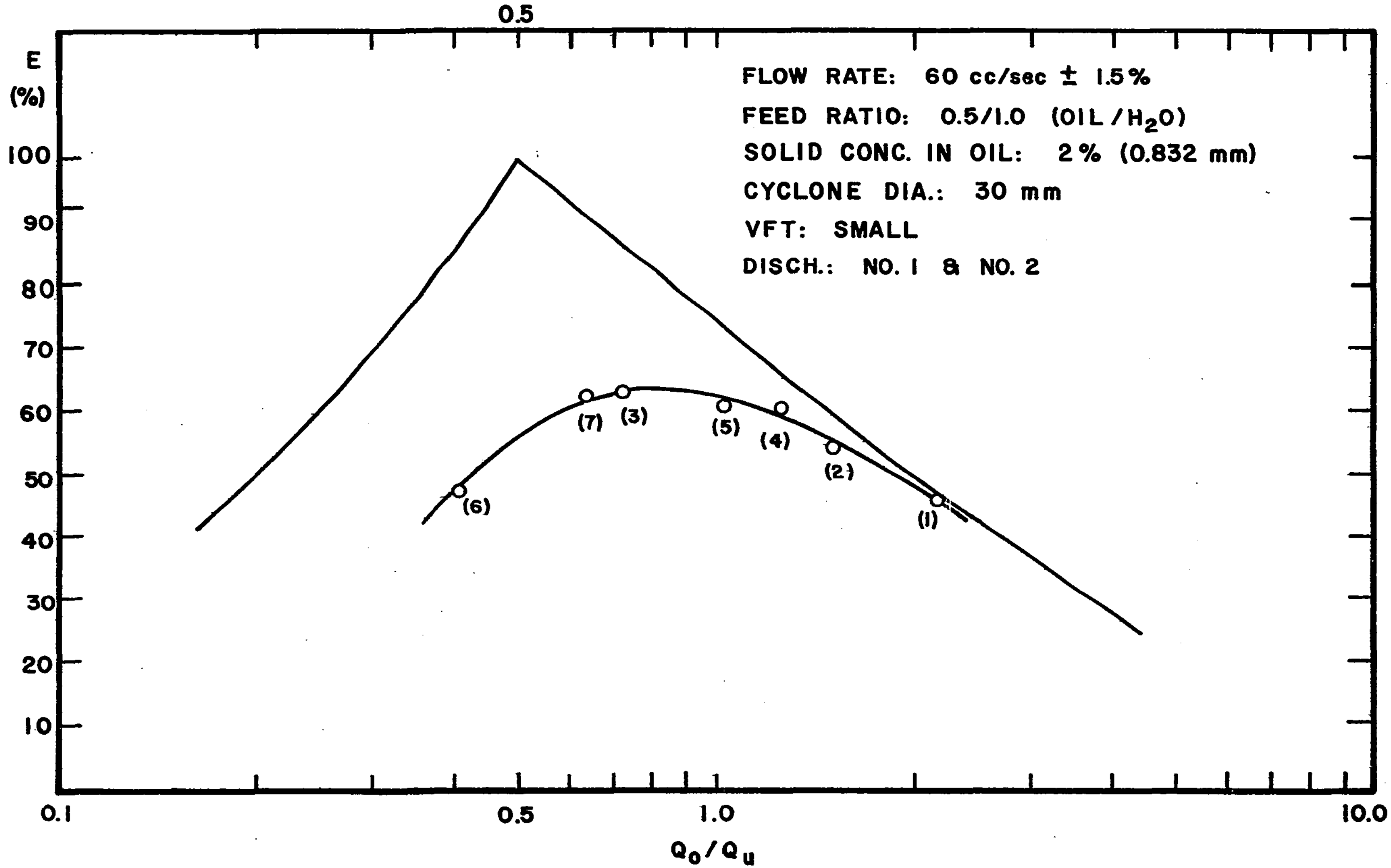

Figure E-1. Overall Efficiency vs. Effluent Split.

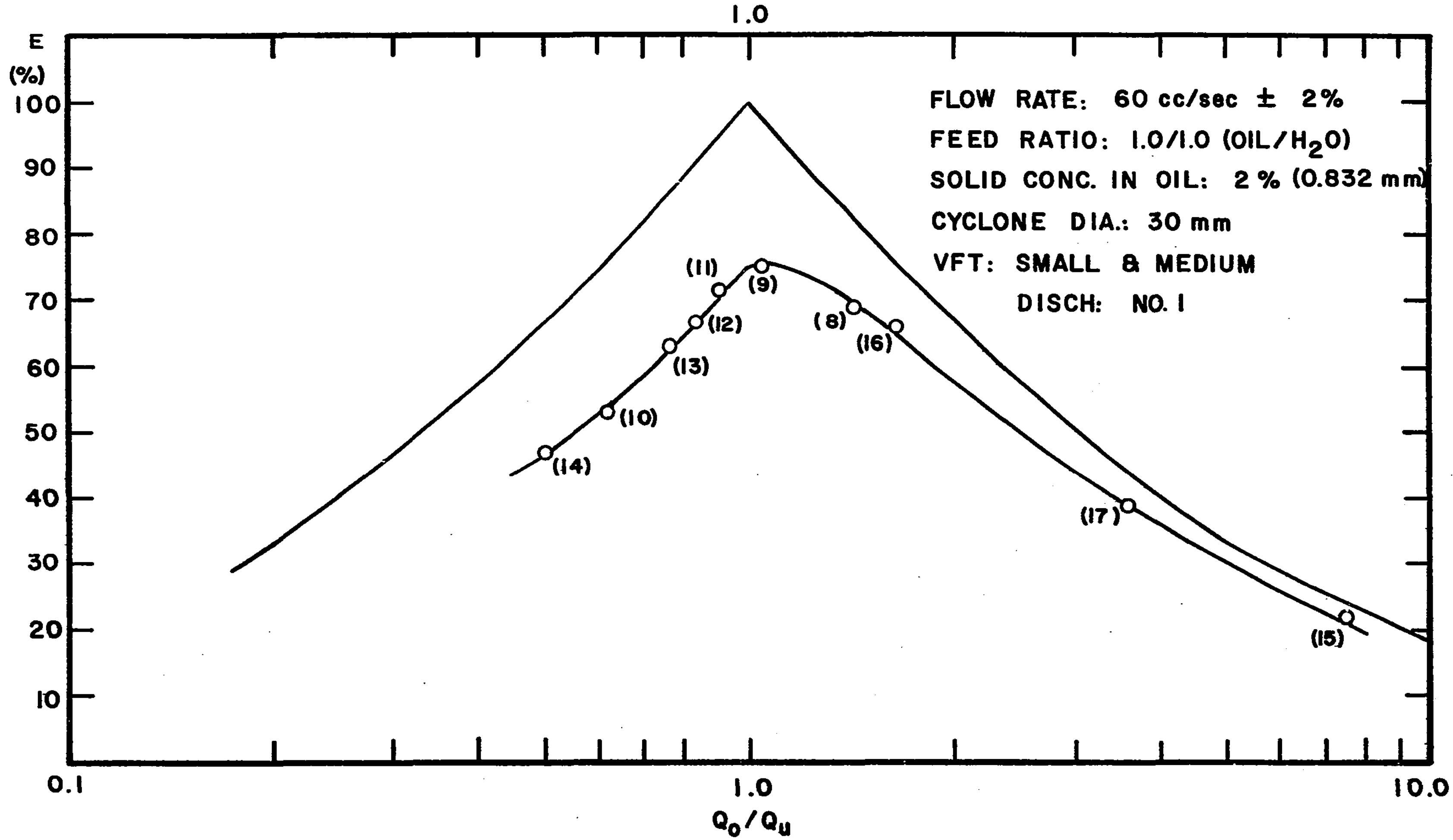

Figure E-2. Overall Efficiency vs. Effluent Split.

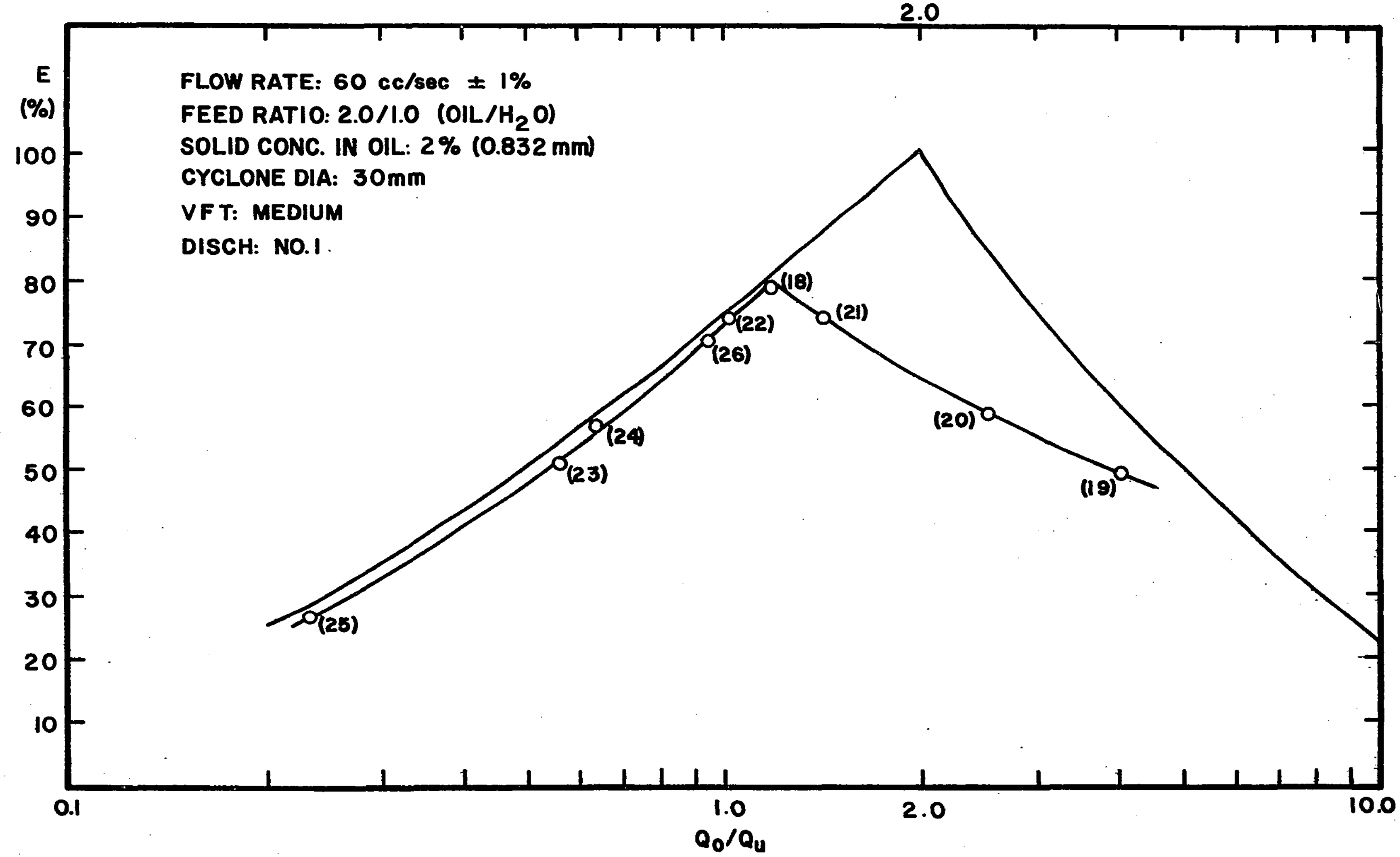

Figure E-3. Overall Efficiency vs. Effluent Split.

116

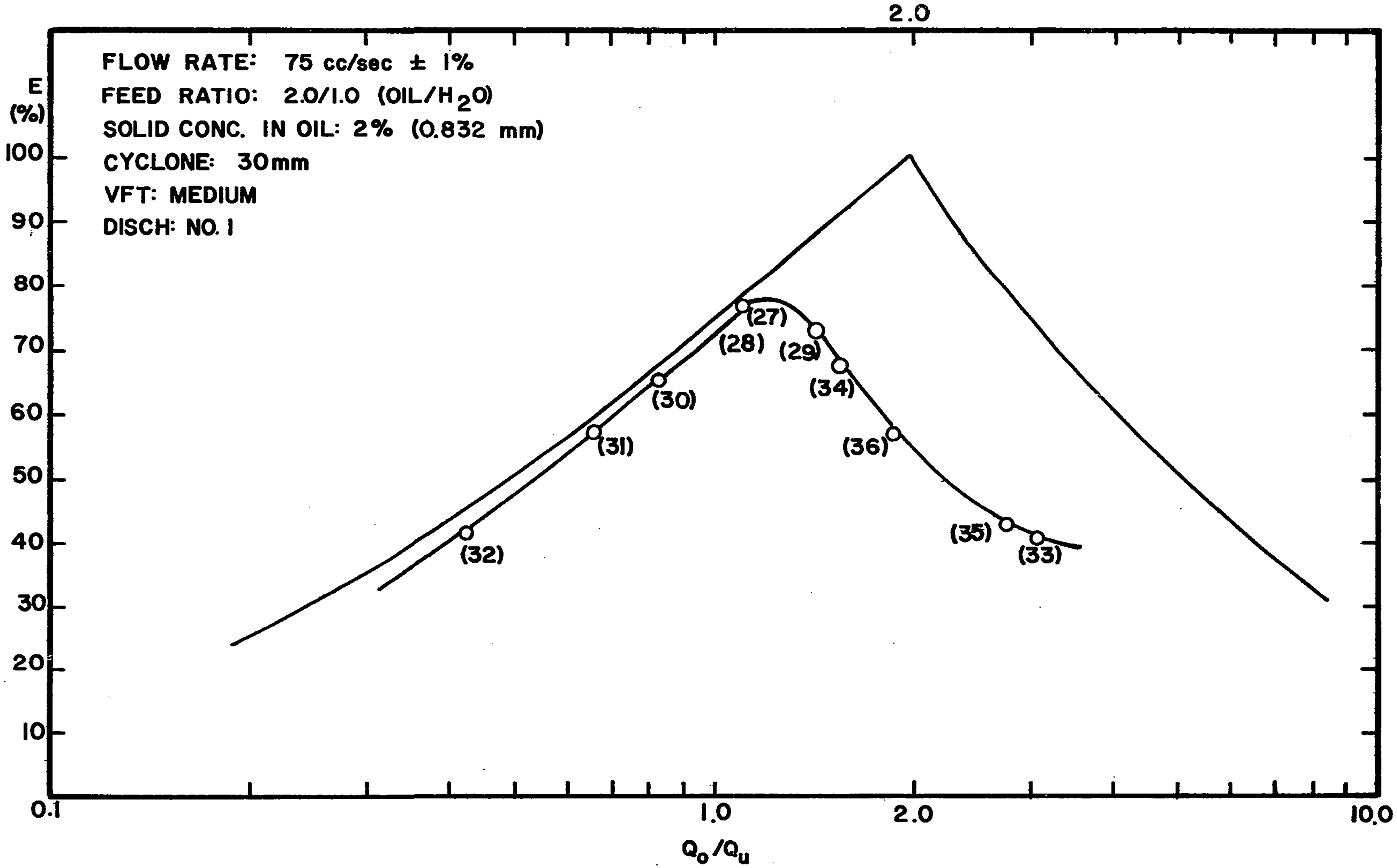

Figure E-4. Overall Efficiency vs. Effluent Split.

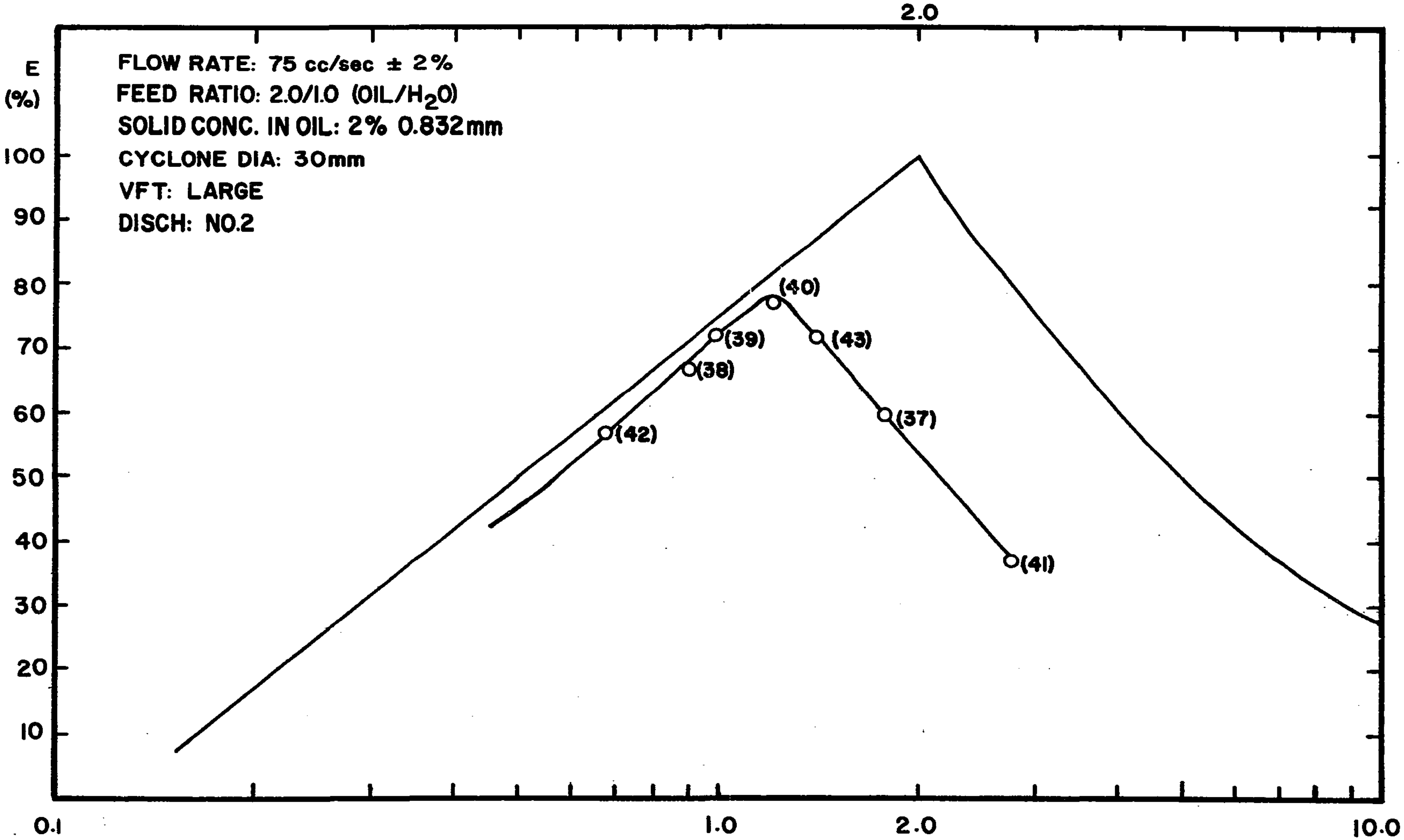

Figure E-5. Overall Efficiency vs. Effluent Split.

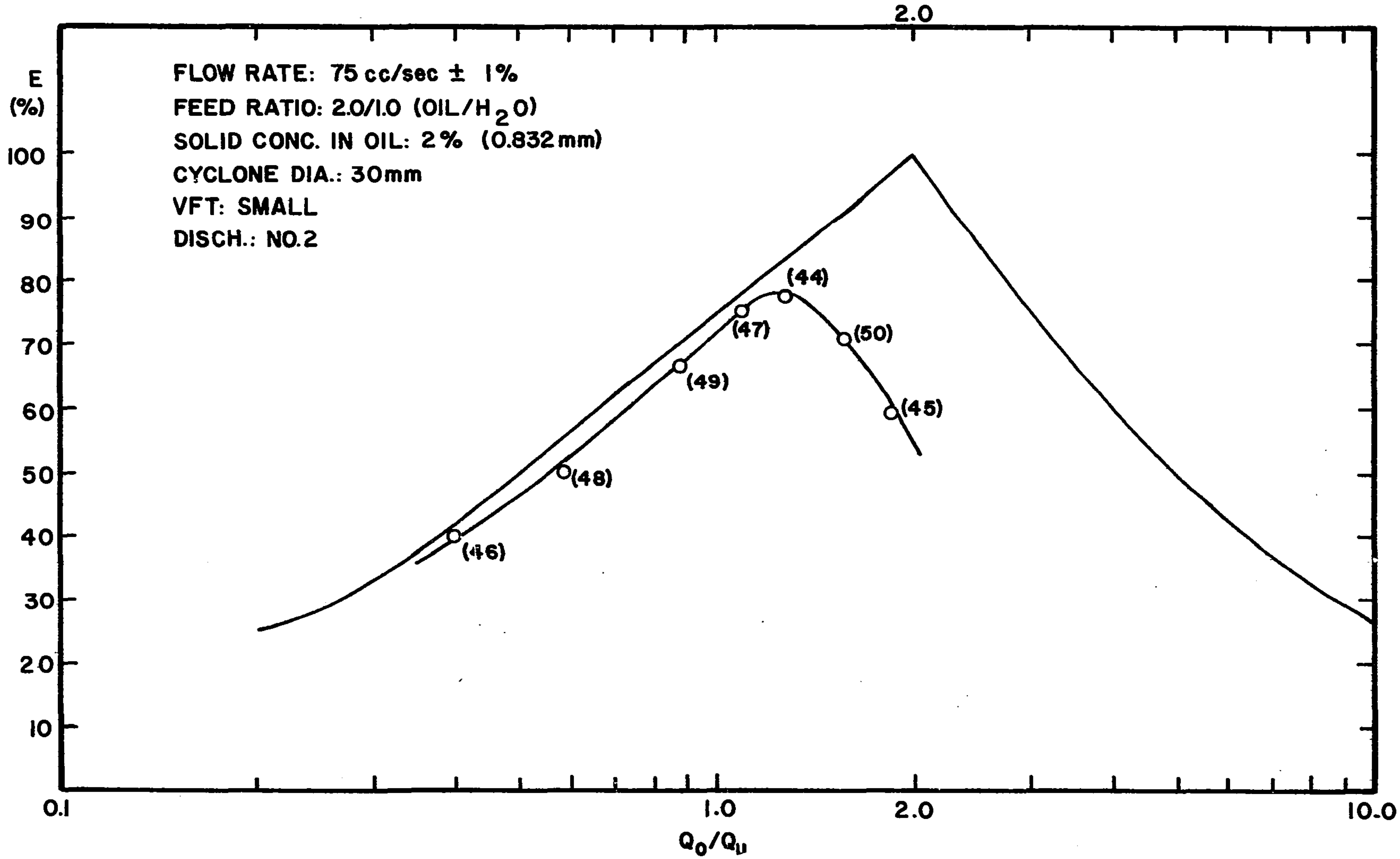

Figure E-6. Overall Efficiency vs. Effluent Split.

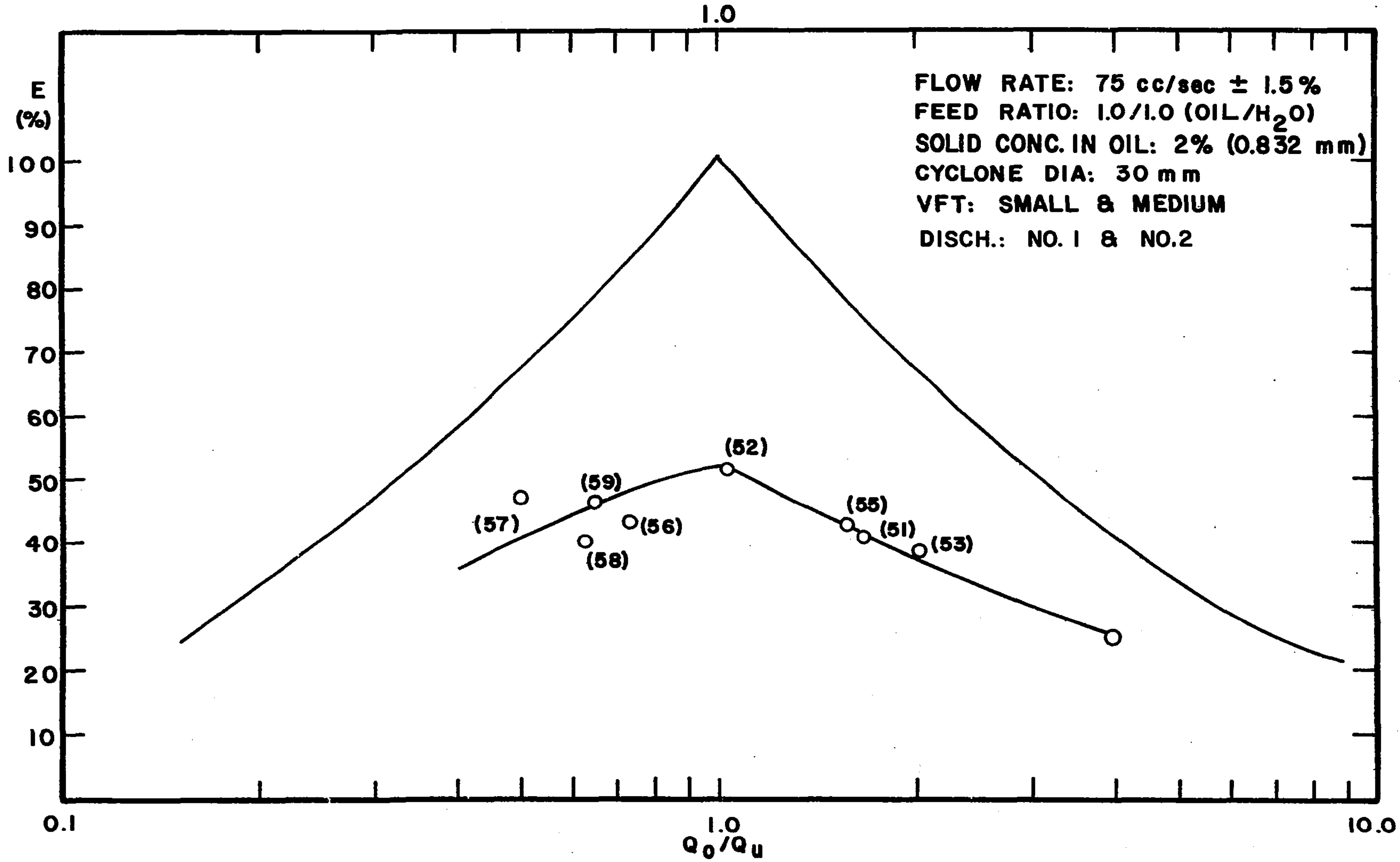

Figure E-7. Overall Efficiency vs. Effluent Split.

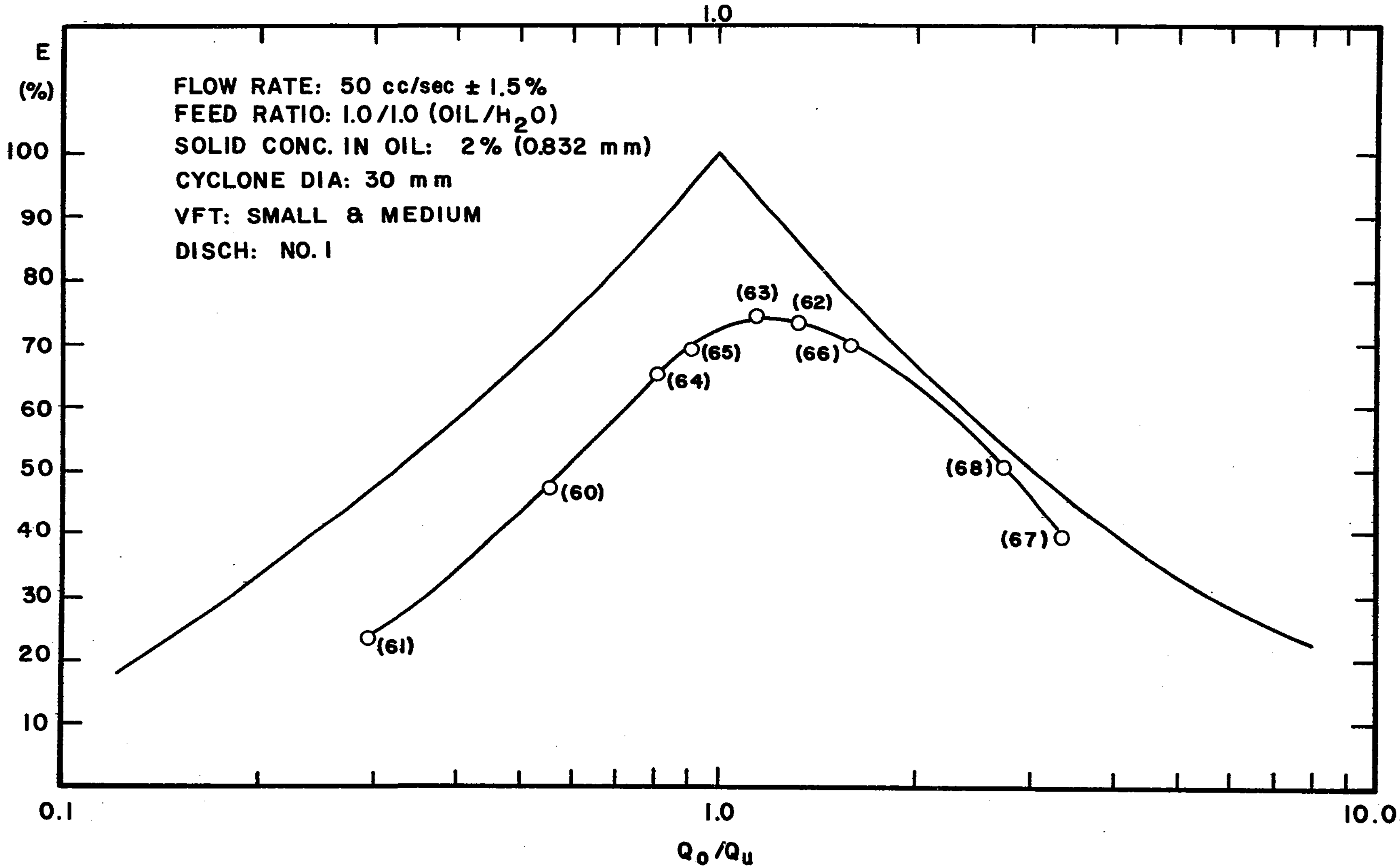

Figure E-8. Overall Efficiency vs. Effluent Split.

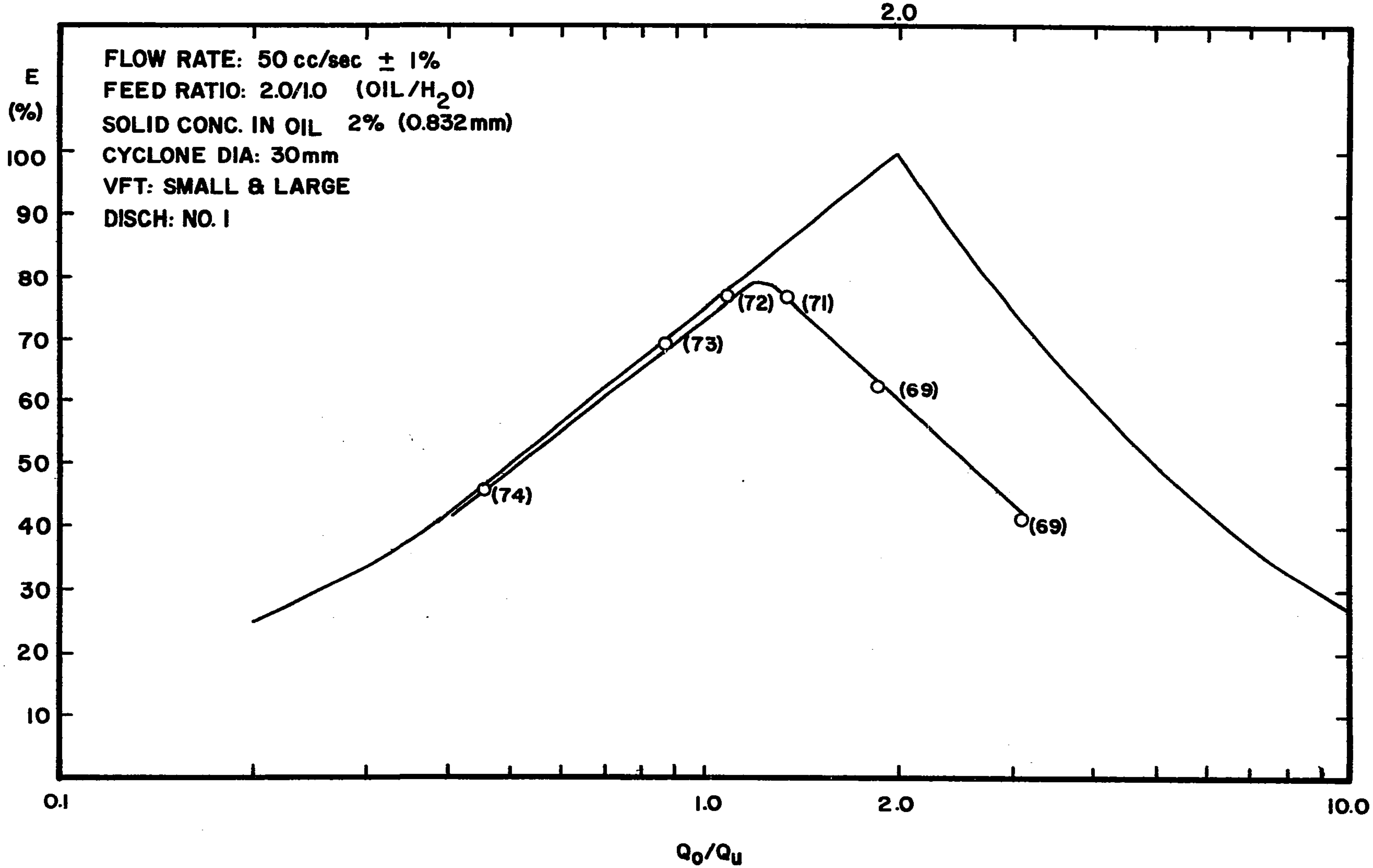

Figure E-9. Overall Efficiency vs. Effluent Split.

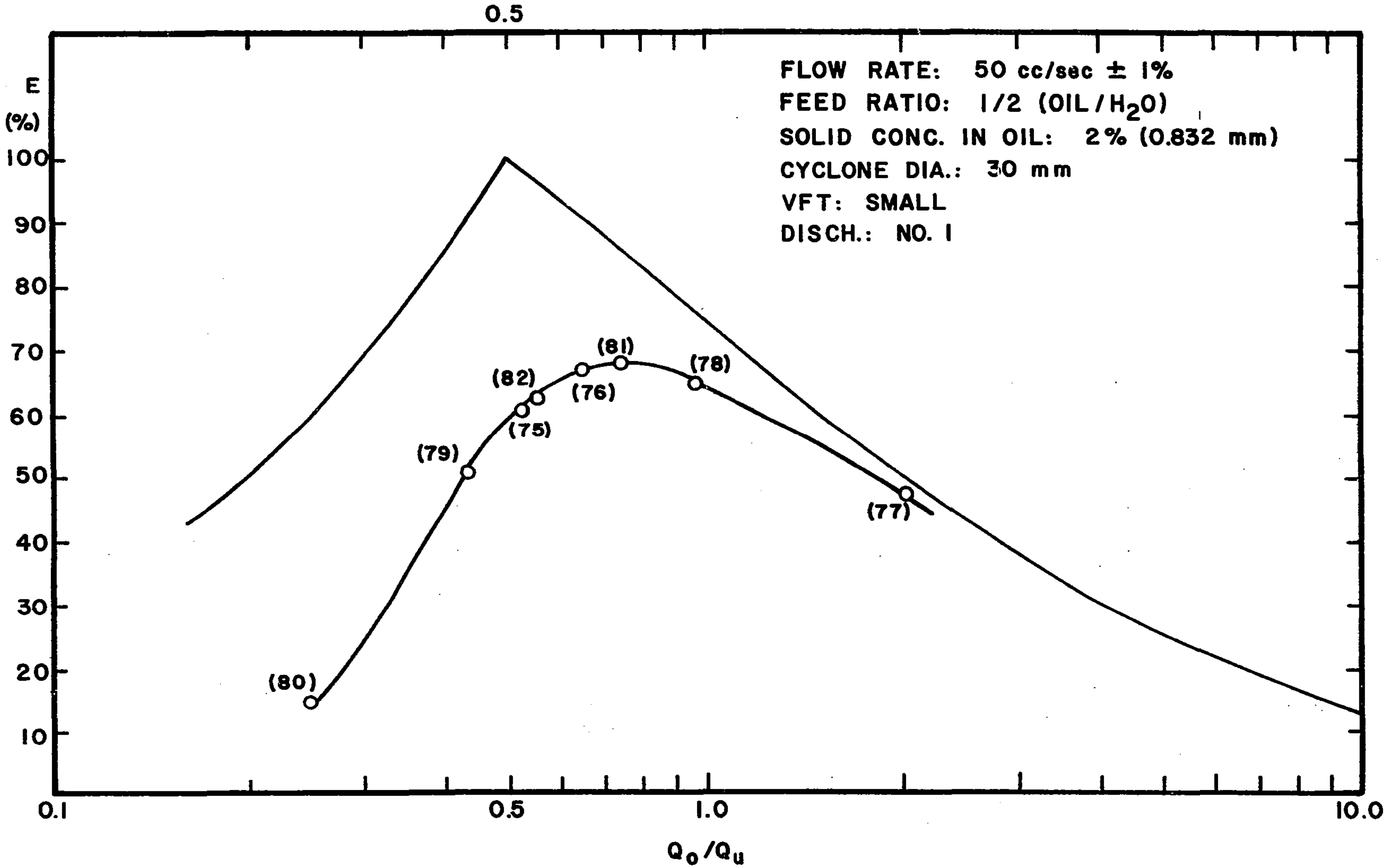

Figure E-10. Overall Efficiency vs. Effluent Split.

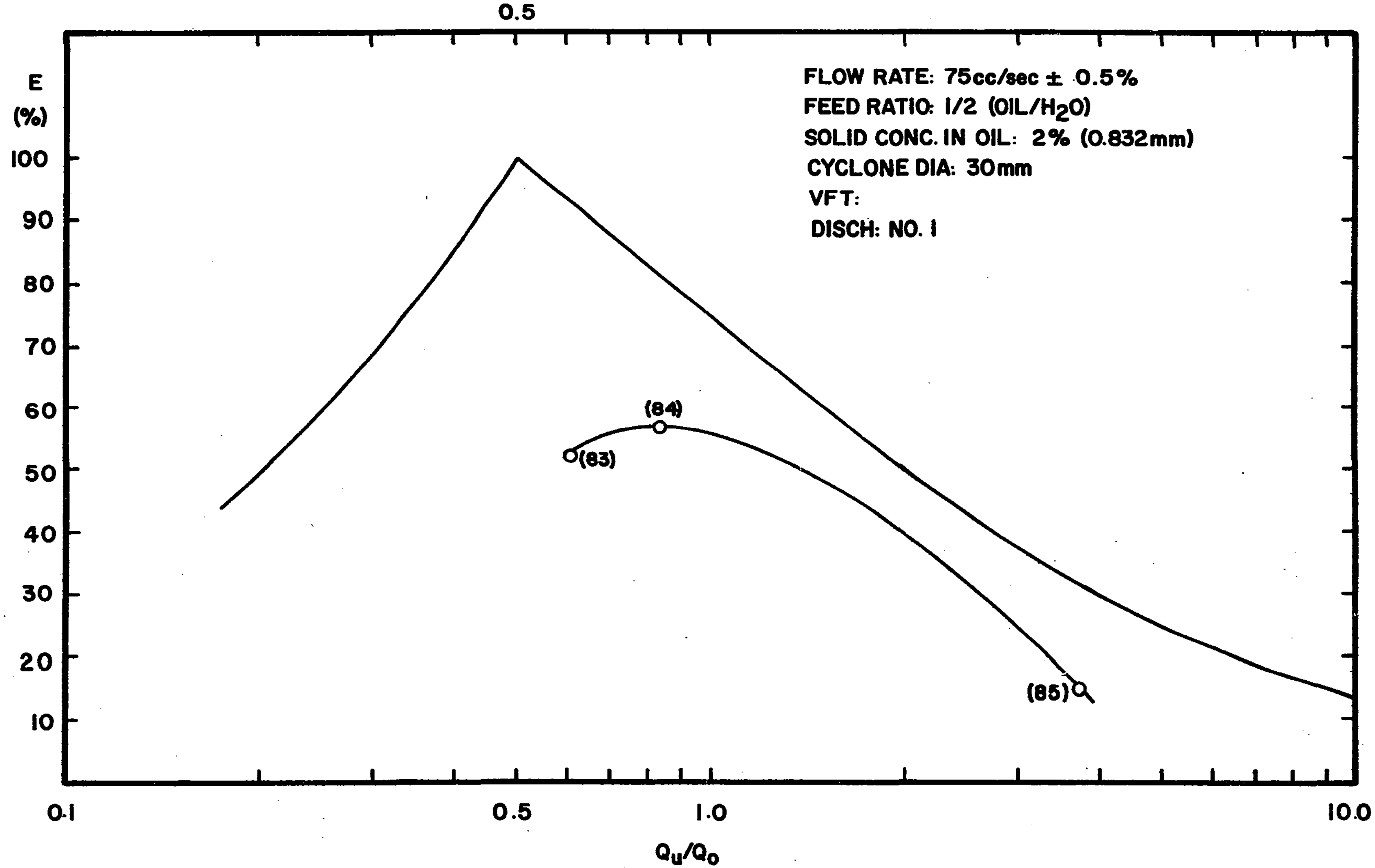

Figure E-11. Overall Efficiency vs. Effluent Split.

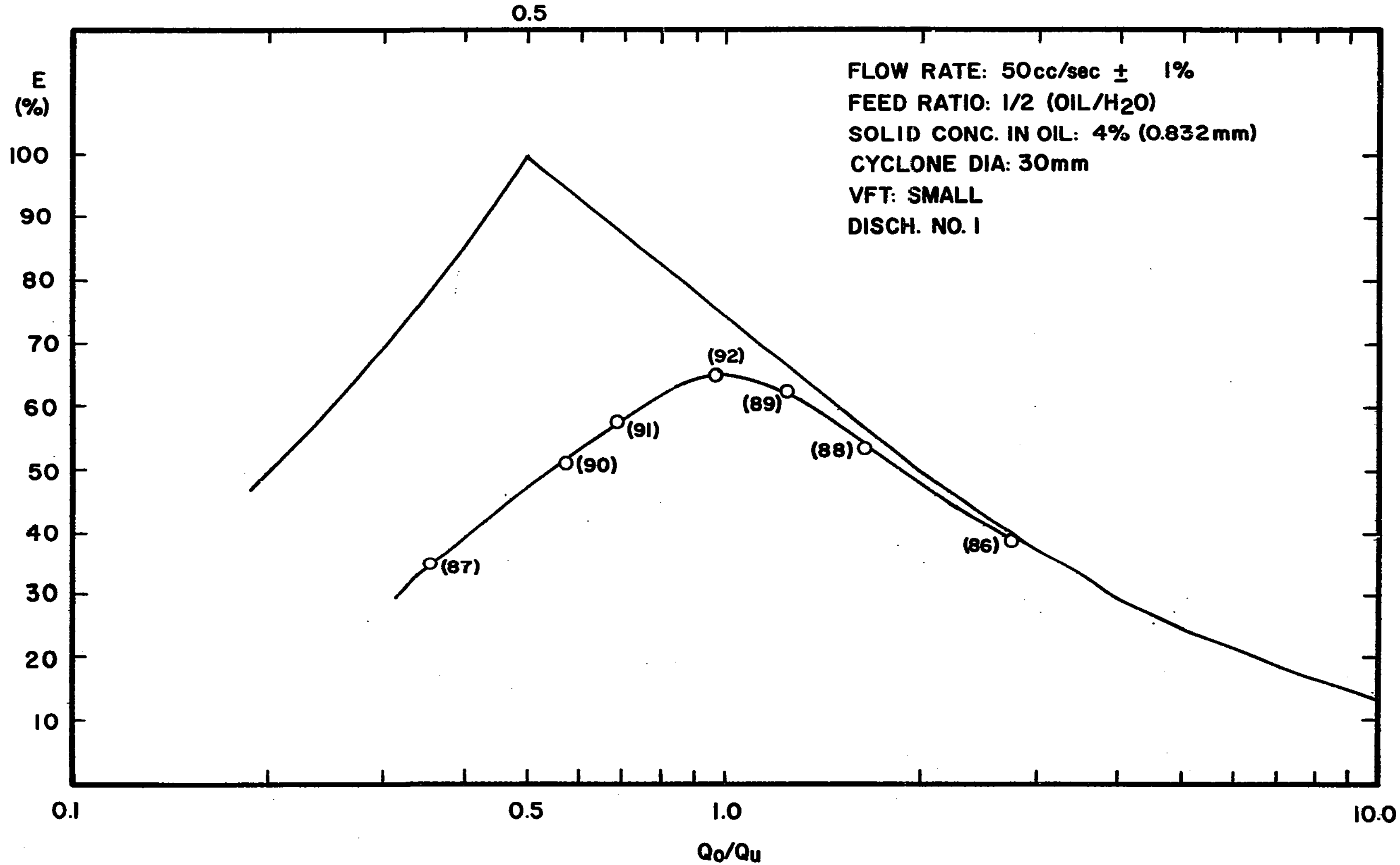

Figure E-12. Overall Efficiency vs. Effluent Split.

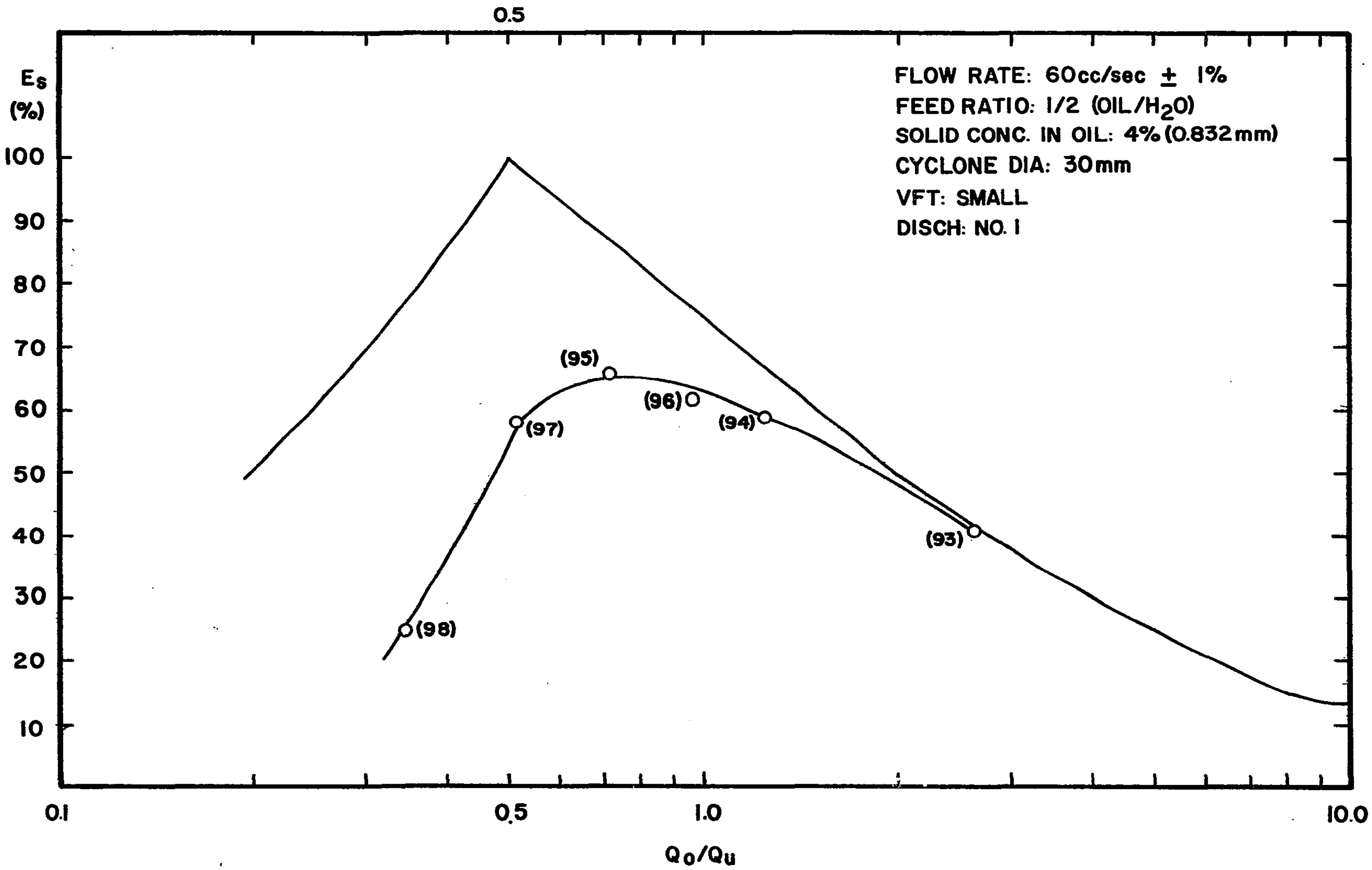

Figure E-13. Overall Efficiency vs. Effluent Split.

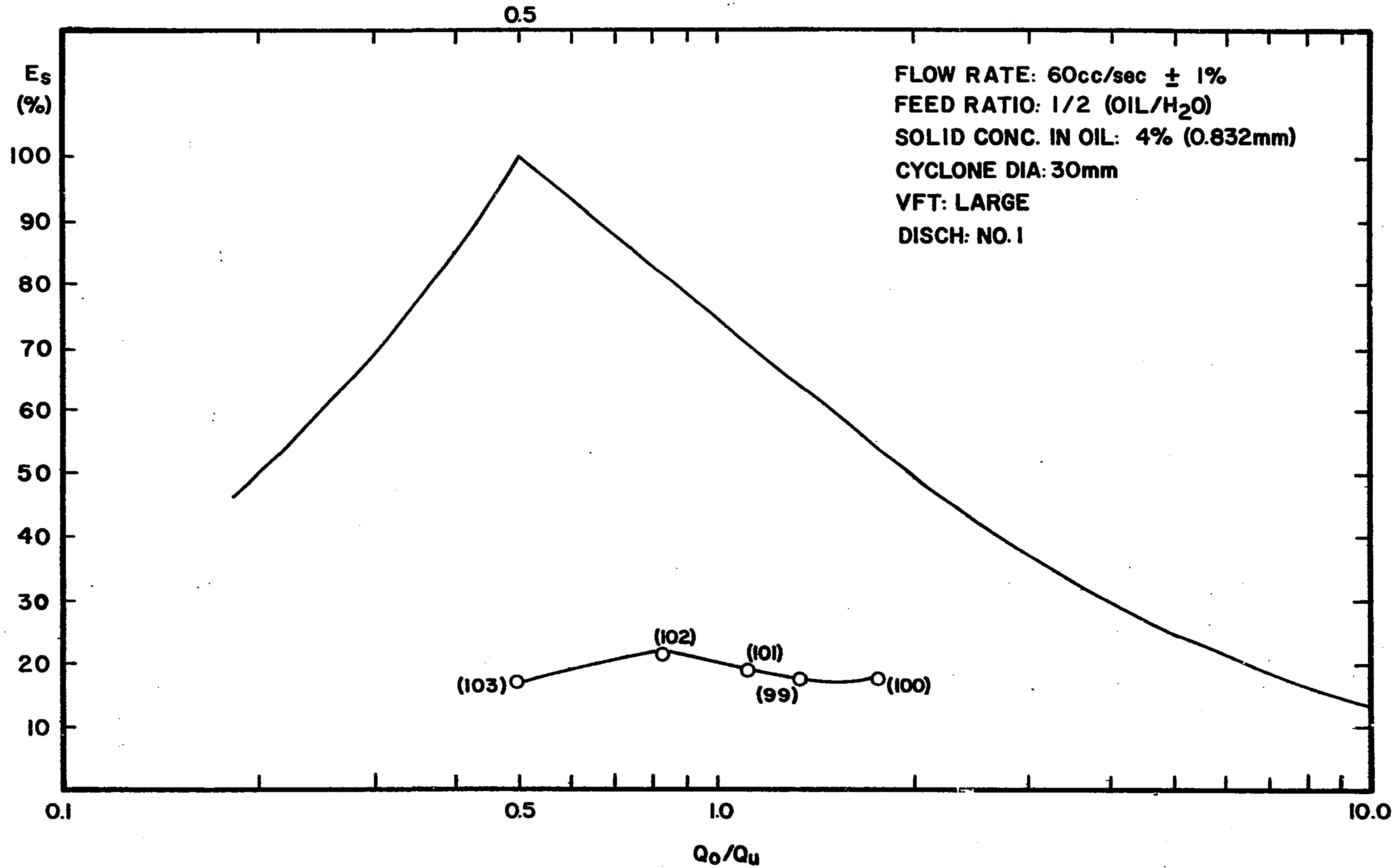

Figure E-14. Overall Efficiency vs. Effluent Split.

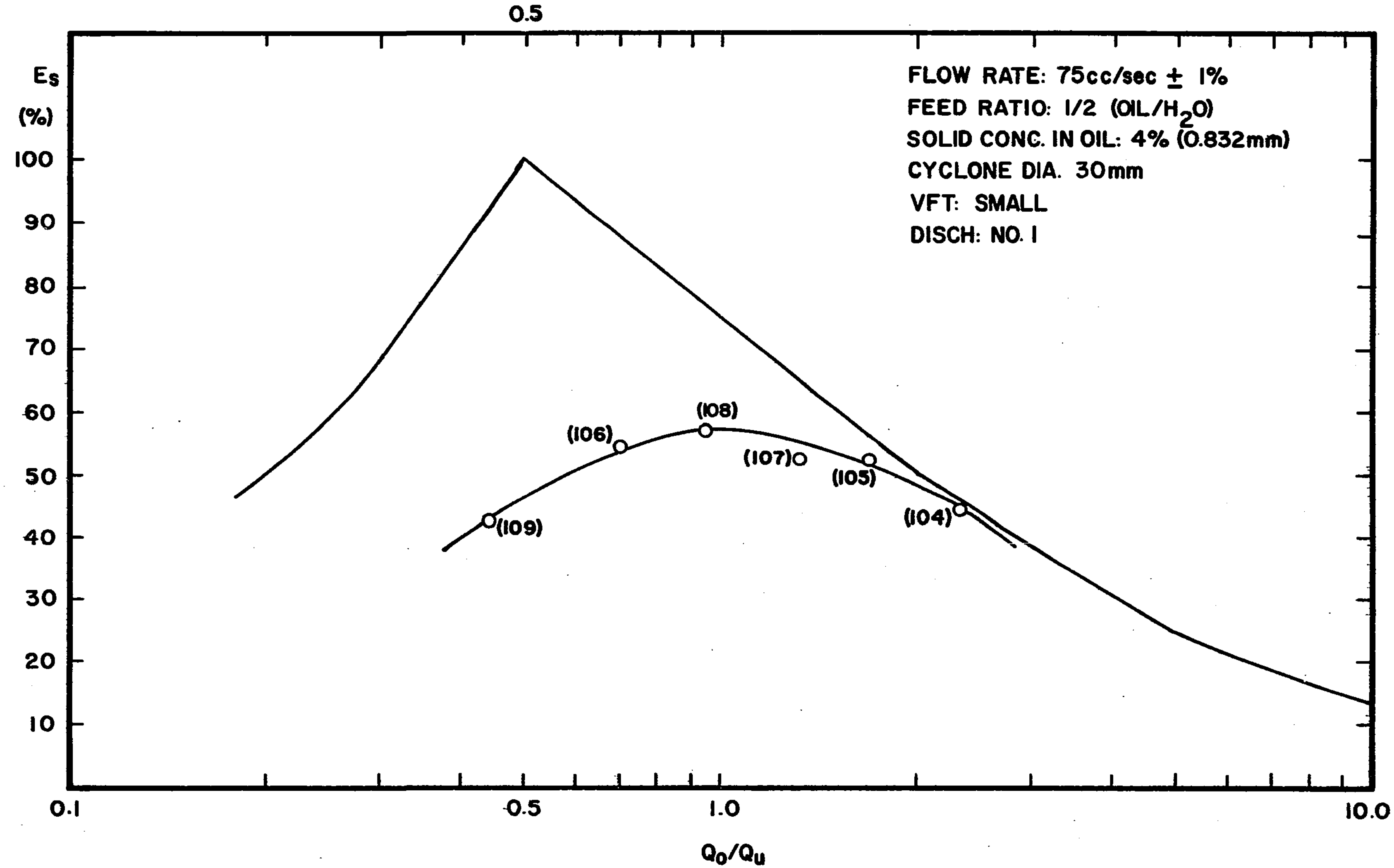

Figure E-15. Overall Efficiency vs. Effluent Split.

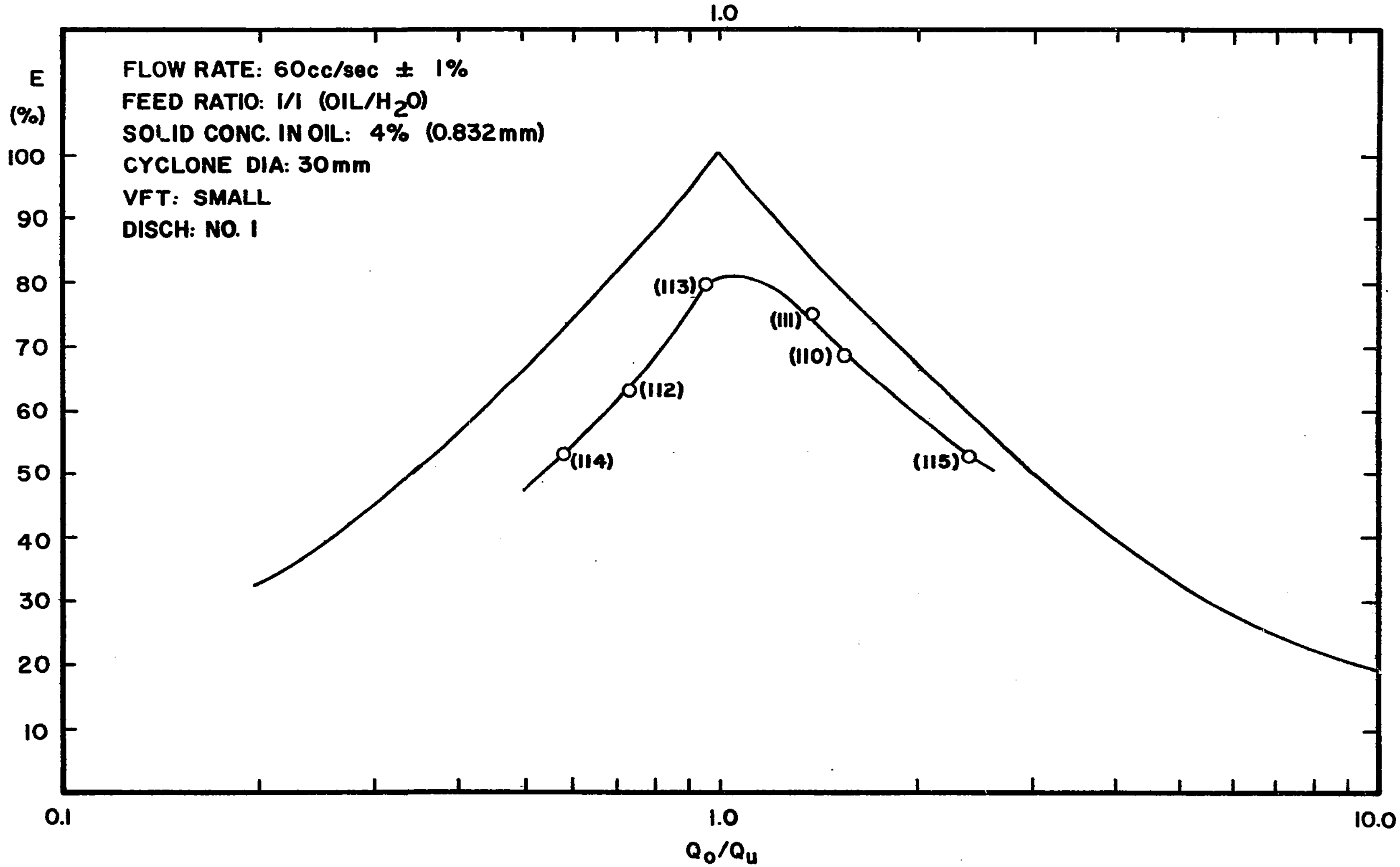

Figure E-16. Overall Efficiency vs. Effluent Split.

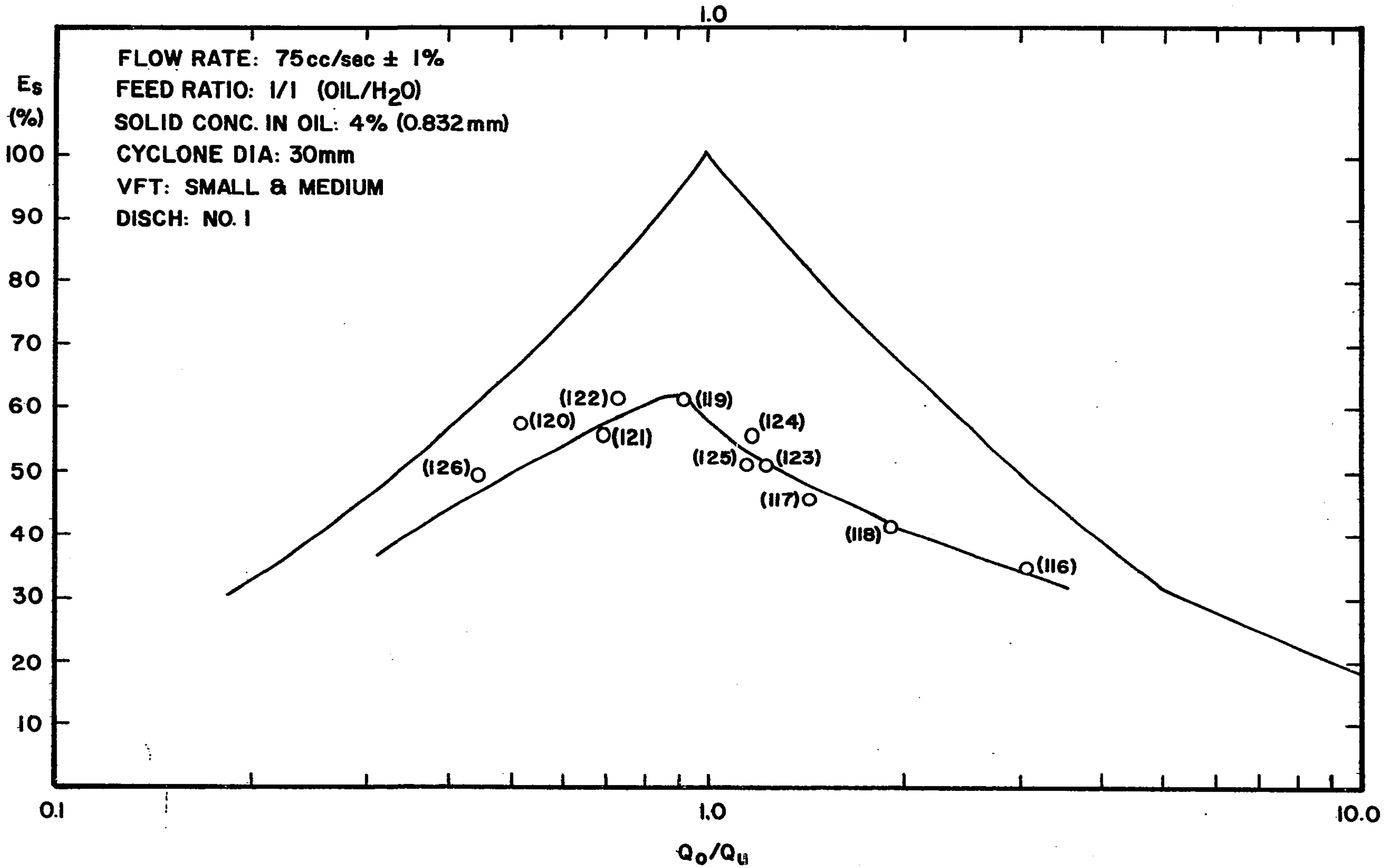

Figure E-17. Overall Efficiency vs. Effluent Split.

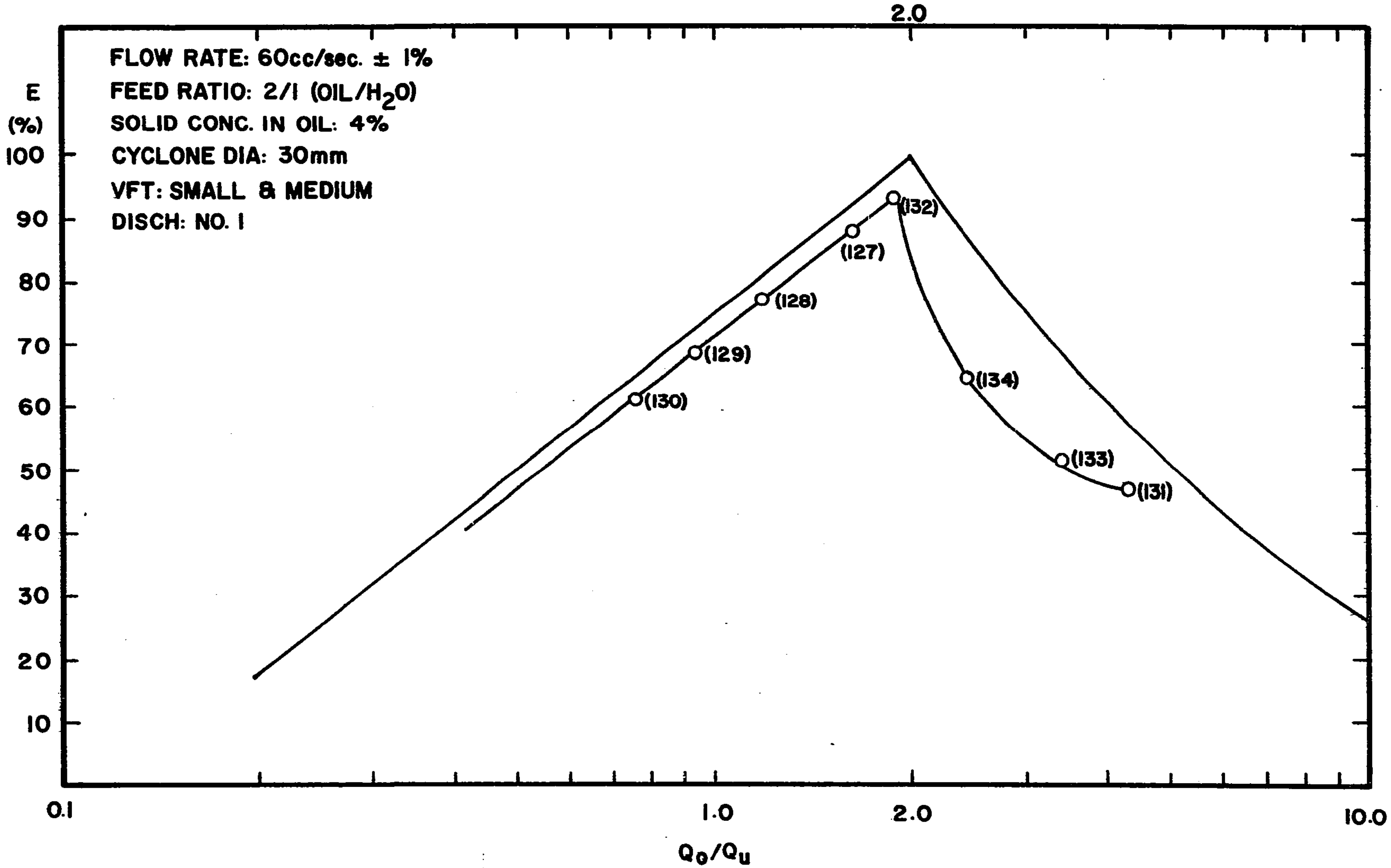

Figure E-18. Overall Efficiency vs. Effluent Split.

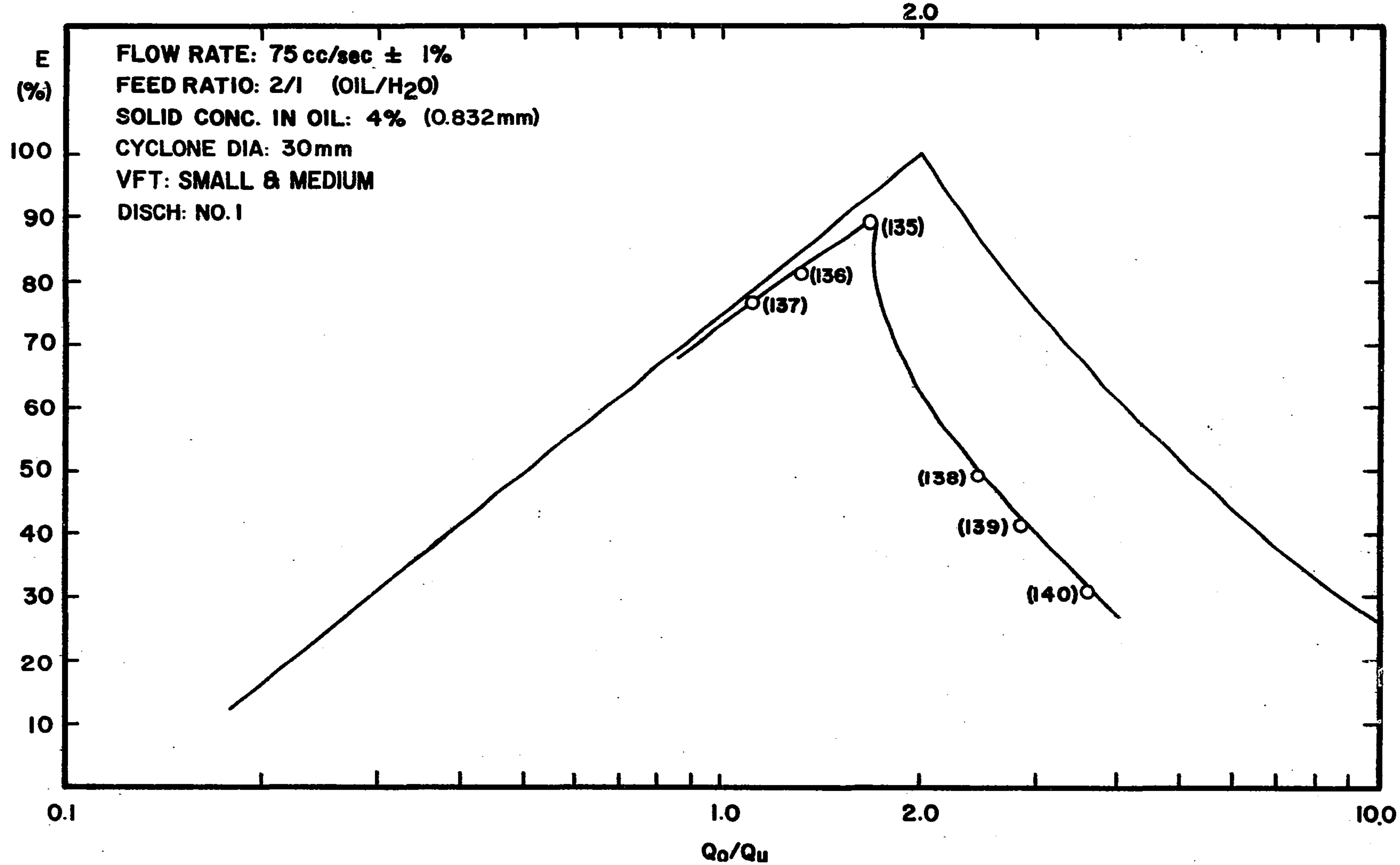

Figure E-19. Overall Efficiency vs. Effluent Split.

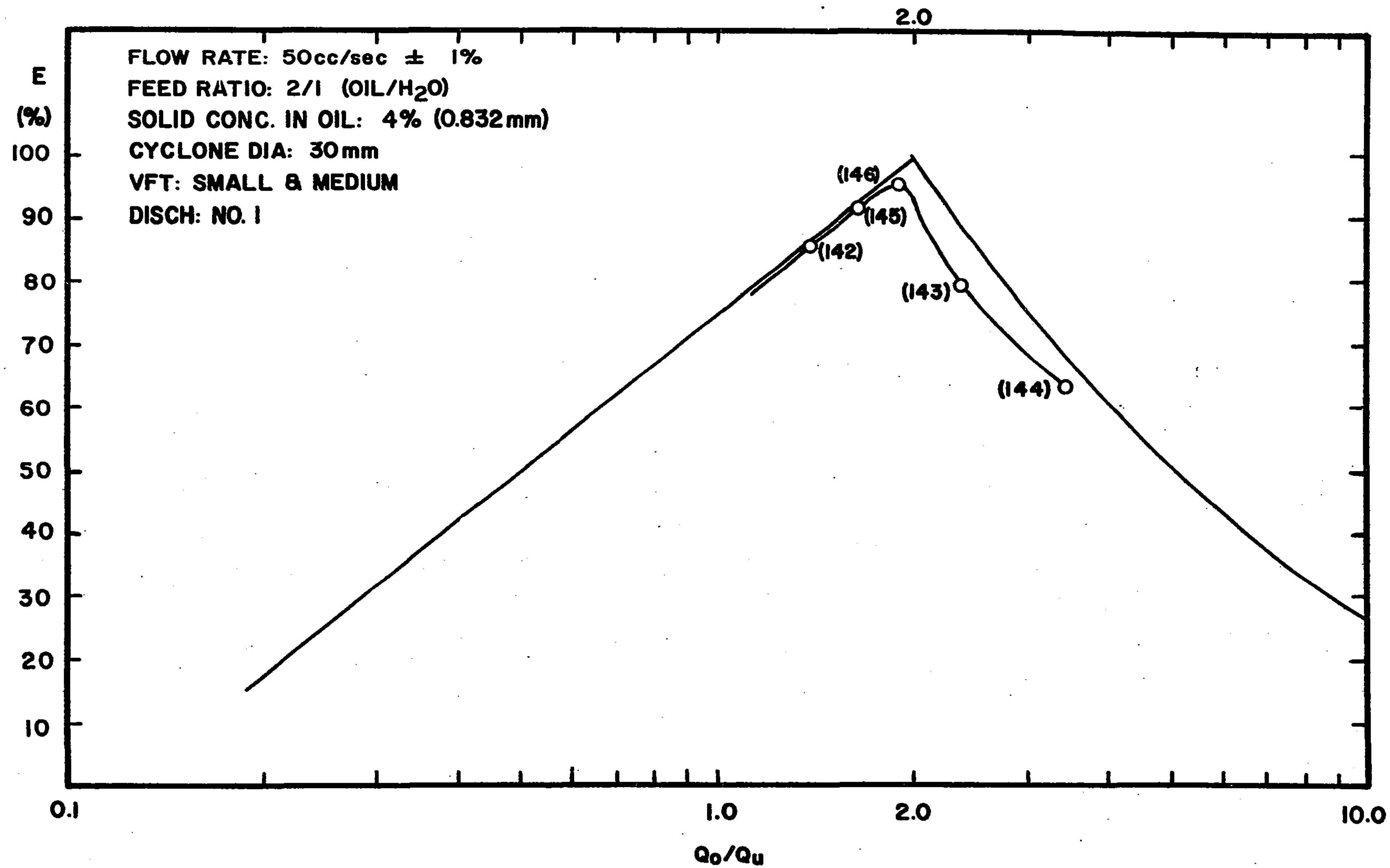

Figure E-20. Overall Efficiency vs. Effluent Split.

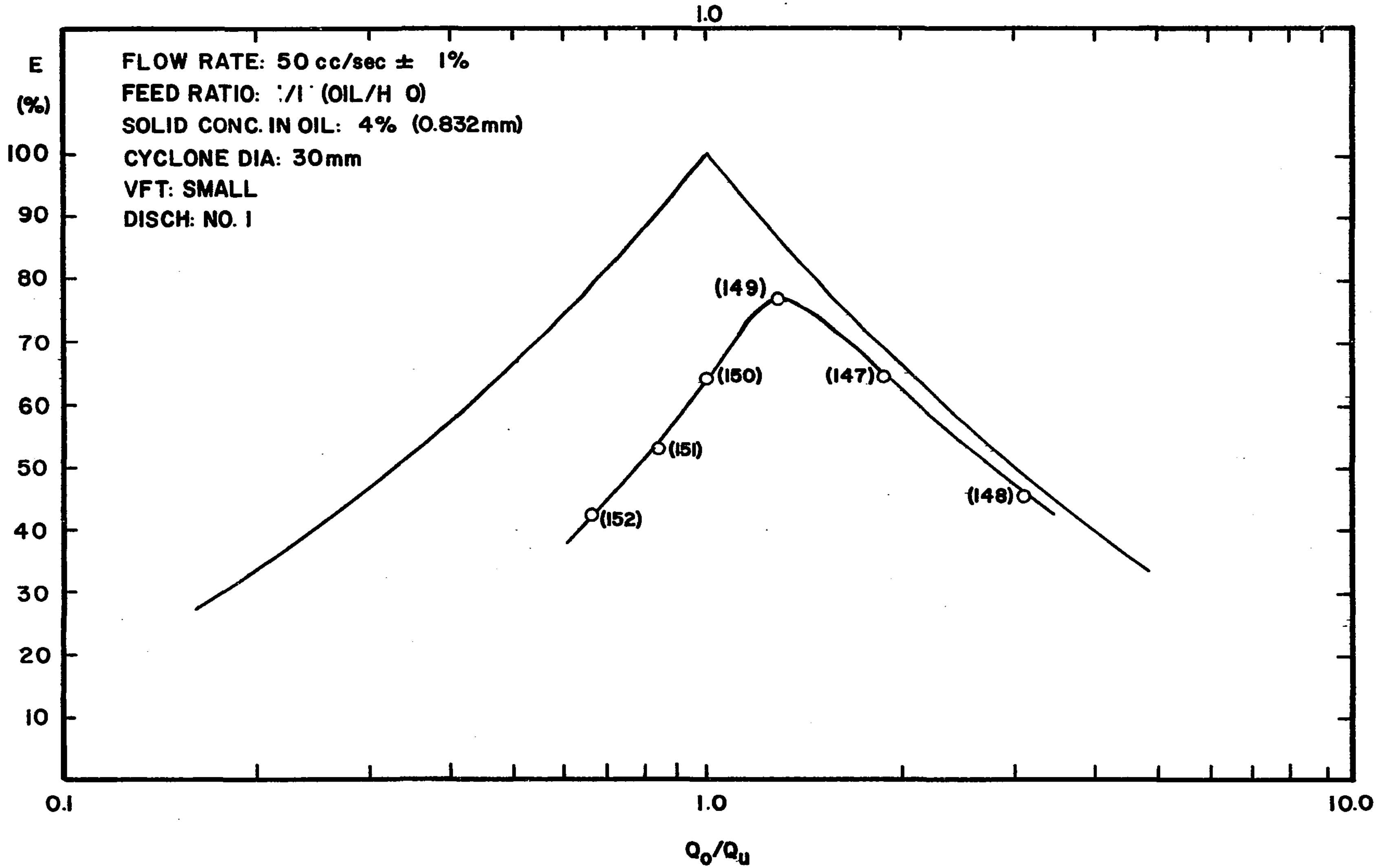

Figure E-21. Overall Efficiency vs. Effluent Split.

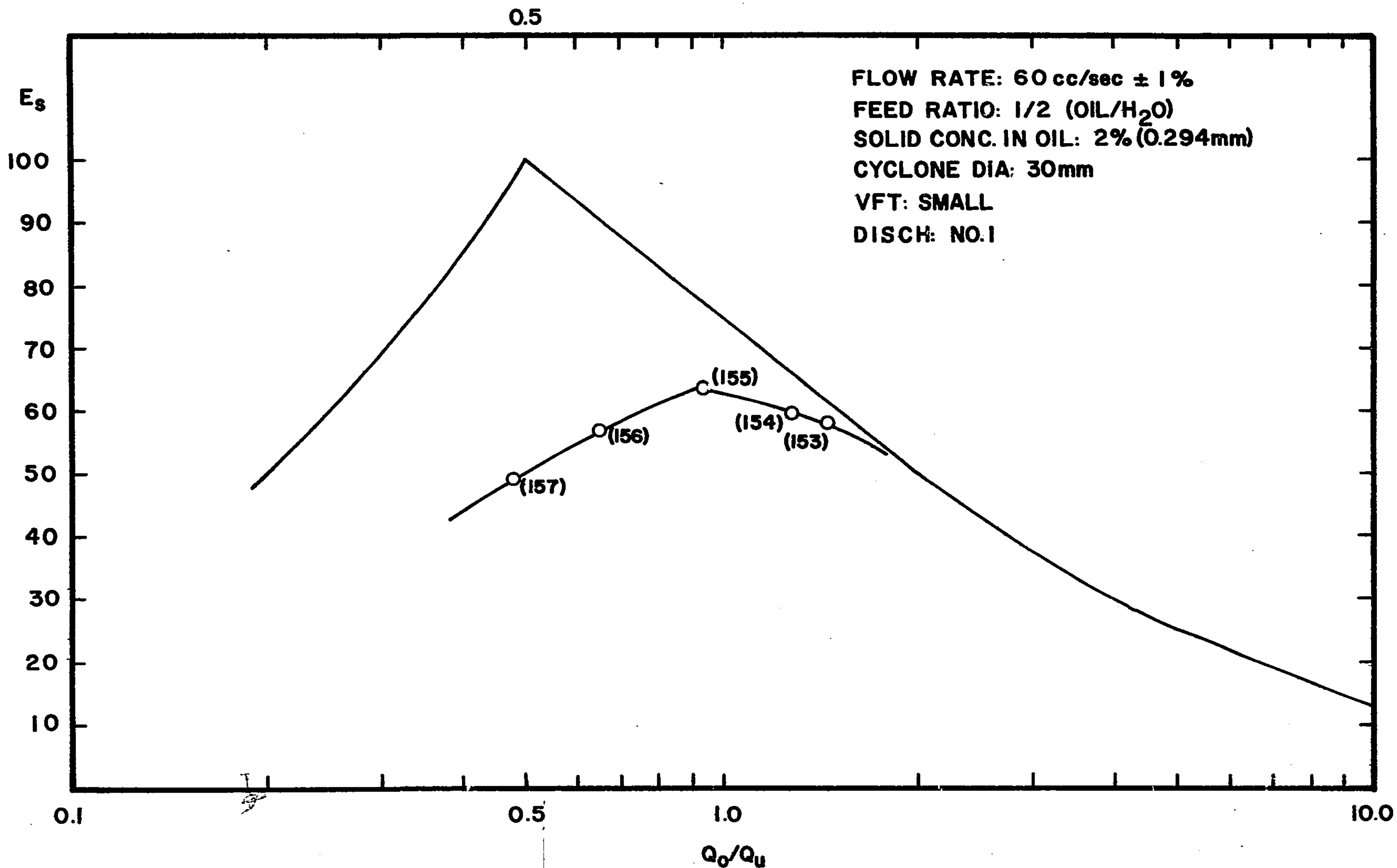

Figure E-22. Overall Efficiency vs. Effluent Split.

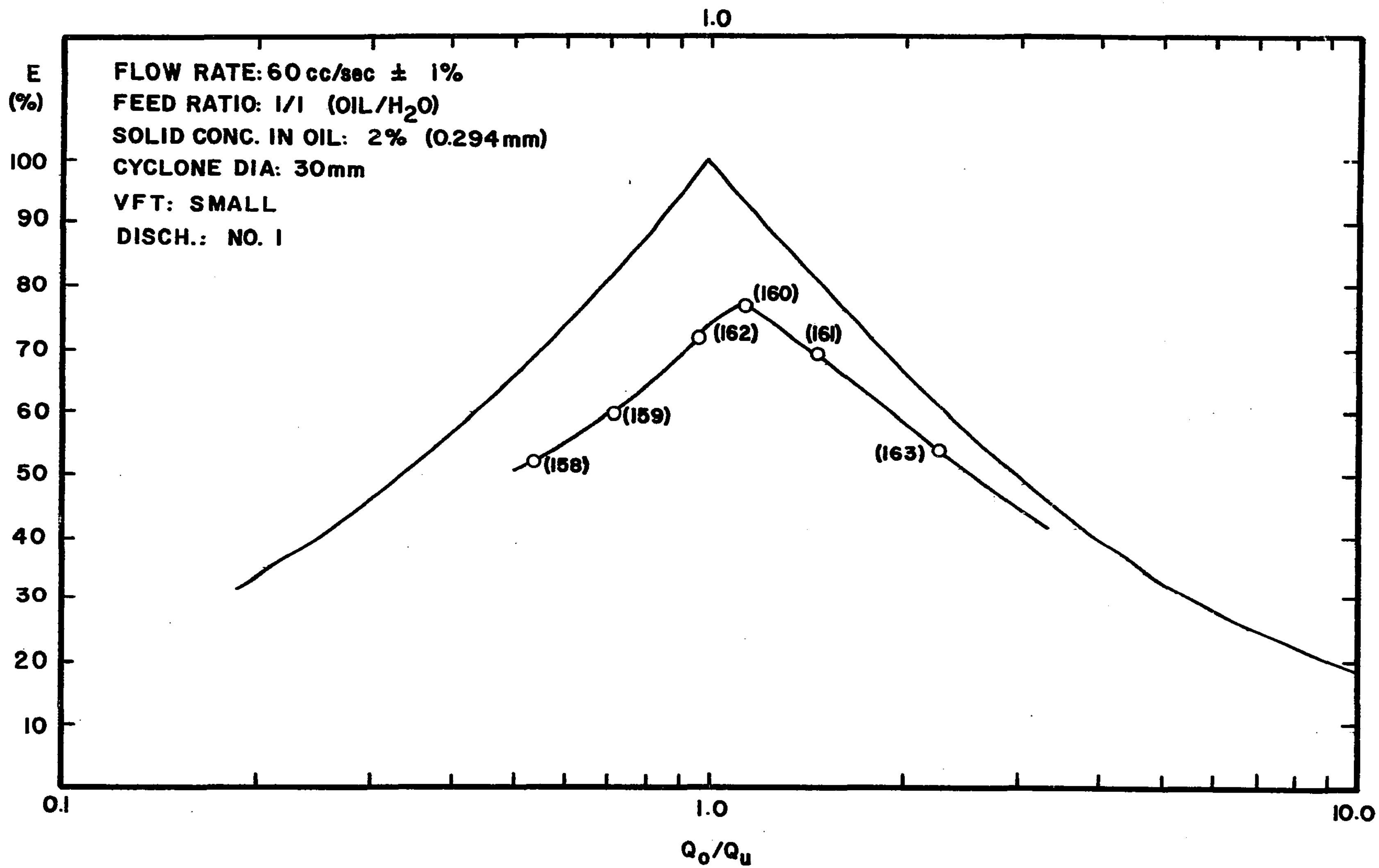

Figure E-23. Overall Efficiency vs. Effluent Split.

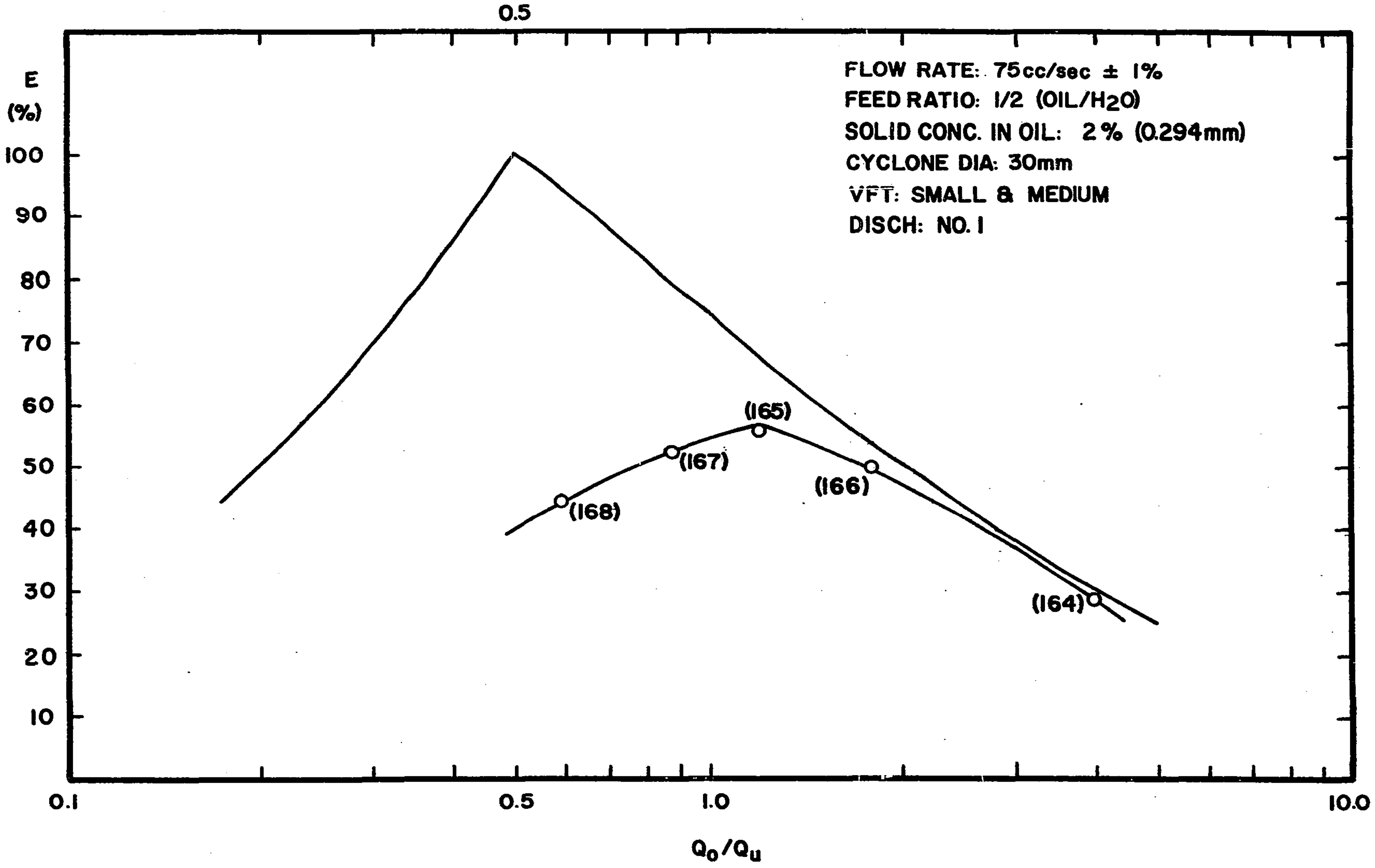

Figure E-24. Overall Efficiency vs. Effluent Split.

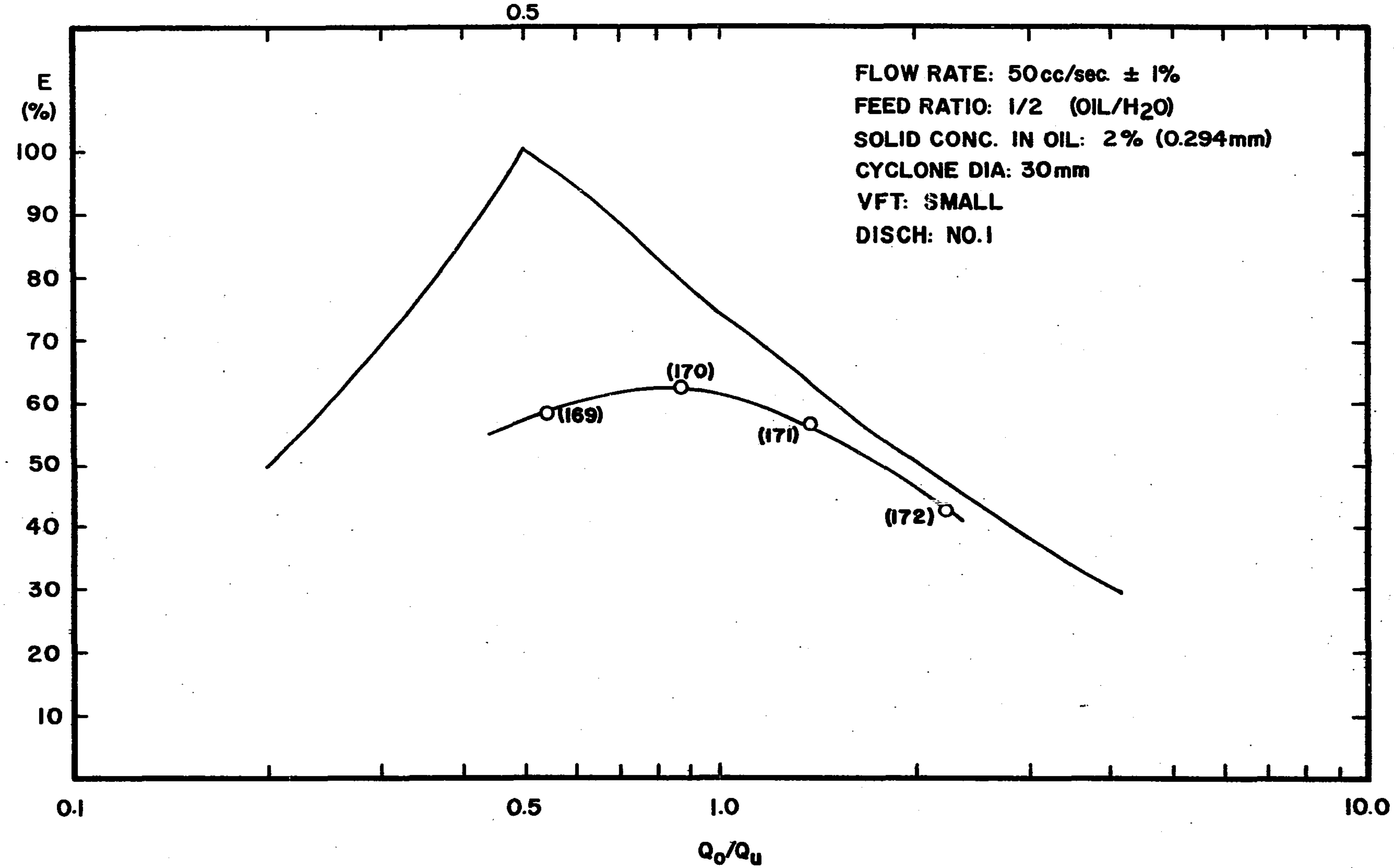

Figure E-25. Overall Efficiency vs. Effluent Split.

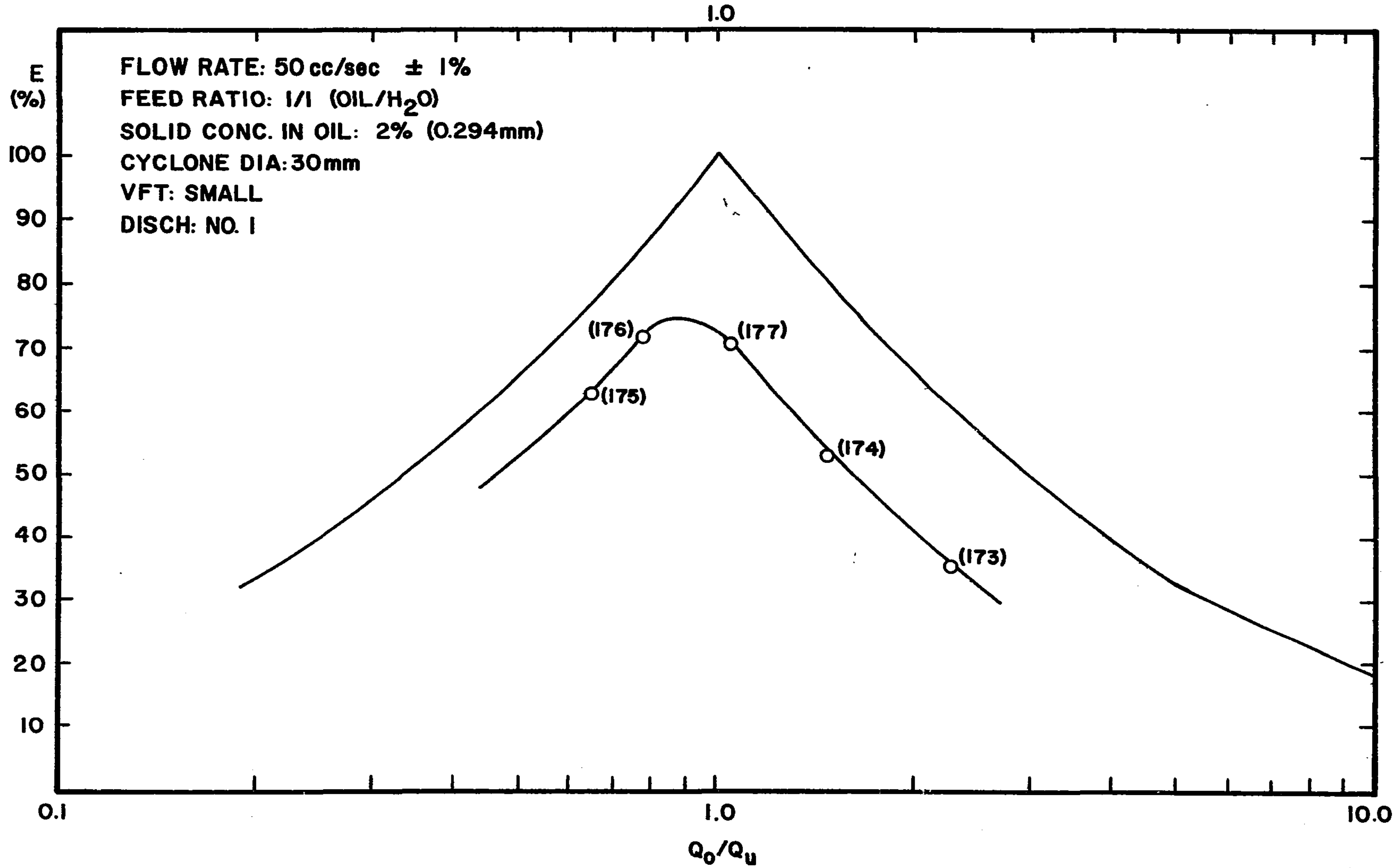

Figure E-26. Overall Efficiency vs. Effluent Split.

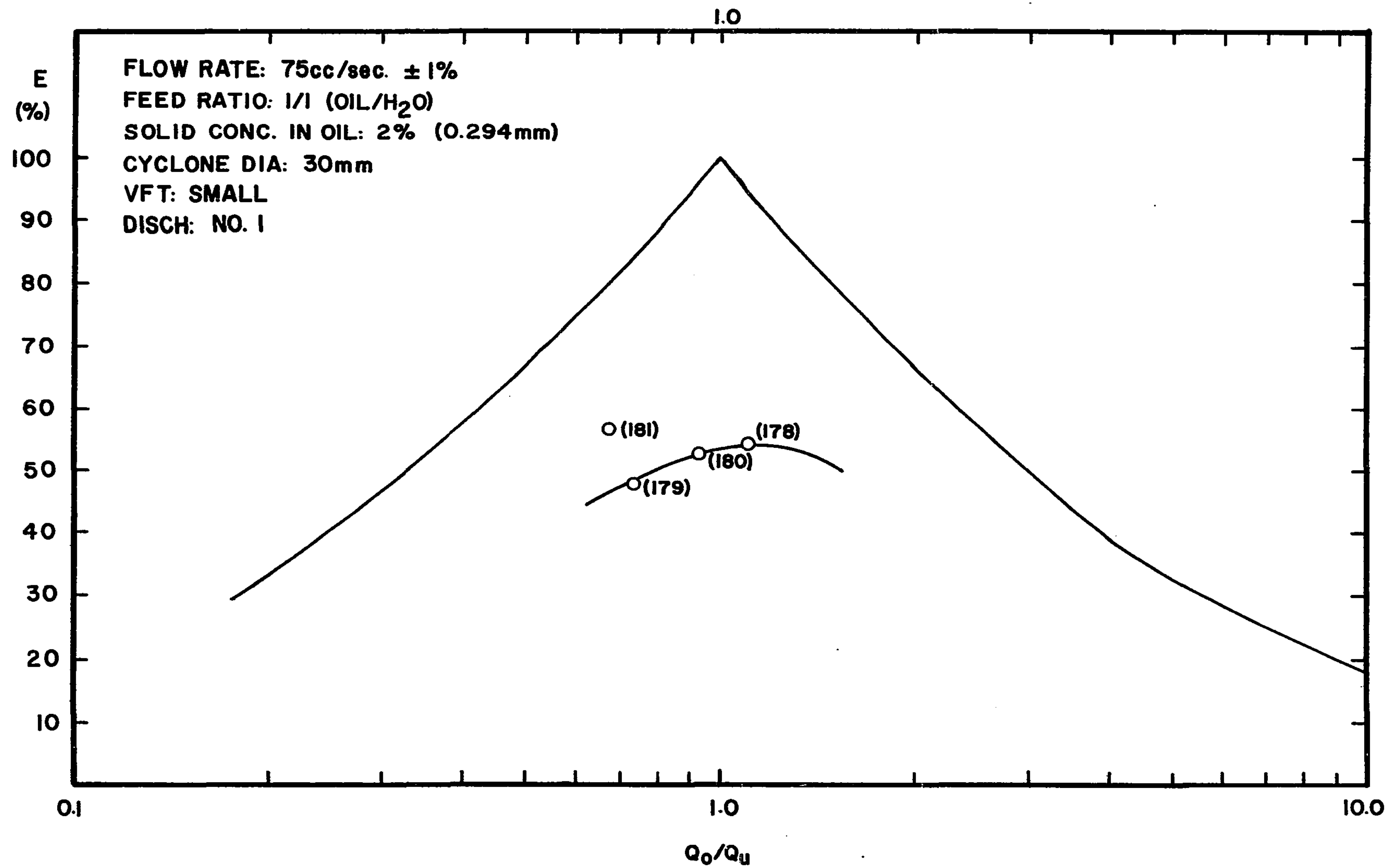

Figure E-27. Overall Efficiency vs. Effluent Split.

140

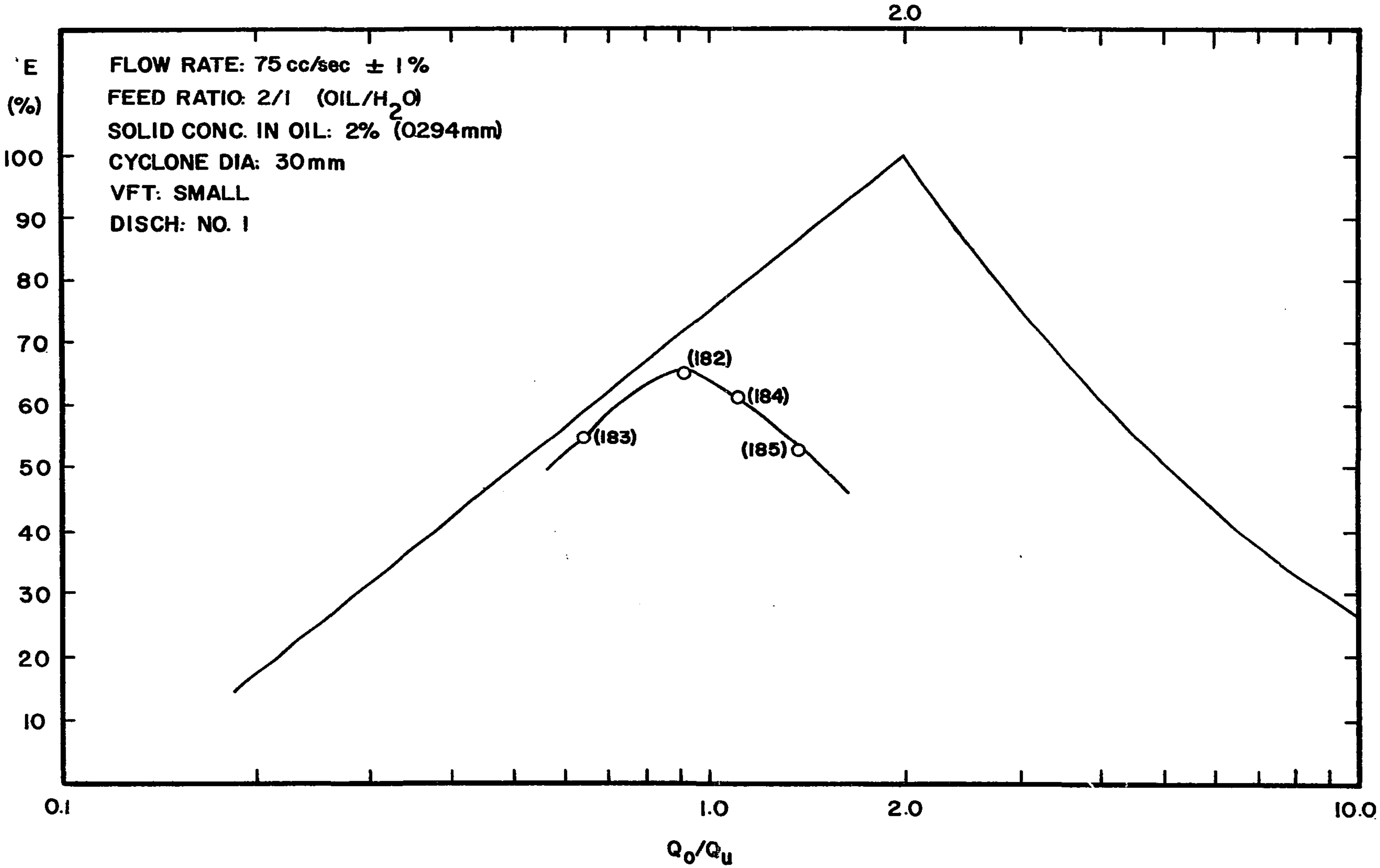

Figure E-28. Overall Efficiency vs. Effluent Split.

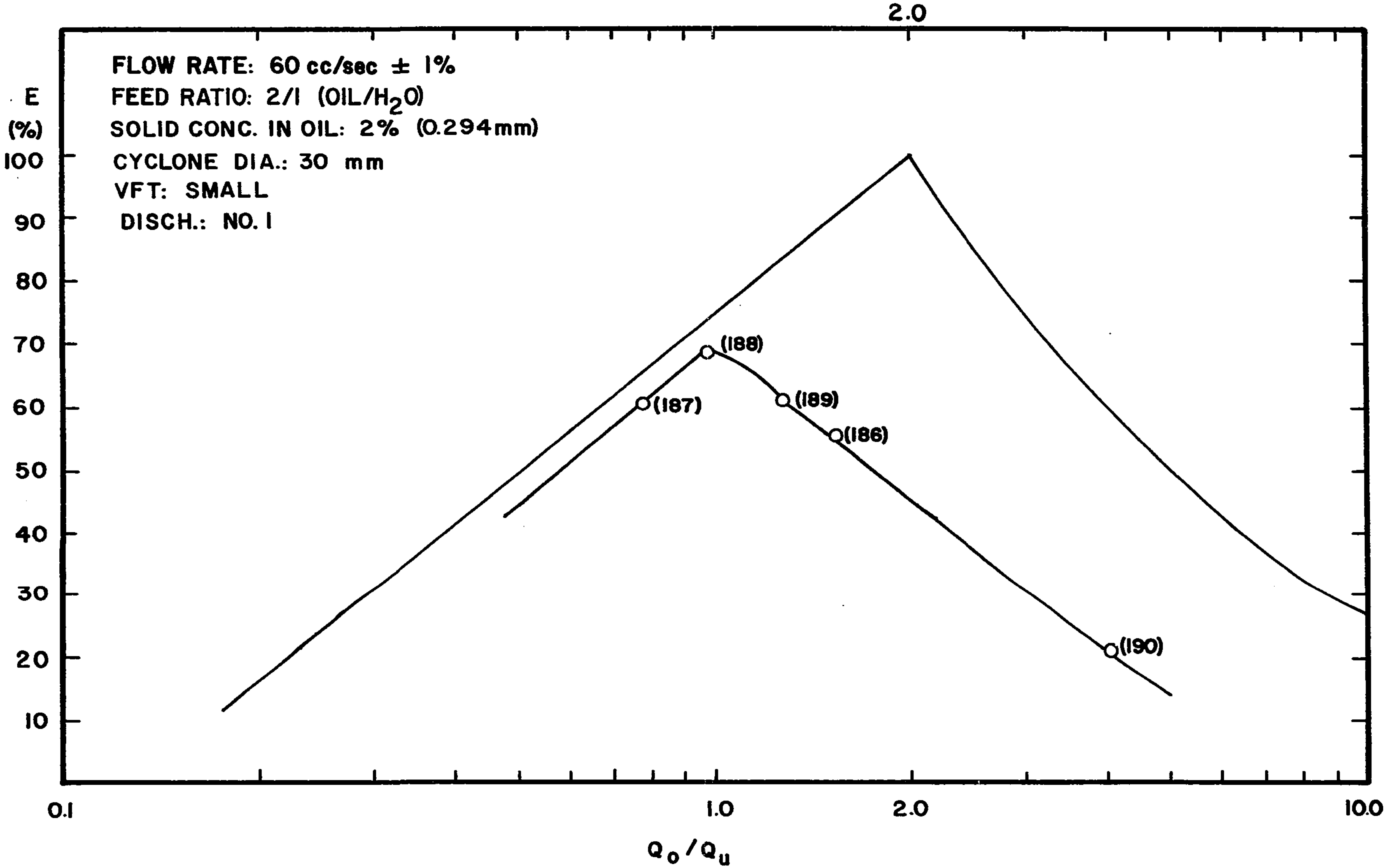

Figure E-29. Overall Efficiency vs. Effluent Split.

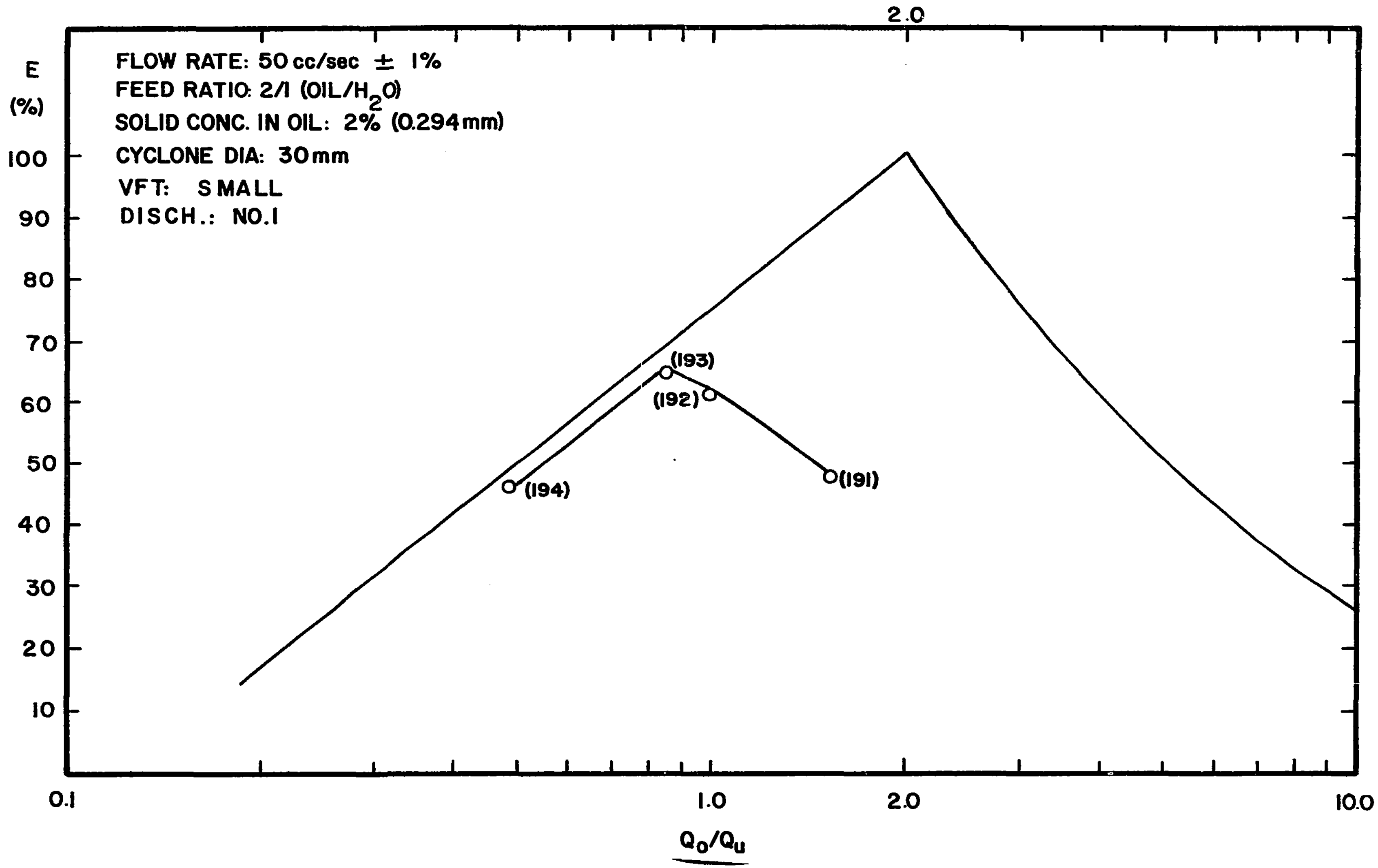

Figure E-30. Overall Efficiency vs. Effluent Split.

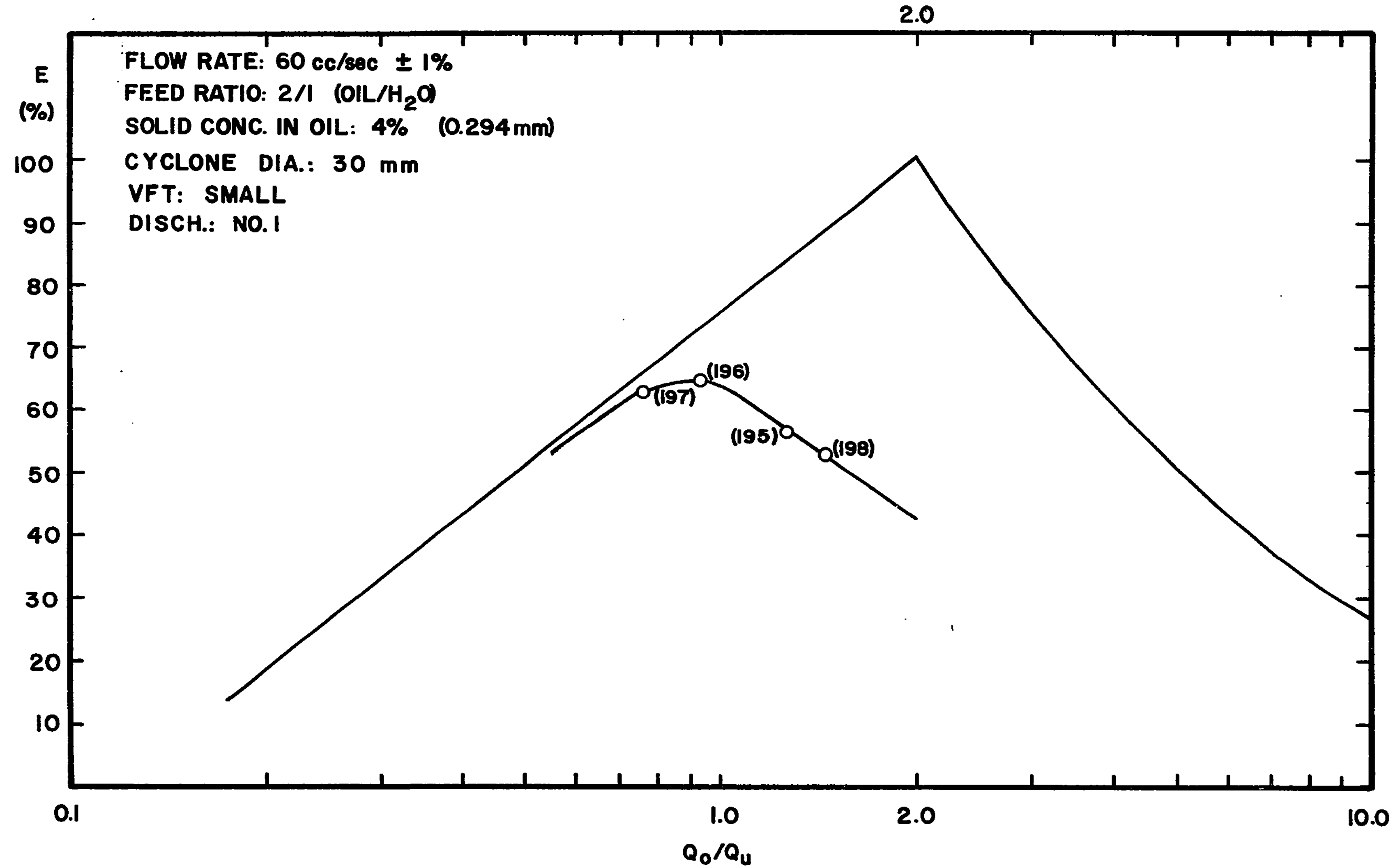

Figure E-31. Overall Efficiency vs. Effluent Split.

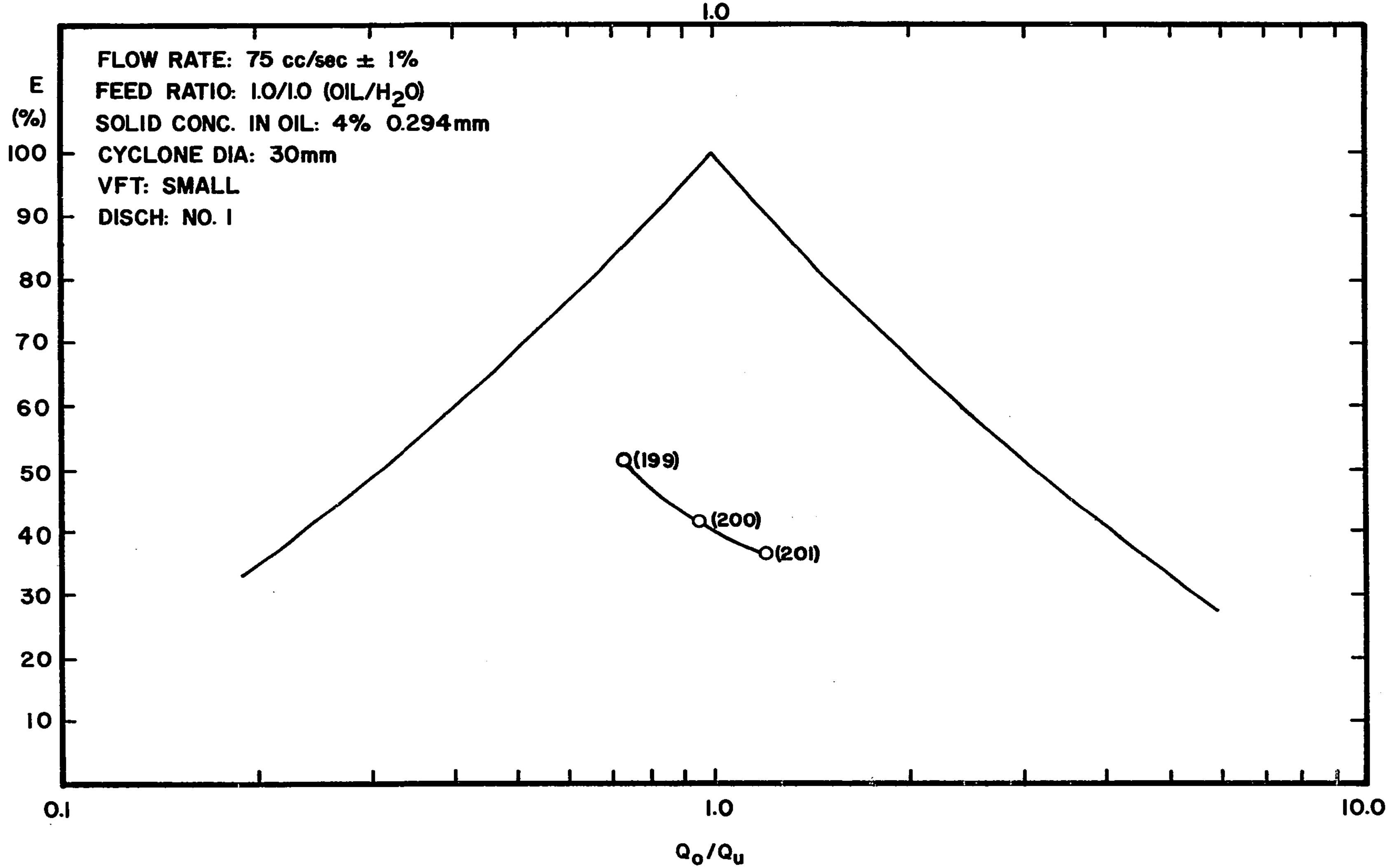

Figure E-32. Overall Efficiency vs. Effluent Split.

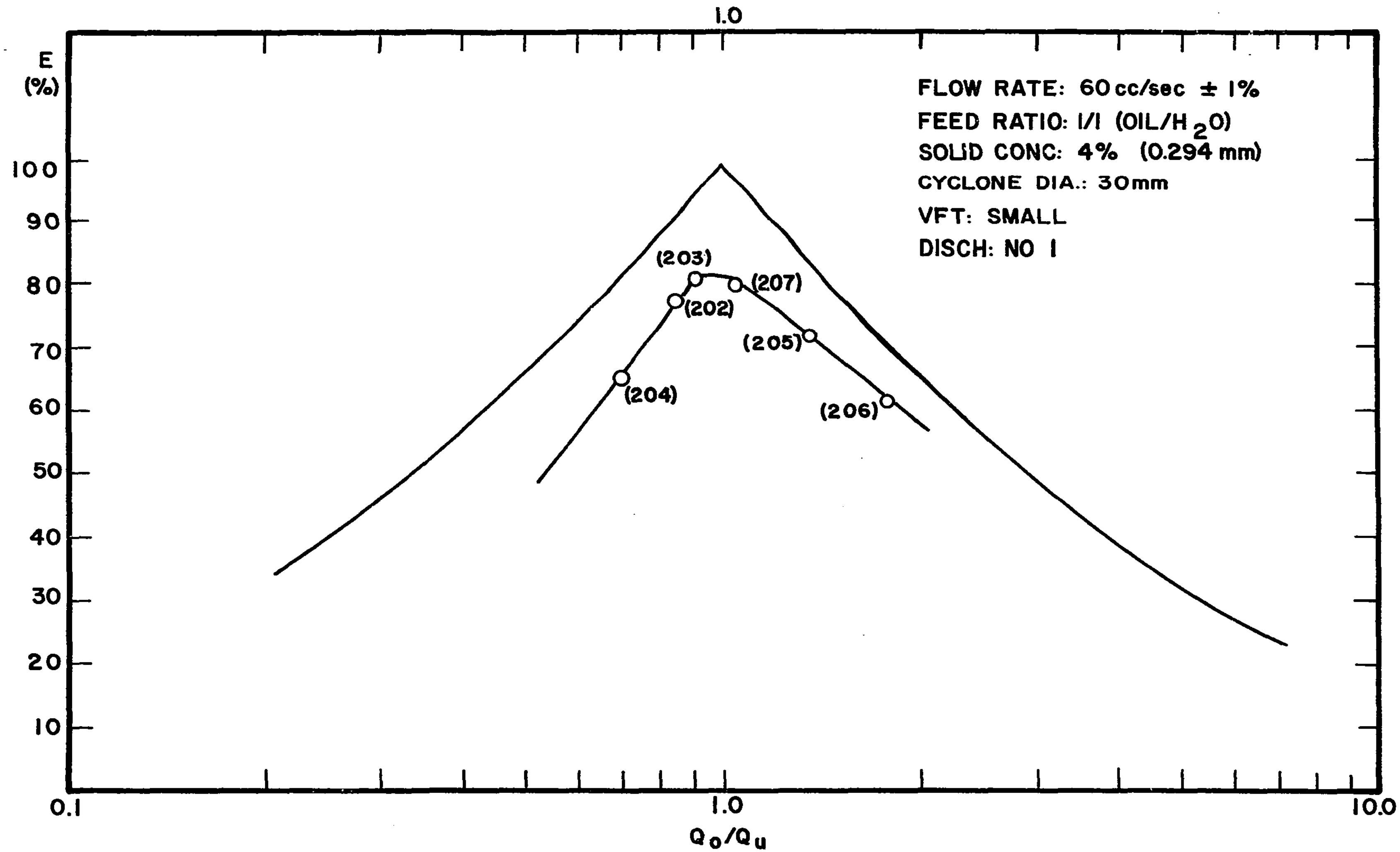

Figure E-33. Overall Efficiency vs. Effluent Split.

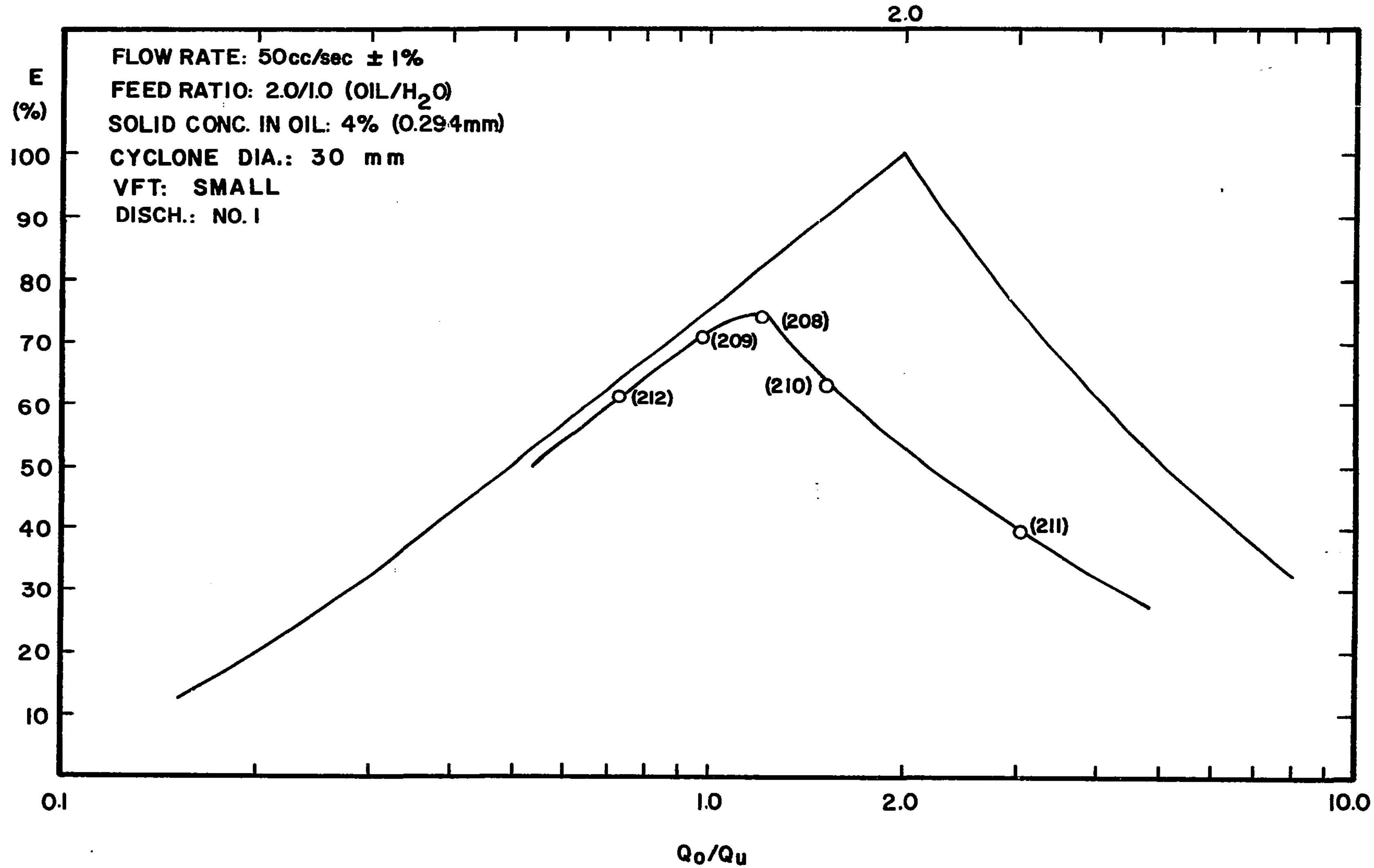

Figure E-34. Overall Efficiency vs. Effluent Split.

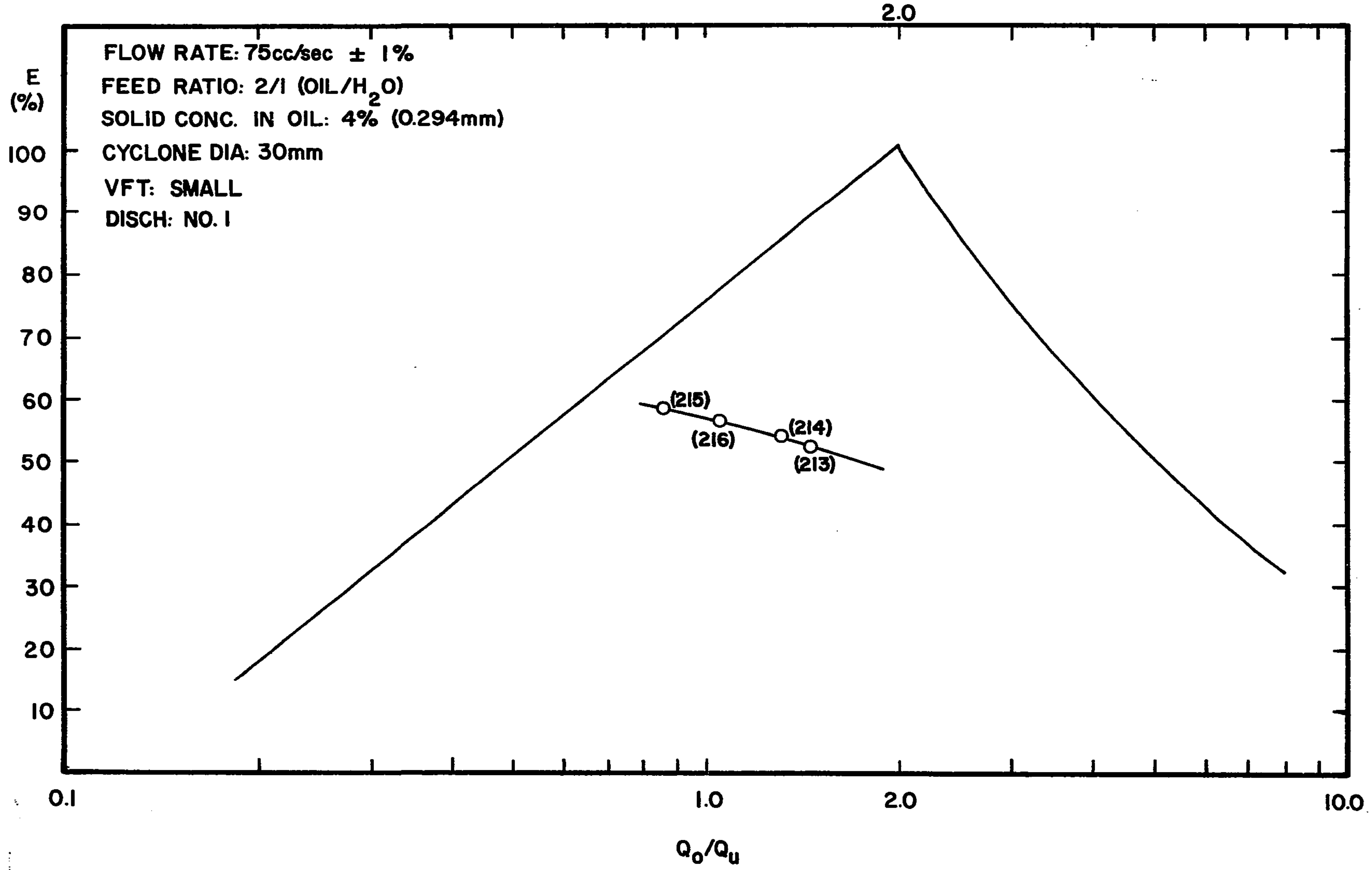

Figure E-35. Overall Efficiency vs. Effluent Split.

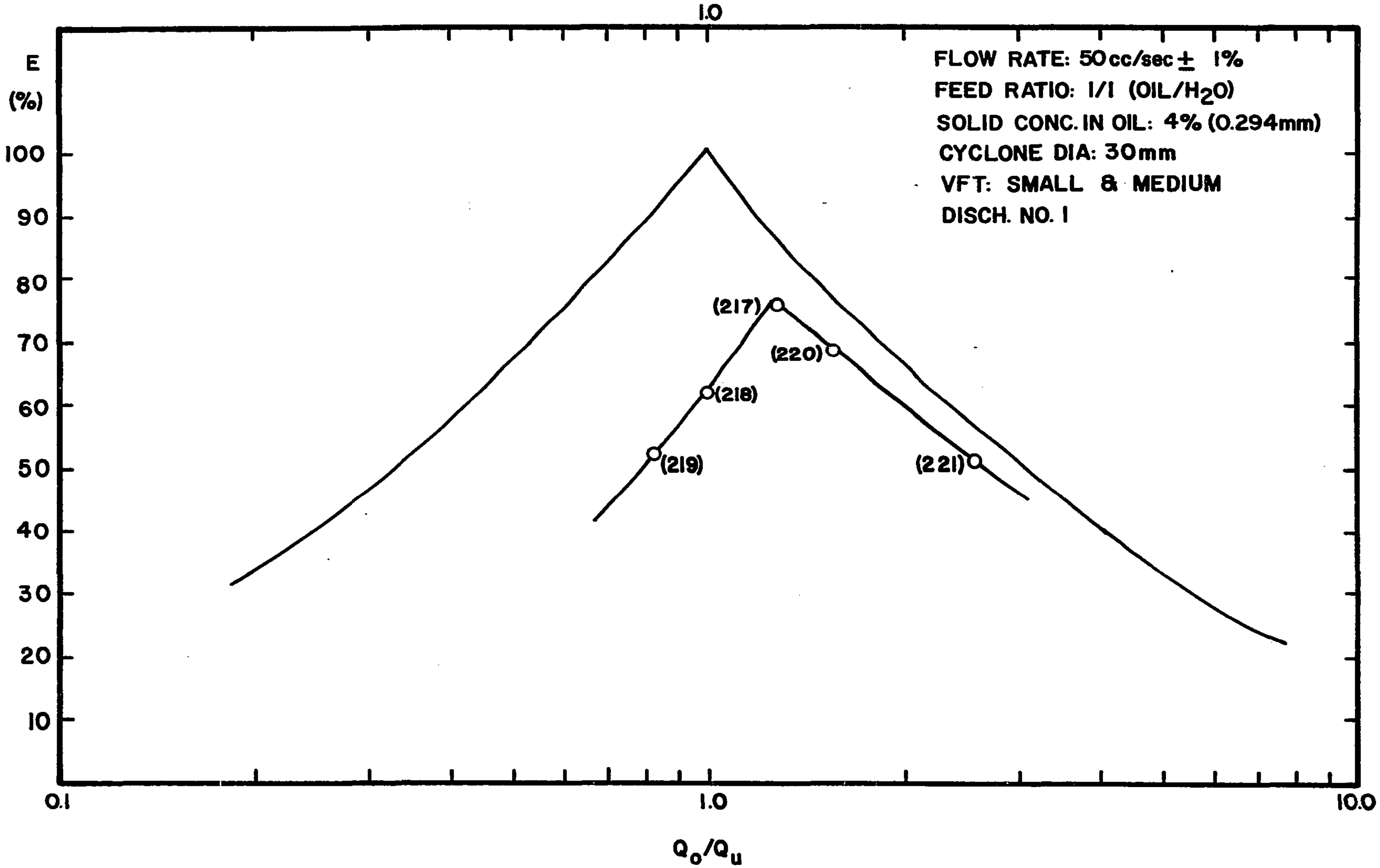

Figure E-36. Overall Efficiency vs. Effluent Split.

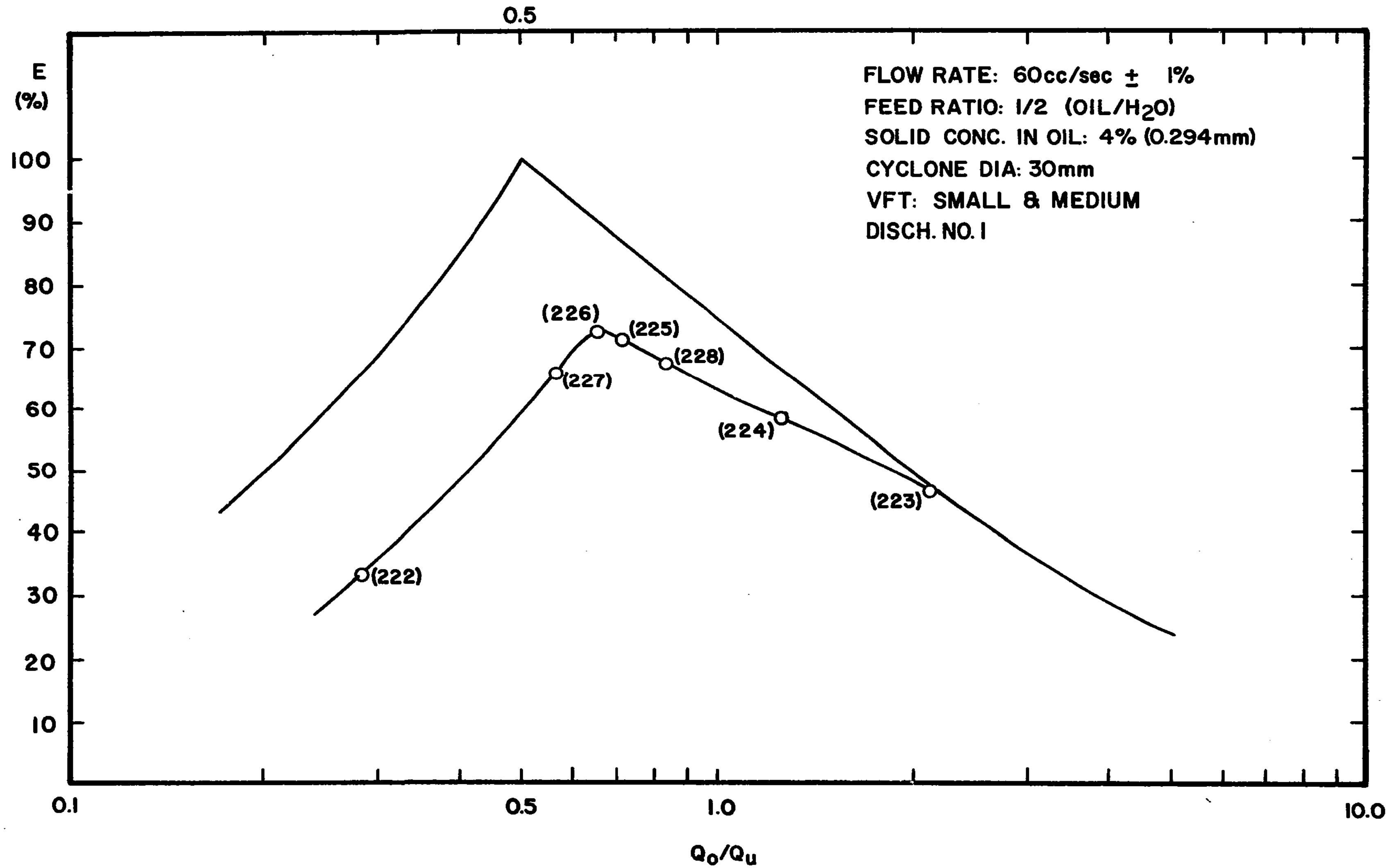

Figure E-37. Overall Efficiency vs. Effluent Split.

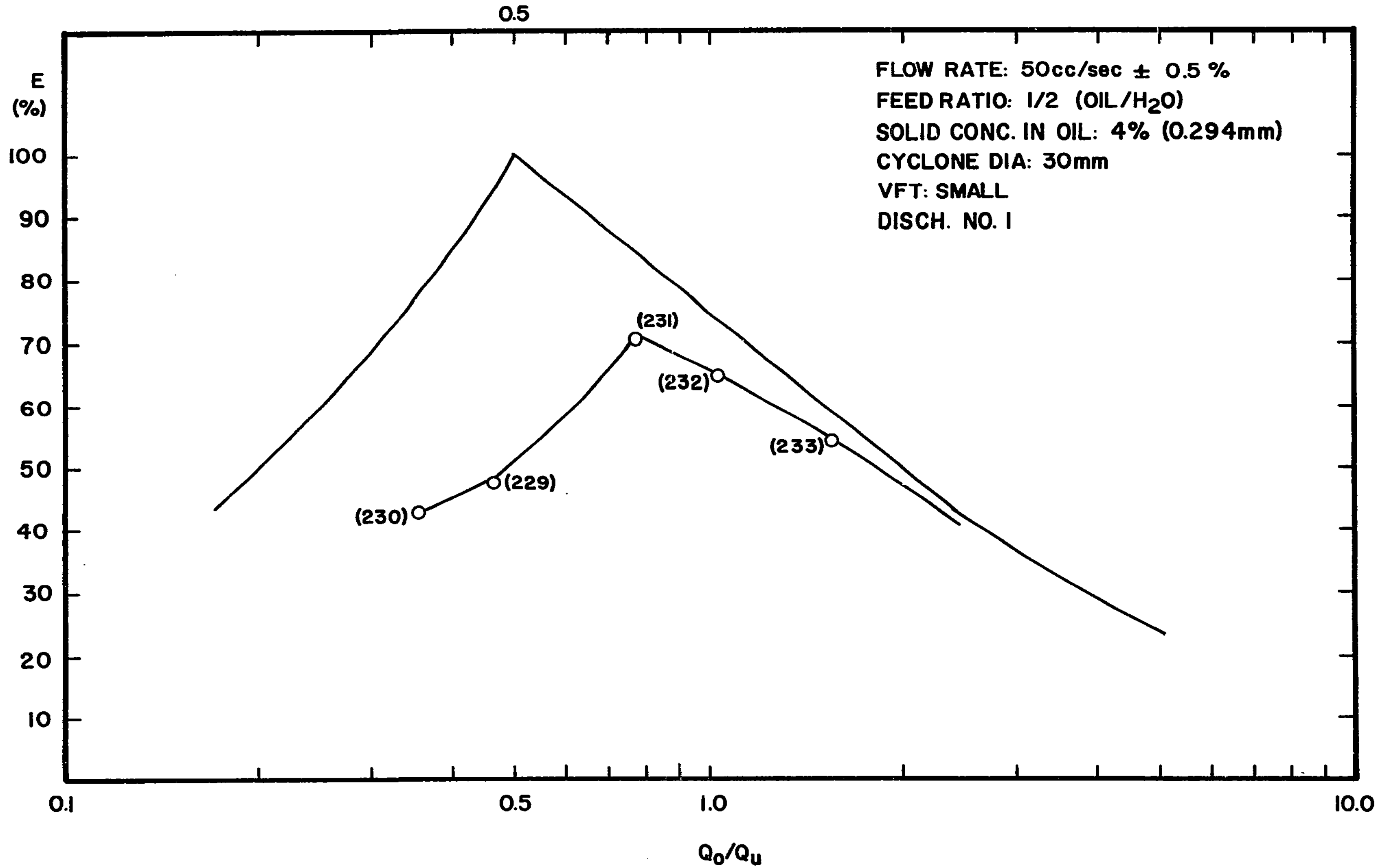

Figure E-38. Overall Efficiency vs. Effluent Split.

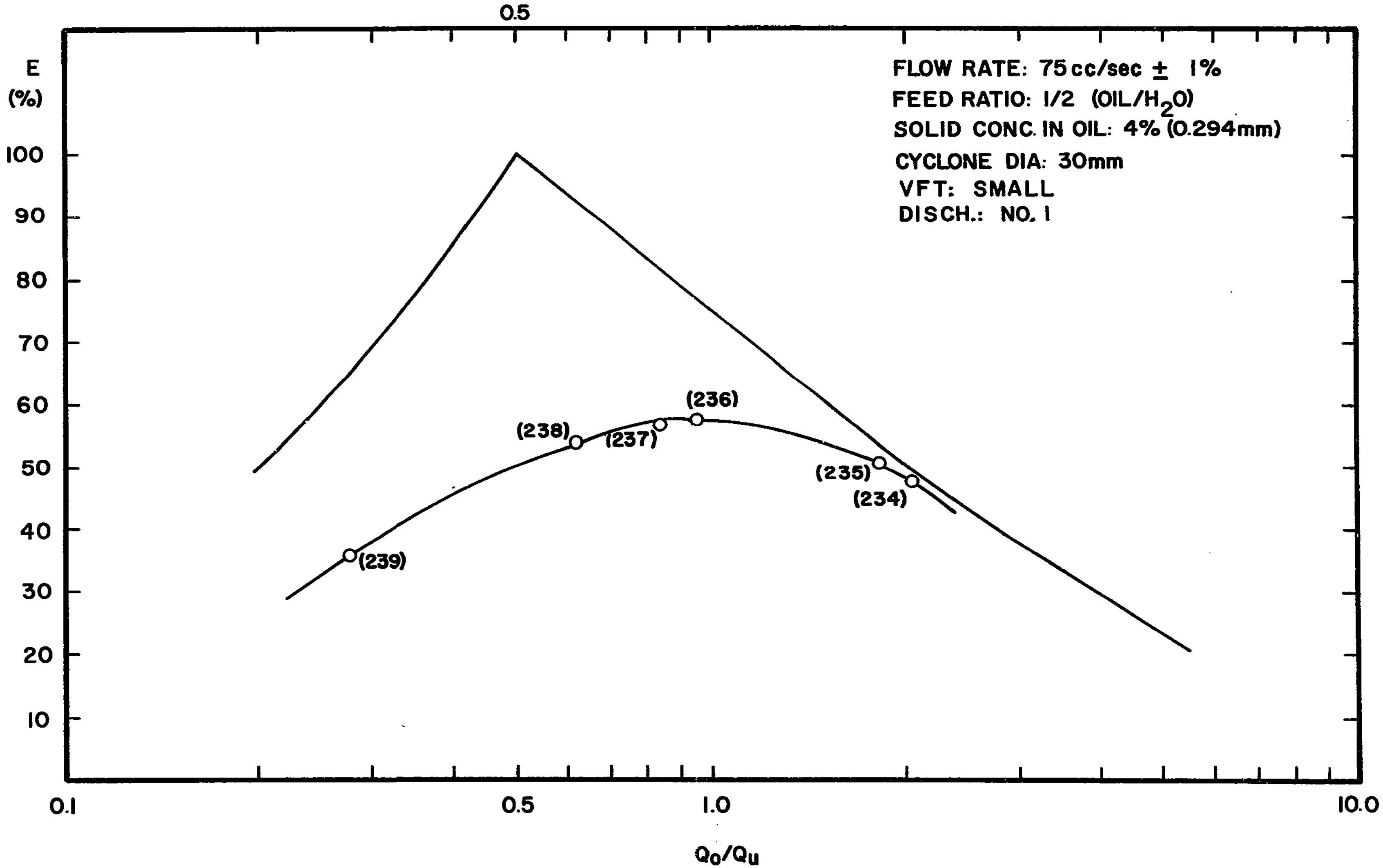

Figure E-39. Overall Efficiency vs. Effluent Split.

TABLE E-2

SUMMARY OF EXPERIMENTAL RESULTS

Run	x_f+z_f	Q_f cc/sec	x_o+z_o	Q_o cc/sec	y_u	Q_u cc/sec	E	Q_o/Q_u	$\frac{Q_o y_o}{Q_u y_u}$	$\frac{Q_o(x_o+z_o)}{Q_u(x_u+z_u)}$	$\frac{Q_o x_o}{Q_u x_u}$	$\frac{Q_o z_o}{Q_u z_u}$	Solid %
1	0.336	60.48	0.487	41.520	0.993	18.960	0.463	2.190	1.130	145.00	143.00	∞	1.93
2	0.340	60.40	0.542	36.350	0.965	24.050	0.541	1.511	0.720	23.66	23.34	78.300	2.05
3	0.355	60.00	0.703	25.300	0.896	34.700	0.636	0.729	0.240	4.94	5.12	1.350	2.12
4	0.339	60.79	0.582	33.960	0.969	26.830	0.606	1.266	0.545	23.80	23.40	76.000	2.08
5	0.338	59.71	0.613	30.400	0.947	29.310	0.625	1.037	0.424	11.98	11.83	25.500	2.03
6	0.330	59.90	0.691	17.500	0.821	42.400	0.479	0.413	0.155	1.60	1.64	0.503	2.01
7	0.347	60.14	0.711	23.500	0.885	36.600	0.629	0.642	0.210	3.94	4.11	0.870	2.06
8	0.504	59.82	0.798	35.150	0.916	24.700	0.692	1.423	0.314	13.55	13.51	15.500	2.14
9	0.502	60.04	0.869	30.830	0.885	29.210	0.753	1.055	0.150	7.95	7.99	6.330	2.12
10	0.501	60.24	0.844	23.290	0.716	36.950	0.531	0.630	0.140	1.87	1.97	0.037	1.98
11	0.495	59.80	0.873	28.400	0.846	31.400	0.717	0.904	0.140	5.16	5.43	1.150	2.11
12	0.499	59.58	0.863	27.230	0.807	32.350	0.665	0.842	0.143	3.76	3.98	0.240	2.00
13	0.501	59.99	0.868	26.100	0.781	33.890	0.638	0.770	0.130	3.06	3.29	0.190	2.02
14	0.502	60.19	0.854	20.190	0.676	40.000	0.473	0.505	0.109	1.33	1.40	0.022	2.04
15	0.501	60.34	0.562	53.300	0.972	7.040	0.218	7.571	3.400	147.00	144.00	∞	2.01
16	0.499	60.19	0.765	37.450	0.938	22.740	0.661	1.647	0.410	20.20	20.10	29.700	2.01
17	0.496	60.20	0.620	47.200	0.958	13.000	0.391	3.631	1.440	53.10	52.70	73.200	1.98
18	0.668	60.06	0.993	32.490	0.715	27.570	0.793	1.178	0.012	4.11	4.54	0.066	2.03
19	0.667	60.45	0.803	48.400	0.880	12.050	0.490	4.017	0.900	26.80	27.30	25.000	2.00
20	0.668	60.11	0.848	43.000	0.785	17.110	0.581	2.513	0.490	9.95	9.96	7.950	1.98
21	0.661	59.90	0.942	35.300	0.745	24.600	0.741	1.435	0.190	5.29	5.61	1.050	1.92
22	0.666	60.18	0.995	30.380	0.671	29.800	0.748	1.019	0.009	3.08	3.33	0.061	2.02
23	0.664	60.10	0.988	21.350	0.515	38.750	0.516	0.551	0.013	1.12	1.17	0.027	2.01
24	0.670	60.43	0.989	23.550	0.534	36.880	0.563	0.639	0.013	1.35	1.42	0.030	1.94
25	0.669	60.05	0.985	11.140	0.404	48.850	0.264	0.228	0.081	0.04	0.04	0.014	1.93
26	0.672	60.52	0.992	29.720	0.630	30.800	0.717	0.965	0.011	2.59	2.78	0.059	2.06
27	0.662	74.30	0.989	39.100	0.703	35.200	0.770	1.111	0.016	3.70	4.04	0.048	2.02
28	0.665	74.78	0.985	38.460	0.675	36.320	0.740	1.059	0.023	3.21	3.47	0.092	2.00
29	0.663	75.12	0.942	44.250	0.736	30.870	0.735	1.433	0.114	5.12	5.37	0.820	2.01
30	0.666	75.50	0.985	34.300	0.600	41.200	0.650	0.833	0.020	2.04	2.17	0.048	2.01
31	0.667	74.90	0.987	29.900	0.544	45.000	0.574	0.664	0.015	1.44	1.51	0.026	2.10
32	0.676	75.58	0.980	22.580	0.453	53.000	0.414	0.426	0.019	0.76	0.79	0.017	1.98
33	0.668	74.92	0.789	56.700	0.699	18.220	0.407	3.112	0.951	8.10	8.11	6.710	2.06
34	0.667	75.35	0.912	45.750	0.709	29.400	0.667	1.556	0.194	4.86	4.90	2.860	2.00
35	0.670	74.81	0.797	55.060	0.688	19.750	0.424	2.788	0.819	7.12	7.18	5.540	2.09
36	0.673	75.43	0.864	49.110	0.683	26.320	0.565	1.866	0.371	5.08	5.13	3.430	2.02
37	0.664	74.85	0.832	48.000	0.664	26.850	0.483	1.788	0.447	4.45	4.46	3.320	2.08
38	0.671	75.16	0.978	36.090	0.613	39.070	0.668	0.924	0.033	2.33	2.48	0.078	1.97
39	0.656	74.30	0.976	37.100	0.665	37.200	0.709	0.997	0.035	2.90	3.10	0.103	1.92
40	0.668	75.70	0.981	41.900	0.717	33.800	0.779	1.240	0.033	4.32	4.77	0.647	1.96

TABLE E-2 (continued)

Run	x_f+z_f	Q_f cc/sec	x_o+z_o	Q_o cc/sec	y_u	Q_u cc/sec	E	Q_o/Q_u	$\frac{Q_o y_o}{Q_u y_u}$	$\frac{Q_o(x_o+z_o)}{Q_u(x_u+z_u)}$	$\frac{Q_o x_o}{Q_u x_u}$	$\frac{Q_o z_o}{Q_u z_u}$	Solid %
41	0.665	74.60	0.777	54.850	0.653	19.750	0.372	2.777	0.940	6.33	6.33	6.250	1.88
42	0.666	75.10	0.978	30.400	0.546	44.700	0.568	0.680	0.026	1.46	1.53	0.027	1.95
43	0.673	75.50	0.942	44.250	0.708	31.250	0.716	1.416	0.116	4.56	5.05	0.074	1.95
44	0.665	74.80	0.971	42.400	0.737	37.400	0.820	1.134	0.522	4.83	5.40	0.060	1.89
45	0.674	74.60	0.867	48.500	0.680	26.100	0.569	1.858	0.374	5.02	5.12	3.570	1.95
46	0.665	75.21	0.981	21.610	0.462	53.600	0.407	0.403	0.014	0.74	0.79	0.019	1.80
47	0.665	74.65	0.985	39.050	0.687	35.600	0.752	1.097	0.024	3.46	3.70	0.152	1.77
48	0.669	75.17	0.972	27.670	0.510	47.500	0.506	0.583	0.028	1.16	1.21	0.043	1.77
49	0.665	74.95	0.982	35.250	0.616	39.700	0.669	0.888	0.028	2.26	2.39	0.074	1.89
50	0.666	75.00	0.922	46.000	0.745	29.000	0.709	1.586	0.163	5.76	6.02	1.420	2.06
51	0.499	74.70	0.661	46.900	0.775	27.800	0.407	1.687	0.735	4.95	4.93	6.300	2.11
52	0.496	74.50	0.750	38.000	0.767	36.500	0.517	1.041	0.340	3.35	3.56	2.730	1.99
53	0.495	74.87	0.641	50.250	0.800	24.620	0.390	2.041	0.914	6.62	6.56	8.490	2.12
54	0.506	74.93	0.584	59.920	0.796	15.010	0.246	3.992	2.080	11.50	11.41	18.200	2.08
55	0.503	75.55	0.680	46.300	0.777	29.200	0.433	1.586	0.653	4.84	4.84	6.210	2.03
56	0.501	75.25	0.755	31.750	0.690	43.500	0.432	0.730	0.258	1.78	1.77	1.960	1.95
57	0.500	75.50	0.850	25.250	0.676	50.250	0.468	0.502	0.069	1.43	1.42	1.680	1.94
58	0.494	75.00	0.758	29.000	0.674	46.000	0.410	0.630	0.226	1.46	1.46	1.670	2.01
59	0.505	75.25	0.807	29.750	0.692	45.500	0.460	0.654	0.183	1.72	1.73	1.070	1.99
60	0.496	49.80	0.826	17.800	0.687	32.000	0.471	0.556	0.142	1.47	1.45	0.053	1.99
61	0.507	50.30	0.795	11.400	0.577	38.900	0.237	0.293	0.104	0.55	0.56	0.053	1.99
62	0.508	50.60	0.840	28.900	0.940	21.700	0.738	1.332	0.224	19.20	19.30	13.500	1.98
63	0.505	50.00	0.857	26.700	0.901	23.300	0.738	1.146	0.178	10.00	10.90	1.160	1.87
64	0.504	50.13	0.872	22.510	0.795	27.620	0.646	0.815	0.131	3.47	3.76	0.079	1.96
65	0.500	50.25	0.860	24.050	0.832	26.200	0.691	0.918	0.154	4.68	5.21	0.080	1.93
66	0.504	50.25	0.789	31.000	0.950	19.250	0.700	1.610	0.361	25.80	25.70	29.900	1.91
67	0.496	50.18	0.620	39.850	0.981	10.330	0.393	3.858	1.480	149.00	152.00	80.000	2.00
68	0.503	50.47	0.678	36.910	0.971	13.560	0.511	2.722	0.901	64.10	63.00	73.100	1.94
69	0.663	49.90	0.880	32.600	0.742	17.300	0.632	1.884	0.307	6.45	6.52	4.400	1.99
70	0.668	50.40	0.787	38.190	0.698	12.300	0.405	3.105	0.960	8.12	8.17	6.190	2.07
71	0.670	49.65	0.966	28.600	0.733	21.050	0.772	1.359	0.062	4.88	5.24	0.454	1.91
72	0.660	50.11	0.996	26.110	0.694	24.000	0.785	1.088	0.007	3.54	3.84	0.900	1.94
73	0.666	50.02	0.994	23.450	0.628	26.570	0.693	0.883	0.005	2.37	2.50	0.069	1.93
74	0.656	49.95	0.993	15.600	0.497	34.350	0.466	0.454	0.006	0.90	0.92	0.072	1.96
75	0.334	49.83	0.717	17.280	0.869	32.550	0.596	0.531	0.173	2.90	3.10	0.170	2.06
76	0.332	50.05	0.715	19.850	0.911	30.200	0.669	0.657	0.204	5.66	5.91	1.410	1.94
77	0.334	50.12	0.492	33.600	0.989	16.520	0.478	2.034	1.050	73.70	72.60	167.000	2.01
78	0.332	50.01	0.624	24.610	0.952	25.400	0.650	0.969	0.382	13.10	13.00	12.200	1.83

TABLE E-2 (continued)

Run	x_f+z_f	Q_f cc/sec	x_o+z_o	Q_o cc/sec	y_u	Q_u cc/sec	E	Q_o/Q_u	$\frac{Q_oy_o}{Q_uy_u}$	$\frac{Q_o(x_o+z_o)}{Q_u(x_u+z_u)}$	$\frac{Q_ox_o}{Q_ux_u}$	$\frac{Q_oz_o}{Q_uz_u}$	Solid %
79	0.332	50.25	0.696	15.320	0.829	34.950	0.503	0.438	0.161	1.78	1.86	0.051	1.87
80	0.330	50.40	0.508	10.000	0.714	40.400	0.160	0.248	0.171	0.44	0.45	0.016	1.87
81	0.341	50.35	0.698	21.500	0.925	28.850	0.678	0.745	0.242	7.19	7.21	4.970	2.03
82	0.336	50.16	0.729	17.830	0.882	32.330	0.626	0.551	0.169	3.39	3.62	0.278	1.93
83	0.336	75.20	0.640	28.500	0.850	41.700	0.480	0.683	0.258	2.60	2.59	4.550	1.92
84	0.336	74.88	0.607	34.150	0.900	40.730	0.566	0.838	0.370	4.72	4.67	12.700	1.99
85	0.347	75.20	0.389	59.400	0.812	15.800	0.147	3.759	2.820	7.78	7.68	194.000	2.12
86	0.338	49.70	0.453	36.600	0.992	13.100	0.385	2.794	1.540	199.00	199.00	200.000	4.04
87	0.336	49.90	0.647	13.100	0.774	36.800	0.364	0.356	0.162	1.03	1.09	0.189	3.94
88	0.333	50.10	0.529	31.200	0.989	18.900	0.548	1.651	0.786	71.50	70.40	94.500	4.15
89	0.334	50.33	0.590	28.580	0.980	21.750	0.625	1.314	0.574	35.00	34.80	38.200	4.12
90	0.336	50.42	0.650	18.420	0.843	32.000	0.511	0.576	0.238	2.40	2.54	0.632	4.05
91	0.326	49.88	0.607	20.330	0.902	29.500	0.584	0.689	0.313	3.15	3.42	0.650	4.18
92	0.328	50.40	0.619	24.900	0.951	25.500	0.644	0.976	0.390	12.30	12.80	5.900	3.82
93	0.333	59.92	0.458	43.560	0.995	16.360	0.405	2.663	1.450	333.00	320.00	∞	4.07
94	0.333	59.80	0.566	33.200	0.960	26.600	0.585	1.248	0.565	17.10	16.70	36.100	4.00
95	0.332	60.20	0.683	25.200	0.920	35.000	0.661	0.720	0.248	6.13	6.45	2.370	3.91
96	0.332	60.30	0.600	29.700	0.927	30.600	0.593	0.971	0.418	8.17	7.97	14.850	4.07
97	0.335	60.30	0.715	20.500	0.861	39.850	0.581	0.514	0.171	2.64	2.98	0.224	4.07
98	0.341	60.30	0.558	15.420	0.735	44.880	0.250	0.344	0.207	0.72	0.76	0.075	4.02
99	0.331	60.19	0.400	34.450	0.761	25.740	0.178	1.338	1.050	2.24	2.23	2.390	3.94
100	0.333	59.80	0.394	38.300	0.776	21.500	0.176	1.781	1.390	3.14	3.11	4.410	4.02
101	0.335	60.20	0.415	31.800	0.754	28.400	0.189	1.120	0.868	1.88	1.87	2.350	3.94
102	0.338	59.80	0.446	27.100	0.751	32.700	0.218	0.829	0.670	1.49	1.50	1.300	4.07
103	0.332	59.60	0.447	19.900	0.725	39.700	0.172	0.501	0.382	0.82	0.80	1.310	3.80
104	0.334	75.30	0.478	52.500	0.995	22.800	0.449	2.303	1.210	230.00	230.00	∞	4.12
105	0.330	74.86	0.514	47.040	0.983	27.820	0.525	1.691	0.841	57.50	56.00	140.000	3.98
106	0.332	75.50	0.622	31.400	0.875	44.100	0.545	0.712	0.307	3.54	3.48	6.280	4.05
107	0.330	74.90	0.533	42.840	0.941	32.060	0.525	1.336	0.663	12.20	11.70	72.300	4.02
108	0.338	75.47	0.601	36.770	0.911	39.700	0.581	0.926	0.416	6.47	6.23	41.300	3.90
109	0.331	74.72	0.632	23.100	0.805	51.620	0.423	0.448	0.205	1.44	1.47	0.953	4.08
110	0.499	59.80	0.781	36.400	0.941	23.400	0.688	1.556	0.363	20.30	20.10	24.200	3.89
111	0.494	59.98	0.827	34.900	0.940	25.080	0.750	1.392	0.254	19.50	19.30	24.200	3.98
112	0.504	60.10	0.873	25.500	0.770	34.600	0.629	0.737	0.120	2.78	3.23	0.071	4.00
113	0.501	60.30	0.907	29.500	0.890	30.800	0.797	0.958	0.099	7.88	9.88	0.600	3.89
114	0.499	60.30	0.856	22.200	0.708	38.100	0.524	0.583	0.118	1.71	1.97	0.038	3.98

TABLE E-2 (continued)

Run	x_f+z_f	Q_f cc/sec	x_o+z_o	Q_o cc/sec	y_u	Q_u cc/sec	E	Q_o/Q_u	$\frac{Q_o y_o}{Q_u y_u}$	$\frac{Q_o(x_o+z_o)}{Q_u(x_u+z_u)}$	$\frac{Q_o x_o}{Q_u x_u}$	$\frac{Q_o z_o}{Q_u z_u}$	Solid %
115	0.498	59.72	0.686	42.160	0.956	17.560	0.532	2.401	0.785	38.10	38.20	34.000	3.89
116	0.507	74.75	0.625	55.250	0.825	19.500	0.348	2.833	1.290	10.30	10.20	10.600	3.95
117	0.505	75.60	0.697	44.550	0.769	31.100	0.452	1.432	0.565	4.27	4.26	4.720	4.12
118	0.505	75.05	0.662	49.400	0.805	25.650	0.419	1.926	0.803	6.65	6.47	7.750	4.00
119	0.500	75.07	0.819	36.310	0.798	38.760	0.616	0.937	0.212	3.79	3.83	2.860	4.12
120	0.499	75.25	0.921	25.750	0.715	49.500	0.570	0.520	0.067	1.66	1.78	0.320	4.05
121	0.502	74.90	0.844	30.500	0.731	44.400	0.555	0.687	0.146	2.17	2.29	0.700	4.06
122	0.494	75.30	0.855	31.800	0.770	43.500	0.610	0.731	0.138	2.72	2.96	0.581	4.05
123	0.501	75.05	0.731	41.400	0.785	33.650	0.510	1.230	0.420	4.20	4.20	4.380	4.18
124	0.498	74.70	0.756	40.500	0.810	34.200	0.562	1.184	0.357	4.67	4.67	4.780	4.00
125	0.502	75.30	0.741	40.300	0.777	35.000	0.515	1.151	0.382	3.83	3.82	4.230	4.03
126	0.504	75.45	0.905	23.450	0.676	52.000	0.497	0.451	0.062	1.27	1.21	5.130	3.92
127	0.665	60.06	0.981	37.260	0.850	22.800	0.879	1.634	0.034	10.75	13.00	1.320	3.85
128	0.667	60.46	0.982	32.860	0.710	27.600	0.770	1.191	0.030	4.03	4.76	0.235	4.01
129	0.666	60.12	0.980	29.220	0.628	30.900	0.684	0.946	0.030	2.49	2.82	0.118	3.91
130	0.666	60.30	0.980	26.000	0.574	34.300	0.610	0.758	0.025	1.74	1.92	0.121	4.04
131	0.666	59.80	0.793	48.500	0.886	11.300	0.465	4.292	1.000	29.60	29.30	31.800	3.94
132	0.669	59.60	0.987	39.000	0.932	20.600	0.939	1.893	0.026	27.20	27.80	18.600	3.90
133	0.665	59.74	0.814	46.200	0.841	13.540	0.516	3.412	0.754	17.60	17.80	13.200	4.05
134	0.668	60.30	0.869	42.800	0.824	17.500	0.643	2.446	0.389	12.00	12.00	10.300	4.02
135	0.670	75.00	0.985	47.000	0.865	28.000	0.896	1.679	0.024	12.40	16.60	1.000	3.92
136	0.666	74.90	0.980	42.800	0.769	32.100	0.815	1.333	0.016	5.72	7.64	0.055	3.95
137	0.662	75.00	0.990	39.500	0.703	35.500	0.772	1.113	0.015	3.74	4.50	0.086	3.95
138	0.664	75.60	0.820	53.600	0.715	22.000	0.495	2.436	0.611	7.04	7.10	6.180	3.96
139	0.669	75.05	0.790	55.700	0.688	19.350	0.409	2.879	0.876	7.25	7.25	7.470	3.90
140	0.661	74.72	0.784	58.600	0.820	16.120	0.442	3.635	0.910	16.20	16.35	13.400	4.00
141	0.667	49.95	0.994	28.750	0.779	21.200	0.847	1.356	0.010	6.13	7.63	0.390	4.04
142	0.666	49.70	0.996	28.800	0.791	20.900	0.861	1.378	0.060	6.62	8.27	0.410	3.84
143	0.666	50.12	0.915	35.300	0.932	14.820	0.791	2.382	0.213	33.00	34.20	17.000	3.98
144	0.665	49.63	0.849	38.400	0.950	11.230	0.634	3.419	0.547	57.70	60.04	30.600	3.81
145	0.666	49.67	0.995	31.650	0.906	18.220	0.939	1.737	0.010	18.50	20.90	4.110	3.79
146	0.671	49.94	0.992	32.800	0.942	17.140	0.952	1.914	0.020	31.50	32.70	15.500	3.92
147	0.503	50.17	0.748	32.750	0.962	17.420	0.643	1.880	0.490	38.80	39.90	22.500	4.02
148	0.500	50.00	0.648	38.040	0.968	11.960	0.449	3.181	1.160	65.78	64.60	78.700	3.99
149	0.503	50.00	0.845	28.300	0.947	21.700	0.778	1.304	0.210	20.30	20.80	13.000	3.82
150	0.495	49.90	0.815	25.200	0.835	24.700	0.650	1.020	0.224	4.96	6.33	0.050	3.91
151	0.500	50.00	0.792	22.900	0.748	27.100	0.536	0.845	0.235	2.66	3.11	0.026	4.07
152	0.503	50.10	0.768	20.100	0.674	30.000	0.425	0.670	0.231	1.58	1.76	0.013	3.97

TABLE E-2 (continued)

Run	x_f+z_f	Q_f cc/sec	x_o+z_o	Q_o cc/sec	y_u	Q_u cc/sec	E	Q_o/Q_u	$\frac{Q_o y_o}{Q_u y_u}$	$\frac{Q_o(x_o+z_o)}{Q_u(x_u+z_u)}$	$\frac{Q_o x_o}{Q_u x_u}$	$\frac{Q_o z_o}{Q_u z_u}$	Solid %
153	0.335	60.36	0.554	35.800	0.983	24.560	0.582	1.458	0.664	43.00	42.70	92.200	2.02
154	0.333	59.99	0.567	33.370	0.960	26.620	0.586	1.254	0.566	17.30	17.50	39.600	2.01
155	0.337	59.90	0.631	29.000	0.940	30.900	0.639	0.939	0.368	9.60	9.43	17.900	2.02
156	0.329	59.64	0.641	23.540	0.875	36.100	0.559	0.652	0.270	3.34	3.31	7.940	2.03
157	0.332	60.10	0.672	19.500	0.830	40.600	0.495	0.480	0.190	1.88	1.91	1.160	2.09
158	0.501	60.19	0.884	20.990	0.704	39.200	0.534	0.535	0.088	1.60	1.66	0.260	2.06
159	0.500	59.93	0.893	22.890	0.743	39.040	0.617	0.586	0.089	2.15	2.24	0.330	2.11
160	0.501	60.34	0.862	32.100	0.910	28.240	0.769	1.137	0.171	10.90	10.98	8.500	2.07
161	0.505	60.10	0.797	35.720	0.925	24.380	0.696	1.465	0.321	15.10	15.10	17.000	2.06
162	0.502	60.04	0.869	29.550	0.855	30.540	0.724	0.968	0.148	5.79	6.14	1.040	2.11
163	0.503	60.18	0.705	41.600	0.947	18.580	0.557	2.239	0.700	29.10	29.70	37.800	2.04
164	0.334	75.17	0.415	60.000	0.990	15.170	0.297	3.955	2.340	143.00	143.20	98.000	1.97
165	0.336	74.92	0.566	40.880	0.940	34.040	0.562	1.201	0.555	11.35	11.11	51.700	1.97
166	0.333	75.02	0.512	48.130	0.985	26.890	0.514	1.790	0.887	63.50	62.50	375.000	1.96
167	0.334	75.32	0.568	35.060	0.885	40.260	0.528	0.871	0.410	4.51	4.42	28.700	1.96
168	0.335	75.13	0.604	27.750	0.823	47.380	0.447	0.586	0.280	2.00	1.97	10.500	2.06
169	0.337	50.37	0.707	17.670	0.865	32.600	0.584	0.542	0.180	0.81	2.89	0.720	1.88
170	0.329	49.90	0.625	23.300	0.930	26.600	0.626	0.876	0.350	7.72	7.70	9.800	1.94
171	0.331	50.27	0.550	29.050	0.970	21.220	0.573	1.369	0.632	26.00	26.00	32.900	2.00
172	0.331	49.82	0.466	34.410	0.972	15.410	0.423	2.233	1.220	38.50	38.00	62.000	1.90
173	0.500	49.95	0.625	34.800	0.783	15.150	0.346	2.297	1.100	6.60	6.57	8.900	2.02
174	0.498	50.00	0.720	29.900	0.837	20.100	0.535	1.488	0.495	6.57	6.53	8.270	1.99
175	0.505	50.15	0.909	19.750	0.756	30.400	0.635	0.650	0.077	2.44	2.67	0.210	1.88
176	0.500	49.85	0.915	21.750	0.821	28.100	0.724	0.774	0.080	3.98	3.98	3.870	1.99
177	0.502	50.30	0.844	25.900	0.864	24.400	0.707	1.061	0.190	6.57	6.52	8.120	2.04
178	0.498	75.35	0.752	39.950	0.780	35.400	0.531	1.129	0.355	4.00	3.99	4.480	1.83
179	0.509	75.30	0.792	32.100	0.701	43.200	0.482	0.743	0.220	1.95	1.96	1.850	1.89
180	0.503	75.10	0.770	36.300	0.745	38.800	0.514	0.936	0.290	2.82	2.82	3.130	2.02
181	0.500	75.00	0.850	30.400	0.738	44.600	0.567	0.682	0.140	2.22	2.26	0.830	1.81
182	0.665	74.90	0.966	36.000	0.615	38.900	0.651	0.925	0.052	2.31	2.37	0.740	1.91
183	0.667	75.45	0.975	29.650	0.532	45.800	0.545	0.647	0.027	1.35	1.40	0.120	1.84
184	0.670	74.90	0.930	39.300	0.617	35.600	0.617	1.104	0.123	2.69	2.70	2.200	1.89
185	0.665	74.60	0.872	43.100	0.620	31.500	0.538	1.368	0.280	3.14	3.14	2.920	2.04
186	0.662	60.26	0.866	36.510	0.650	23.750	0.551	1.537	0.320	3.81	3.81	3.920	1.99

TABLE E-2 (continued)

Run	x_f+z_f	Q_f cc/sec	x_o+z_o	Q_o cc/sec	y_u	Q_u cc/sec	E	Q_o/Q_u	$\frac{Q_o y_o}{Q_u y_u}$	$\frac{Q_o(x_o+z_o)}{Q_u(x_u+z_u)}$	$\frac{Q_o x_o}{Q_u x_u}$	$\frac{Q_o z_o}{Q_u z_u}$	Solid %
187	0.667	60.06	0.975	26.420	0.577	33.640	0.612	0.785	0.032	1.81	1.89	0.330	2.11
188	0.669	60.00	0.980	29.800	0.632	30.200	0.693	0.987	0.033	2.62	2.75	0.364	2.04
189	0.670	60.10	0.911	33.700	0.637	26.400	0.611	1.277	0.180	3.20	3.20	2.920	1.81
190	0.663	60.10	0.723	48.300	0.581	11.800	0.215	4.093	1.940	7.08	7.06	9.300	2.04
191	0.667	49.90	0.842	30.250	0.602	19.650	0.477	1.539	0.400	3.26	3.28	3.420	1.86
192	0.670	49.95	0.940	24.950	0.600	25.000	0.610	0.998	0.100	2.35	2.36	1.910	1.90
193	0.668	50.25	0.982	23.100	0.602	27.150	0.653	0.851	0.023	2.10	2.18	0.340	1.91
194	0.666	50.26	0.980	16.360	0.486	33.900	0.460	0.483	0.018	0.92	0.95	0.150	2.04
195	0.665	59.70	0.888	33.500	0.619	26.200	0.561	1.279	0.240	2.96	2.96	2.860	4.03
196	0.666	60.16	0.963	28.920	0.609	31.240	0.642	0.926	0.056	2.28	2.31	1.830	3.93
197	0.666	60.08	0.988	26.060	0.580	34.020	0.627	0.766	0.017	1.80	1.93	0.390	4.07
198	0.665	60.45	0.862	35.650	0.622	24.800	0.524	1.437	0.318	3.27	3.30	3.030	4.16
199	0.498	75.55	0.802	31.950	0.725	43.600	0.515	0.733	0.199	2.14	2.22	0.995	4.00
200	0.500	75.00	0.706	37.000	0.700	38.000	0.406	0.974	0.407	2.30	2.34	2.540	3.76
201	0.502	75.00	0.669	41.050	0.698	33.950	0.364	1.209	0.572	2.69	2.68	2.990	3.94
202	0.501	60.28	0.925	27.580	0.855	32.700	0.774	0.843	0.074	5.43	6.24	0.770	4.07
203	0.499	59.95	0.920	28.620	0.886	31.330	0.804	0.914	0.081	7.30	7.71	2.840	3.94
204	0.500	60.13	0.896	24.850	0.778	35.280	0.654	0.704	0.045	2.84	3.22	0.200	4.03
205	0.501	60.04	0.816	34.620	0.928	25.420	0.727	1.362	0.270	15.52	15.40	17.300	3.96
206	0.498	60.16	0.737	38.600	0.931	21.560	0.614	1.790	0.470	19.22	18.96	25.100	4.01
207	0.497	59.60	0.884	30.660	0.912	28.940	0.795	1.059	0.135	10.66	10.74	8.600	4.08
208	0.663	50.11	0.958	28.180	0.713	21.930	0.740	1.285	0.076	4.29	4.54	1.460	3.83
209	0.667	50.17	0.984	25.000	0.647	25.170	0.711	0.993	0.025	2.77	2.84	1.490	3.78
210	0.665	49.90	0.897	30.110	0.687	19.790	0.628	1.521	0.229	4.34	4.34	4.240	4.00
211	0.670	49.95	0.785	37.630	0.683	12.320	0.392	3.054	0.960	7.57	7.47	8.490	3.88
212	0.669	50.30	0.991	21.200	0.567	29.100	0.614	0.729	0.011	1.68	1.79	0.330	3.90
213	0.665	75.25	0.860	44.750	0.622	30.500	0.521	1.467	0.330	3.35	3.36	3.260	4.09
214	0.666	75.40	0.871	43.000	0.610	32.900	0.531	1.307	0.280	2.96	2.97	2.870	3.84
215	0.670	74.85	0.950	34.600	0.570	40.250	0.585	0.860	0.075	1.90	1.92	1.480	3.85
216	0.668	74.85	0.910	38.750	0.591	36.100	0.564	1.073	0.166	2.38	2.38	2.050	3.88
217	0.501	50.00	0.841	28.000	0.931	22.000	0.758	1.273	0.215	16.55	16.93	9.720	3.72
218	0.504	50.32	0.811	24.660	0.790	25.660	0.601	0.961	0.230	3.75	4.51	0.089	3.95
219	0.497	50.25	0.791	22.750	0.745	27.500	0.531	0.827	0.238	2.58	2.98	0.048	4.08
220	0.500	50.11	0.781	30.660	0.942	19.450	0.687	1.576	0.364	21.20	21.26	19.300	3.91
221	0.496	50.08	0.676	36.000	0.964	14.080	0.517	2.557	0.859	48.70	48.30	58.400	4.06

TABLE E-2 (continued)

Run	x_f+z_f	Q_f cc/sec	x_o+z_o	Q_o cc/sec	y_u	Q_u cc/sec	E	Q_o/Q_u	$\frac{Q_o y_o}{Q_u y_u}$	$\frac{Q_o(x_o+z_o)}{Q_u(x_u+z_u)}$	$\frac{Q_o x_o}{Q_u x_u}$	$\frac{Q_o z_o}{Q_u z_u}$	Solid %
222	0.336	60.10	0.677	13.300	0.761	46.800	0.338	0.284	0.120	0.80	0.85	0.104	4.09
223	0.331	59.90	0.483	40.850	0.993	19.050	0.466	2.144	1.120	132.00	136.00	104.000	3.81
224	0.333	59.78	0.566	33.400	0.962	26.380	0.586	1.266	0.570	19.30	19.10	25.300	3.97
225	0.337	60.07	0.716	25.070	0.935	35.000	0.709	0.716	0.217	7.92	8.07	5.420	4.11
226	0.337	60.24	0.740	24.250	0.935	35.990	0.727	0.674	0.187	7.67	8.09	3.010	4.11
227	0.337	60.35	0.742	21.900	0.893	38.450	0.656	0.570	0.165	3.96	4.36	0.750	3.94
228	0.331	59.90	0.655	27.500	0.944	32.400	0.672	0.849	0.310	10.00	9.98	10.360	3.79
229	0.333	50.00	0.668	15.820	0.822	34.180	0.477	0.463	0.187	1.74	1.79	0.914	3.88
230	0.331	50.10	0.685	13.400	0.800	36.700	0.431	0.365	0.144	1.23	1.34	0.078	4.03
231	0.336	50.20	0.687	21.900	0.946	28.300	0.704	0.774	0.256	9.67	9.72	8.210	3.88
232	0.333	50.10	0.615	25.600	0.957	24.650	0.645	1.039	0.416	14.75	14.88	12.300	3.93
233	0.336	50.18	0.535	30.490	0.974	19.690	0.544	1.549	0.739	31.85	31.66	55.400	3.88
234	0.333	75.05	0.490	51.000	0.996	24.050	0.477	2.121	1.080	500.00	600.00	92.500	3.82
235	0.332	74.85	0.505	48.500	0.986	26.350	0.505	1.841	0.922	70.00	69.00	119.000	3.98
236	0.334	74.90	0.602	35.500	0.910	39.400	0.575	0.901	0.400	5.85	5.68	16.900	3.96
237	0.332	74.70	0.609	34.200	0.900	40.500	0.569	0.844	0.366	5.23	5.07	15.900	4.07
238	0.332	75.05	0.645	28.660	0.864	46.390	0.544	0.618	0.254	2.90	2.84	5.280	3.99
239	0.337	74.90	0.710	16.400	0.765	58.500	0.360	0.280	0.107	0.85	0.89	0.165	3.90
240	0.331	75.55	0.542	42.500	0.936	33.050	0.530	1.286	0.628	11.10	10.92	30.000	4.01

IBM 360/40 FORTRAN PROGRAM

(TABLE E-2)

```
C       SEPARATION EXPERIMENT    PROGRAM 1
        DIMENSION COL(17)
        EQUIVALENCE(QO,COL(4)),(YF,COL(6)),(YU,COL(8)),(Qu,COL(12)),
       1(QF,COL(15))
        FLAG=1.0
        INCT=48.0
100     CONTINUE
        READ (1,5000) COL(1),COL(2),QO,YF, YU,QU,QF,RUN
        IF(COL(1))300,200,300
200     CONTINUE
        IF(FLAG) 210,220,210
210     CONTINUE
        FLAG=0.0
        WRITE(3,5200)
        LNCT=LNCT+ 2.0
        GO TO 100
220     CONTINUE
        STOP
300     CONTINUE
        FLAG=1.0
        READ(1,5500) WATER,OILSO,OIL,SOLID,PSOLID,IRAN
        NRUN=RUN
        IF(NRUN-IRAN) 325,800,325
325     CONTINUE
        WRITE (3,5600)
        GO TO 220
800     CONTINUE
        COL(3)=COL(1)-COL(2)
        COL(5)=COL(3)*COL(4)
        COL(7)=COL(5)/COL(6)
        COL(9)=COL(8)-COL(6)
        COL(10)=COL(2)
        COL(11)=COL(9)/COL(10)
        COL(13)=COL(11)*COL(12)
        COL(14)=COL(7)+COL(13)
        COL(16)=COL(14)/COL(15)
        COL(17)=COL(4)/COL(12)
        IF(LNCT-48.0) 900,850,850
850     CONTINUE
        WRITE (3,5700)
        LNCT=0
900     LNCT=LNCT+1.0
```

```
      WRITE(3,5100)NRUN,COL(2),QF,COL(1), QO,YU,QU,COL(16),COL(17),WATER
     1OILSO,OIL,SOLID,PSOLID
      GO TO 100
5000  FORMAT(8F10.3)
5100  FORMAT('      ',I3,F8.3,F8.2,F8.3,F9.3,F8.3,F9.3,3F8.3,F10.2,F10.2,
     1F10.3,F8.2)
5200  FORMAT('0')
5500  FORMAT(6X,F6.4,2F12.3,F12.4,F9.3,15X,I4)
5600  FORMAT('PHASE ERROR')
5700  FORMAT('1'/'0'/'0'/'0')
      END
```

TABLE E-3

SUMMARY OF PROCESSED DATA

RUN	x_f+z_f	Q_f cc/sec	x_o+z_o	Q_o cc/sec	y_u	Q_u cc/sec	Q_o/Q_u	E	$Q_f x_f$ cc/sec	$\frac{Q_o x_o}{Q_f x_f}$	E_s	E/E_s	$\left(\frac{Q_o x_o}{Q_f x_f}\right)_I$	$\frac{Q_o x_o}{(Q_o x_o)_I}$	d cm.	EVF	ϕ (%)
C 1	0.341	60.00	0.710	17.50	0.812	42.50	0.412	0.480	20.44	0.608	0.856	0.561	0.856	0.710	8.17	0.12	6.71
C 2	0.341	60.00	0.721	19.50	0.842	40.50	0.482	0.550	20.44	0.688	0.954	0.577	0.954	0.721	7.64	0.14	8.36
C 3	0.341	60.00	0.712	21.50	0.867	38.50	0.559	0.593	20.44	0.749	0.973	0.609	1.000	0.749	6.91	0.19	11.34
C 4	0.341	60.00	0.696	23.50	0.888	36.50	0.644	0.620	20.44	0.801	0.923	0.672	1.000	0.801	6.12	0.24	16.00
C 5	0.341	60.00	0.679	25.51	0.909	34.49	0.739	0.640	20.44	0.847	0.872	0.734	1.000	0.847	5.19	0.31	22.86
C 6	0.341	60.00	0.654	27.51	0.925	32.49	0.847	0.640	20.44	0.880	0.821	0.779	1.000	0.880	4.43	0.38	29.67
C 7	0.341	60.00	0.628	29.51	0.938	30.49	0.968	0.630	20.44	0.907	0.771	0.817	1.000	0.907	3.69	0.46	37.46
C 8	0.341	60.00	0.605	31.51	0.952	28.49	1.106	0.618	20.44	0.933	0.720	0.858	1.000	0.933	2.94	0.55	46.83
C 9	0.341	60.00	0.581	33.51	0.964	26.49	1.265	0.598	20.44	0.953	0.670	0.893	1.000	0.953	2.32	0.63	55.96
C 10	0.341	60.00	0.557	35.51	0.973	24.49	1.450	0.570	20.44	0.968	0.619	0.921	1.000	0.968	1.60	0.73	67.24
C 11	0.341	60.00	0.533	37.52	0.980	22.48	1.669	0.535	20.44	0.978	0.568	0.941	1.000	0.978	0.90	0.84	79.21
C 12	0.341	60.00	0.511	39.52	0.988	20.48	1.929	0.500	20.44	0.988	0.518	0.966	1.000	0.988	0.19	0.96	93.10
C 13	0.341	60.00	0.487	41.52	0.987	18.48	2.247	0.450	20.44	0.989	0.467	0.963	1.000	0.989	0.00	1.00	96.32
C 14	0.500	60.00	0.849	20.19	0.677	39.81	0.507	0.470	30.00	0.571	0.673	0.698	0.673	0.849	6.67	0.20	14.05
C 15	0.500	60.00	0.850	22.26	0.707	37.74	0.590	0.520	30.00	0.631	0.742	0.701	0.742	0.850	6.13	0.24	16.62
C 16	0.500	60.00	0.851	24.33	0.740	35.67	0.682	0.570	30.00	0.690	0.811	0.703	0.811	0.851	5.60	0.28	19.49
C 17	0.500	60.00	0.864	26.40	0.786	33.60	0.786	0.640	30.00	0.760	0.880	0.727	0.880	0.864	4.89	0.34	24.54
C 18	0.500	60.00	0.869	28.47	0.833	31.53	0.903	0.700	30.00	0.824	0.949	0.738	0.949	0.869	4.34	0.39	28.72
C 19	0.500	60.00	0.871	30.54	0.884	29.46	1.036	0.755	30.00	0.886	0.982	0.769	1.000	0.886	3.62	0.47	35.83
C 20	0.500	60.00	0.840	32.61	0.905	27.39	1.190	0.740	30.00	0.913	0.913	0.810	1.000	0.913	2.85	0.56	45.15
C 21	0.500	60.00	0.807	34.68	0.921	25.32	1.369	0.710	30.00	0.933	0.844	0.841	1.000	0.933	2.11	0.66	55.21
C 22	0.500	60.00	0.769	36.74	0.926	23.26	1.580	0.660	30.00	0.942	0.775	0.851	1.000	0.942	1.40	0.76	64.76
C 23	0.500	60.00	0.732	38.81	0.925	21.19	1.832	0.600	30.00	0.947	0.706	0.850	1.000	0.947	0.82	0.86	72.69
C 24	0.500	60.00	0.704	40.88	0.935	19.12	2.139	0.555	30.00	0.959	0.637	0.871	1.000	0.959	0.09	0.98	85.73
C 25	0.500	60.00	0.671	42.95	0.931	17.05	2.520	0.490	30.00	0.961	0.568	0.862	1.000	0.961	0.00	1.00	86.23
C 26	0.500	60.00	0.645	45.02	0.936	14.98	3.006	0.435	30.00	0.968	0.499	0.871	1.000	0.968	0.00	1.00	87.13
C 27	0.500	60.00	0.623	47.09	0.947	12.91	3.648	0.385	30.00	0.977	0.430	0.895	1.000	0.977	0.00	1.00	89.48
C 28	0.500	60.00	0.601	49.16	0.957	10.84	4.536	0.330	30.00	0.984	0.361	0.913	1.000	0.984	0.00	1.00	91.34
C 29	0.500	60.00	0.579	51.23	0.962	8.77	5.842	0.270	30.00	0.989	0.292	0.924	1.000	0.989	0.00	1.00	92.36
C 30	0.500	60.00	0.556	53.30	0.948	6.70	7.955	0.200	30.00	0.988	0.223	0.895	1.000	0.988	0.00	1.00	89.55
C 31	0.667	60.00	0.978	11.14	0.404	48.86	0.228	0.260	40.03	0.272	0.278	0.934	0.278	0.978	8.91	0.09	8.33
C 32	0.667	60.00	0.980	13.21	0.421	46.79	0.282	0.310	40.03	0.323	0.330	0.939	0.330	0.980	8.17	0.12	11.24
C 33	0.667	60.00	0.981	15.28	0.440	44.72	0.342	0.360	40.03	0.374	0.382	0.943	0.382	0.981	7.44	0.16	14.69
C 34	0.667	60.00	0.982	17.35	0.461	42.65	0.407	0.410	40.03	0.426	0.433	0.946	0.433	0.982	6.89	0.19	17.73
C 35	0.667	60.00	0.983	19.42	0.484	40.58	0.479	0.460	40.03	0.477	0.485	0.948	0.485	0.983	6.17	0.23	22.23
C 36	0.667	60.00	0.983	21.49	0.509	38.51	0.558	0.510	40.03	0.528	0.537	0.950	0.537	0.983	5.62	0.28	26.19
C 37	0.667	60.00	0.984	23.56	0.538	36.44	0.647	0.560	40.03	0.579	0.589	0.952	0.589	0.984	4.92	0.33	31.82
C 38	0.667	60.00	0.984	25.63	0.569	34.37	0.746	0.610	40.03	0.630	0.640	0.953	0.640	0.984	4.37	0.39	36.81
C 39	0.667	60.00	0.985	27.70	0.605	32.30	0.858	0.660	40.03	0.681	0.692	0.954	0.692	0.985	3.69	0.46	43.67
C 40	0.667	60.00	0.989	29.77	0.649	30.23	0.985	0.718	40.03	0.735	0.744	0.966	0.744	0.989	3.12	0.52	50.54
C 41	0.667	60.00	0.989	31.84	0.697	28.16	1.131	0.770	40.03	0.787	0.795	0.968	0.795	0.989	2.45	0.61	59.01

TABLE E-3 (continued)

RUN	x_f+z_f	Q_f cc/sec	x_o+z_o	Q_o cc/sec	Y_u	Q_u cc/sec	Q_o/Q_u	E	Q_fx_f cc/sec	$\frac{Q_ox_o}{Q_fx_f}$	E_s	E/E_s	$\left(\frac{Q_ox_o}{Q_fx_f}\right)_I$	$\frac{Q_ox_o}{(Q_ox_o)_I}$	d cm.	EVF	Φ (%)
C 42	0.667	60.00	0.972	33.91	0.729	26.09	1.300	0.775	40.03	0.823	0.847	0.915	0.847	0.972	2.07	0.66	60.55
C 43	0.667	60.00	0.936	35.98	0.735	24.02	1.498	0.725	40.03	0.841	0.899	0.807	0.899	0.936	1.67	0.72	58.11
C 44	0.667	60.00	0.907	38.05	0.749	21.95	1.733	0.685	40.03	0.862	0.950	0.721	0.950	0.907	1.35	0.77	55.44
C 45	0.667	60.00	0.896	40.12	0.795	19.88	2.018	0.690	40.03	0.898	0.996	0.693	1.000	0.898	0.83	0.85	59.10
C 46	0.667	60.00	0.858	42.19	0.785	17.81	2.369	0.605	40.03	0.904	0.892	0.678	1.000	0.904	0.14	0.97	66.08
C 47	0.667	60.00	0.837	44.26	0.811	15.74	2.812	0.565	40.03	0.926	0.788	0.717	1.000	0.926	0.00	1.00	71.67
C 48	0.667	60.00	0.818	46.33	0.844	13.67	3.389	0.525	40.03	0.947	0.685	0.767	1.000	0.947	0.00	1.00	76.68
C 49	0.667	60.00	0.801	48.40	0.890	11.60	4.172	0.485	40.03	0.968	0.581	0.835	1.000	0.968	0.00	1.00	83.48
C 50	0.668	75.00	0.977	22.58	0.466	52.42	0.431	0.420	50.08	0.441	0.451	0.931	0.451	0.977	6.65	0.20	18.82
C 51	0.668	75.00	0.982	24.59	0.486	50.41	0.488	0.465	50.08	0.482	0.491	0.947	0.491	0.982	6.15	0.24	22.39
C 52	0.668	75.00	0.984	26.59	0.506	48.41	0.549	0.505	50.08	0.522	0.531	0.951	0.531	0.984	5.65	0.27	26.08
C 53	0.668	75.00	0.987	28.60	0.529	46.40	0.616	0.548	50.08	0.563	0.571	0.959	0.571	0.987	5.15	0.31	30.20
C 54	0.668	75.00	0.986	30.61	0.552	44.39	0.690	0.585	50.08	0.603	0.611	0.957	0.611	0.986	4.66	0.36	34.34
C 55	0.668	75.00	0.984	32.62	0.576	42.38	0.770	0.620	50.08	0.641	0.651	0.952	0.651	0.984	4.18	0.41	38.66
C 56	0.668	75.00	0.985	34.62	0.604	40.38	0.857	0.660	50.08	0.681	0.691	0.955	0.691	0.985	3.69	0.46	43.71
C 57	0.668	75.00	0.985	36.63	0.635	38.37	0.955	0.698	50.08	0.720	0.731	0.954	0.731	0.985	3.33	0.50	47.62
C 58	0.668	75.00	0.997	38.64	0.682	36.36	1.063	0.765	50.08	0.769	0.772	0.992	0.772	0.997	2.68	0.58	57.40
C 59	0.668	75.00	0.985	40.64	0.708	34.36	1.183	0.775	50.08	0.799	0.812	0.955	0.812	0.985	2.36	0.62	59.40
C 60	0.668	75.00	0.964	42.65	0.723	32.35	1.318	0.760	50.08	0.821	0.852	0.892	0.852	0.964	2.07	0.66	59.10
C 61	0.668	75.00	0.932	44.66	0.722	30.34	1.472	0.710	50.08	0.831	0.892	0.796	0.892	0.932	1.83	0.70	55.44
C 62	0.668	75.00	0.896	46.66	0.708	28.34	1.647	0.640	50.08	0.835	0.932	0.687	0.932	0.896	1.63	0.73	49.90
C 63	0.668	75.00	0.868	48.67	0.702	26.33	1.849	0.585	50.08	0.843	0.972	0.602	0.972	0.868	1.39	0.76	45.87
C 64	0.668	75.00	0.842	50.68	0.695	24.32	2.084	0.530	50.08	0.852	0.976	0.543	1.000	0.852	1.10	0.81	43.88
C 65	0.668	75.00	0.819	52.69	0.690	22.31	2.361	0.480	50.08	0.862	0.895	0.536	1.000	0.862	0.57	0.90	48.09
C 66	0.668	75.00	0.802	54.69	0.693	20.31	2.693	0.440	50.08	0.875	0.815	0.540	1.000	0.875	0.01	1.00	53.89
C 67	0.668	75.00	0.788	56.70	0.705	18.30	3.098	0.410	50.08	0.892	0.734	0.558	1.000	0.892	0.00	1.00	55.84
C 68	0.666	75.00	0.976	30.40	0.545	44.60	0.682	0.565	49.96	0.594	0.608	0.929	0.608	0.976	4.85	0.34	31.71
C 69	0.666	75.00	0.980	32.44	0.573	42.56	0.762	0.610	49.96	0.636	0.649	0.940	0.649	0.980	4.34	0.39	36.59
C 70	0.666	75.00	0.981	34.47	0.601	40.53	0.851	0.650	49.96	0.677	0.690	0.942	0.690	0.981	3.85	0.44	41.51
C 71	0.666	75.00	0.986	36.51	0.637	38.49	0.949	0.700	49.96	0.721	0.731	0.958	0.731	0.986	3.34	0.50	47.63
C 72	0.666	75.00	0.988	38.55	0.675	36.45	1.058	0.745	49.96	0.763	0.772	0.966	0.772	0.988	2.84	0.56	53.94
C 73	0.666	75.00	0.985	40.59	0.710	34.41	1.179	0.777	49.96	0.801	0.812	0.956	0.812	0.985	2.36	0.62	59.42
C 74	0.666	75.00	0.960	42.62	0.721	32.38	1.317	0.752	49.96	0.819	0.853	0.881	0.853	0.960	2.09	0.66	58.13
C 75	0.666	75.00	0.928	44.66	0.719	30.34	1.472	0.700	49.96	0.829	0.894	0.783	0.894	0.928	1.85	0.69	54.29
C 76	0.666	75.00	0.895	46.70	0.711	28.30	1.650	0.640	49.96	0.836	0.935	0.685	0.935	0.895	1.63	0.73	49.74
C 77	0.666	75.00	0.863	48.74	0.699	26.26	1.856	0.575	49.96	0.842	0.976	0.589	0.976	0.863	1.41	0.76	44.77
C 78	0.666	75.00	0.835	50.77	0.688	24.23	2.096	0.515	49.96	0.849	0.967	0.532	1.000	0.849	1.11	0.81	42.99
C 79	0.666	75.00	0.808	52.81	0.672	22.19	2.380	0.450	49.96	0.854	0.886	0.508	1.000	0.854	0.60	0.89	45.33
C 80	0.666	75.00	0.785	54.85	0.657	20.15	2.722	0.390	49.96	0.862	0.805	0.485	1.000	0.862	0.07	0.99	47.81
C 81	0.667	75.00	0.971	21.61	0.456	53.39	0.405	0.395	50.02	0.420	0.432	0.914	0.432	0.971	6.91	0.19	17.01

TABLE E-3 (continued)

RUN	x_f+z_f	Q_f cc/sec	x_o+z_o	Q_o cc/sec	Y_u	Q_u cc/sec	Q_o/Q_u	E	$Q_f x_f$ cc/sec	$\frac{Q_o x_o}{Q_f x_f}$	E_s	E/E_s	$\left(\frac{Q_o x_o}{Q_f x_f}\right)_I$	$\frac{Q_o x_o}{(Q_o x_o)_I}$	d cm.	EVF	Φ (%)
C 82	0.667	75.00	0.977	23.68	0.476	51.32	0.461	0.440	50.02	0.462	0.473	0.930	0.473	0.977	6.40	0.22	20.35
C 83	0.667	75.00	0.974	25.75	0.494	49.25	0.523	0.475	50.02	0.501	0.515	0.923	0.515	0.974	5.90	0.25	23.48
C 84	0.667	75.00	0.977	27.82	0.516	47.18	0.589	0.518	50.02	0.543	0.556	0.932	0.556	0.977	5.39	0.29	27.40
C 85	0.667	75.00	0.978	29.88	0.539	45.12	0.662	0.558	50.02	0.584	0.597	0.934	0.597	0.978	4.89	0.34	31.49
C 86	0.667	75.00	0.980	31.95	0.565	43.05	0.742	0.600	50.02	0.626	0.639	0.939	0.639	0.980	4.40	0.38	36.09
C 87	0.667	75.00	0.980	34.02	0.593	40.98	0.830	0.640	50.02	0.667	0.680	0.941	0.680	0.980	3.90	0.44	40.94
C 88	0.667	75.00	0.983	36.09	0.626	38.91	0.927	0.685	50.02	0.709	0.721	0.950	0.721	0.983	3.40	0.49	46.61
C 89	0.667	75.00	0.986	38.16	0.663	36.84	1.036	0.730	50.02	0.752	0.763	0.957	0.763	0.986	2.90	0.55	52.75
C 90	0.667	75.00	0.986	40.23	0.702	34.77	1.157	0.770	50.02	0.793	0.804	0.958	0.804	0.986	2.41	0.62	58.90
C 91	0.667	75.00	0.974	42.29	0.730	32.71	1.293	0.780	50.02	0.824	0.845	0.923	0.845	0.974	2.07	0.66	61.03
C 92	0.667	75.00	0.947	44.36	0.738	30.64	1.448	0.745	50.02	0.840	0.887	0.840	0.887	0.947	1.80	0.70	58.80
C 93	0.667	75.00	0.913	46.43	0.732	28.57	1.625	0.685	50.02	0.847	0.928	0.738	0.928	0.913	1.58	0.73	54.17
C 94	0.667	75.00	0.880	48.50	0.723	26.50	1.830	0.620	50.02	0.853	0.970	0.639	0.970	0.880	1.36	0.77	49.12
C 95	0.500	75.00	0.812	25.25	0.658	49.75	0.508	0.420	37.49	0.547	0.673	0.624	0.673	0.812	6.90	0.19	11.63
C 96	0.500	75.00	0.802	27.29	0.673	47.71	0.572	0.440	37.49	0.584	0.728	0.604	0.728	0.802	6.44	0.22	13.05
C 97	0.500	75.00	0.794	29.33	0.689	45.67	0.642	0.460	37.49	0.621	0.782	0.588	0.782	0.794	6.14	0.24	13.92
C 98	0.500	75.00	0.787	31.37	0.706	43.63	0.719	0.480	37.49	0.658	0.837	0.574	0.837	0.787	5.69	0.27	15.53
C 99	0.500	75.00	0.775	33.41	0.721	41.59	0.803	0.490	37.49	0.690	0.891	0.550	0.891	0.775	5.40	0.29	16.15
C100	0.500	75.00	0.770	35.45	0.742	39.55	0.896	0.510	37.49	0.728	0.945	0.539	0.945	0.770	4.95	0.33	17.93
C101	0.500	75.00	0.759	37.49	0.759	37.51	0.999	0.518	37.49	0.759	1.000	0.518	1.000	0.759	4.66	0.36	18.60
C102	0.500	75.00	0.739	39.53	0.767	35.47	1.114	0.505	37.49	0.780	0.946	0.534	1.000	0.780	4.12	0.41	21.99
C103	0.500	75.00	0.714	41.57	0.766	33.43	1.243	0.475	37.49	0.792	0.891	0.533	1.000	0.792	3.61	0.47	24.89
C104	0.500	75.00	0.693	43.60	0.765	31.40	1.389	0.450	37.49	0.806	0.837	0.538	1.000	0.806	3.08	0.53	28.44
C105	0.500	75.00	0.677	45.64	0.775	29.36	1.555	0.430	37.49	0.824	0.783	0.549	1.000	0.824	2.42	0.61	33.72
C106	0.500	75.00	0.657	47.68	0.775	27.32	1.746	0.400	37.49	0.836	0.728	0.549	1.000	0.836	1.89	0.69	37.76
C107	0.500	75.00	0.642	49.72	0.781	25.28	1.967	0.378	37.49	0.852	0.674	0.561	1.000	0.852	1.33	0.77	43.27
C108	0.500	75.00	0.628	51.76	0.787	23.24	2.227	0.355	37.49	0.868	0.620	0.573	1.000	0.868	0.67	0.88	50.40
C109	0.500	75.00	0.615	53.80	0.792	21.20	2.538	0.330	37.49	0.882	0.565	0.584	1.000	0.882	0.11	0.98	57.24
C110	0.500	75.00	0.602	55.84	0.799	19.16	2.915	0.305	37.49	0.897	0.511	0.597	1.000	0.897	0.00	1.00	59.71
C111	0.500	75.00	0.591	57.88	0.807	17.12	3.381	0.280	37.49	0.912	0.456	0.613	1.000	0.912	0.00	1.00	61.35
C112	0.500	75.00	0.580	59.92	0.817	15.08	3.973	0.255	37.49	0.926	0.402	0.634	1.000	0.926	0.00	1.00	63.42
C113	0.503	50.00	0.766	11.40	0.575	38.60	0.295	0.240	25.13	0.347	0.454	0.529	0.454	0.766	8.92	0.09	4.69
C114	0.503	50.00	0.789	13.43	0.603	36.57	0.367	0.308	25.13	0.422	0.535	0.576	0.535	0.789	8.16	0.12	6.92
C115	0.503	50.00	0.810	15.46	0.635	34.54	0.448	0.380	25.13	0.498	0.615	0.617	0.615	0.810	7.39	0.16	9.77
C116	0.503	50.00	0.833	17.50	0.675	32.50	0.538	0.462	25.13	0.580	0.696	0.664	0.696	0.833	6.62	0.20	13.54
C117	0.503	50.00	0.849	19.53	0.720	30.47	0.641	0.542	25.13	0.660	0.777	0.697	0.777	0.849	5.86	0.26	17.96
C118	0.503	50.00	0.863	21.56	0.771	28.44	0.758	0.622	25.13	0.741	0.858	0.725	0.858	0.863	5.10	0.32	23.13
C119	0.503	50.00	0.868	23.59	0.824	26.41	0.893	0.690	25.13	0.815	0.939	0.735	0.939	0.868	4.37	0.39	28.45
C120	0.503	50.00	0.861	25.62	0.874	24.38	1.051	0.735	25.13	0.878	0.980	0.750	1.000	0.878	3.62	0.47	34.95
C121	0.503	50.00	0.837	27.66	0.911	22.34	1.238	0.740	25.13	0.921	0.898	0.824	1.000	0.921	2.62	0.59	48.39

TABLE E-3 (continued)

RUN	x_f+z_f	Q_f cc/sec	x_o+z_o	Q_o cc/sec	Y_u	Q_u cc/sec	Q_o/Q_u	E	Q_fx_f cc/sec	$\frac{Q_ox_o}{Q_fx_f}$	E_s	E/E_s	$\left(\frac{Q_ox_o}{Q_fx_f}\right)_I$	$\frac{Q_ox_o}{(Q_ox_o)_I}$	d cm.	EVF	Φ (%)
C122	0.503	50.00	0.806	29.69	0.941	20.31	1.462	0.720	25.13	0.952	0.817	0.882	1.000	0.952	1.65	0.72	63.69
C123	0.503	50.00	0.771	31.72	0.962	18.28	1.735	0.680	25.13	0.973	0.735	0.925	1.000	0.973	0.82	0.85	79.03
C124	0.503	50.00	0.732	33.75	0.974	16.25	2.078	0.620	25.13	0.983	0.653	0.949	1.000	0.983	0.03	1.00	94.47
C125	0.503	50.00	0.691	35.79	0.972	14.21	2.518	0.540	25.13	0.984	0.571	0.945	1.000	0.984	0.00	1.00	94.49
C126	0.503	50.00	0.648	37.82	0.949	12.18	3.104	0.440	25.13	0.975	0.490	0.898	1.000	0.975	0.00	1.00	89.83
C127	0.503	50.00	0.603	39.85	0.892	10.15	3.926	0.320	25.13	0.956	0.408	0.784	1.000	0.956	0.00	1.00	78.41
C128	0.664	50.00	0.986	15.60	0.482	34.40	0.453	0.450	33.19	0.463	0.470	0.957	0.470	0.986	6.40	0.22	20.91
C129	0.664	50.00	0.997	17.65	0.518	32.35	0.546	0.527	33.19	0.530	0.532	0.991	0.532	0.997	5.63	0.28	27.25
C130	0.664	50.00	0.995	19.71	0.552	30.29	0.651	0.585	33.19	0.591	0.594	0.985	0.594	0.995	4.89	0.34	33.30
C131	0.664	50.00	0.997	21.76	0.593	28.24	0.771	0.650	33.19	0.654	0.656	0.991	0.656	0.997	4.14	0.41	40.67
C132	0.664	50.00	0.996	23.81	0.639	26.19	0.909	0.710	33.19	0.715	0.717	0.990	0.717	0.996	3.40	0.49	48.57
C133	0.664	50.00	0.994	25.87	0.690	24.13	1.072	0.765	33.19	0.775	0.779	0.982	0.779	0.994	2.67	0.58	56.93
C134	0.664	50.00	0.980	27.92	0.735	22.08	1.265	0.790	33.19	0.824	0.841	0.939	0.841	0.980	2.10	0.66	61.68
C135	0.664	50.00	0.932	29.98	0.737	20.02	1.497	0.720	33.19	0.842	0.903	0.797	0.903	0.932	1.69	0.72	57.20
C136	0.664	50.00	0.890	32.03	0.740	17.97	1.782	0.650	33.19	0.859	0.965	0.674	0.965	0.890	1.37	0.77	51.63
C137	0.664	50.00	0.850	34.08	0.736	15.92	2.141	0.570	33.19	0.873	0.947	0.602	1.000	0.873	0.83	0.85	51.37
C138	0.664	50.00	0.815	36.14	0.731	13.86	2.607	0.490	33.19	0.887	0.825	0.594	1.000	0.887	0.01	1.00	59.25
C139	0.664	50.00	0.784	38.19	0.724	11.81	3.234	0.410	33.19	0.902	0.703	0.584	1.000	0.902	0.00	1.00	58.35
C140	0.334	50.00	0.501	10.00	0.708	40.00	0.250	0.150	16.69	0.300	0.599	0.250	0.599	0.501	10.66	0.04	0.96
C141	0.334	50.00	0.609	12.15	0.754	37.85	0.321	0.300	16.69	0.443	0.728	0.412	0.728	0.609	9.43	0.07	2.94
C142	0.334	50.00	0.692	14.29	0.809	35.71	0.400	0.460	16.69	0.592	0.856	0.537	0.856	0.692	8.40	0.11	5.87
C143	0.334	50.00	0.733	16.44	0.862	33.56	0.490	0.590	16.69	0.722	0.985	0.599	0.985	0.733	7.43	0.16	9.36
C144	0.334	50.00	0.723	18.58	0.896	31.42	0.591	0.650	16.69	0.805	0.943	0.689	1.000	0.805	6.39	0.22	15.11
C145	0.334	50.00	0.696	20.73	0.923	29.27	0.708	0.675	16.69	0.864	0.879	0.768	1.000	0.864	5.36	0.30	22.81
C146	0.334	50.00	0.662	22.87	0.943	27.13	0.843	0.675	16.69	0.907	0.814	0.829	1.000	0.907	4.36	0.39	32.16
C147	0.334	50.00	0.621	25.02	0.953	24.98	1.001	0.645	16.69	0.930	0.750	0.860	1.000	0.930	3.41	0.49	42.09
C148	0.334	50.00	0.583	27.16	0.962	22.84	1.189	0.608	16.69	0.948	0.686	0.887	1.000	0.948	2.60	0.59	52.27
C149	0.334	50.00	0.548	29.31	0.970	20.69	1.417	0.565	16.69	0.963	0.621	0.909	1.000	0.963	1.68	0.72	65.28
C150	0.334	50.00	0.518	31.45	0.978	18.55	1.696	0.520	16.69	0.975	0.557	0.934	1.000	0.975	0.87	0.85	79.05
C151	0.334	50.00	0.489	33.60	0.985	16.40	2.049	0.470	16.69	0.985	0.492	0.955	1.000	0.985	0.05	0.99	94.51
C152	0.340	75.00	0.648	28.50	0.850	46.50	0.613	0.523	25.47	0.725	0.939	0.557	1.000	0.725	6.68	0.20	11.15
C153	0.340	75.00	0.645	30.56	0.870	44.44	0.688	0.555	25.47	0.774	0.897	0.619	1.000	0.774	5.94	0.25	15.56
C154	0.340	75.00	0.631	32.62	0.885	42.38	0.770	0.565	25.47	0.808	0.856	0.660	1.000	0.808	5.37	0.30	19.53
C155	0.340	75.00	0.614	34.68	0.896	40.32	0.860	0.565	25.47	0.835	0.814	0.694	1.000	0.835	4.67	0.36	24.80
C156	0.340	75.00	0.596	36.74	0.907	38.26	0.960	0.560	25.47	0.860	0.773	0.725	1.000	0.860	4.12	0.41	29.85
C157	0.340	75.00	0.578	38.80	0.916	36.20	1.072	0.550	25.47	0.881	0.731	0.752	1.000	0.881	3.44	0.49	36.55
C158	0.340	75.00	0.558	40.86	0.921	34.14	1.197	0.530	25.47	0.895	0.689	0.769	1.000	0.895	2.91	0.55	42.24
C159	0.340	75.00	0.540	42.92	0.928	32.08	1.338	0.510	25.47	0.909	0.648	0.787	1.000	0.909	2.37	0.62	48.78
C160	0.340	75.00	0.519	44.98	0.929	30.02	1.498	0.480	25.47	0.917	0.606	0.792	1.000	0.917	1.86	0.69	54.82
C161	0.340	75.00	0.502	47.04	0.934	27.96	1.682	0.455	25.47	0.928	0.565	0.806	1.000	0.928	1.32	0.77	62.36

TABLE E-3 (continued)

RUN	x_f+z_f	Q_f cc/sec	x_o+z_o	Q_o cc/sec	Y_u	Q_u cc/sec	Q_o/Q_u	E	Q_fx_f cc/sec	$\frac{Q_ox_o}{Q_fx_f}$	E_s	E/E_s	$\left(\frac{Q_ox_o}{Q_fx_f}\right)_I$	$\frac{Q_ox_o}{(Q_ox_o)_I}$	d cm.	EVF	ϕ (%)
C162	0.340	75.00	0.482	49.10	0.930	25.90	1.896	0.415	25.47	0.929	0.523	0.794	1.000	0.929	0.82	0.85	67.78
C163	0.340	75.00	0.462	51.16	0.923	23.84	2.146	0.372	25.47	0.928	0.481	0.773	1.000	0.928	0.34	0.94	72.53
C164	0.340	75.00	0.442	53.22	0.911	21.78	2.444	0.325	25.47	0.924	0.440	0.739	1.000	0.924	0.00	1.00	73.90
C165	0.340	75.00	0.423	55.28	0.893	19.72	2.803	0.273	25.47	0.917	0.398	0.686	1.000	0.917	0.00	1.00	68.56
C166	0.340	75.00	0.401	57.34	0.860	17.66	3.247	0.210	25.47	0.903	0.357	0.589	1.000	0.903	0.00	1.00	58.89
C167	0.340	75.00	0.379	59.40	0.811	15.60	3.808	0.140	25.47	0.884	0.315	0.444	1.000	0.884	0.00	1.00	44.44
C168	0.333	50.00	0.630	13.10	0.772	36.90	0.355	0.350	16.65	0.495	0.787	0.445	0.787	0.630	9.14	0.08	3.59
C169	0.333	50.00	0.641	15.24	0.802	34.76	0.438	0.422	16.65	0.586	0.915	0.461	0.915	0.641	8.40	0.11	5.04
C170	0.333	50.00	0.646	17.37	0.834	32.63	0.532	0.490	16.65	0.674	0.978	0.501	1.000	0.674	7.62	0.15	7.31
C171	0.333	50.00	0.651	19.51	0.870	30.49	0.640	0.558	16.65	0.762	0.914	0.610	1.000	0.762	6.38	0.22	13.43
C172	0.333	50.00	0.645	21.65	0.905	28.35	0.763	0.608	16.65	0.838	0.850	0.715	1.000	0.838	5.16	0.31	22.46
C173	0.333	50.00	0.637	23.78	0.942	26.22	0.907	0.650	16.65	0.909	0.786	0.827	1.000	0.909	3.94	0.43	35.61
C174	0.333	50.00	0.609	25.92	0.964	24.08	1.076	0.643	16.65	0.947	0.722	0.890	1.000	0.947	3.07	0.53	47.21
C175	0.333	50.00	0.574	28.05	0.976	21.95	1.278	0.610	16.65	0.968	0.658	0.927	1.000	0.968	2.13	0.65	60.61
C176	0.333	50.00	0.541	30.19	0.984	19.81	1.524	0.565	16.65	0.981	0.594	0.951	1.000	0.981	1.32	0.77	73.65
C177	0.333	50.00	0.506	32.33	0.984	17.67	1.829	0.505	16.65	0.983	0.530	0.953	1.000	0.983	0.45	0.92	87.54
C178	0.333	50.00	0.476	34.46	0.985	15.54	2.218	0.445	16.65	0.986	0.466	0.955	1.000	0.986	0.00	1.00	95.52
C179	0.333	50.00	0.451	36.60	0.990	13.40	2.731	0.390	16.65	0.992	0.402	0.971	1.000	0.992	0.00	1.00	97.06
C180	0.334	60.00	0.559	15.42	0.744	44.58	0.346	0.260	20.06	0.430	0.769	0.338	0.769	0.559	9.44	0.07	2.39
C181	0.334	60.00	0.622	17.43	0.783	42.57	0.409	0.375	20.06	0.540	0.869	0.432	0.869	0.622	8.67	0.10	4.24
C182	0.334	60.00	0.681	19.44	0.832	40.56	0.479	0.505	20.06	0.660	0.969	0.521	0.969	0.681	7.89	0.13	6.90
C183	0.334	60.00	0.714	21.45	0.877	38.55	0.556	0.610	20.06	0.764	0.965	0.632	1.000	0.764	6.88	0.19	11.85
C184	0.334	60.00	0.699	23.46	0.900	36.54	0.642	0.640	20.06	0.817	0.915	0.700	1.000	0.817	5.93	0.25	17.62
C185	0.334	60.00	0.675	25.47	0.917	34.53	0.738	0.650	20.06	0.857	0.865	0.752	1.000	0.857	5.16	0.31	23.57
C186	0.334	60.00	0.648	27.48	0.931	32.52	0.845	0.645	20.06	0.887	0.814	0.792	1.000	0.887	4.41	0.38	30.31
C187	0.334	60.00	0.623	29.49	0.944	30.51	0.967	0.637	20.06	0.916	0.764	0.834	1.000	0.916	3.56	0.46	38.45
C188	0.334	60.00	0.594	31.50	0.953	28.50	1.105	0.613	20.06	0.933	0.714	0.859	1.000	0.933	2.94	0.55	46.88
C189	0.334	60.00	0.569	33.51	0.963	26.49	1.265	0.590	20.06	0.951	0.663	0.890	1.000	0.951	2.33	0.63	55.65
C190	0.334	60.00	0.545	35.52	0.971	24.48	1.451	0.560	20.06	0.965	0.613	0.914	1.000	0.965	1.61	0.73	66.54
C191	0.334	60.00	0.528	37.53	0.977	22.47	1.670	0.525	20.06	0.962	0.563	0.931	1.000	0.962	1.07	0.81	75.50
C192	0.334	60.00	0.500	39.54	0.985	20.46	1.933	0.490	20.06	0.985	0.512	0.957	1.000	0.985	0.29	0.95	90.49
C193	0.334	60.00	0.479	41.55	0.991	18.45	2.252	0.450	20.06	0.992	0.462	0.974	1.000	0.992	0.00	1.00	97.41
C194	0.334	60.00	0.460	43.56	0.999	16.44	2.650	0.410	20.06	0.999	0.412	0.996	1.000	0.999	0.00	1.00	99.60
C195	0.334	60.00	0.448	19.90	0.723	40.10	0.496	0.170	20.03	0.445	0.994	0.171	0.994	0.448	9.19	0.08	1.35
C196	0.334	60.00	0.446	21.94	0.731	38.06	0.577	0.185	20.03	0.489	0.952	0.194	1.000	0.489	8.64	0.10	1.93
C197	0.334	60.00	0.445	23.99	0.740	36.01	0.666	0.200	20.03	0.533	0.901	0.222	1.000	0.533	7.88	0.13	2.95
C198	0.334	60.00	0.447	26.03	0.753	33.97	0.766	0.220	20.03	0.580	0.850	0.259	1.000	0.580	6.93	0.18	4.78
C199	0.334	60.00	0.438	28.08	0.758	31.92	0.880	0.220	20.03	0.615	0.799	0.275	1.000	0.615	6.19	0.23	6.42
C200	0.334	60.00	0.425	30.12	0.758	29.88	1.008	0.205	20.03	0.639	0.747	0.274	1.000	0.639	5.63	0.28	7.55
C201	0.334	60.00	0.415	32.17	0.760	27.83	1.156	0.195	20.03	0.666	0.696	0.280	1.000	0.666	4.89	0.34	9.46

TABLE E-3 (continued)

RUN	x_f+z_f	Q_f cc/sec	x_o+z_o	Q_o cc/sec	Y_u	Q_u cc/sec	Q_o/Q_u	E	Q_fx_f cc/sec	$\frac{Q_ox_o}{Q_fx_f}$	E_s	E/E_s	$\left(\frac{Q_ox_o}{Q_fx_f}\right)_I$	$\frac{Q_ox_o}{\left(Q_ox_o\right)_I}$	d cm.	EVF	Φ (%)
C202	0.334	60.00	0.404	34.21	0.759	25.79	1.327	0.180	20.03	0.690	0.645	0.279	1.000	0.690	4.16	0.41	11.38
C203	0.334	60.00	0.399	36.26	0.766	23.74	1.527	0.178	20.03	0.723	0.594	0.300	1.000	0.723	3.38	0.49	14.76
C204	0.334	60.00	0.396	38.30	0.776	21.70	1.765	0.178	20.03	0.757	0.543	0.328	1.000	0.757	2.59	0.59	19.38
C205	0.332	75.00	0.650	23.10	0.809	51.90	0.445	0.440	24.94	0.602	0.926	0.475	0.926	0.650	8.19	0.12	5.63
C206	0.332	75.00	0.643	25.20	0.825	49.80	0.506	0.470	24.94	0.650	0.995	0.472	1.000	0.650	7.90	0.13	6.25
C207	0.332	75.00	0.637	27.30	0.842	47.70	0.572	0.500	24.94	0.698	0.953	0.525	1.000	0.698	7.15	0.17	9.00
C208	0.332	75.00	0.630	29.40	0.859	45.60	0.645	0.525	24.94	0.742	0.911	0.576	1.000	0.742	6.42	0.22	12.54
C209	0.332	75.00	0.620	31.50	0.876	43.50	0.724	0.545	24.94	0.784	0.869	0.627	1.000	0.784	5.68	0.27	16.99
C210	0.332	75.00	0.610	33.60	0.893	41.40	0.812	0.560	24.94	0.822	0.827	0.677	1.000	0.822	5.10	0.32	21.60
C211	0.332	75.00	0.598	35.70	0.909	39.30	0.908	0.570	24.94	0.856	0.785	0.726	1.000	0.856	4.37	0.39	28.07
C212	0.332	75.00	0.586	37.80	0.925	37.20	1.016	0.575	24.94	0.888	0.743	0.774	1.000	0.888	3.65	0.46	35.75
C213	0.332	75.00	0.570	39.90	0.938	35.10	1.137	0.570	24.94	0.912	0.701	0.813	1.000	0.912	3.08	0.53	43.02
C214	0.332	75.00	0.554	42.00	0.950	33.00	1.273	0.560	24.94	0.934	0.659	0.850	1.000	0.934	2.39	0.62	52.49
C215	0.332	75.00	0.540	44.10	0.964	30.90	1.427	0.550	24.94	0.955	0.617	0.891	1.000	0.955	1.70	0.72	63.77
C216	0.332	75.00	0.523	46.20	0.974	28.80	1.604	0.530	24.94	0.970	0.575	0.921	1.000	0.970	1.14	0.80	73.95
C217	0.332	75.00	0.510	48.30	0.989	26.70	1.809	0.515	24.94	0.988	0.533	0.966	1.000	0.988	0.55	0.90	87.06
C218	0.332	75.00	0.491	50.40	0.992	24.60	2.049	0.480	24.94	0.992	0.491	0.977	1.000	0.992	0.01	1.00	97.44
C219	0.332	75.00	0.475	52.50	1.000	22.50	2.333	0.450	24.94	1.000	0.449	1.000	1.000	1.000	0.00	1.00	100.00
C220	0.499	60.00	0.861	22.20	0.713	37.80	0.587	0.535	29.95	0.638	0.741	0.722	0.741	0.861	6.12	0.24	17.20
C221	0.499	60.00	0.870	24.42	0.755	35.58	0.686	0.603	29.95	0.709	0.815	0.740	0.815	0.870	5.40	0.29	21.73
C222	0.499	60.00	0.882	26.64	0.807	33.36	0.798	0.680	29.95	0.784	0.889	0.765	0.889	0.882	4.67	0.36	27.36
C223	0.499	60.00	0.905	28.85	0.876	31.15	0.926	0.780	29.95	0.872	0.963	0.810	0.963	0.905	3.91	0.43	35.12
C224	0.499	60.00	0.894	31.07	0.925	28.93	1.074	0.818	29.95	0.928	0.963	0.850	1.000	0.928	3.15	0.52	44.25
C225	0.499	60.00	0.851	33.29	0.939	26.71	1.246	0.780	29.95	0.945	0.889	0.877	1.000	0.945	2.39	0.62	54.19
C226	0.499	60.00	0.803	35.51	0.942	24.49	1.450	0.720	29.95	0.952	0.815	0.883	1.000	0.952	1.67	0.72	63.57
C227	0.499	60.00	0.762	37.72	0.945	22.28	1.694	0.660	29.95	0.959	0.741	0.890	1.000	0.959	1.05	0.82	72.74
C228	0.499	60.00	0.721	39.94	0.942	20.06	1.991	0.590	29.95	0.961	0.667	0.884	1.000	0.961	0.34	0.94	82.84
C229	0.499	60.00	0.690	42.16	0.951	17.84	2.363	0.535	29.95	0.971	0.594	0.901	1.000	0.971	0.00	1.00	90.11
C230	0.502	75.00	0.877	23.45	0.669	51.55	0.455	0.470	37.62	0.547	0.623	0.754	0.623	0.877	6.92	0.19	13.98
C231	0.502	75.00	0.872	25.57	0.690	49.43	0.517	0.505	37.62	0.593	0.680	0.743	0.680	0.872	6.43	0.22	16.08
C232	0.502	75.00	0.864	27.69	0.710	47.31	0.585	0.535	37.62	0.636	0.736	0.727	0.736	0.864	6.12	0.24	17.33
C233	0.502	75.00	0.856	29.81	0.732	45.19	0.660	0.563	37.62	0.678	0.792	0.710	0.792	0.856	5.64	0.27	19.46
C234	0.502	75.00	0.845	31.93	0.753	43.07	0.741	0.585	37.62	0.717	0.849	0.689	0.849	0.845	5.19	0.31	21.46
C235	0.502	75.00	0.837	34.05	0.778	40.95	0.831	0.610	37.62	0.758	0.905	0.674	0.905	0.837	4.87	0.34	22.88
C236	0.502	75.00	0.818	36.17	0.793	38.83	0.931	0.610	37.62	0.786	0.962	0.634	0.962	0.818	4.59	0.37	23.20
C237	0.502	75.00	0.781	38.29	0.790	36.71	1.043	0.570	37.62	0.795	0.982	0.580	1.000	0.795	4.19	0.40	23.51
C238	0.502	75.00	0.747	40.41	0.786	34.59	1.168	0.530	37.62	0.803	0.925	0.573	1.000	0.803	3.68	0.46	26.27
C239	0.502	75.00	0.720	42.53	0.784	32.47	1.310	0.495	37.62	0.814	0.869	0.570	1.000	0.814	3.17	0.52	29.54
C240	0.502	75.00	0.699	44.65	0.789	30.35	1.471	0.470	37.62	0.830	0.812	0.579	1.000	0.830	2.62	0.59	33.96
C241	0.502	75.00	0.679	46.77	0.793	28.23	1.657	0.443	37.62	0.844	0.755	0.587	1.000	0.844	2.07	0.66	38.81

TABLE E-3 (continued)

RUN	x_f+z_o	Q_f cc/sec	x_o+z_o	Q_o cc/sec	Y_u	Q_u cc/sec	Q_o/Q_u	E	$Q_f x_o$ cc/sec	$\frac{Q_o x_o}{Q_f x_f}$	E_s	E/E_s	$\left(\frac{Q_o x_o}{Q_f x_f}\right)_I$	$\frac{Q_o x_o}{(Q_o x_o)_I}$	d cm.	EVF	Φ (%)
C242	0.502	75.00	0.663	48.89	0.800	26.11	1.872	0.420	37.62	0.861	0.698	0.601	1.000	0.861	1.40	0.76	45.79
C243	0.502	75.00	0.648	51.01	0.810	23.99	2.126	0.393	37.62	0.879	0.642	0.620	1.000	0.879	0.82	0.86	53.06
C244	0.502	75.00	0.635	53.13	0.823	21.87	2.429	0.378	37.62	0.897	0.585	0.646	1.000	0.897	0.12	0.98	63.13
C245	0.502	75.00	0.622	55.25	0.835	19.75	2.797	0.355	37.62	0.914	0.528	0.672	1.000	0.914	0.00	1.00	67.20
C246	0.667	60.00	0.980	26.00	0.572	34.00	0.765	0.610	40.00	0.637	0.650	0.939	0.650	0.980	4.34	0.39	36.61
C247	0.667	60.00	0.982	28.05	0.610	31.95	0.876	0.663	40.00	0.668	0.701	0.946	0.701	0.982	3.65	0.46	43.74
C248	0.667	60.00	0.984	30.09	0.652	29.91	1.006	0.715	40.00	0.740	0.752	0.951	0.752	0.984	3.09	0.53	50.12
C249	0.667	60.00	0.982	32.14	0.697	27.86	1.153	0.760	40.00	0.789	0.805	0.946	0.803	0.982	2.43	0.61	57.92
C250	0.667	60.00	0.983	34.18	0.752	25.82	1.324	0.810	40.00	0.840	0.854	0.948	0.854	0.983	1.87	0.69	65.45
C251	0.667	60.00	0.981	36.25	0.813	23.77	1.524	0.855	40.00	0.849	0.906	0.944	0.906	0.981	1.31	0.77	73.15
C252	0.667	60.00	0.982	38.27	0.889	21.73	1.761	0.905	40.00	0.939	0.957	0.946	0.957	0.982	0.65	0.88	83.66
C253	0.667	60.00	0.938	40.32	0.885	19.68	2.046	0.820	40.00	0.945	0.984	0.833	1.000	0.945	0.36	0.93	77.87
C254	0.667	60.00	0.868	42.36	0.817	17.64	2.402	0.640	40.00	0.919	0.852	0.726	1.000	0.919	0.02	1.00	72.30
C255	0.667	60.00	0.836	44.41	0.816	15.59	2.848	0.565	40.00	0.925	0.780	0.725	1.000	0.928	0.00	1.00	72.46
C256	0.667	60.00	0.810	46.45	0.825	13.55	3.429	0.500	40.00	0.941	0.677	0.738	1.000	0.941	0.00	1.00	73.80
C257	0.667	60.00	0.793	48.50	0.867	11.50	4.217	0.460	40.00	0.962	0.575	0.800	1.000	0.962	0.00	1.00	79.98
C258	0.665	75.00	0.989	39.50	0.695	35.50	1.113	0.765	49.90	0.783	0.792	0.966	0.792	0.989	2.60	0.59	56.94
C259	0.665	75.00	0.988	41.62	0.737	33.38	1.247	0.805	49.90	0.824	0.834	0.965	0.834	0.988	2.10	0.66	63.41
C260	0.665	75.00	0.986	43.74	0.783	31.26	1.400	0.840	49.90	0.864	0.877	0.958	0.877	0.986	1.61	0.73	69.83
C261	0.665	75.00	0.986	45.87	0.839	29.13	1.574	0.880	49.90	0.906	0.919	0.957	0.919	0.986	1.11	0.81	77.27
C262	0.665	75.00	0.931	47.99	0.806	27.01	1.777	0.763	49.90	0.895	0.962	0.793	0.962	0.931	1.07	0.81	64.55
C263	0.665	75.00	0.875	50.11	0.757	24.89	2.013	0.630	49.90	0.879	0.992	0.635	1.000	0.879	0.94	0.83	53.03
C264	0.665	75.00	0.840	52.23	0.734	22.77	2.294	0.545	49.90	0.879	0.907	0.601	1.000	0.879	0.54	0.90	54.22
C265	0.665	75.00	0.809	54.36	0.713	20.64	2.633	0.468	49.90	0.881	0.822	0.569	1.000	0.881	0.03	0.99	56.61
C266	0.665	75.00	0.781	56.48	0.686	18.52	3.049	0.390	49.90	0.884	0.738	0.528	1.000	0.884	0.00	1.00	52.85
C267	0.665	75.00	0.754	58.60	0.650	16.40	3.573	0.310	49.90	0.885	0.653	0.474	1.000	0.885	0.00	1.00	47.44
C268	0.667	50.00	0.991	28.75	0.772	21.25	1.353	0.840	33.34	0.855	0.862	0.974	0.862	0.991	1.67	0.72	70.07
C269	0.667	50.00	0.993	31.16	0.873	18.84	1.654	0.915	33.34	0.928	0.935	0.979	0.935	0.993	0.85	0.85	83.20
C270	0.667	50.00	0.971	33.57	0.955	16.43	2.044	0.920	33.34	0.978	0.986	0.933	1.000	0.978	0.10	0.98	91.62
C271	0.667	50.00	0.898	35.99	0.928	14.01	2.568	0.750	33.34	0.970	0.841	0.892	1.000	0.970	0.00	1.00	89.16
C272	0.667	50.00	0.855	38.40	0.956	11.60	3.310	0.650	33.34	0.985	0.696	0.933	1.000	0.985	0.00	1.00	93.34
C273	0.501	50.00	0.765	20.10	0.677	29.90	0.672	0.425	25.03	0.614	0.803	0.529	0.803	0.765	6.15	0.24	12.51
C274	0.501	50.00	0.789	22.34	0.732	27.66	0.808	0.515	25.03	0.704	0.893	0.577	0.893	0.789	5.35	0.30	17.18
C275	0.501	50.00	0.818	24.58	0.807	25.42	0.967	0.625	25.03	0.804	0.982	0.636	0.982	0.818	4.38	0.39	24.56
C276	0.501	50.00	0.845	26.83	0.897	23.17	1.158	0.733	25.03	0.905	0.928	0.795	1.000	0.905	2.95	0.55	43.36
C277	0.501	50.00	0.830	29.07	0.956	20.93	1.389	0.765	25.03	0.963	0.838	0.913	1.000	0.963	1.83	0.70	63.48
C278	0.501	50.00	0.778	31.31	0.964	18.69	1.676	0.695	25.03	0.973	0.749	0.929	1.000	0.973	0.91	0.84	77.95
C279	0.501	50.00	0.728	33.55	0.963	16.45	2.040	0.610	25.03	0.976	0.659	0.926	1.000	0.976	0.11	0.98	90.64
C280	0.501	50.00	0.687	35.80	0.970	14.20	2.520	0.535	25.03	0.983	0.569	0.940	1.000	0.983	0.00	1.00	94.05
C281	0.501	50.00	0.649	38.04	0.970	11.96	3.181	0.450	25.03	0.985	0.479	0.939	1.000	0.985	0.00	1.00	93.94

TABLE E-3 (continued)

RUN	x_f+z_f	Q_f cc/sec	x_o+z_o	Q_o cc/sec	Y_u	Q_u cc/sec	Q_o/Q_u	E	$Q_f x_f$ cc/sec	$\frac{Q_o x_o}{Q_f x_f}$	E_s	E/E_s	$\left(\frac{Q_o x_o}{Q_f x_f}\right)_I$	$\frac{Q_o x_o}{(Q_o x_o)_I}$	d cm	EVF	ϕ (%)
C282	0.333	60.00	0.668	19.50	0.828	40.50	0.481	0.490	19.99	0.652	0.975	0.502	0.975	0.668	7.91	0.13	6.61
C283	0.333	60.00	0.661	21.54	0.850	38.46	0.560	0.530	19.99	0.712	0.961	0.551	1.000	0.712	7.15	0.17	9.47
C284	0.333	60.00	0.653	23.57	0.874	36.43	0.647	0.565	19.99	0.770	0.910	0.621	1.000	0.770	6.19	0.23	14.48
C285	0.333	60.00	0.644	25.61	0.899	34.39	0.745	0.598	19.99	0.826	0.860	0.696	1.000	0.826	5.38	0.30	20.55
C286	0.333	60.00	0.632	27.65	0.922	32.35	0.855	0.620	19.99	0.874	0.809	0.767	1.000	0.874	4.43	0.38	29.19
C287	0.333	60.00	0.616	29.69	0.944	30.31	0.979	0.630	19.99	0.915	0.758	0.832	1.000	0.915	3.64	0.46	38.57
C288	0.333	60.00	0.593	31.72	0.958	28.28	1.122	0.618	19.99	0.941	0.707	0.874	1.000	0.941	2.88	0.55	48.41
C289	0.333	60.00	0.568	33.76	0.969	26.24	1.287	0.595	19.99	0.959	0.656	0.907	1.000	0.959	2.15	0.65	59.08
C290	0.333	60.00	0.548	35.80	0.985	24.20	1.479	0.578	19.99	0.982	0.605	0.956	1.000	0.982	1.39	0.76	72.94
C291	0.502	60.00	0.877	20.99	0.700	39.01	0.538	0.525	30.12	0.611	0.697	0.753	0.697	0.877	6.37	0.22	16.64
C292	0.502	60.00	0.866	23.05	0.725	36.95	0.624	0.560	30.12	0.663	0.765	0.732	0.765	0.866	5.86	0.26	18.84
C293	0.502	60.00	0.863	25.11	0.758	34.89	0.720	0.605	30.12	0.720	0.834	0.726	0.834	0.863	5.19	0.31	22.60
C294	0.502	60.00	0.864	27.17	0.797	32.83	0.828	0.655	30.12	0.779	0.902	0.726	0.902	0.864	4.66	0.36	26.05
C295	0.502	60.00	0.869	29.23	0.847	30.77	0.950	0.715	30.12	0.843	0.971	0.737	0.971	0.869	4.11	0.41	30.42
C296	0.502	60.00	0.869	31.29	0.898	28.71	1.090	0.765	30.12	0.903	0.961	0.796	1.000	0.903	3.33	0.50	39.76
C297	0.502	60.00	0.837	33.36	0.917	26.64	1.252	0.745	30.12	0.927	0.892	0.835	1.000	0.927	2.57	0.59	49.62
C298	0.502	60.00	0.798	35.42	0.925	24.58	1.441	0.700	30.12	0.939	0.823	0.851	1.000	0.939	1.85	0.69	58.97
C299	0.502	60.00	0.762	37.48	0.931	22.52	1.664	0.650	30.12	0.948	0.754	0.862	1.000	0.948	1.15	0.80	69.08
C300	0.502	60.00	0.728	39.54	0.934	20.46	1.932	0.595	30.12	0.955	0.685	0.869	1.000	0.955	0.54	0.90	78.39
C301	0.502	60.00	0.697	41.60	0.938	18.40	2.261	0.540	30.12	0.962	0.616	0.877	1.000	0.962	0.00	1.00	87.69
C302	0.334	75.00	0.602	27.75	0.823	47.25	0.587	0.445	25.08	0.666	0.947	0.470	1.000	0.666	7.19	0.17	7.96
C303	0.334	75.00	0.598	29.77	0.839	45.23	0.658	0.470	25.08	0.710	0.906	0.519	1.000	0.710	6.63	0.20	10.56
C304	0.334	75.00	0.594	31.78	0.857	43.22	0.735	0.495	25.08	0.753	0.866	0.572	1.000	0.753	5.89	0.25	14.57
C305	0.334	75.00	0.589	33.80	0.874	41.20	0.820	0.515	25.08	0.793	0.825	0.624	1.000	0.793	5.16	0.31	19.55
C306	0.334	75.00	0.584	35.81	0.894	39.19	0.914	0.535	25.08	0.834	0.785	0.682	1.000	0.834	4.43	0.38	25.93
C307	0.334	75.00	0.577	37.83	0.913	37.17	1.018	0.550	25.08	0.870	0.745	0.739	1.000	0.870	3.84	0.44	32.62
C308	0.334	75.00	0.570	39.84	0.933	35.16	1.133	0.563	25.08	0.906	0.704	0.799	1.000	0.906	3.11	0.53	42.00
C309	0.334	75.00	0.559	41.86	0.949	33.14	1.263	0.563	25.08	0.933	0.664	0.848	1.000	0.933	2.41	0.61	52.15
C310	0.334	75.00	0.544	43.88	0.961	31.12	1.410	0.550	25.08	0.951	0.623	0.882	1.000	0.951	1.85	0.69	61.14
C311	0.334	75.00	0.525	45.89	0.967	29.11	1.576	0.525	25.08	0.961	0.583	0.900	1.000	0.961	1.32	0.77	69.65
C312	0.334	75.00	0.509	47.91	0.974	27.09	1.768	0.500	25.08	0.972	0.543	0.921	1.000	0.972	0.69	0.88	80.81
C313	0.334	75.00	0.493	49.92	0.982	25.08	1.991	0.475	25.08	0.982	0.502	0.946	1.000	0.982	0.15	0.97	91.99
C314	0.334	75.00	0.479	51.94	0.991	23.06	2.252	0.450	25.08	0.992	0.462	0.974	1.000	0.992	0.00	1.00	97.40
C315	0.334	75.00	0.463	53.95	0.995	21.05	2.563	0.415	25.08	0.996	0.422	0.984	1.000	0.996	0.00	1.00	98.43
C316	0.334	75.00	0.448	55.97	0.999	19.03	2.941	0.380	25.08	0.999	0.381	0.997	1.000	0.999	0.00	1.00	99.67
C317	0.334	75.00	0.431	57.98	0.994	17.02	3.408	0.335	25.08	0.996	0.341	0.983	1.000	0.996	0.00	1.00	98.28
C318	0.334	75.00	0.414	60.00	0.983	15.00	4.000	0.285	25.08	0.990	0.300	0.948	1.000	0.990	0.00	1.00	94.85
C319	0.332	50.00	0.702	17.67	0.870	32.33	0.547	0.590	16.60	0.748	0.968	0.610	1.000	0.748	6.94	0.18	11.23
C320	0.332	50.00	0.674	19.76	0.892	30.24	0.654	0.610	16.60	0.803	0.905	0.674	1.000	0.803	5.94	0.25	16.93
C321	0.332	50.00	0.649	21.85	0.914	28.15	0.777	0.625	16.60	0.855	0.843	0.742	1.000	0.855	4.94	0.33	24.71

TABLE E-3 (continued)

RUN	x_f+z_f	Q_f cc/sec	x_o+z_o	Q_o cc/sec	Y_u	Q_u cc/sec	Q_o/Q_u	E	$Q_f x_f$ cc/sec	$\frac{Q_o x_o}{Q_f x_f}$	E_s	E/E_s	$\left(\frac{Q_o x_o}{Q_f x_f}\right)_I$	$\frac{Q_o x_o}{\left(Q_o x_o\right)_I}$	d cm.	EVF	Φ (%)
C322	0.332	50.00	0.621	23.95	0.934	26.05	0.919	0.625	16.60	0.896	0.780	0.801	1.000	0.896	4.09	0.42	33.29
C323	0.332	50.00	0.592	26.04	0.950	23.96	1.087	0.610	16.60	0.928	0.717	0.850	1.000	0.928	3.12	0.52	44.58
C324	0.332	50.00	0.561	28.13	0.962	21.87	1.286	0.580	16.60	0.950	0.655	0.886	1.000	0.950	2.18	0.65	57.20
C325	0.332	50.00	0.530	30.22	0.971	19.78	1.528	0.540	16.60	0.965	0.592	0.912	1.000	0.965	1.38	0.76	69.70
C326	0.332	50.00	0.502	32.32	0.978	17.68	1.828	0.495	16.60	0.977	0.529	0.935	1.000	0.977	0.57	0.90	83.84
C327	0.332	50.00	0.472	34.41	0.977	15.59	2.207	0.435	16.60	0.979	0.467	0.932	1.000	0.979	0.00	1.00	93.19
C328	0.501	50.00	0.903	.9.75	0.761	30.25	0.653	0.635	25.05	0.712	0.788	0.805	0.788	0.903	5.40	0.29	23.67
C329	0.501	50.00	0.912	21.90	0.819	28.10	0.779	0.720	25.05	0.797	0.874	0.824	0.874	0.912	4.63	0.36	29.79
C330	0.501	50.00	0.891	24.05	0.860	25.95	0.927	0.750	25.05	0.855	0.960	0.781	0.960	0.891	4.09	0.42	32.44
C331	0.501	50.00	0.830	26.20	0.861	23.80	1.101	0.690	25.05	0.868	0.954	0.723	1.000	0.868	3.43	0.49	35.22
C332	0.501	50.00	0.763	28.35	0.843	21.65	1.309	0.595	25.05	0.864	0.868	0.686	1.000	0.864	2.84	0.56	38.30
C333	0.501	50.00	0.710	30.50	0.826	19.50	1.564	0.510	25.05	0.864	0.782	0.653	1.000	0.864	2.11	0.66	42.85
C334	0.501	50.00	0.668	32.65	0.812	17.35	1.882	0.435	25.05	0.870	0.695	0.626	1.000	0.870	1.34	0.77	48.19
C335	0.501	50.00	0.630	34.80	0.793	15.20	2.289	0.358	25.05	0.875	0.609	0.588	1.000	0.875	0.57	0.90	52.73
C336	0.502	75.00	0.789	30.40	0.693	44.60	0.682	0.465	37.69	0.637	0.807	0.576	0.807	0.789	5.91	0.25	14.61
C337	0.502	75.00	0.787	32.79	0.719	42.21	0.777	0.498	37.69	0.685	0.870	0.572	0.870	0.787	5.42	0.29	16.73
C338	0.502	75.00	0.780	35.17	0.742	39.83	0.883	0.520	37.69	0.728	0.933	0.557	0.933	0.780	4.94	0.33	18.55
C339	0.502	75.00	0.770	37.56	0.765	37.44	1.003	0.535	37.69	0.767	0.997	0.537	0.997	0.770	4.62	0.36	19.48
C340	0.502	75.00	0.757	39.95	0.788	35.05	1.140	0.543	37.69	0.803	0.939	0.578	1.000	0.803	3.86	0.44	25.40
C341	0.667	75.00	0.981	29.65	0.539	45.35	0.654	0.560	50.01	0.582	0.593	0.944	0.593	0.981	4.91	0.34	31.71
C342	0.667	75.00	0.985	31.89	0.569	43.11	0.740	0.610	50.01	0.629	0.638	0.956	0.638	0.985	4.39	0.39	36.84
C343	0.667	75.00	0.980	34.13	0.595	40.87	0.835	0.642	50.01	0.669	0.683	0.941	0.683	0.980	3.89	0.44	41.04
C344	0.667	75.00	0.967	36.37	0.616	38.63	0.942	0.655	50.01	0.703	0.727	0.900	0.727	0.967	3.42	0.49	43.98
C345	0.667	75.00	0.939	38.62	0.622	36.38	1.061	0.630	50.01	0.725	0.772	0.816	0.772	0.939	3.13	0.52	42.63
C346	0.667	75.00	0.905	40.86	0.619	34.14	1.197	0.585	50.01	0.740	0.817	0.716	0.817	0.905	2.87	0.55	39.71
C347	0.667	75.00	0.877	43.10	0.618	31.90	1.351	0.545	50.01	0.756	0.862	0.632	0.862	0.877	2.60	0.59	37.28
C348	0.666	60.00	0.976	26.42	0.577	33.58	0.787	0.613	39.97	0.645	0.661	0.927	0.661	0.976	4.16	0.41	37.86
C349	0.666	60.00	0.979	28.61	0.619	31.39	0.911	0.670	39.97	0.700	0.716	0.936	0.716	0.979	3.58	0.47	44.04
C350	0.666	60.00	0.961	30.80	0.644	29.20	1.055	0.680	39.97	0.740	0.770	0.883	0.770	0.961	2.95	0.55	48.12
C351	0.666	60.00	0.925	32.98	0.650	27.02	1.221	0.640	39.97	0.763	0.825	0.776	0.825	0.925	2.63	0.59	45.40
C352	0.666	60.00	0.886	35.17	0.645	24.83	1.417	0.580	39.97	0.780	0.880	0.659	0.880	0.886	2.34	0.62	41.13
C353	0.666	60.00	0.855	37.36	0.646	22.64	1.650	0.530	39.97	0.800	0.935	0.567	0.935	0.855	1.92	0.68	38.74
C354	0.666	60.00	0.827	39.55	0.645	20.45	1.934	0.477	39.97	0.818	0.989	0.482	0.989	0.827	1.60	0.73	35.19
C355	0.666	60.00	0.797	41.74	0.633	18.26	2.285	0.410	39.97	0.832	0.912	0.450	1.000	0.832	0.91	0.84	37.76
C356	0.666	60.00	0.769	43.92	0.616	16.08	2.732	0.340	39.97	0.846	0.803	0.424	1.000	0.846	0.16	0.97	41.08
C357	0.666	60.00	0.744	46.11	0.593	13.89	3.320	0.270	39.97	0.859	0.693	0.389	1.000	0.859	0.00	1.00	38.94
C358	0.666	60.00	0.724	48.30	0.573	11.70	4.128	0.210	39.97	0.875	0.584	0.359	1.000	0.875	0.00	1.00	35.95
C359	0.668	50.00	0.980	16.36	0.484	33.64	0.486	0.460	33.39	0.480	0.490	0.939	0.490	0.980	6.15	0.24	22.13
C360	0.668	50.00	0.983	18.67	0.520	31.33	0.596	0.530	33.39	0.550	0.559	0.948	0.559	0.983	5.36	0.30	28.11
C361	0.668	50.00	0.985	20.99	0.562	29.01	0.724	0.600	33.39	0.619	0.629	0.954	0.629	0.985	4.43	0.38	36.33

TABLE E-3 (continued)

RUN	x_f+z_f	Q_f cc/sec	x_o+z_o	Q_o cc/sec	Y_u	Q_u cc/sec	Q_o/Q_u	E	$Q_f x_f$ cc/sec	$\frac{Q_o x_o}{Q_f x_f}$	E_s	E/E_s	$\left[\frac{Q_o x_o}{Q_f x_f}\right]_I$	$\frac{Q_o x_o}{[Q_o x_o]_I}$	d cm.	EVF	ϕ (%)
C362	0.668	50.00	0.975	23.30	0.600	26.70	0.873	0.645	33.39	0.680	0.698	0.924	0.698	0.975	3.68	0.46	42.38
C363	0.668	50.00	0.930	25.62	0.608	24.38	1.051	0.605	33.39	0.713	0.767	0.788	0.767	0.930	3.19	0.52	40.68
C364	0.668	50.00	0.892	27.93	0.616	22.07	1.266	0.565	33.39	0.746	0.837	0.675	0.837	0.892	2.68	0.58	39.08
C365	0.668	50.00	0.844	30.25	0.602	19.75	1.532	0.480	33.39	0.764	0.906	0.530	0.906	0.844	2.36	0.62	32.94
C366	0.665	60.00	0.988	26.06	0.583	33.94	0.768	0.630	39.90	0.645	0.653	0.965	0.653	0.988	4.17	0.41	39.24
C367	0.665	60.00	0.968	28.46	0.608	31.54	0.902	0.645	39.90	0.690	0.713	0.904	0.713	0.968	3.63	0.46	41.97
C368	0.665	60.00	0.929	30.85	0.615	29.15	1.059	0.610	39.90	0.719	0.773	0.789	0.773	0.929	3.17	0.52	40.84
C369	0.665	60.00	0.896	33.25	0.622	26.75	1.243	0.575	39.90	0.747	0.833	0.690	0.833	0.896	2.82	0.56	38.69
C370	0.665	60.00	0.862	35.65	0.623	24.35	1.464	0.525	39.90	0.770	0.893	0.588	0.893	0.862	2.38	0.62	36.40
C371	0.500	75.00	0.799	31.95	0.722	43.05	0.742	0.510	37.50	0.681	0.852	0.599	0.852	0.799	5.60	0.28	16.59
C372	0.500	75.00	0.752	34.22	0.712	40.78	0.839	0.460	37.50	0.686	0.913	0.504	0.913	0.752	5.40	0.29	14.82
C373	0.500	75.00	0.713	36.50	0.702	38.50	0.948	0.415	37.50	0.694	0.973	0.426	0.973	0.713	5.18	0.31	13.31
C374	0.500	75.00	0.689	38.77	0.702	36.23	1.070	0.390	37.50	0.712	0.966	0.404	1.000	0.712	4.85	0.34	13.79
C375	0.500	75.00	0.667	41.05	0.702	33.95	1.209	0.365	37.50	0.730	0.905	0.403	1.000	0.730	4.16	0.41	16.44
C376	0.499	60.00	0.898	24.85	0.782	35.15	0.707	0.660	29.96	0.745	0.829	0.796	0.829	0.898	5.13	0.32	25.19
C377	0.499	60.00	0.917	27.14	0.845	32.86	0.826	0.755	29.96	0.830	0.906	0.833	0.906	0.917	4.37	0.39	32.25
C378	0.499	60.00	0.912	29.43	0.898	30.57	0.963	0.810	29.96	0.896	0.982	0.824	0.982	0.912	3.68	0.46	37.84
C379	0.499	60.00	0.870	31.72	0.917	28.28	1.122	0.785	29.96	0.922	0.941	0.834	1.000	0.922	3.07	0.53	44.20
C380	0.499	60.00	0.821	34.02	0.922	25.98	1.309	0.730	29.96	0.932	0.865	0.844	1.000	0.932	2.33	0.63	52.84
C381	0.499	60.00	0.776	36.31	0.925	23.69	1.533	0.670	29.96	0.941	0.789	0.850	1.000	0.941	1.59	0.73	62.20
C382	0.499	60.00	0.739	38.60	0.933	21.40	1.804	0.617	29.96	0.952	0.712	0.866	1.000	0.952	0.83	0.85	73.92
C383	0.667	50.00	0.986	21.20	0.568	28.80	0.736	0.610	33.34	0.627	0.636	0.959	0.636	0.986	4.39	0.38	36.88
C384	0.667	50.00	0.984	23.25	0.609	26.75	0.869	0.665	33.34	0.687	0.697	0.953	0.697	0.984	3.66	0.46	43.96
C385	0.667	50.00	0.983	25.31	0.657	24.69	1.025	0.720	33.34	0.746	0.759	0.949	0.759	0.983	2.93	0.55	51.87
C386	0.667	50.00	0.967	27.36	0.696	22.64	1.209	0.740	33.34	0.794	0.821	0.902	0.821	0.967	2.37	0.62	55.86
C387	0.667	50.00	0.916	29.41	0.689	20.59	1.429	0.660	33.34	0.808	0.882	0.748	0.882	0.916	2.08	0.66	49.39
C388	0.667	50.00	0.873	31.47	0.684	18.53	1.698	0.585	33.34	0.824	0.944	0.620	0.944	0.873	1.66	0.72	44.68
C389	0.667	50.00	0.837	33.52	0.680	16.48	2.034	0.515	33.34	0.842	0.989	0.521	1.000	0.842	1.31	0.78	40.36
C390	0.667	50.00	0.809	35.58	0.684	14.42	2.466	0.455	33.34	0.863	0.866	0.526	1.000	0.863	0.38	0.93	48.96
C391	0.667	50.00	0.782	37.63	0.683	12.37	3.042	0.390	33.34	0.883	0.743	0.525	1.000	0.883	0.00	1.00	52.52
C392	0.667	75.00	0.949	34.60	0.574	40.40	0.856	0.585	50.04	0.656	0.691	0.846	0.691	0.949	3.93	0.43	36.52
C393	0.667	75.00	0.931	36.63	0.584	38.37	0.955	0.580	50.04	0.681	0.732	0.792	0.732	0.931	3.64	0.46	36.76
C394	0.667	75.00	0.911	38.66	0.592	36.34	1.064	0.565	50.04	0.703	0.773	0.731	0.773	0.911	3.35	0.50	36.32
C395	0.667	75.00	0.894	40.69	0.601	34.31	1.186	0.553	50.04	0.727	0.813	0.680	0.813	0.894	2.94	0.55	37.16
C396	0.667	75.00	0.878	42.72	0.611	32.28	1.323	0.540	50.04	0.749	0.854	0.633	0.854	0.878	2.64	0.58	36.93
C397	0.667	75.00	0.863	44.75	0.622	30.25	1.479	0.525	50.04	0.771	0.894	0.587	0.894	0.863	2.35	0.62	36.58
C398	0.500	50.00	0.788	22.75	0.741	27.25	0.835	0.525	24.98	0.718	0.911	0.576	0.911	0.788	5.15	0.31	18.13
C399	0.500	50.00	0.810	24.96	0.810	25.04	0.997	0.620	24.98	0.809	0.999	0.621	0.999	0.810	4.35	0.39	24.11
C400	0.500	50.00	0.833	27.17	0.897	22.83	1.190	0.725	24.98	0.906	0.913	0.794	1.000	0.906	2.88	0.55	43.96
C401	0.500	50.00	0.810	29.37	0.943	20.63	1.424	0.730	24.98	0.953	0.824	0.886	1.000	0.953	1.82	0.70	61.81

TABLE E-3 (continued)

RUN	x_f+z_f	Q_f cc/sec	x_o+z_o	Q_o cc/sec	Y_u	Q_u cc/sec	Q_o/Q_u	E	Q_fx_f cc/sec	$\frac{Q_ox_o}{Q_fx_f}$	E_s	E/E_s	$\left[\frac{Q_ox_o}{Q_fx_f}\right]_I$	$\frac{Q_ox_o}{[Q_ox_o]_I}$	d cm.	EVF	Φ (%)
C402	0.500	50.00	0.760	31.58	0.947	18.42	1.715	0.658	24.98	0.961	0.736	0.894	1.000	0.961	0.91	0.84	75.03
C403	0.500	50.00	0.718	33.79	0.955	16.21	2.085	0.590	24.98	0.971	0.648	0.911	1.000	0.971	0.08	0.98	89.66
C404	0.500	50.00	0.678	36.00	0.960	14.00	2.571	0.515	24.98	0.978	0.560	0.920	1.000	0.978	0.00	1.00	92.04
C405	0.335	60.00	0.666	13.30	0.760	46.70	0.285	0.330	20.07	0.441	0.663	0.498	0.663	0.666	9.44	0.07	3.53
C406	0.335	60.00	0.703	15.42	0.793	44.58	0.346	0.425	20.07	0.540	0.768	0.553	0.768	0.703	8.69	0.10	5.40
C407	0.335	60.00	0.712	17.54	0.821	42.46	0.413	0.495	20.07	0.622	0.874	0.567	0.874	0.712	8.16	0.12	6.79
C408	0.335	60.00	0.729	19.66	0.857	40.34	0.487	0.580	20.07	0.714	0.979	0.592	0.979	0.729	7.44	0.16	9.21
C409	0.335	60.00	0.755	21.78	0.905	38.22	0.570	0.685	20.07	0.819	0.957	0.716	1.000	0.819	6.41	0.22	15.60
C410	0.335	60.00	0.737	23.90	0.932	36.10	0.662	0.720	20.07	0.877	0.904	0.796	1.000	0.877	5.44	0.29	23.13
C411	0.335	60.00	0.691	26.02	0.939	33.98	0.766	0.695	20.07	0.896	0.851	0.816	1.000	0.896	4.85	0.34	27.88
C412	0.335	60.00	0.649	28.13	0.943	31.87	0.883	0.662	20.07	0.909	0.798	0.829	1.000	0.909	4.12	0.41	34.13
C413	0.335	60.00	0.613	30.25	0.948	29.75	1.017	0.630	20.07	0.923	0.745	0.846	1.000	0.923	3.40	0.49	41.49
C414	0.335	60.00	0.582	32.37	0.956	27.63	1.172	0.600	20.07	0.939	0.692	0.867	1.000	0.939	2.67	0.58	50.30
C415	0.335	60.00	0.553	34.49	0.961	25.51	1.352	0.565	20.07	0.951	0.639	0.884	1.000	0.951	2.06	0.66	58.63
C416	0.335	60.00	0.530	36.61	0.971	23.39	1.565	0.535	20.07	0.966	0.586	0.913	1.000	0.966	1.32	0.77	70.72
C417	0.335	60.00	0.507	38.73	0.979	21.27	1.821	0.500	20.07	0.978	0.533	0.939	1.000	0.978	0.58	0.90	84.11
C418	0.335	60.00	0.487	40.85	0.990	19.15	2.133	0.465	20.07	0.990	0.480	0.969	1.000	0.990	0.00	1.00	96.94
C419	0.332	50.00	0.695	13.40	0.800	36.60	0.366	0.438	16.62	0.560	0.806	0.543	0.806	0.695	8.66	0.10	5.37
C420	0.332	50.00	0.675	15.54	0.822	34.46	0.451	0.480	16.62	0.631	0.935	0.514	0.935	0.675	8.14	0.12	6.21
C421	0.332	50.00	0.675	17.67	0.855	32.33	0.547	0.545	16.62	0.717	0.969	0.563	1.000	0.717	7.17	0.17	9.61
C422	0.332	50.00	0.688	19.81	0.901	30.19	0.656	0.635	16.62	0.820	0.905	0.702	1.000	0.820	5.89	0.25	17.89
C423	0.332	50.00	0.689	21.94	0.946	28.06	0.782	0.705	16.62	0.909	0.841	0.839	1.000	0.909	4.63	0.36	30.33
C424	0.332	50.00	0.646	24.08	0.959	25.92	0.929	0.680	16.62	0.936	0.777	0.876	1.000	0.936	3.68	0.46	40.22
C425	0.332	50.00	0.603	26.22	0.966	23.78	1.102	0.640	16.62	0.952	0.713	0.898	1.000	0.952	2.88	0.55	49.72
C426	0.332	50.00	0.563	28.35	0.970	21.65	1.310	0.590	16.62	0.961	0.649	0.910	1.000	0.961	2.10	0.66	59.86
C427	0.332	50.00	0.530	30.49	0.976	19.51	1.563	0.543	16.62	0.972	0.585	0.929	1.000	0.972	1.19	0.79	73.74
C428	0.333	75.00	0.699	16.40	0.769	58.60	0.280	0.360	24.97	0.459	0.657	0.548	0.657	0.699	9.41	0.07	3.93
C429	0.333	75.00	0.703	18.44	0.788	56.56	0.326	0.410	24.97	0.519	0.738	0.555	0.738	0.703	8.92	0.09	4.92
C430	0.333	75.00	0.695	20.47	0.803	54.53	0.375	0.445	24.97	0.570	0.820	0.543	0.820	0.695	8.45	0.11	5.83
C431	0.333	75.00	0.685	22.51	0.818	52.49	0.429	0.475	24.97	0.617	0.901	0.527	0.901	0.685	8.17	0.12	6.30
C432	0.333	75.00	0.672	24.54	0.832	50.46	0.486	0.500	24.97	0.661	0.983	0.509	0.983	0.672	7.89	0.13	6.74
C433	0.333	75.00	0.659	26.58	0.846	48.42	0.549	0.520	24.97	0.701	0.968	0.537	1.000	0.701	7.19	0.17	9.09
C434	0.333	75.00	0.647	28.61	0.861	46.39	0.617	0.540	24.97	0.742	0.927	0.582	1.000	0.742	6.64	0.20	11.82
C435	0.333	75.00	0.636	30.65	0.876	44.35	0.691	0.557	24.97	0.780	0.887	0.628	1.000	0.780	5.91	0.25	15.91
C436	0.333	75.00	0.624	32.68	0.891	42.32	0.772	0.570	24.97	0.816	0.846	0.674	1.000	0.816	5.20	0.31	20.91
C437	0.333	75.00	0.611	34.72	0.907	40.28	0.862	0.580	24.97	0.850	0.805	0.720	1.000	0.850	4.63	0.36	26.06
C438	0.333	75.00	0.595	36.75	0.919	38.25	0.961	0.578	24.97	0.876	0.765	0.756	1.000	0.876	3.94	0.43	32.60
C439	0.333	75.00	0.580	38.79	0.932	36.21	1.071	0.575	24.97	0.901	0.724	0.794	1.000	0.901	3.37	0.49	39.25
C440	0.333	75.00	0.564	40.82	0.942	34.18	1.194	0.565	24.97	0.921	0.683	0.827	1.000	0.921	2.70	0.58	47.70
C441	0.333	75.00	0.551	42.86	0.957	32.14	1.333	0.560	24.97	0.945	0.643	0.872	1.000	0.945	2.12	0.65	57.06

TABLE E-3 (continued)

RUN	x_f+z_f	Q_f cc/sec	x_o+z_o	Q_o cc/sec	Y_u	Q_u cc/sec	Q_o/Q_u	E	$Q_f x_f$ cc/sec	$\frac{Q_o x_o}{Q_f x_f}$	E_s	E/E_s	$\left(\frac{Q_o x_o}{Q_f x_f}\right)_I$	$\frac{Q_o x_o}{(Q_o x_o)_I}$	d cm.	EVF	ϕ (%)
C442	0.333	75.00	0.534	44.89	0.967	30.11	1.491	0.543	24.97	0.961	0.602	0.902	1.000	0.961	1.56	0.74	66.40
C443	0.333	75.00	0.519	46.93	0.979	28.07	1.672	0.525	24.97	0.976	0.561	0.936	1.000	0.976	0.91	0.84	78.65
C444	0.333	75.00	0.503	48.96	0.987	26.04	1.881	0.500	24.97	0.986	0.520	0.961	1.000	0.986	0.36	0.93	89.76
C445	0.333	75.00	0.490	51.00	1.000	24.00	2.125	0.480	24.97	1.000	0.480	1.000	1.000	1.000	0.00	1.00	100.00

IBM 360/40 FORTRAN PROGRAM

(TABLE E-3)

```
C       SEPARATION EXPERIMENT - PROGRAM 2
        REAL MIN,MAX
        TOL=0.00001
        H=16.1
        DOL=0.025
        PI=3.1415
        WRITE(3,5700)
        LNCT=0
100     CONTINUE
        FLAG=0.0
        MAX=0.0
        MIN=100.0
        CT=0.0
        AVG2=0.0
150     CONTINUE
        READ(1,5000) COL2, QO,QF
        IF(QO)400,200,400
200     CONTINUE
        IF(FLAG)900,300,900
300     CONTINUE
        CALL EXIT
400     CONTINUE
        CT=CT+1.0
        AVG2=AVG2+COL2
        FLAG=1.0
        IF(QO-MAX)600,600,500
500     CONTINUE
        MAX=QO
600     CONTINUE
        IF(QO-MIN)700,800,800
700     CONTINUE
        MIN=QO
800     CONTINUE
        QSAVE=QF
        GOTO150
900     CONTINUE
        QF=QSAVE
        COL2=AVG2/CT
        WRITE(3,5100)
        LNCT=LNCT+2.0
```

```
      DIF=MAX-MIN
      J=DIF/2.0
      DEL=DIF/FLOAT(J)
      MIN=MIN-DEL
      J=J+1
      IF(QF-52.0)1000,1000,1100
 1000 CONTINUE
      QF=50.0
      GOTO1400
 1100 CONTINUE
      IF(QF-62.0)1200,1200,1300
 1200 CONTINUE
      QF=60.0
      GOTO1400
 1300 CONTINUE
      QF=75.0
 1400 CONTINUE
      DO2900I=1,J
      MIN=MIN+DEL
      QU=QF-MIN
      COL17=MIN/QU
      READ(1,5300)ICT,COL16
      IF(ICT) 1550,1550,1600
 1550 CONTINUE
      WRITE(3,5400)
      GOTO300
 1600 CONTINUE
      A2=MIN
      A3=QU
      A4=QF*(1.0-COL2)
      A5=A3/(QF*COL2)
      A1=COL16+((A2*COL2)/A4)+(A5*(1.0-COL2))
      COL1=(A1*A3-A4*A5+A2*A5)/(A2*A3/A4+A2*A5
      COL8=(A2*COL1-A2+A4)/A3
      COL24=COL2*QF
      COL25=MIN*COL1
      COL26=QU*(1.0-COL8)
      COL27=COL25/COL24
      COL28=COL26/COL24
      YF=1.0-COL2
```

```
      IF(COL17-(COL2/YF))1610,1620,1630
1610  CONTINUE
      XO=1.0
      YU=1.0-(QF*COL2-MIN)/QU
      GOTO1640
1620  CONTINUE
      XO=1.0
      YU=1.0
      GOTO1640
1630  CONTINUE
      YU=1.0
      XO=1.0-(QF*(1.0-COL2)-QU)/MIN
1640  CONTINUE
      E1=((XO-COL2)/(1.0-COL2))*(MIN/QF)
      E2=((YU-YF)/COL2)*(QU/QF)
      COL29=E1+E2
      COL30=COL16/COL29
      COL31=(MIN*XO)/(QF*COL2)
      COL32=COL27/COL31
      D=0.1
      DO=D
      DD=0.25
1800  Z=H-D
      X=1.5*Z/H
      XX=2.25*Z*Z/(H*H)
      CS=(COL32*(XX-0.03))+0.03
      QOL=(QF+QU)/202.22
      CF=(2.25*H)/(XX*Z)
      T=(CS-0.03)*CF/(2*QOL)
      DC =  (2.25*H-(XX*MIN*TC)/(PI*(2.25-0.03)))/2.25+XX+1.5*X)
      IF(DC)  2700,2300,2300
2300  CONTINUE
      C6=D-DC
      IF(ABS(C6)-DOL)  2800,2800,2400
2400  CONTINUE
      IF(C6)2500,2800,2600
2500  CONTINUE
      DO=D
      D=D+DD
      GOTO1800
```

```
2600   CONTINUE
       DD=DD/2.0
       D=DO+DD
       GOTO1800
2700   CONTINUE
       DC=0.0001
2800   CONTINUE
       A=3*DC/16.1
       B=-3*(DC*DC)/(16.1*16.1)
       C=(DC*DC*DC)/(16.1*16.1*16.1)
       VF=1.0-(A+B+C)
       PER=COL 30*VF*100.0
       WRITE (3,5200) ICT,COL2,QF,COL1,MIN,COL8,QU,COL17,COL16,COL24,
      1 COL27,COL28,COL29,COL30,COL31,COL32,DC,VF,PER
       IF(LNCT-45.0) 2770,2750,2750
2750   CONTINUE
       WRITE (3,5700)
       LNCT=0
2770   LNCT=LNCT+1.0
2900   CONTINUE
       READ (1,5300)ICT
       IF (ICT)3000,100,3000
3000   CONTINUE
       WRITE (3,5400)
       GO TO 300
5000   FORMAT (10X,2F10.8,30X,F10.0)
5100   FORMAT ('0')
5200   FORMAT ('C',13,F7.3,F7.2,F7.3,F7.2,F7.3,F7.2,F8.3,F7.3,F7.2,5F8.3,
      1 F9.3,F7.2,F8.3)
5300   FORMAT (2X,12,5X,F10.3)
5400   FORMAT ('PHASE EFFOR')
5700   FORMAT ('1'/'0'/'0'/'0'/)
       END
```

APPENDIX F

TESTING THE PROPOSED MODEL

It is evident that prior to the utilization of Eq. 44 and Eq. 51, the liquid particle size of the dispersed phase must be known. In Eq. 51, both the air core radius "a" and the air core velocity V_o must also be evaluated. In the absence of any elaborate measuring apparatus on hand, high-speed motion pictures were taken for a particular run and the results are described as below.

Reduction of Mathematical Equations

The air core radius, measured by the movie film, was found to be about 0.132 cm in comparison with the known radius of the discharge apex—0.150 cm. The proximity of these two values seems to concur reasonably well with the observation made when the cyclone was in operation. The film also revealed that the liquid (oil) particle is about the same size as the solid (polyethylene) particle. Since the solid particle is believed to be practically indivisible in the cyclone and the exact size ($2\sigma_s$ = 0.298 mm) is already known, the liquid particle radius can be approximated to be about $2\sigma_\ell$ = 0.030 cm (or σ_ℓ = 0.015 cm).

Substituting this value into Eq. 44 and assuming a range of t from 0.01 to 1.00 sec, it is discovered that the first term of Eq. 44, Z_m, is negligibly small (less than 10%) in comparison with the second term, Z_o, which contains the quantity Q_o (ranging from 20 to 60 cc/sec). Hence Eq. 44 can be reduced to

$$Z = \frac{Q_o\, t}{\pi (b^2 - a^2)} \qquad (44)$$

<u>Selection of the Appropriate Model by Experimental Data</u>

<u>Phase Separation by Combined Streamline Flow and Centrifugal Action</u>: At the onset of fitting the experimental data into the proposed mathematical model (Eq. 51), a computer program was written to evaluate both the air core tangential velocity, V_o, and the turbulent length, "d", by a double trial and error procedure. Unfortunately, many hours of computer time and human effort failed to fit even one set of runs into the model. A brief recount of this model-fitting endeavor is given as follows.

First, a particular set of runs was chosen (Set No. 10 or Run C-140 to C-151). The basis for such a selection was:

a) oil, having a density less than water, is a dispersed phase. (Note: if otherwise, then both $\overline{v}_r$ and $\overline{v}_o$ components, represented by Eq. 21 and Eq. 22 respectively, could not be neglected).

b) The throughput or feed rate (Q_f = 50 cc/sec) is so low that emulsification should not be a prime concern. The computer program was tailored to the trial and error procedure for two "loops"; the "inner loop" was aimed to converge the fixed t_1/t_2 with the calculated t_1/t_2 at a certain V_o while the "outer loop" was to converge the assumed turbulent length with the calculated length. After the initial effort, which failed to converge both desired variables, a correction factor (CF) was arbitrarily assigned to the first term of Eq. 51. This factor can be justified only on the empirical ground that the first term in Eq. 51, representing only the streamline flow, predominates over the second term which is incorporated with the centrifugal influence. However, it was soon discovered that the correction factor is quite sensitive and a value less than 1.80 would help to converge only the calculated t_1/t_2 with the fixed t_1/t_2 within the "inner loop," but not the turbulent length of the "outer loop." An attempt was also made to replace Eq. 52

$$\frac{(c_o)^2 - a^2}{R^2 - a^2} = \frac{(Q_o x_o)_{exp}}{(Q_o x_o)_{ideal}} \tag{52}$$

by the following expression

$$\frac{(c_o)^2 - a^2}{R^2 - a^2} = \frac{(Q_o x_o)_{exp.}}{(Q_f x_f)_{exp.}} \tag{F-1}$$

The tabulated results showed that only two pairs of adjacent runs (C142-143 and C143-C144) converged for both t_1/t_2 and "d" values but failed to converge beyond these two pairs. The following is a segment of computer results:

C142-C143

Z	$(Q/L)_1$	$(Q/L)_2$	t_1/t_2	V_o	t_1	t_2	t_1/t_2	d*	d (calc)
8.10	0.32	0.33	0.94	578.8	0.16	0.17	0.94	8.00	9.07
7.20	0.32	0.33	0.94	522.5	0.12	0.13	0.94	8.90	9.27
C143-C144									
8.10	0.33	0.34	0.96	397.5	0.3[illegible]	0.40	0.96	8.00	0.55
3.60	0.33	0.34	0.96	325.6	0.01	0.01	0.96	12.50	12.1

*Assumed turbulent length.

Here both t_1 and t_2 of approximately 0.01 second seemed to be unrealistic since they represented the time required for the dispersed particle to reach the air core from a radius C_o by way of a streamline flow path.

Phase Separation Controlled by Centrifugal Action: After the initial failure of fitting Eq. 51 with the experimental data, it was postulated that the separation was dominated by the centrifugal action alone and hence Eq. 49a was applied instead

$$t = \frac{9\,\mu(C_o^4 - a^4)}{8(\rho - \rho')\,a^2(\sigma_\ell \cdot V_o)^2} \qquad (49a)$$

where σ_ℓ and V_o are the dispersed liquid particle radius and the air core velocity, respectively. In order to simplify the calculation, values of both σ_ℓ and V_o (average) from the previous trial and error procedure were used. Therefore

$$\sigma_\ell \cdot V_o = 0.005 \times 400 = 2.0 \text{ cm}^2/\text{sec}*$$

Substituting "a" = 0.132 cm with other constant values into Eq. 49a yields the following expression

$$t = 0.613 \ (C_o^4 - a^4)$$

Unfortunately, no run ever converged for d, and any correction factor applied would be unreasonably large because t decreased rapidly as C_o was gradually reduced during the trial and error routine.

<u>Phase Separation Controlled by Streamline Flow</u>: Now, it appeared that the only alternative would be to consider the streamline flow as the controlling mechanism, so only Eq. 46

$$t = \frac{C_o^2 - a^2}{2(Q/L)} \tag{46}$$

---

*If σ_ℓ = 0.015 cm were used for the previous double trial and error procedure, the resultant V_o would be 167 cm/sec since σ_ℓ and V_o both appear in the second term. The product of σ_ℓ and V_o would remain the same. Qualitatively, it also seems reasonable that under higher air core velocity, the liquid particle would be smaller.

should be applied. Since V_o was no longer needed, the trial and error procedure was reduced to seeking a single converging value for the turbulent length, d. A correction factor designated as

$$CF = \frac{b^2}{R^2}\frac{H}{Z} = \frac{2.25}{R^2}\frac{H}{Z}$$

was applied. Eq. 46 was then written as

$$t = \frac{(C_o^2 - 0.02)(CF)}{2(Q/L)} \tag{46a}$$

while both Eq. 35 and Eq. 52 remained unchanged. This correction factor is justified on the ground that the time required for a particle following the streamline path until it reaches the effective region is proportional to the ratio of total volume of the cyclone to the volume of the effective region (measured by Z). In other words, Eq. 46 without the correction factor simply overlooked the fact that a particle might encounter delay caused by turbulence prior to its arrival at the destination--the effective region. Therefore, in reality, it seems logical to apply the correction factor (always greater than 1.0) so that the total residence time of a particle in the cyclone was prolonged by the "intensity" or turbulence which could be partially attributed to rotational flow. Consequently, d values for all the runs were converged. The detailed trial and error procedure is listed in the FORTRAN program in Table E-3. A segment of the intermediate computer results is repeated as follows:

Z	x^2	c_o^2	Q/L	CF	t	d (assumed)	d* (calc.)
RUN NO. C-1							
16.00	2.22	1.587	0.507	1.019	1.38	0.10	4.10
7.87	0.52	0.380	0.507	8.965	2.98	8.13	8.17
RUN NO. C-2							
16.00	2.22	1.610	0.497	1.019	1.610	0.10	3.90
8.38	0.61	0.480	0.497	7.104	3.39	7.73	7.64

Here, only the last column "d" (calculated) is shown in Table E-3.

---

*In lieu of Eq. 47

$$Z = H-d$$

the d is calculated from the following volume balance

$$V_z = V_H - V_d$$

where V_z = the lower conic volume with a height Z.

V_H = the total cyclone volume with a height H

V_d = the upper truncated conic volume with a height d.

The details of mathematical manipulation are presented in the computer program in Table E-3.

However, it must be emphasized that the abandonment of the centrifugal term in Eq. 51 neither implied an absence of centrifugal force nor negated its influence within the cyclone. In analogy to an ordinary mechanics problem, when the trajectory of a projectile is prescribed, it is difficult to determine exactly all the contributing vectors present in the field. In the case of the hydrocyclone, when the streamline flow pattern is postulated, it is impossible to isolate all the contributing forces interacting in a highly irreversible state.

APPENDIX G

REFERENCES

1. Bird, R. B., Stewart, W. E., and Lightfoot, E. N., Transport Phenomena. J. Wiley, (1960).

2. Bradley, D., United Kingdom Atomic Energy Authority Report, AERECE/M. 177 (1956) "The Hydraulic Cyclone as a Liquid-Liquid Contractor and Separator."

3. Bradley, D., The Hydrocyclone, Pergamon Press (1965).

4. Breeze, J. C., "Design and Performance of a Dual-Clone Liquid Separator," Oak Ridge National Laboratory, Oak Ridge, Tenn., U.S. AEC CF-56-3-171, (March, 1956).

5. Crainer, H. E., "The Vortex Thickner," Rev. Indus. Min. Special Issue, No. 5, pp. 627-43, (April, 1951).

6. Driessen, M. G., "Theory of Flow in a Cyclone" Rev. of Indus. Mining Special Issue, No. 4, pp. 449-61, (1951).

7. Ellefson, R. R., M.S. Thesis, Northwestern Univ., (1952).

8. Fontein, F. J., "Separation by Cyclone According to Specific Gravity," Cyclone in Industry, p. 118, Elsevier Publishing Co. (1961).

9. Goldstein, Herbert, Classical Mechanics, p. 135, Edison-Wesley Co. (1950).

10. Hitchon, J. W., U.K. Atomic Energy Authority Report AERECE/R 2777, (1959) "Cyclone as Liquid-liquid Contractor-Separators."

11. Kelsell, D. F., "A Study of the Motion of Solid Particles in a Hydraulic Cyclone," Trans. Inst. Chem. Eng., Vol. 30, 87, (1952).

12. Klein, F. G., M.S. Thesis, Northwestern Univ., (1950).

13. McCracken, D. D, and Dorn, W. S., Numerical Methods and FORTRAN Programming, John Wiley, (1964).

14. Mixon, F. O., "An Analytical Study of Separation in a Liquid-Liquid Cyclone as Applied to the Sweet Water Process," Final Report for Office of Saline Water, U.S. Dept. of Interior, (1967).

15. Molyneaux, F., "Extraction in the Hydraulic Cyclone." Chem. & Process Engineering, Vol. 43, p. 502 (Oct. 1962).

16. Neumark, Stefan, "Acceleration Resistance of Rectilinear Moving Body in an Ideal Fluid," Zeit, Für Argevante Mathematik Und Mechanik, Vol. 16, p. 117, (1936).

17. Rietema, K., "Performance and Design of Hydrocyclones," Chem. Eng. Science, Vol. 15, pp. 298-325, (1961).

18. Simkin, D. J., and Olney, R. B., "Phase Separation and Mass Transfer in a Liquid-Liquid Cyclone," A.I.Ch.E. Journal, Vol. 2, No. 4, pp. 545-551, (1956).

19. Sweet Water Development Co., Final Report for Contract No. 14-01-0001-341, (1967).

20. Tengbergen, H. J., and Rietema, K., "Efficiency of Phase Separations," Cyclones in Industry, p. 23, Elsevier Publishing Co., (1961).

21. Tepe, J. B., and Woods, W. K., U.S. Atomic Energy Commission Report AECD 2864 (Jan. 1943), "Designing of Ether-Water Contracting Systems."

22. Vallentine, H. R., Applied Hydrodynamics, p. 28-29, Butterworths Scientific Publication (1959).

23. Van Rossum, J. J., "Separation of Emulsions in a Cyclone," from Cyclones in Industry, Chapter 9, Edited by K. Rietema and C. G. Verver, Elsevier Publishing Co., (1961).

APPENDIX H

NOMENCLATURE

A the lighter component of a system to be treated by a cyclone.

a radius of the air core (cm).

B the denser component of a system to be treated by a cyclone.

b radius of the upper base of a cyclone (cm).

C_o radius of a hypothetical cone with a height Z from the apex of the cyclone (cm).

D differential operator of a vector.

d length of the turbulent region extended downward from the upper base - this region is completely ineffective for separation (cm).

e base, natural logarithms = 2.71828.

$\hat{e}$ a unit vector in curvilinear coordinates.

E overall separation efficiency (dimensionless).

E_s ideal overall separation efficiency (dimensionless).

EVF effective volume fraction - complementary volume fraction for ineffective separation determined by "d".

F a function analytical in a complex plane.

g gravitational acceralation (cm/sec^2).

g_c gravitational conversion factor (dimensionless).

H height of a cyclone including the distance extrapolated from the apex (cm).

h_1 height of the cylindrical (vertical) section of a cyclone (cm).

h_2 height of the conical section of a cyclone (cm).

$\hat{i}$ a unit vector in a x-direction of Cartesian coordinates.

$\hat{j}$ a unit vector in the y-direction of Cartesian coordinates.

k a viscous term = $6\pi\mu\sigma$ when the particle reaches its terminal velocity in a continuous phase.

K' an arbitrary constant.

$\hat{k}$ a unit vector in the z-direction of Cartesian coordinates.

L average length of an element normal to flow in a cyclone (cm).

M mass of the liquid displaced by a solid or a liquid particle of a dispersed phase (gm).

m mass of the dispersed particle (gm).

m' slope of a line.

m_o the apparent mass of a particle moving in a fluid (gm).

m° abbreviated for m-M.

n an exponential order.

P pressure (gm/cm-sec^2).

Q_f volumetric flow rate of the feed (cc/sec).

Q_o volumetric flow rate of the overflow (cc/sec).

Q_u volumetric flow rate of the underflow (cc/sec).

r radius in cylindrical coordinates (cm).

R radius of the conic section of the cyclone (cm).

S shape factor for the moving particle displacing the fluid.

t time (sec).

$\bar{v}$ relative velocity of a particle with respect to the continuous fluid phase in motion (cm/sec).

V_O tangential velocity at the outer perimeter of the air core (cm/sec).

V_r radial velocity (cm/sec).

V_θ tangential velocity (cm/sec).

V_z vertical velocity (cm/sec).

W a function of designated variables.

x volumetric fraction of the lighter liquid component.

y volumetric fraction of the heavier liquid component.

Z height of the cyclone effective in separation (cm).

z volumetric fraction of the solids in the flow.

Greek

σ radius of the particle of the dispersed phase (cm).

α apex angle (degree).

Δ gradient of a potential.

ν kinematic viscosity (cm^2/sec).

θ angle (degree).

μ viscosity (gm/cm-sec).

ξ a reduced dimensionless quantity $= \frac{(Q/L)}{\nu}$ (dimensionless).

π 3.14159.

ρ density (gm/cm^3).

Φ cyclone performance $= (E/E_s) \times$ EVF (dimensionless).

ψ streamline function orthogonal to the potential function.

ω angular velocity (radian/sec).